CRANFIELD UNIVERSITY

**KONSTANTINOS G. KYPRIANIDIS**

# On Gas Turbine Conceptual Design

SCHOOL OF AEROSPACE, TRANSPORT AND MANUFACTURING
Propulsion Engineering Centre

PhD Thesis
Academic Year 2018-19

Supervisor: Dr. V. Sethi
January 2019

CRANFIELD UNIVERSITY

SCHOOL OF AEROSPACE, TRANSPORT AND MANUFACTURING
Propulsion Engineering Centre

PhD Thesis

Academic Year 2018-19

KONSTANTINOS G. KYRPIANIDIS

# On Gas Turbine Conceptual Design

Supervisor: Dr. V. Sethi

January 2019

This thesis is submitted in partial fulfillment of the requirements for the degree of Doctor of Philosophy

# Abstract

The thesis begins with a review of the evolution of the industry's vision for the aero-engine design of the future. Appropriate research questions are set that can influence how this vision may further evolve in the years to come. Design constraints, material technology, customer requirements, noise and emissions legislation, technology risk and economic considerations and their effect on optimal concept selection are discussed in detail. Different aspects of the pedagogy of gas turbine conceptual design as well as information on the Swedish and Brazilian educational systems are also presented.

A multi-disciplinary aero-engine conceptual design tool is utilised for assessing engine/aircraft environmental performance. The tool considers a variety of disciplines that span conceptual design including: engine performance, engine aerodynamic and mechanical design, aircraft design and performance, emissions prediction and environmental impact, engine and airframe noise, and production, maintenance and direct operating costs.

With respect to addressing the research questions set, several novel engine cycles and technologies - currently under research - are identified. It is shown that there is great potential to reduce fuel consumption for the different concepts identified, and consequently decrease the $CO_2$ emissions. Furthermore, this can be achieved with sufficient margin from the $NO_x$ certification limits set by International Civil Aviation Organisation, and in line with the medium-term and long-term goals set through it's Committee on Aviation Environmental Protection.

The option of an intercooled-core geared-fan aero-engine for long-haul applications is assessed by means of a detailed design space exploration. An attempt is made to identify the fuel burn optimal values for a set of engine design parameters by varying them all simultaneously, as well as in isolation. Different fuel optimal designs are developed based on different sets of assumptions. Evidence is provided that higher overall pressure ratio intercooled engine cycles become more attractive in aircraft applications that require larger engine sizes.

The trade-off between the ever-increasing energy efficiency of modern aero-engines and their $NO_x$ performance is assessed. Improving engine thermal efficiency has a detrimental effect on $NO_x$ emissions for traditional combustors, both at high altitude and particularly at sea-level conditions. Lean-combustion technology does not demonstrate such behaviour and can therefore help decouple $NO_x$ emissions performance from engine thermal efficiency. If we are to reduce the contribution of aviation to global warming, however, future certification legislation may need to become more stringent and comprehensive, i.e., cover high altitude conditions. By doing so we can help unlock the competitive advantage of lean burn technology in relation to cruise $NO_x$ and mission performance.

Finally, some insight is provided on the potential benefits to be tapped from a transition from the traditional deterministic approach for system analysis to a stochastic (robust design) approach for economic decision-making under uncertainty. A basic methodology is outlined and applied on a specific conceptual design case for a conventional turbofan engine. The sensitivity of an optimal engine design obtained deterministically to real-life uncertainties is found to be far from negligible. The considerable impact of production scatter, measurement uncertainties as well as component performance deterioration, on engine performance must be catered for; this includes taking into consideration control system design aspects. A fast analytical approach is shown to be sufficiently accurate for the conceptual design process, particularly for estimating key performance parameters. These relate to type-test certification and performance retention guarantees including preliminary estimates of engine production margins.

Lessons learned are presented from: (i) the integration of different elements of conceptual design in a new BSc course and an existing traditional MSc course on gas turbine technology, (ii) the development of an intensive course on gas turbine multi-disciplinary conceptual design. The results from the use of problem-based learning are very encouraging, in terms of enhancing student learning and developing engineering skills.

# Acknowledgments

Parts of the work presented in this thesis have been performed under the project NEWAC (European Commission Contract No. AIP5-CT-2006-030876) and this funding is acknowledged. Within project NEWAC, the work has been performed under WP1.3, "Techno-Economic and Environmental Risk Analysis", in close collaboration with L. Xu (Siemens), A. Alexiou (National Technical University of Athens), and B. Lehmayr (Continental Automotive GmbH). Their contributions in developing the NEWAC TERA2020 framework are gratefully acknowledged, and their support in the work presented in this thesis is much appreciated.

Stimulating discussions with J.A. Borradaile, C.J. Begley (Rolls-Royce), M. Horobin (Rolls-Royce), R.J. Tunstall (Rolls-Royce), S. Bake (Rolls-Royce Deutschland), S. Donnerhack (MTU Aero Engines), R. Singh (Cranfield University), S.O.T. Ogaji, D. Nalianda (Cranfield University), P. Giannakakis (Snecma), A. Lundbladh (GKN Aerospace) and L. Larsson (GKN Aerospace) on advanced concepts and aero engine design practice and pedagogy are gratefully acknowledged. I am grateful to R. Avellán (GKN Aerospace) for providing the transport efficiency data used in this work. Many thanks go to A.I. Kaflas (Aristotle University of Thessaloniki), A.M. Rolt (Cranfield University), E. Dahlquist (Mälardalen University), I. Aslanidou (Mälardalen University), N. Zimmerman (Mälardalen University), V. Zaccaria (Mälardalen University), E. Pontika (Cranfield University), B. Sauter (Mälardalen University), J. Barbosa, T. Grönstedt (Chalmers University of Technology), C. Gkoudesnes and W. Camilleri for the fruitful collaborations that have resulted in the different published articles that this thesis is based on.

I am indebted to Prof. P. Pilidis for giving me the opportunity to pursue a second PhD degree. I would also like to thank my supervisor Dr. V. Sethi for his help in bringing this research work forward. Finally, I would like to thank the reviewers of this research for their constructive suggestions to improve the overall quality and clarity of this report and associated articles.

*Konstantinos G. Kyprianidis*
*January 2019*

# Contents

# List of Figures

# List of Tables

# Nomenclature

## Acronyms and abbreviations

| | |
|---|---|
| ACARE | Advisory Council for Aeronautical Research in Europe |
| ASA | Adaptive Simulated Annealing |
| ATM | Air Traffic Management |
| CAEP | Committee on Aviation Environmental Protection |
| CFD | Computational Fluid Dynamics |
| $CO_2$ | Carbon dioxide |
| Comb. | Combustor |
| CRTF | Counter-Rotating TurboFan |
| DDTF | Direct Drive TurboFan |
| DOC | Direct Operating Costs |
| DOE | Design Of Experiments |
| DREAM | valiDation of Radical Engine Architecture systeMs |
| EIS | Entry Into Service |
| EOR | End Of Runway |
| EU | European Union |
| FAR | Federal Aviation Regulations |
| FL350 | Flight Level, 35000 [ft] |
| GTF | Geared TurboFan |
| GOR | Geared Open Rotor |
| HD | Hot-Day |
| HPC | High Pressure Compressor |
| HPT | High Pressure Turbine |
| IC | InterCooled aero engine |
| ICAO | International Civil Aviation Organisation |
| Id. | Ideal |
| IPC | Intermediate Pressure Compressor |
| IPCC | International Panel on Climate Change IPT |
| IPT | Intermediate Pressure Turbine |
| IRA | Intercooled Recuperated Aero engine |
| ISA | International Standard Atmosphere |
| ITA | Instituto Technologico de Aeronautica |

| | |
|---|---|
| LDI | Lean Direct Injection |
| LP | Low Pressure |
| LPP | Lean Pre-mixed Pre-vaporised |
| LPT | Low Pressure Turbine |
| LR | Long Range |
| LT | Long Term |
| LTO | Landing and Take-Off cycle |
| MCR | Mid-Cruise |
| MT | Medium Term |
| NEWAC | NEW Aero engine Core concepts |
| NGV | Nozzle Guide Vane |
| $NO_x$ | Nitrogen oxides |
| OEM | Original Equipment Manufacturer |
| Opt. | Optimisation |
| PERM | Partial Evaporation & Rapid Mixing |
| Ref. | Reference |
| RQL | Rich-burn/Quick-quench/Lean-burn |
| SQP | Sequential Quadratic Programming |
| SR | Short Range |
| TBC | Thermal Barrier Coatings |
| TERA2020 | Techno-economic, Environmental and Risk Assessment for 2020 |
| T-O | Take-Off |
| TBC | Thermal Barrier Coating |
| TOC | Top-Of-Climb |
| TRL | Technology Readiness Level |
| UDF | UnDucted Fan |
| UHBR | Ultra High Bypass Ratio |
| VITAL | enVIronmenTALly Friendly Aero Engines |

# Equation and parameter symbols

| | |
|---|---|
| AFR | Air to Fuel Ratio |
| $BPR$ | Bypass ratio |
| $c$ | Factor |
| dP/Pin | Fractional pressure loss [%] |
| $EINO_x$ | Nitrogen Oxides Emissions Index [g $NO_x$ / kg fuel] |
| $f$ | Performance model residual |
| $FN$ | Engine net thrust [N] |
| $FPR$ | Fan pressure ratio |
| $g$ | Whole system performance parameter |
| $H_{Blade}$ | Blade height [mm] |
| $\dot{m}$ | Mass flow rate [kg/s] |
| $N$ | Shaft rotational speed [rpm] |

| | |
|---|---|
| $N_{46}$ | Low pressure shaft rotational speed [rpm] |
| $n$ | Pressure ratio split exponent |
| $OPR$ | Engine overall pressure ratio |
| $P$ | Total pressure [Pa] |
| | or Performance model component parameter |
| Pol. Eff. | Polytropic efficiency [%] |
| $Q$ | Performance model independent parameter |
| $SFC$ | Engine specific fuel consumption [g/(kN*s)] |
| $SFN$ | Engine specific thrust [m/s] |
| $T$ | Total temperature [K] |
| Tex | Average external surface blade metal temperature [K] |
| $T_m$ | Metal temperature [K] |
| $\mathrm{T}_4$ | Combustor outlet temperature [K] |
| $\mathrm{T}_{41}$ | High Pressure Turbine Rotor Inlet Temperature [K] |
| $V_{id}$ | Jet velocity from full expansion in an ideal [m/s] |
| | convergent-divergent nozzle |
| $W$ | Mass flow [kg/s] |
| $W132Q25$ | Intercooler mass flow ratio |
| $x$ | Performance model independent variable |
| $\Delta$ | Difference |
| $\eta$ | Component efficiency |
| 2 | Fan entry |
| 24 | IPC entry |
| 25 | IPC delivery |
| 26 | HPC entry |
| 3 | HPC delivery |
| 31 | Combustor entry |
| 4 | Combustor delivery |
| 41 | HPT rotor entry |
| 47 | LPT NGV entry |
| 47 | LPT rotor entry |
| 8 | Core nozzle throat |
| 18 | Bypass nozzle throat |
| 132 | Intercooler cold side entry |
| 138 | Intercooler auxiliary nozzle throat |

# Chapter 1

# Introduction

## 1.1 Problem area

Public awareness and political concern over aviation-induced pollution has increased substantially in recent decades, driving policy and technological developments. The Intergovernmental Panel on Climate Change [3] provides a good introduction to the impact of aviation induced emissions on the global atmosphere; the interested reader may refer to the latest synthesis report [4]. In the Vision 2020 report made by the Advisory Council for Aeronautical Research in Europe [5], goals are set to reduce noise and emissions produced by the ever increasing global air traffic. Emissions legislation, set by the International Civil Aviation Organisation (ICAO) and it's Committee on Aviation Environmental Protection (CAEP), is becoming ever more stringent, creating a strong driver for investigating novel aero engine designs that produce less $CO_2$ and $NO_x$ emissions.

On the other hand, airline companies need to continuously reduce their operating costs in order to increase, or at least maintain, their profitability. This introduces an additional design challenge as new aero engine designs need to be conceived for reduced environmental impact as well as direct operating costs. Decision making on optimal engine cycle selection needs to consider mission fuel burn, direct operating costs, engine and airframe noise, pollutant emissions and global warming impact.

$CO_2$ emissions are directly proportional to aircraft fuel burn and one way to minimise the latter is by having engines with reduced Specific Fuel Consumption (SFC) and installations that minimise nacelle drag and weight. Reducing engine weight results in a lower aircraft maximum take-off weight, which in turn leads to reduced thrust requirements for a given aircraft lift to drag ratio. Reducing engine size – predominantly engine nacelle diameter and length – reduces nacelle drag and therefore also leads to reduced thrust requirements. For a given engine

SFC, a reduction in thrust requirements essentially results in lower fuel burn. Significant factors affecting SFC are propulsive efficiency and thermal efficiency; SFC is inversely proportional to both thermal and propulsive efficiency.

## 1.2 Research questions

Propulsive efficiency has been improved by designing turbofan engines with larger fans to give lower specific thrust (net thrust divided by fan inlet mass flow) until increased engine weight and nacelle drag have started to outweigh the benefits. Propulsive efficiency improvements at a constant weight are directly dependent on weight reduction technologies such as light weight fan designs and new shaft materials. Increasing engine bypass ratio aggravates the speed mismatch between the fan and the Low Pressure Turbine (LPT). Introduction of a gearbox can relieve this issue by permitting the design of these two components at their optimal speeds, and can hence reduce engine weight (primarily through the reduced LPT stage count), as well as improve component efficiency. The first research question therefore rises:

***R.Q.1: How low can we really go on specific thrust?***

Thermal efficiency has been improved mainly by increasing the Overall Pressure Ratio (OPR) and High Pressure Turbine (HPT) rotor inlet temperature $T_{41}$ to the extent possible with current materials and design technologies. In more detail, increasing OPR further than current engine designs is hindered by limitations in high pressure compressor delivery temperature at take-off. Increasing $T_{41}$ is limited by maximum permissable HPT rotor metal temperatures at take-off and top of climb. Increasing turbine cooling flows for this purpose is also fairly limited as a strategy; cooling flows essentially represent losses in the thermodynamic cycle, and increasing them eventually leads to severe thermal efficiency deficits [6, 7]. Designing a combustor at very low air to fuel ratio levels is also limited by the need for adequate combustor liner film-cooling air as well as maintaining an acceptable temperature traverse quality [8]. The second research question therefore rises:

***R.Q.2: How high can we really go on OPR and $T_{41}$?***

Although $CO_2$ emissions per passenger-kilometer have been decreasing the same cannot be said for $NO_x$ emissions. Aggressive turbofan designs that reduce $CO_2$ emissions – such as increased OPR and $T_{41}$ designs – can increase the production of $NO_x$ emissions due to higher flame temperatures resulting in less mixing air being available for emissions control. Furthermore, emissions legislation is becoming ever more stringent, creating a strong driver for more environmentally friendly designs. The third research question therefore rises:

> ***R.Q.3: What is the trade-off between low $CO_2$ and $NO_x$ considering the influence of current and future emissions legislation?***

It is a common approach within most gas turbine conceptual design codes to address the decision making problem in a deterministic manner. In reality however, all engineering designs are subject to some level of uncertainty. Accounting for production scatter, measurement uncertainties as well as component performance deterioration early in the design process, and in a computationally efficient manner, can reduce development time and cost, reduce risk, and identify more competitive engine designs. The fourth research question therefore rises:

> ***R.Q.4: How sensitive is an optimal design obtained deterministically to production scatter, component deterioration as well as measurement uncertainty?***

Despite the need for highly qualified experts, gas turbine conceptual design has not been a common study topic in traditional post-graduate curriculums. In fact, the provision of dedicated formal education on multi-disciplinary gas turbine conceptual design to future engineers has been rather rare. Teaching conceptual design as part of a post-graduate curriculum, or as an intensive short course, may help to address the industrial need for engineers with early qualifications on the topic i.e., prior to starting their careers in the company. The fifth research question therefore rises:

> ***R.Q.5: How can gas turbine conceptual design be introduced effectively in traditional post-graduate curriculums?***

Part of the research work presented in this thesis will focus on assessing several novel engine cycles and technologies - currently under research - in relation to the first two research questions raised. These concepts will be evaluated based on their potential to reduce $CO_2$ and $NO_x$ emissions for engine designs entering service between 2020 and 2025. Design constraints, material technology, customer requirements, noise and emissions legislation, technology risk and economic considerations and their effect on optimal concept selection will also be discussed in detail.

The option of an intercooled core geared fan aero engine for long–haul applications will be further assessed by means of a detailed design space exploration. An attempt will be made to identify the fuel burn optimal values for a set of engine design parameters by varying them all simultaneously, as well as in isolation. Different fuel optimal designs will be developed based on different sets of assumptions. The analysis will focus on the following six major design parameters: specific thrust, jet velocity ratio, intercooler effectiveness, intercooler mass flow ratio, pressure ratio split exponent and overall pressure ratio.

With the third research question in mind, the trade-off between the ever-increasing energy efficiency of modern aero-engines and their $NO_x$ performance will be assessed. The analysis will focus on the effect of improving engine thermal and propulsive efficiency on $NO_x$ emissions from traditional and lean-burn combustors. Consideration will be given on current emissions certification legislation and the potential need for it to become more stringent and comprehensive in the future.

Furthermore, some insight will be provided on the potential benefits to be tapped from a transition from the traditional deterministic approach for system analysis to a stochastic (robust design) approach for economic decision-making under uncertainty. The sensitivity of an optimal engine design obtained deterministically will be assessed from a robust design point of view. The impact of production scatter, measurement uncertainties as well as component performance deterioration, on engine performance will be estimated. Focus will be given on the validation of a fast analytical method for estimating key performance parameters. These relate to type-test certification and performance retention guarantees including preliminary estimates of engine production margins.

Finally, the fifth research question set will be explored. Lessons learned will be presented from the integration of different elements of conceptual design in a new BSc course and an existing traditional MSc course on gas turbine technology, as well as an intensive course on gas turbine multi-disciplinary conceptual design.

## 1.3 Research approach

A rather traditional research approach has been followed for the present work as illustrated in Fig. 1.1. In the first stage focus was given on identifying a specific set of scientific and societal needs. Afterwards, the literature in the public domain was reviewed extensively with the aim of framing in detail the current gap in the literature. Particular focus was given on the evolution of aero engine designs, recent European research initiatives on enabling technologies, and different aspects of the pedagogy of gas turbine conceptual design. A number of important research questions were consequently framed – as presented in the section above – focused on engine design targets and the innovative technologies that can help realise them.

A detailed and novel methodology was then established in order to assess the identified technologies in a holistic and consistent manner. This included existing validated tools from past work as well new models and analysis approaches. A

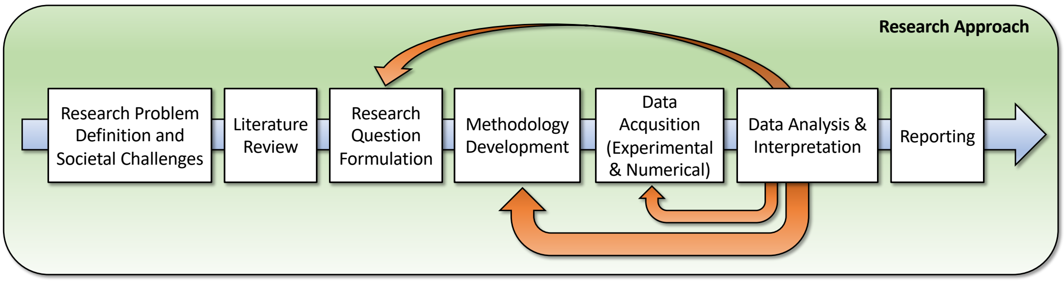


Figure 1.1: Research approach employed in the present thesis.

number of different engine concepts were then developed and the methodology was applied systematically; the methodology was refined in an iterative manner as initial results were generated.

In the next step, the knowledge gained from applying the methodology was generalised and was prepared for presentation in the form of detailed technical analysis, supported by a large number of figures. A further extension of the work was focused on formalising the lessons learned from developing courses on the subject matter of the present thesis. In a final stage, overall conclusions and recommendations for future work were drawn. A key focus has been on identifying the contribution to knowledge stemming from the present work, and providing answers to the research questions set. In parallel to the write-up of the present thesis, the underlying research was presented in a number of peer-reviewed articles.

## 1.4 Publications

The research work presented in the main body of this thesis is based on a foundation built through approximately 60 peer-reviewed journal and conference papers. These works have been published in a collaborative effort with other academic and industrial partners over a period of several years. For practical reasons, a selection has been made based primarily on the following criteria: (i) the work has been carried out by the doctoral candidate as the principal investigator and, (ii) the work has a strong connection to the main theme of this thesis.

The research effort presented is therefore based strictly on material from the following publications:

[1] K.G. Kyprianidis. Future Aero Engine Designs: An Evolving Vision. In Benini, E., editor, *Advances in Gas Turbine Technology*, chapter 1, pages 3–24. InTech, ISBN 978–953–307–611–9, Rijeka, Croatia, November 2011. DOI: 10.5772/19689.

[2] K.G. Kyprianidis, T. Grönstedt, and J.R. Barbosa. Lessons Learned from the

Development of Courses on Gas Turbine Multi-disciplinary Conceptual Design. In *ASME Journal of Engineering for Gas Turbines and Power*, 135(7), July 2013. DOI: 10.1115/1.4023616.

[3] K.G. Kyprianidis, A.M. Rolt, and T. Grönstedt. Multi-disciplinary Analysis of a Geared Fan Intercooled Core Aero-Engine. In *ASME Journal of Engineering for Gas Turbines and Power*, 136(1), January 2014. **ASME IGTI Best Paper Award.** DOI: 10.1115/1.4025244.

[4] K.G. Kyprianidis, and A.M. Rolt. On the Optimisation of a Geared Fan Intercooled Core Engine Design. In *ASME Journal of Engineering for Gas Turbines and Power*, 137(4), April 2015. DOI:10.1115/1.4028544.

[5] K.G. Kyprianidis, C. Gkoudesnes, and W. Camilleri. Gas Turbines for Power and Propulsion. In J. Jan and U. Desideri, editors, Handbook of Clean Energy Systems, Volume 2: Clean Energy Conversion Technologies. chapter 5, pages 825–850. John Wiley & Sons Ltd, ISBN 978–11–189–9197–8, Chichester, United Kingdom, 2015. DOI: 10.1002/9781118991978.hces140

[6] K.G. Kyprianidis, and E. Dahlquist. On the Trade-Off Between Aviation $NO_x$ and Energy Efficiency. In *Applied Energy*, 187(2):1506–1516, January 2017. DOI:10.1016/j.apenergy.2015.12.055.

[7] I. Aslanidou, V. Zaccaria, E. Pontika, N. Zimmerman, A.I. Kalfas, and K.G. Kyprianidis. Teaching Gas Turbine Technology to Undergraduate Students in Sweden. In *ASME TURBO EXPO 2018 Proceedings*, Paper No. GT2018-77074, pp. V006T07A004, Oslo, Norway, June 2018. **ASME IGTI Best Paper Award.** DOI:10.1115/GT2018-77074.

## 1.5 Thesis overview

The main contents of this thesis have been organised in the following chapters:

- In Chapter 2, a short literature review is presented focusing on the evolution of aero engine designs, recent European research initiatives on enabling technologies, and different aspects of the pedagogy of gas turbine conceptual design.
- In Chapter 3, the methodology derived/employed for assessing innovative engine technologies is discussed.
- In Chapter 4, results from the detailed assessment of different engine concepts are presented.
- In Chapter 5, lessons learned from the development of courses on gas turbine conceptual design are presented.
- In Chapter 6, overall conclusions are drawn from the work carried out and recommendations for future work are made.

# Chapter 2

# Literature Review

## 2.1 An evolving vision

Numerous feasibility studies have been published over the years focusing on future engine and aircraft designs that can reduce fuel consumption; a brief review of some of these publications will be carried out here.

One of the earliest discussions on the subject of improving engine fuel efficiency is provided by Gray and Witherspoon [9], looking at conventional and heat exchanged cores, as well as non-steady flow combustion processes and open rotor configurations. A similar study focusing on geared and open rotor arrangements as well as heat exchanged cycles is presented by Hirschkron and Neitzel [10].

An interesting discussion on how specific thrust levels were expected to evolve in the mid-70's based on the economic and technological projections of that time period is given by Jackson [11]; the author has also provided an update to that discussion based on current economical and technological projections [12]. Wilde [13], Young [14], and Pope [15] provide a good reference on how the future for civil turbofan engines for medium and long range applications was envisaged in the late 70's. Some early discussions on future trends in commercial aviation from the aircraft manufacturer's perspective can be found in Swihart [16] and Bates and Morris [17], while Watts [18] provides an airliner's view of the future.

A review on the several technical and economic obstacles that were identified in the late 80's with respect to the realization of the Ultra-High Bypass Ratio (UHBR) turbofan concept is provided by Borradaile [19] and by Zimbrick and Colehour [20]. Peacock and Sadler [21] give an update on the subject, focusing further on engine design constraints and the technology advancements required for producing a competitive UHBR configuration. Potential year 2020 scenarios are explored by Birch [22] while an overview of current aero engine technology and some insight on the future of aircraft propulsion is given by

Ruffles [23]. Sieber [24] and Schimming [25] provide an excellent discussion on counter-rotating fan designs. Finally, for a review on the development of civil propulsion from the early 50's to recent years the interested reader is referred to Saravanamuttoo [26].

The focus of the next section will be given on recent European research initiatives on enabling technologies relevant to the research questions that have been set.

## 2.2 Enabling technologies and recent research

### 2.2.1 Propulsor technologies

Within the EU Framework Program 6 research project VITAL [27] a number of low pressure system component technologies have been investigated [28, 29]. The emerging progress will allow the design of new powerplants capable of providing a step reduction in fuel consumption and generated noise.

The VITAL project concentrated on new technologies for the low pressure system of the engine, which enable the development of low noise and low weight fan architectures for UHBR engines. To achieve these objectives, the VITAL project has investigated three different low pressure configurations, leading to low noise and high efficiency power plants. The three configurations are the DDTF (Direct Drive TurboFan) supported by Rolls-Royce, the GTF (Geared TurboFan) by MTU and the CRTF (Counter-Rotating TurboFan) by Snecma.

The DDTF architecture offers a re-optimised trade-off between fan and turbine requirements considering the low weight technologies introduced by the VITAL programme. The GTF combines a fan with a reduction gear train, to allow different rotating speeds for the fan on one hand, and the booster and turbine on the other. The CRTF offers a configuration with two fans turning in opposite directions, allowing for lower rotational speeds, since the two fan rotors split the loads involved.

The technologies being built into the VITAL engines include [28, 29]:

- New fan concepts with the emphasis on two types: counter-rotating and lightweight fans.
- New booster technologies for different operational requirements; low and high speed, associated aerodynamic technologies, new lightweight materials and associated coating and noise reduction design.
- Polymer composites and corresponding structural design and manufacturing techniques are studied in parallel with advances in metallic materials and manufacturing processes.

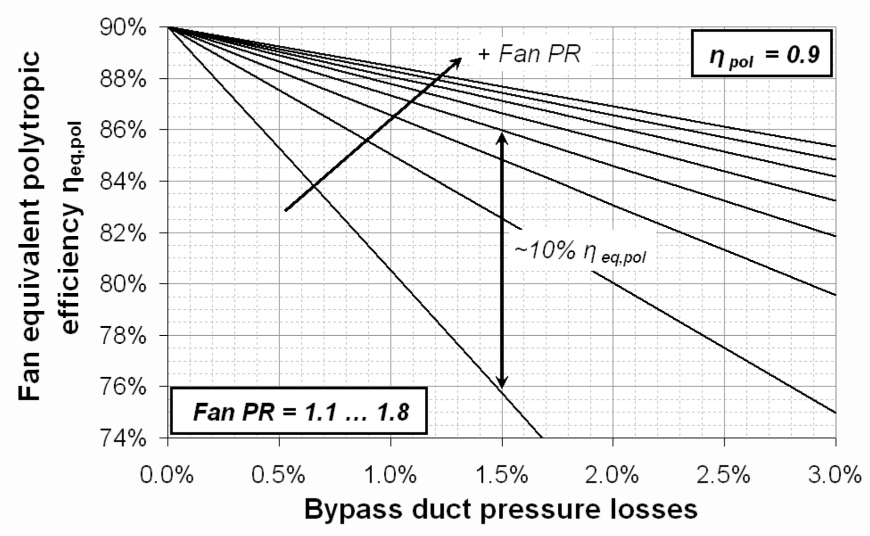


Figure 2.1: Effect of fan tip pressure ratio and bypass duct pressure losses on fan equivalent polytropic efficiency

- Shaft torque density capabilities through the development of metal matrix composites and multi metallic shafts.
- Low pressure turbine weight savings through ultra high lift airfoil design, ultra high stage loading, lightweight materials and design solutions.
- Technologies for light weight and low drag installation of high bypass ratio engines related to nozzle, nacelle and thrust reverser.

For very low specific thrust levels open rotor designs may be considered [2, 30]. The open rotor engine concept, for high subsonic flight speeds, has risen as a candidate for improving fuel consumption on several occasions since the advent of the first high bypass ratio turbofan engine. Such engine configurations, often referred to as propfans in the literature, are direct competitors to ultra high bypass ratio turbofan engines. Their are located at the ultra-low specific thrust region of the design space, where propulsive efficiency benefits for turbofans are negated by very low transfer efficiencies. As illustrated in Fig. 2.1, this is due to the dominant effect on transfer efficiency that bypass duct pressure losses have when looking at low fan tip pressure ratio engine designs, i.e. low specific thrust. Open rotor engines do not suffer from bypass duct pressure losses and can therefore achieve a very high propulsive efficiency at a good level of transfer efficiency. Compared to turbofans, propfans also benefit from reduced nacelle drag and weight penalties.

Several open rotor programs took place during the 80's, resulting in engine demonstrators and flight tests. The purpose of these projects was to develop propfan concepts that could fly efficiently at speeds comparable to high bypass

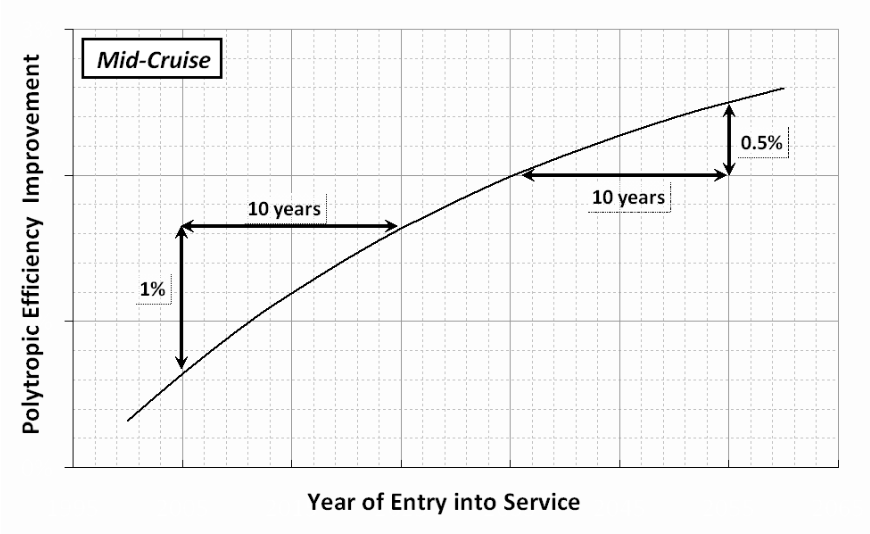


Figure 2.2: Compressor efficiency improvement with year of entry into service.

ratio turbofans, i.e. close to Mach 0.8. General Electric proposed the UDF (Un-Ducted Fan), a pusher configuration with counter-rotating propellers driven by a counter-rotating low pressure turbine [31]. The 578-DX, a pusher configuration with counter-rotating propellers driven by a more conventional low pressure turbine through a differential planetary differential gearbox, was the result of a joint effort by Pratt & Whitney, Hamilton Standard, and Allison.

Both projects were eventually put on hold towards the end of the decade as fuel prices fell significantly. Nevertheless, the open rotor concept has now resurfaced within the EU Framework Program 7 research project DREAM [32] and the Clean Sky Joint Technology Initiative [33]. Within DREAM, the feasibility of two different open rotor architectures is evaluated including noise. Within Clean Sky, research work is being carried out by some of Europe's largest aero engine manufacturers, such as Rolls-Royce and Snecma, focused on designing, building and testing an open rotor demonstrator.

### 2.2.2 Core technologies

Improving core component efficiencies (including reducing losses in the cycle such as duct pressure losses) is one way of improving the engine thermal efficiency. Nevertheless, modern CFD-assisted designs are already quite aggressive and limited benefit may be envisaged by such future advancements [34]; the increasing effort required to improve an already very good axial compressor design is illustrated in Fig.2.2.

Within the EU Framework Program 6 research project NEWAC [35] a number of advanced core component technologies have been investigated that include [36,

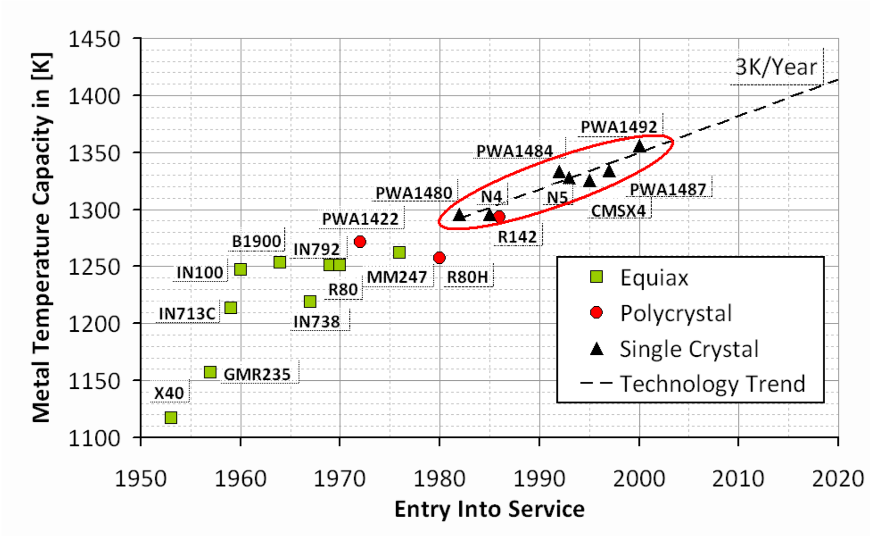


Figure 2.3: Evolution of turbine material capability and future trend.

37]:

- Improved high pressure compressor aero design and blade tip rub management.
- Flow control technologies including aspirated compression systems.
- Active control of surge and tip clearance in compressors.
- Active control of a cooled cooling air system.

As mentioned earlier another way of improving engine thermal efficiency is to raise the cycle OPR. For conventional cores, increasing OPR and $T_4$ depends primarily on future advancements in material and cooling technology. The evolution of turbine material capability over a period of 50 years is illustrated in Fig. 2.3. As can be observed, only mild improvements have been achieved so far and this seems to be a continuing trend; the potential introduction of ceramics would form a major improvement in the field, but substantially more research is still required before realising this. Despite the low improvement rate in turbine material technology (roughly 3 [K/year]) aero engine designs have seen substantial increases in $T_4$ over the last 60 years (roughly 10 [K/year]); this is illustrated in Fig. 2.4 for engines designed for long-haul applications. The main reason behind these improvements in $T_4$ has been the introduction of cooling and Thermal Barrier Coatings (TBC) in turbine designs; the interested reader is referred to Downs and Kenneth [38] for a good overview of the evolution of turbine cooling systems design.

It is perhaps debatable whether an improvement rate of 10 [K/year] in $T_4$ can be maintained in the future, and for that reason the design focus for more aggressive

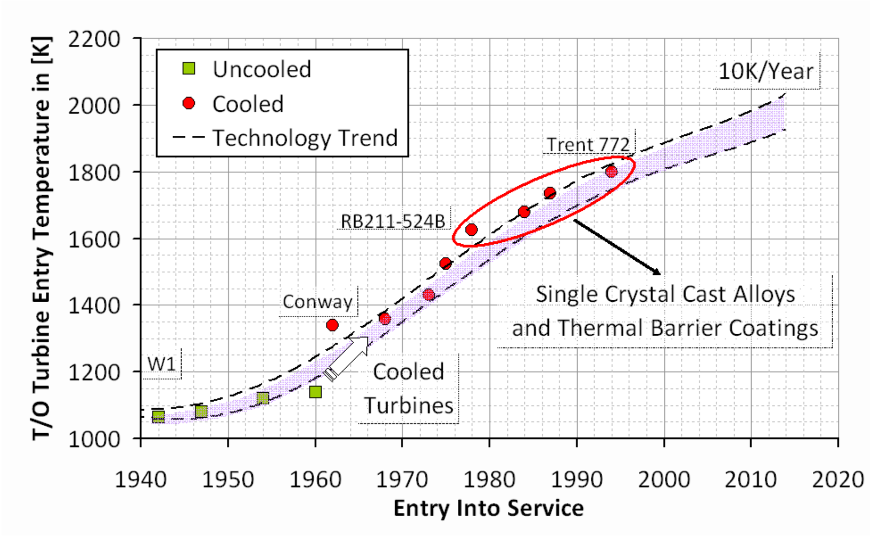


Figure 2.4: Evolution of turbine entry temperature and future trend.

thermal efficiency improvements could very well be redirected to the introduction of heat-exchanged cores and advanced compressor technologies for future turbofan designs. In that respect, some of the technologies researched under the NEWAC project can be perceived as intermediate enabling steps for realising new engine core concepts that could improve the core thermal efficiency. These new core concepts comprise of:

- Ultra-high OPR core with intercooling.
- Medium OPR intercooled recuperated core.
- High OPR flow controlled core.
- High OPR active core including active cooling air cooling.

When considering intercooling for an aero engine design, a common textbook misconception is that the thermal efficiency of an intercooled core will always be lower than a conventional core's for a fixed OPR and specific thrust [39]. The argument behind this is that the heat removed by the intercooler will largely need to be reintroduced in the combustor by burning more fuel, while the reduction in compression work and increase in bypass stream thrust (due to the heat rejection) will only partially compensate for the loss in cycle efficiency, at a fixed specific thrust and $T_4$. Adding the expected intercooler pressure losses in the cycle calculations would further worsen the SFC deficit and make the increase in specific thrust less marked.

However, cycle calculations based on half-ideal gas properties and no dissociation (i.e. isobaric heat capacity dependent on temperature), presented by Walsh and

Fletcher [40], give a slightly different picture on intercooling. For a given $T_4$, the optimal OPR for an intercooled core will be much higher than that for a conventional core. Comparing the two concepts at their optimal OPR levels, for a given technology level, can make the intercooled core more attractive with respect to thermal efficiency and not just specific thrust. Caniére et al. [41] and da Cunha Alves et al. [42] also reached the same conclusion about the thermal efficiency of the intercooled cycle while studying this concept for gas turbines used in power generation.

Papadopoulos and Pilidis [43] worked on the introduction of intercooling, by means of heat pipes, in an aero engine design for long haul applications. Xu et al. [44] performed a mission optimization to assess the potential of a tubular intercooler. Recent work by Xu and Grönstedt [45] presents a refined tubular configuration estimating a potential block fuel benefit of 3.4%. The work addresses the limitation that short high pressure compressor blade lengths and related low compression efficiencies may impose on engines designed for short range missions, and suggest a novel gas path layout as a remedy to this constraint. A design study of a high OPR intercooled aero engine is described in Rolt [46] and Rolt and Baker [47]. Details on the aerodynamic challenges in designing a duct system to transfer the core air into and out of the intercooler are presented by Walker et al. [48]. Overall system performance assessment results are provided in Rolt and Kyprianidis [37].

The introduction of recuperation in an aero engine, for high thermal efficiency at low OPR, has also been the focus of different researchers. Lundbladh and Sjunnesson [49] performed a feasibility study for InterCooled (IC) and Intercooled Recuperated Aero engines (IRA) that consider cycle benefits, weights and direct operating costs. Boggia and Rud [50] provide an extended discussion on the thermodynamic cycle and the technological innovations necessary for realizing the intercooled recuperated core concept. Work by Xu et al. [51, 52] presents insight into specific thermodynamic aspects of the IRA concept, such as variable geometry and hot cooling bleeds, as well as aircraft system level performance considerations. Various aspects of the thermo-mechanical design of a compact heat exchanger have been presented by Pellischek and Kumpf [53] and Schoenenborn et al. [54]. For a comprehensive review on the development activities for recuperated aero engines since the late 60's the interested reader can refer to McDonald et al. [55–57].

A good review on aero engine pollutant emissions, and an introduction to some of the technologies for reducing them, is given by Wulff and Hourmouziadis [58]. Mongia [59], Matthes [60], Lieuwen and Yang [61] and Masiol and Harrison [62] provide a fresh perspective on the topic and a comprehensive summary of the latest technological developments. Three different types of lean-burn combustor technology were researched within NEWAC [36] with the objective of reducing emissions of oxides of nitrogen ($NO_x$):

- Lean Direct Injection (LDI) combustor for high and ultra-high OPR cores.
- Partial Evaporation and Rapid Mixing (PERM) combustor for high OPR cores.
- Lean Premixed Pre-vaporized (LPP) combustor for medium OPR cores.

## 2.3 Robust conceptual design

It can be argued that the current state of the art in multidisciplinary engine simulation tools is represented by an extended suite of tools comprising of: NPSS (Numerical Propulsion System Simulation), WATE (Weight Analysis of Turbine Engines), FLOPS (FLight OPtimization System), and ANOPP (Aircraft Noise Prediction Program). These codes and their integration are discussed in great detail in an array of references spanning several decades [63–69], most recently through the works of Antoine et al. [70] and Mercer et al. [71]. A review of several other conceptual design tools is presented in [1] including an analysis of their individual merits and shortfalls.

One common characteristic of these gas turbine conceptual design codes is that they largely approach the decision making problem in a deterministic manner. Allowance for design uncertainty and life-cycle deterioration is restricted to uncertainty quantification exercises, generally only after an optimal design has been proposed and/or hardware has been built and validated. Some early use of the Monte Carlo simulation method for uncertainty quantification is reported by Abernathy and Sammons [72]. Interesting works in the field include that by Mavris and Roth [73] and Kurzke [74]. A generic probabilistic approach for quantifying the impact of uncertainty, and for allowing for uncertainty-mitigating decisions in the design process, is suggested by Roth and Mavris [75]. A foundation for considering uncertainty and risk in engine technology selection is provided by Roth et al [76].

A common fast alternative to the Monte Carlo, the root-sum-squared method is often utilised in industry for ballpark estimates; its assumption of statistically independent influence factors make it unsuitable for accurate analysis work. Analytical uncertainty propagation methods offer high accuracy at very low computational cost, but their implementation is not straightforward, particularly with legacy codes. The successful use for robust design of advanced propagation methods such as the Univariate Reduced Quadrature (URQ) and the Bivariate Reduced Quadrature (BRQ) techniques is reported by Padulo et al. [77] and Padulo and Liou [77]. Unfortunately the reported use was limited to aircraft system design, not considering propulsion system design.

Overall, none of the works available in the open literature has so far attempted to account for method uncertainty, production scatter and future engine deterioration within the (robust) conceptual design optimization process itself. Doing so in a computationally efficient and integrated manner, could reduce development time, cost and technical risk as well as identify more competitive designs.

# Chapter 3

# Methodology

## 3.1 System modelling

To effectively explore the design space a tool is required that can consider the main disciplines typically encountered in conceptual design. The prediction of engine performance, aircraft design and performance, direct operating costs, and emissions for the concepts analysed in this study was made using the EVA code [78]. Another code, WeiCo [2, 79], was also used for carrying out mechanical and aerodynamic design in order to derive engine component weight and dimensions. The two tools have been integrated together within an optimiser environment [80] as illustrated in Fig. 3.1 with a large amount of information being made available to the user during the design iteration. The integration was based on lessons learned from the development of the TERA2020 tool [81, 82]. This integration allows for multi-objective optimization, design studies, parametric studies, and sensitivity analysis.

### 3.1.1 Engine baseline modelling

The engine models utilised in the present thesis are largely based on the work already presented in [1]. The interested reader is therefore referred to that earlier work for the full implementation details, including code verification and model validation. A short description of the key modelling methods utilised as well as specific improvements made to the respective models are presented below and in Chapter 4.

The baseline engine considered in this work is a three–shaft turbofan engine for long–haul applications, i.e., 70,000lbf thrust, and is assumed to have 1995 as the year of Entry Into Service (EIS). A schematic of the engine performance model is illustrated in Fig. 3.2. Along with the full flight mission profile three major

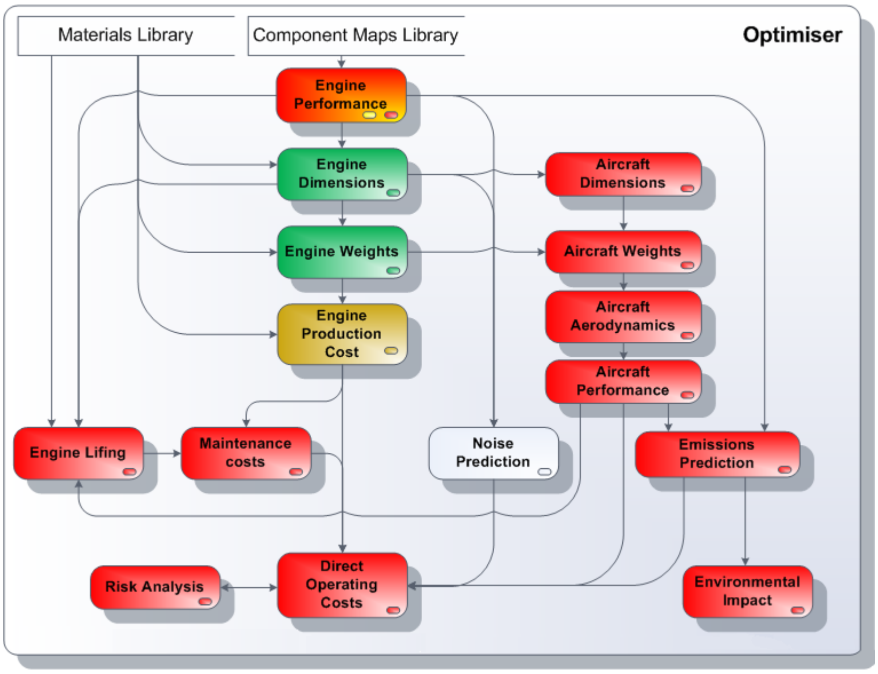


Figure 3.1: Conceptual design tool algorithm [1].

engine operating points were considered: Hot–Day Top–of–Climb (HD TOC), End–Of–Runway Hot–Day Take–Off (EOR HD TO), and ISA Mid–Cruise (ISA MCR).

Engine performance modelling was primarily based on the use of generic compressor and turbine characteristics as well as empirical correlations [40]. All thermodynamic calculations were based on the assumption of an ideal gas (i.e., variable specific heat capacity); therefore, the main thermodynamic equation used was the Gibbs equation. The HPT Thermal Barrier Coating (TBC) average external surface blade metal temperature and corresponding cooling flows have been modelled using the simplified approach presented in [83]. The correlations presented in [1,84] were used for estimating the $NO_x$ emissions of future aero-engine designs incorporating modern Rich-burn Quick-quench Lean-burn (RQL) and lean-burn combustor technology.

The engine turbomachinery (including discs and casings), the intercooler and the nacelle are major contributors to the powerplant weight. The assessment of the dimensions and weight of the turbomachinery components was based on a mean line design approach very similar to the one described in [65]. However, many design factors, such as the flow coefficient, stage loading factor, etc., were updated to better capture trends in modern gas turbines. The size and weight of the intercooler were mainly determined through surface-area requirements. They were in turn determined by the heat transfer coefficients on internal and external surfaces presented in [85].

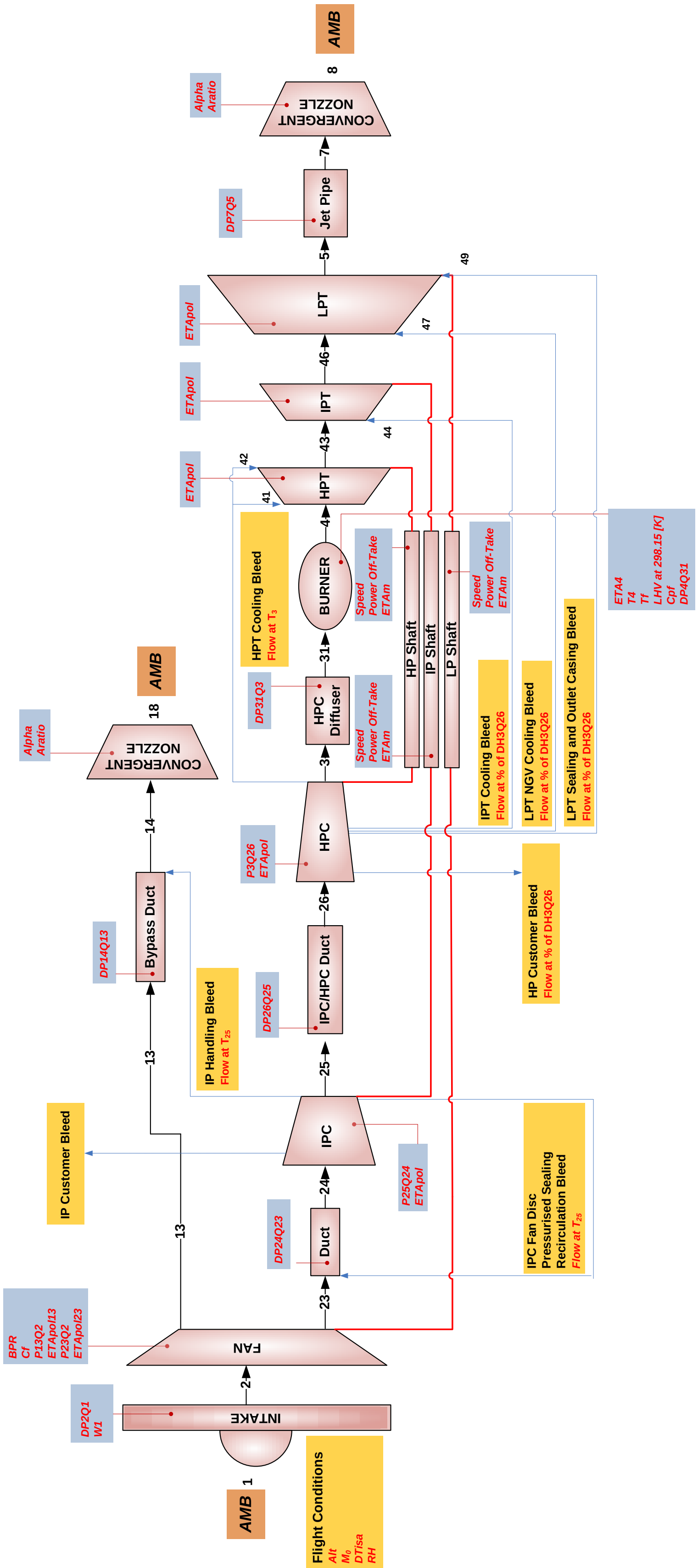


Figure 3.2: Performance model of the 3-shaft turbofan configuration.

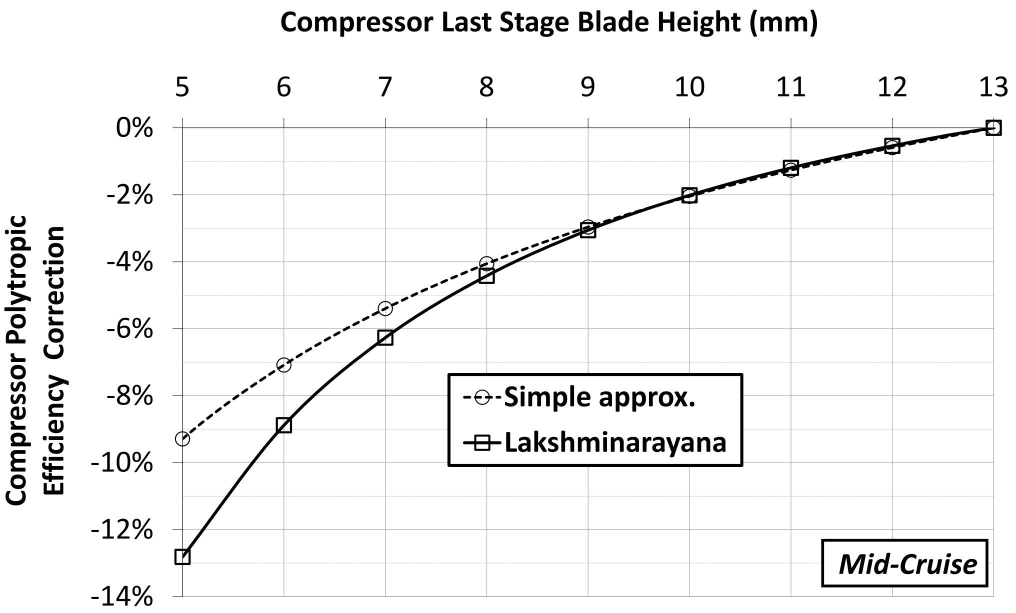


Figure 3.3: Compressor polytropic efficiency correction vs. last stage blade height.

Engine designs of very high overall pressure ratio and relative small core flow can suffer from increased tip leakage losses due to very low High Pressure Compressor (HPC) last stage blade heights. A correction needs to be applied on the HPC polytropic efficiency levels assumed to cater for this effect. An efficiency correction based on author experience is proposed in the present work and has been set up as a simple exponential function of HPC last stage blade height as shown in Eq. (3.1).

$$\Delta\eta_{HPC} = 0.12 \cdot \left(1 - \left(\frac{1}{\left(\frac{H_{blade,HPC}}{13}\right)^{0.6}}\right)\right) \tag{3.1}$$

A comparison against the detailed method suggested in [86] is illustrated in Fig. 3.3. The proposed empirical approximation follows reasonably well the more complex method for blades above 9 mm and can therefore be considered suitable for the purposes of gas turbine conceptual design.

The correction has been applied in three steps:

1. A correction to the HPC polytropic efficiency is determined based on the calculated last stage blade height.
2. The component efficiency correction is converted to a specific fuel consump-

tion and business case block fuel correction using appropriate exchange rates.

3. The block fuel correction is applied to the business case figure that has been calculated using the rubberised-wing aircraft model.

### 3.1.2 Engine parameter definitions

The definitions of jet velocity ratio and specific thrust for a conventional turbofan engine are given in Eq. (3.2) and Eq. (3.3), respectively. For an intercooled turbofan configuration the author has worked with the definition given in Eq. (3.4) which uses a mass-averaged jet velocity for the intercooler and bypass nozzle. It should be noted that although engine thrusts have been calculated using estimates of real nozzle performance, the "jet velocity ratio" parameter is calculated assuming full expansion of each stream as in an ideal convergent-divergent nozzle.

$$\frac{V_{cold}}{V_{hot}} = \frac{V_{id,18}}{V_{id,8}} \tag{3.2}$$

$$SFN = \left(\frac{FN}{W_2}\right), \qquad [\mathrm{m\,s^{-1}}] \tag{3.3}$$

$$\frac{V_{cold}}{V_{hot}} = \frac{(\dot{m}_{18}V_{id,18}) + (\dot{m}_{138}V_{id,138})}{(\dot{m}_{18} + \dot{m}_{138})} \cdot \frac{1}{V_{id,8}} \tag{3.4}$$

The definition of intercooler mass flow ratio is provided in Eq. (3.5).

$$W132Q25 = \left(\frac{\dot{m}_{132}}{\dot{m}_{25}}\right) \tag{3.5}$$

The definition of OPR is provided in Eq. (3.6).

$$OPR = \left(\frac{P_3}{P_2}\right) \tag{3.6}$$

The definition of the pressure ratio split exponent is provided in Eq. (3.7) while Fig. 3.4 illustrates the relationship between IPC and HPC pressure ratios and pressure ratio split exponent at different overall pressure ratio levels.

$$n = \log_{OPR}\left(\frac{P_{25}}{P_2}\right) \tag{3.7}$$

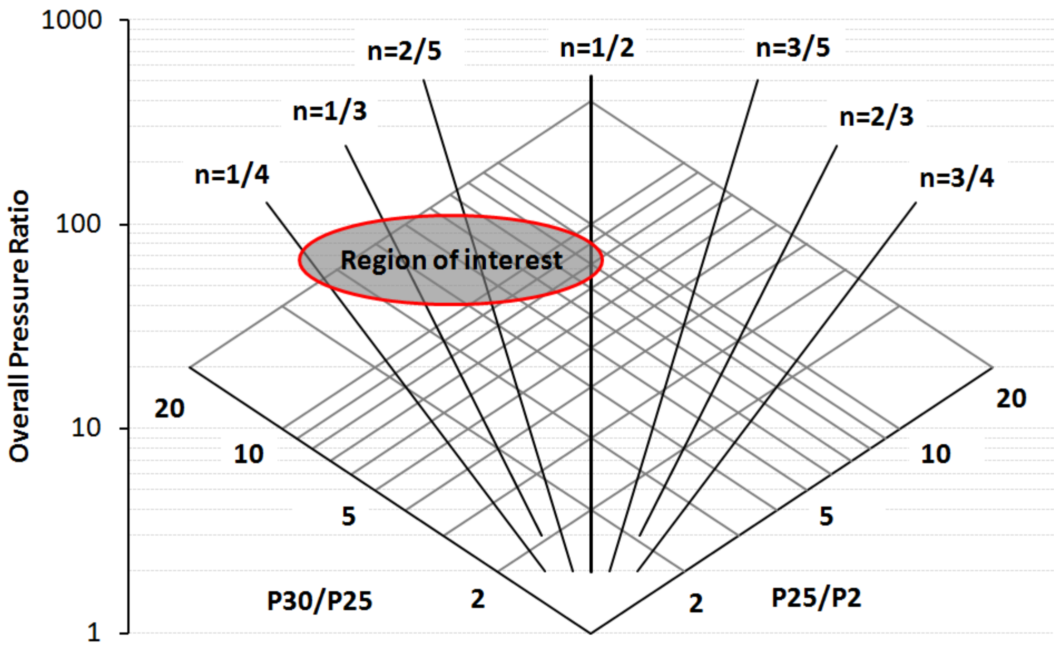


Figure 3.4: OPR vs pressure ratio split exponent.

Core efficiency is defined in this thesis as the ratio of the useful energy at the core exit divided by the fuel heat input. Transfer efficiency is defined as the ratio of the summation of useful energy at each nozzle exit divided by the useful energy at the core exit. Core exit is defined as the position in the LPT expansion process at which the Intermediate Pressure Compressor (IPC) and fan root power requirements have been satisfied while useful energy refers to the kinetic energy of the flow following an ideal full expansion to ambient pressure. Thermal efficiency is defined as the product of core and transfer efficiency while overall efficiency as the product of propulsive and thermal efficiency i.e., the ratio of propulsive power divided by the fuel heat input. These turbofan engine efficiency definitions are provided in Eq. (3.8) to Eq. (3.14), and are illustrated in Fig. 3.5.

$$\dot{E}_{kin,id,out} = \dot{E}_{kin,cold,id,out} - \dot{E}_{kin,hot,id,out}, \qquad [\mathrm{J\,s^{-1}}] \tag{3.8}$$

$$\dot{E}_{kin,cold,id,out} = \dot{m}_{cold,out} \cdot \frac{C^2_{cold,id,out}}{2}, \qquad [\mathrm{J\,s^{-1}}] \tag{3.9}$$

$$\dot{E}_{kin,hot,id,out} = \dot{m}_{hot,out} \cdot \frac{C^2_{hot,id,out}}{2}, \qquad [\mathrm{J\,s^{-1}}] \tag{3.10}$$

$$\dot{E}_{core,id} = \dot{E}_{core,id,out} - \dot{E}_{core,in}, \qquad [\mathrm{J\,s^{-1}}] \tag{3.11}$$

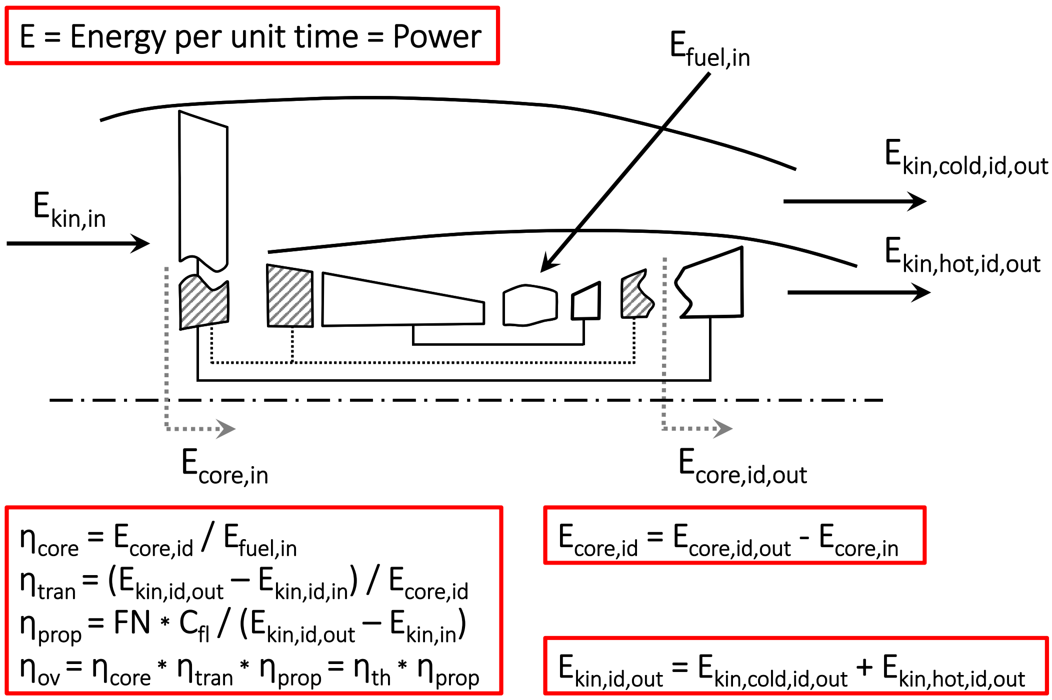


Figure 3.5: Turbofan engine efficiency definitions.

$$\dot{E}_{core,id,out} = \dot{m}_{core,out} \cdot \frac{C^2_{core,id,out}}{2}, \qquad [\mathrm{J\,s^{-1}}] \tag{3.12}$$

$$\dot{E}_{core,in} = \dot{m}_{core,in} \cdot \frac{C^2_{fl}}{2}, \qquad [\mathrm{J\,s^{-1}}] \tag{3.13}$$

$$\dot{E}_{kin,in} = \dot{m}_{in} \cdot \frac{C^2_{fl}}{2}, \qquad [\mathrm{J\,s^{-1}}] \tag{3.14}$$

For more details on performance parameters that have not been defined explicitly in this thesis - such as engine bypass ratio - the reader is referred to [40].

### 3.1.3 Engine multi-point synthesis

An engine steady-state performance model comprises:

1. A large number of equations that describe the performance of each engine component, and
2. A set of governing equations that describe the interactions between different

components.

The latter are derived using a set of compatibility requirements such as energy and mass flow balances, as described in [87]. For a generic engine configuration, the mathematical description of the steady-state performance model will comprise a square matrix of $n$ non-linear equations and $n$ unknowns, as described by Eq. (3.15).

$$\begin{aligned} f_1\left(x_1, ..., x_n, P_1, ..., P_m, Q_1, ..., Q_l\right) &= 0 \\ f_2\left(x_1, ..., x_n, P_1, ..., P_m, Q_1, ..., Q_l\right) &= 0 \\ &\vdots \\ f_n\left(x_1, ..., x_n, P_1, ..., P_m, Q_1, ..., Q_l\right) &= 0 \end{aligned} \tag{3.15}$$

In the present work, the necessary independent variables and residuals were selected automatically by the code to formulate the model's mathematical description as given in Table 3.1. The independent variables $x_1, x_2, ..., x_n$ are iterated until all residuals $f_1, f_2, ..., f_n$ reach a value sufficiently close to zero, typically around $10^{-7}$ or less depending on the convergence criteria set. When the mathematical model has converged for a specific engine operating condition a set of $k$ dependent whole system performance parameters $g_1, g_2, ..., g_k$ will have been determined.

The independent parameters $Q_1, Q_2, ..., Q_l$ are boundary conditions (such as altitude, flight Mach number etc.) and can be considered as "input" to the mathematical model. Every engine operating point will have a dedicated set of $\boldsymbol{Q}$ vector values that are needed as "input" to solve the steady-state performance model.

The parameters $P_1, P_2, ..., P_m$ are component performance parameters such as compressor and turbine pressure ratio, burner and duct pressure losses etc. They can be considered as independent parameters and "input" to the mathematical model only for one engine operating condition, the reference point, often termed the "engine design point" in the open literature. All nozzle throat areas as well as the scaling factors of the component characteristics used will be determined at that reference or design point, based on the procedure outlined in [88]. All nozzle throat areas as well as the scaling factors will consequently be fixed for all other engine steady-state operating points. The parameters $P_1, P_2, ..., P_m$ can therefore be considered as dependent parameters for all other engine steady-state operating points - apart from the design point - and therefore part of the $\boldsymbol{g}$ vector.

In the present work, the hot-day top of climb condition was chosen as the reference or design point. This particular choice for the reference condition is consistent with the modelling work presented in [89]. For the baseline engine

Table 3.1: Mathematical model for the three-shaft turbofan engine.

| Engine component | Independent variable $x_i$ | Residual $f_i$ | Engine control parameter |
|---|---|---|---|
| Low pressure shaft | Rotational speed | Work balance | |
| Intermediate pressure shaft | Rotational speed | Work balance | |
| High pressure shaft | Rotational speed | Work balance | |
| Intake | Inlet corrected mass flow | | |
| Fan | Root map beta | Root mass flow balance | |
| | Tip map beta | Tip mass flow balance | |
| | Bypass ratio | | |
| Fan disc pressurised sealing bleed | Mass flow | Mass flow balance | |
| (recirculating flow) | Temperature | Temperature balance | |
| Intermediate pressure compressor | Map beta | Mass flow balance | |
| High pressure compressor | Map beta | Mass flow balance | |
| Burner | Fuel flow | | |
| High pressure turbine | Map beta | Mass flow balance | |
| Intermediate pressure turbine | Map beta | Mass flow balance | |
| Low pressure turbine | Map beta | Mass flow balance | |
| Core nozzle | | Mass flow balance | |
| Bypass nozzle | | Mass flow balance | |
| Performance monitor | | Net thrust balance | Net thrust |
| Total | 15 | 15 | 1 |

| Key engine parameters | Units | Hot-day top-of-climb conditions (ISA+10, FL350, Mach 0.82) | Hot-day end-of-runway take-off conditions (ISA+15, FL0, Mach 0.25) | Mid-cruise conditions (ISA, FL350, Mach 0.82) |
|---|---|---|---|---|
| Specific thrust | m/s | Out of the wash | Out of the wash | Out of the wash |
| Jet velocity ratio | - | Out of the wash | Out of the wash | Out of the wash |
| Pressure ratio split exponent | - | Out of the wash | Out of the wash | Out of the wash |
| Fan tip over hub pressure rise ratio | - | Out of the wash | Out of the wash | Out of the wash |
| Overall pressure ratio | - | Out of the wash | Out of the wash | Out of the wash |
| HPC outlet temperature | K | Out of the wash | Out of the wash | Out of the wash |
| HPT NGV TBC metal temperature | K | Out of the wash | Out of the wash | Out of the wash |
| HPT rotor TBC metal temperature | K | Out of the wash | Out of the wash | Out of the wash |
| IPT NGV TBC metal temperature | K | Out of the wash | Out of the wash | Out of the wash |
| IPT rotor TBC metal temperature | K | Out of the wash | Out of the wash | Out of the wash |
| IPT cooling flow mixing pressure ratio | - | Out of the wash | Out of the wash | Out of the wash |
| LPT NGV TBC metal temperature | K | Out of the wash | Out of the wash | Out of the wash |
| LPT NGV cooling flow mixing pressure ratio | - | Out of the wash | Out of the wash | Out of the wash |
| Combustor outlet temperature | K | Out of the wash | Out of the wash | Out of the wash |
| Thrust | kN | **Target 1** | **Target 1** | **Target 1** |
| Engine inlet mass flow | kg/s | **User Input** | Out of the wash | Out of the wash |
| Fan tip pressure ratio | - | **User Input** | Out of the wash | Out of the wash |
| Bypass ratio | - | **User Input** | Out of the wash | Out of the wash |
| Fan root pressure ratio | - | **User Input** | Out of the wash | Out of the wash |
| IPC pressure ratio | - | **User Input** | Out of the wash | Out of the wash |
| HPC pressure ratio | - | **User Input** | Out of the wash | Out of the wash |
| HPT NGV cooling flow (% HPC flow) | % | **User Input** | same as @ToC | same as @ToC |
| HPT rotor cooling flow (% HPC flow) | % | **User Input** | same as @ToC | same as @ToC |
| IPT NGV cooling flow (% HPC flow) | % | **User Input** | same as @ToC | same as @ToC |
| IPT rotor cooling flow (% HPC flow) | % | **User Input** | same as @ToC | same as @ToC |
| IPT cooling flow extraction point (% HPC enthalpy rise) | % | **User Input** | same as @ToC | same as @ToC |
| LPT NGV cooling flow (% HPC flow) | % | **User Input** | same as @ToC | same as @ToC |
| LPT NGV cooling flow extraction point (% HPC enthalpy rise) | % | **User Input** | same as @ToC | same as @ToC |
| LPT sealing flow (% HPC flow) | % | **User Input** | same as @ToC | same as @ToC |
| Fan disc pressurised sealing flow (% IPC flow) | % | **User Input** | same as @ToC | same as @ToC |
| Combustor fuel flow | kg/s | **Variable 1** | **Variable 1** | **Variable 1** |
| Core nozzle area | m2 | Out of the wash | Out of the wash | Out of the wash |
| Bypass nozzle area | m2 | Out of the wash | Out of the wash | Out of the wash |
| Core inlet mass flow | kg/s | Out of the wash | Out of the wash | Out of the wash |
| High pressure turbine rotor inlet temperature | K | Out of the wash | Out of the wash | Out of the wash |
| Fan tip polytropic efficiency | % | **User Input** | Out of the wash | Out of the wash |
| Fan root polytropic efficiency | % | **User Input** | Out of the wash | Out of the wash |
| IPC polytropic efficiency | % | **User Input** | Out of the wash | Out of the wash |
| HPC polytropic efficiency | % | **User Input** | Out of the wash | Out of the wash |
| HPT polytropic efficiency | % | **User Input** | Out of the wash | Out of the wash |
| IPT polytropic efficiency | % | **User Input** | Out of the wash | Out of the wash |
| LPT polytropic efficiency | % | **User Input** | Out of the wash | Out of the wash |
| Engine intake pressure loss dP/P | % | **User Input** | Out of the wash | Out of the wash |
| IPC inlet duct pressure loss dP/P | % | **User Input** | Out of the wash | Out of the wash |
| IPC/HPC intercompressor duct pressure loss dP/P | % | **User Input** | Out of the wash | Out of the wash |
| HPC outlet diffuser pressure loss dP/P | % | **User Input** | Out of the wash | Out of the wash |
| HPT/IPT interturbine duct pressure loss dP/P | % | **User Input** | Out of the wash | Out of the wash |
| IPT/LPT interturbine duct pressure loss dP/P | % | **User Input** | Out of the wash | Out of the wash |
| Combustor pressure loss dP/P | % | **User Input** | Out of the wash | Out of the wash |
| Jet pipe pressure loss dP/P | % | **User Input** | Out of the wash | Out of the wash |
| Bypass duct pressure loss dP/P | % | **User Input** | Out of the wash | Out of the wash |
| Bypass nozzle thrust coefficient | % | **User Input** | Out of the wash | Out of the wash |
| Core nozzle thrust coeffficient | % | **User Input** | Out of the wash | Out of the wash |
| HP shaft mechanical efficiency | % | **User Input** | Out of the wash | Out of the wash |
| IP shaft mechanical efficiency | % | **User Input** | Out of the wash | Out of the wash |
| LP shaft mechanical efficiency | % | **User Input** | Out of the wash | Out of the wash |

Figure 3.6: Baseline matching scheme for 3-shaft turbofan.

| Key engine parameters | Units | Hot-day top-of-climb conditions (ISA+10, FL350, Mach 0.82) | Hot-day end-of-runway take-off conditions (ISA+15, FL0, Mach 0.25) | Mid-cruise conditions (ISA, FL350, Mach 0.82) |
|---|---|---|---|---|
| Specific thrust | m/s | **Target 2** | Out of the wash | Out of the wash |
| Jet velocity ratio | - | **Target 3** | Out of the wash | Out of the wash |
| Pressure ratio split exponent | - | **Target 5** | Out of the wash | Out of the wash |
| Fan tip over hub pressure rise ratio | - | **Target 4** | Out of the wash | Out of the wash |
| Overall pressure ratio | - | **Target 6** | Out of the wash | Out of the wash |
| HPC outlet temperature | K | Out of the wash | Out of the wash | Out of the wash |
| HPT NGV TBC metal temperature | K | **Target 7** | Out of the wash | Out of the wash |
| HPT rotor TBC metal temperature | K | **Target 8** | Out of the wash | Out of the wash |
| IPT NGV TBC metal temperature | K | **Target 9** | Out of the wash | Out of the wash |
| IPT rotor TBC metal temperature | K | **Target 10** | Out of the wash | Out of the wash |
| IPT cooling flow mixing pressure ratio | - | **Target 11** | Out of the wash | Out of the wash |
| LPT NGV TBC metal temperature | K | **Target 12** | Out of the wash | Out of the wash |
| LPT cooling flow mixing pressure ratio | - | **Target 13** | Out of the wash | Out of the wash |
| Combustor outlet temperature | K | **Target 14** | Out of the wash | Out of the wash |
| Thrust | kN | **Target 1** | **Target 1** | **Target 1** |
| Engine inlet mass flow | kg/s | **Variable 1** | Out of the wash | Out of the wash |
| Fan tip pressure ratio | - | **Variable 2** | Out of the wash | Out of the wash |
| Bypass ratio | - | **Variable 3** | Out of the wash | Out of the wash |
| Fan root pressure ratio | - | **Variable 4** | Out of the wash | Out of the wash |
| IPC pressure ratio | - | **Variable 5** | Out of the wash | Out of the wash |
| HPC pressure ratio | - | **Variable 6** | Out of the wash | Out of the wash |
| HPT NGV cooling flow (% HPC flow) | % | **Variable 7** | same as @ToC | same as @ToC |
| HPT rotor cooling flow (% HPC flow) | % | **Variable 8** | same as @ToC | same as @ToC |
| IPT NGV cooling flow (% HPC flow) | % | **Variable 9** | same as @ToC | same as @ToC |
| IPT rotor cooling flow (% HPC flow) | % | **Variable 10** | same as @ToC | same as @ToC |
| IPT cooling flow extraction point (% HPC enthalpy rise) | % | **Variable 11** | same as @ToC | same as @ToC |
| LPT NGV cooling flow (% HPC flow) | % | **Variable 12** | same as @ToC | same as @ToC |
| LPT NGV cooling flow extraction point (% HPC enthalpy rise) | % | **Variable 13** | same as @ToC | same as @ToC |
| LPT sealing flow (% HPC flow) | % | **User Input** | same as @ToC | same as @ToC |
| Fan disc pressurised sealing flow (% IPC flow) | % | **User Input** | same as @ToC | same as @ToC |
| Combustor fuel flow | kg/s | **Variable 14** | **Variable 1** | **Variable 1** |
| Core nozzle area | m2 | Out of the wash | Out of the wash | Out of the wash |
| Bypass nozzle area | m2 | Out of the wash | Out of the wash | Out of the wash |
| Core inlet mass flow | kg/s | Out of the wash | Out of the wash | Out of the wash |
| High pressure turbine rotor inlet temperature | K | Out of the wash | Out of the wash | Out of the wash |
| Fan tip polytropic efficiency | % | **User Input** | Out of the wash | Out of the wash |
| Fan root polytropic efficiency | % | **User Input** | Out of the wash | Out of the wash |
| IPC polytropic efficiency | % | **User Input** | Out of the wash | Out of the wash |
| HPC polytropic efficiency | % | **User Input** | Out of the wash | Out of the wash |
| HPT polytropic efficiency | % | **User Input** | Out of the wash | Out of the wash |
| IPT polytropic efficiency | % | **User Input** | Out of the wash | Out of the wash |
| LPT polytropic efficiency | % | **User Input** | Out of the wash | Out of the wash |
| Engine intake pressure loss dP/P | % | **User Input** | Out of the wash | Out of the wash |
| IPC inlet duct pressure loss dP/P | % | **User Input** | Out of the wash | Out of the wash |
| IPC/HPC intercompressor duct pressure loss dP/P | % | **User Input** | Out of the wash | Out of the wash |
| HPC outlet diffuser pressure loss dP/P | % | **User Input** | Out of the wash | Out of the wash |
| HPT/IPT interturbine duct pressure loss dP/P | % | **User Input** | Out of the wash | Out of the wash |
| IPT/LPT interturbine duct pressure loss dP/P | % | **User Input** | Out of the wash | Out of the wash |
| Combustor pressure loss dP/P | % | **User Input** | Out of the wash | Out of the wash |
| Jet pipe pressure loss dP/P | % | **User Input** | Out of the wash | Out of the wash |
| Bypass duct pressure loss dP/P | % | **User Input** | Out of the wash | Out of the wash |
| Bypass nozzle thrust coefficient | % | **User Input** | Out of the wash | Out of the wash |
| Core nozzle thrust coeffficient | % | **User Input** | Out of the wash | Out of the wash |
| HP shaft mechanical efficiency | % | **User Input** | Out of the wash | Out of the wash |
| IP shaft mechanical efficiency | % | **User Input** | Out of the wash | Out of the wash |
| LP shaft mechanical efficiency | % | **User Input** | Out of the wash | Out of the wash |

Figure 3.7: Reference-point matching scheme for 3-shaft turbofan.

| **Key engine parameters** | **Units** | **Hot-day top-of-climb conditions (ISA+10, FL350, Mach 0.82)** | **Hot-day end-of-runway take-off conditions (ISA+15, FL0, Mach 0.25)** | **Mid-cruise conditions (ISA, FL350, Mach 0.82)** |
|---|---|---|---|---|
| Specific thrust | m/s | Out of the wash | Out of the wash | **Synthesis Target 1** |
| Jet velocity ratio | - | Out of the wash | Out of the wash | **Synthesis Target 2** |
| Pressure ratio split exponent | - | Out of the wash | Out of the wash | **Synthesis Target 4** |
| Fan tip over hub pressure rise ratio | - | Out of the wash | Out of the wash | **Synthesis Target 3** |
| Overall pressure ratio | - | Out of the wash | Out of the wash | **Synthesis Target 5** |
| HPC outlet temperature | K | Out of the wash | Out of the wash | Out of the wash |
| HPT NGV TBC metal temperature | K | Out of the wash | **Synthesis Target 6** | Out of the wash |
| HPT rotor TBC metal temperature | K | Out of the wash | **Synthesis Target 7** | Out of the wash |
| IPT NGV TBC metal temperature | K | Out of the wash | **Synthesis Target 8** | Out of the wash |
| IPT rotor TBC metal temperature | K | Out of the wash | **Synthesis Target 9** | Out of the wash |
| IPT cooling flow mixing pressure ratio | - | Out of the wash | **Synthesis Target 10** | Out of the wash |
| LPT NGV TBC metal temperature | K | Out of the wash | **Synthesis Target 11** | Out of the wash |
| LPT NGV cooling flow mixing pressure ratio | - | Out of the wash | **Synthesis Target 12** | Out of the wash |
| Combustor outlet temperature | K | Out of the wash | Out of the wash | **Synthesis Target 13** |
| Thrust | kN | **Target** | **Target** | **Target** |
| Engine inlet mass flow | kg/s | **Synthesis Variable 1** | Out of the wash | **Out of the wash †** |
| Fan tip pressure ratio | - | **Variable** | Out of the wash | Out of the wash |
| Bypass ratio | - | **Synthesis Variable 2** | Out of the wash | **Out of the wash †** |
| Fan root pressure ratio | - | **Synthesis Variable 3** | Out of the wash | **Out of the wash †** |
| IPC pressure ratio | - | **Synthesis Variable 4** | Out of the wash | **Out of the wash †** |
| HPC pressure ratio | - | **Synthesis Variable 5** | Out of the wash | **Out of the wash †** |
| HPT NGV cooling flow (% HPC flow) | % | **Synthesis Variable 6** | **same as @ToC †** | same as @ToC |
| HPT rotor cooling flow (% HPC flow) | % | **Synthesis Variable 7** | **same as @ToC †** | same as @ToC |
| IPT NGV cooling flow (% HPC flow) | % | **Synthesis Variable 8** | **same as @ToC †** | same as @ToC |
| IPT rotor cooling flow (% HPC flow) | % | **Synthesis Variable 9** | **same as @ToC †** | same as @ToC |
| IPT cooling flow extraction point (% HPC enthalpy rise) | % | **Synthesis Variable 10** | **same as @ToC †** | same as @ToC |
| LPT NGV cooling flow (% HPC flow) | % | **Synthesis Variable 11** | **same as @ToC †** | same as @ToC |
| LPT NGV cooling flow extraction point (% HPC enthalpy | % | **Synthesis Variable 12** | **same as @ToC †** | same as @ToC |
| LPT sealing flow (% HPC flow) | % | **User Input** | same as @ToC | same as @ToC |
| Fan disc pressurised sealing flow (% IPC flow) | % | **User Input** | same as @ToC | same as @ToC |
| Combustor fuel flow | kg/s | **Synthesis Variable 13** | **Variable** | **Variable** |
| Core nozzle area | m2 | Out of the wash | Out of the wash | Out of the wash |
| Bypass nozzle area | m2 | Out of the wash | Out of the wash | Out of the wash |
| Core inlet mass flow | kg/s | Out of the wash | Out of the wash | Out of the wash |
| High pressure turbine rotor inlet temperature | K | Out of the wash | Out of the wash | Out of the wash |
| Fan tip polytropic efficiency | % | **User Input** | Out of the wash | Out of the wash |
| Fan root polytropic efficiency | % | **User Input** | Out of the wash | Out of the wash |
| IPC polytropic efficiency | % | **User Input** | Out of the wash | Out of the wash |
| HPC polytropic efficiency | % | **User Input** | Out of the wash | Out of the wash |
| HPT polytropic efficiency | % | **User Input** | Out of the wash | Out of the wash |
| IPT polytropic efficiency | % | **User Input** | Out of the wash | Out of the wash |
| LPT polytropic efficiency | % | **User Input** | Out of the wash | Out of the wash |
| Engine intake pressure loss dP/P | % | **User Input** | Out of the wash | Out of the wash |
| IPC inlet duct pressure loss dP/P | % | **User Input** | Out of the wash | Out of the wash |
| IPC/HPC intercompressor duct pressure loss dP/P | % | **User Input** | Out of the wash | Out of the wash |
| HPC outlet diffuser pressure loss dP/P | % | **User Input** | Out of the wash | Out of the wash |
| HPT/IPT interturbine duct pressure loss dP/P | % | **User Input** | Out of the wash | Out of the wash |
| IPT/LPT interturbine duct pressure loss dP/P | % | **User Input** | Out of the wash | Out of the wash |
| Combustor pressure loss dP/P | % | **User Input** | Out of the wash | Out of the wash |
| Jet pipe pressure loss dP/P | % | **User Input** | Out of the wash | Out of the wash |
| Bypass duct pressure loss dP/P | % | **User Input** | Out of the wash | Out of the wash |
| Bypass nozzle thrust coefficient | % | **User Input** | Out of the wash | Out of the wash |
| Core nozzle thrust coeffficient | % | **User Input** | Out of the wash | Out of the wash |
| HP shaft mechanical efficiency | % | **User Input** | Out of the wash | Out of the wash |
| IP shaft mechanical efficiency | % | **User Input** | Out of the wash | Out of the wash |
| LP shaft mechanical efficiency | % | **User Input** | Out of the wash | Out of the wash |

***† Varied as needed for convergence of synthesis target using corresponding synthesis variable at top-of-climb condition***

Figure 3.8: Multi-point synthesis matching scheme for 3-shaft turbofan.

configuration considered in the present study, the mathematical model could therefore be described by Fig. 3.6, in addition to Table 3.1).

In gas turbine conceptual design however, it is important that cycle parameters such as compressor pressure ratio, bypass ratio, cooling flow etc. are at their optimal values. The traditional approach is to therefore vary some of the independent parameters $P_1, P_2, ..., P_m$ at the reference condition in order to satisfy an equal number of specific performance targets and/or constraints at the same condition. The mathematical model is therefore modified in this case in accordance with Fig. 3.7.

An extension to the reference-point-based matching scheme for cycle design is proposed in this thesis. The key idea is to match the cycle not only at the reference condition but at multiple operating points, an approach that will be termed "multi-point synthesis" in the present work. In this approach some of the independent parameters $P_1, P_2, ..., P_m$ will be varied at the reference condition in order to satisfy an equal number of specific performance targets and/or constraints at other operating conditions. The proposed modified mathematical model is presented in Fig. 3.8.

### 3.1.4 Aircraft baseline modelling

The aircraft dimensions modelling was based on [90], while aircraft weight modelling followed the principles outlined in [90–92]. The aircraft aerodynamics were modeled according to [90, 93], and aircraft performance modelling was based on [90, 94].

Rather than simply using fixed engine thrust requirements, a rubberized-wing aircraft model was also utilised in these studies to capture "snowball effects" with respect to maximum take-off weight variation due to improvements in engine weight and specific fuel consumption. For every engine design variant the aircraft is scaled on a constant wing loading basis to achieve a design range mission and cargo load. The scaled aircraft is then used in conjunction with a typical business case mission for predicting block fuel.

Two baseline aircraft models have been used herein; one model for long range applications and one for short range. The former model is largely based on public domain information available for the Airbus A330-200 while the latter model is based on the Airbus A320-200. The short range aircraft was designed to carry 150 [pax] for a distance of 3000 [nmi] and a typical business case of 500 [nmi]; for long range applications it was designed for 253 [pax], 6750 [nmi] and 3000 [nmi], respectively. For the step-up cruise procedure, a minimum residual rate of climb of 300 [ft/min] was set as a constraint for flying at the cruise altitude for maximum specific range.

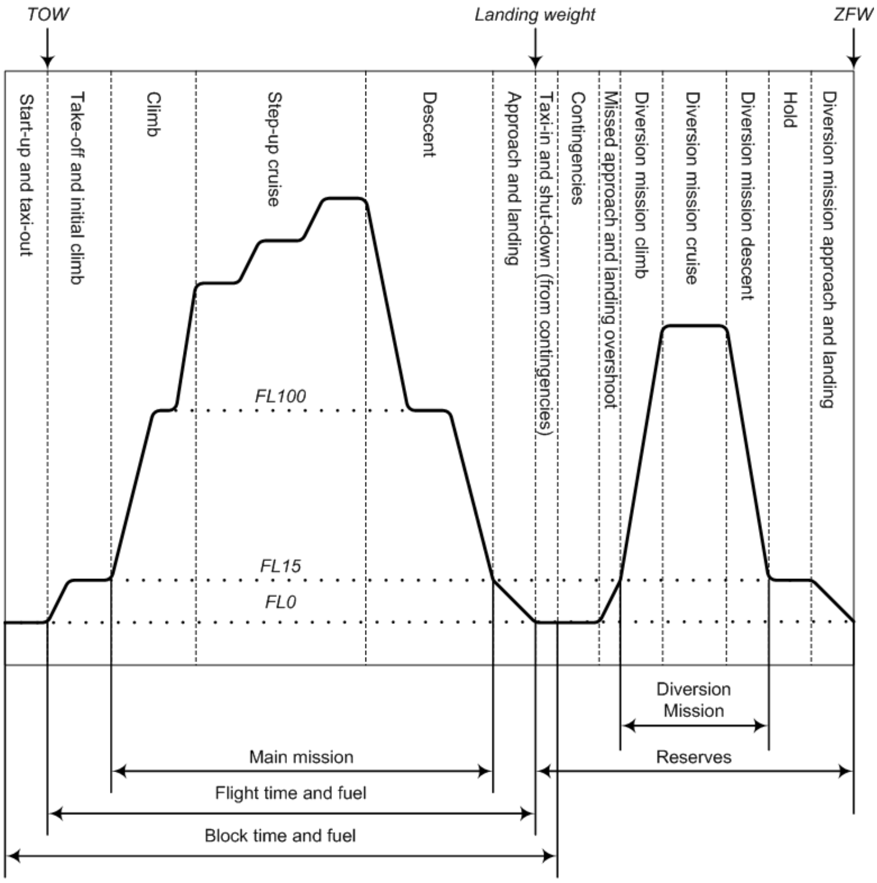


Figure 3.9: Typical flight cycle.

The aircraft drag polar and weight breakdown were predicted at component level from the aircraft geometry and high lift device settings for the take-off and approach phases. Fuel burnt was calculated for the entire flight mission including reserves assuming ISA conditions, as illustrated in Fig. 3.9. Cruise is performed at the optimum altitude for specific range (fixed cruise Mach number) using a step-up cruise procedure as the aircraft gets lighter. A comprehensive take-off field length calculation is performed for all engines operating and one engine inoperative conditions up to 1500 [ft].

## 3.2 Conceptual design considerations

### 3.2.1 Feasibility and design constraints

Aero-engine designs are subject to a large number of constraints and these need to be considered during conceptual design. Constraints can be applied within the optimiser environment at the end of the calculation sequence i.e., after the last design module has been executed. During a numerical optimisation, the optimiser will select a new set of input design parameters for every iteration and the resulting combination of aircraft and engine will be assessed. Using user specified objective functions the optimiser will home in on the best engine designs, determining the acceptability/feasibility of each design through the constraints set by the user. Infeasible designs will be ruled out, while non-optimum design values will result in engine designs with non-optimum values for the objective function selected. The optimiser will therefore avoid regions in the design pool that result in infeasible or non-optimum engine designs.

Design constraints set by the user include among others:

- Take-off HPC delivery temperature and other important performance parameters.
- FAR (Federal Aviation Regulations) take-off field length for all engines operating and balanced field length for one engine inoperative conditions.
- Time to height.
- LTO (Landing and Take-Off) cycle $D_pNO_x/F_{oo}$ vs. ICAO certification limits and CAEP medium and long term goals.
- Cumulative EPNL vs. ICAO certification limits.
- Engine time between overhaul.

Where component design is concerned, for a conventional core the High Pressure Compressor (HPC) delivery temperature, and hence the engine OPR, is typically constrained by the mechanical properties of the HPC disc or HPC rear drive cone or High Pressure Turbine (HPT) disc material [47]. For an intercooled core, the OPR value is no longer constrained by a maximum allowable HPC delivery temperature. Nevertheless, the intercooling process increases the air density in the gas path and as a result the compressor blades tend to become smaller. Losses from tip clearances become increasingly important and a minimum compressor blade height limitation needs to be applied to maintain state of the art compressor efficiency.

Core architecture selections for the conventional core set an upper limit to the HPC design pressure ratio that can achieved when driven by a single-stage HPT. A transonic single-stage HPT design can allow for relatively higher HPC pressure ratios at the expense of a lower polytropic efficiency. A two-stage HPT can offer high HPC pressure ratios at a high polytropic efficiency but a trade-off arises with respect to the need for more cooling air and increased engine length associated with the introduction of a second row of vanes and blades.

With respect to the intercooled core, the minimum design pressure ratio for the Intermediate Pressure Compressor (IPC) can in some cases be limited by icing considerations during the descent flight phase. The maximum area variation that may be achieved by the variable area auxiliary nozzle is also constrained by mechanical (and aerodynamic) considerations.

As discussed earlier, designing a combustor at very low air to fuel ratio levels is also limited by the need for adequate combustor liner film-cooling air as well as maintaining an acceptable temperature traverse quality [8]; this sets an upper bound on combustor outlet temperature. Furthermore, a maximum permissible mean metal temperature needs to be set to consider turbine blade material limitations. A lower bound on engine time between overhaul also needs to be set to limit the frequency of workshop visits. For short range applications the minimum engine time between overhaul was set to 18000 [hr] while for long range applications to 23000 [hr]. This reflects the fact that designs for short range applications are typically operated at high power conditions for a significantly larger part of their operational life. Significantly lower levels of maximum combustor outlet temperature and turbine blade mean metal temperature had to be selected, compared to what could be selected for engine designs for long range applications that are often operated at derated thrust levels and spend most of their life at cruise.

A choice was made to assume an aircraft load factor of 1 and no cargo. Whilst this choice can be considered sensible it also does not necessarily constitute a typical airline practice. The maximum values for FAR take-off field length and time to height were set accordingly, based on customer operational requirements as the aircraft needs to be able to:

1. Take-off from a large number of airports around the world, and
2. Climb to the initial cruise altitude sufficiently fast to ease operations with local air traffic control, and hence reduce waiting time on the ground.

A cumulative distribution of the world's major runway lengths, based on data from Jenkinson et al. [90], is illustrated in Fig. 3.10. For short range applications fairly stringent constraints are typically set for the maximum take-off distance and time to height; in this study these were set to 2.0 [km] and 25 [min], respectively. For long range applications a maximum take-off distance of 2.5 [km] was set instead. Stringent constraints result in bigger engines but allow for greater flexibility for engine derating at a smaller block fuel cost.

During a block fuel optimization all engine aircraft combinations which do not fulfil the take-off and time to height criteria set will be discarded as infeasible. Due to the underlying physics, this will naturally lead to an optimal engine and aircraft combination for the defined objective function. All large engines will produce heavier aircraft with more drag and thus higher block fuel weight. Engines which are too small will not deliver enough thrust to satisfy the take-off and time to height criteria set.

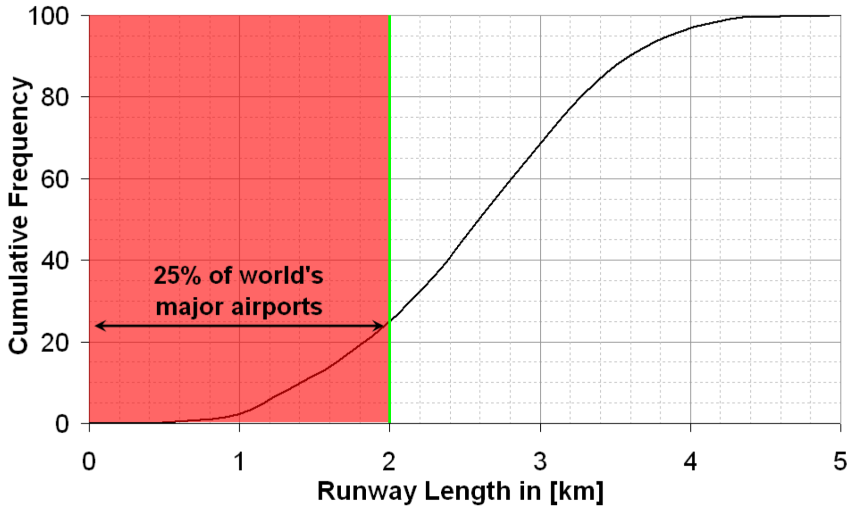


Figure 3.10: Cumulative distribution of world's major runway lengths (based on data from Jenkinson et al. [90]).

### 3.2.2 Engine design optimality

Whereas optimisation constraints can help ensure the feasibility of an engine design, they do little to help with it's optimality. The optimality of the engine design will depend on the careful selection of the figures of merit used during the optimisation process, such as minimum block fuel, maximum time between overhaul, minimum direct operating costs, minimum noise and LTO $NO_x$ emissions etc.

Determining the optimal aero-engine design is essentially the subject of a multi-objective optimisation, and therefore Pareto fronts need typically be constructed to visualize the region of optimal designs within the design space. A simplified example of utilizing the tool for design space exploration, with active constraints, is illustrated in Fig. 3.11. In principle, nacelle drag should also be added as a third dimension when plotting design space exploration results that consider varying levels of specific thrust, but this has been omitted here in order to simplify the plot. The aircraft exchange rates for the baseline design were used for plotting a constant block fuel line (ignoring nacelle drag effects and nonlinearities) and this iso-line therefore defines, in a simple manner, the boundaries of trading specific fuel consumption for weight. During a block fuel optimization, the optimizer continuously evaluates different engine designs as it searches for the optimal solution. Designs that fail to meet constraints set by the user are discarded and have been labeled as infeasible in the plot.

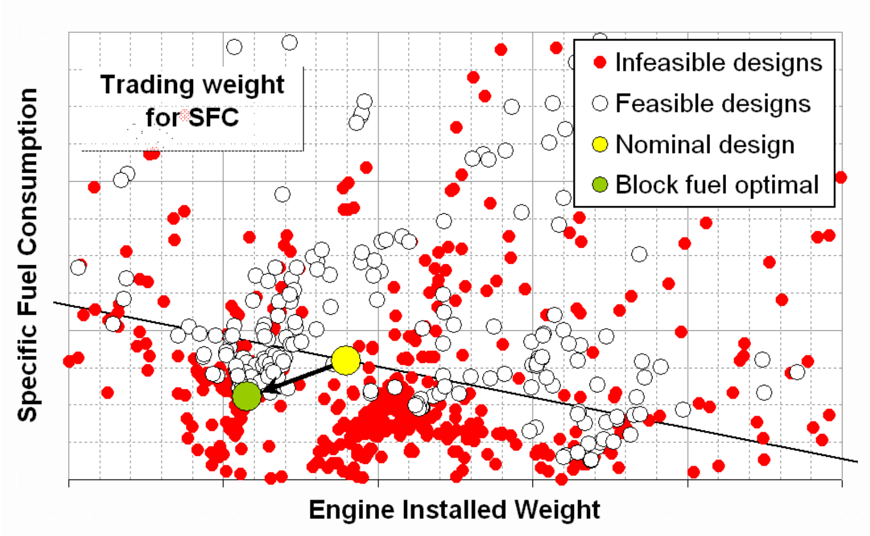


Figure 3.11: Visualization example of constrained design space exploration.

### 3.2.3 Economic considerations

Safety considerations aside, civil aero engine design has been driven primarily by economic considerations even from its fairly early days. A testament to this has been the advent of the world's first commercial jet-airliner, the de Havilland Comet, powered by 4 Rolls-Royce Avon turbojet engines. Although it burned nearly four times as much fuel compared to piston-driven engines, it's business case was very strong since it permitted significantly higher flight speeds resulting in reduced flight times (i.e. a better airline product) and increased aircraft annual utilization. Furthermore, the excellent power to weight ratio of the turbojet engine meant that it could be used to power aircrafts with significantly higher passenger capacities than what was feasible before. The evolution of aircraft transport efficiency since the late 30's is summarised in Fig. 3.12 based on data from Avellán [95].

The aero-engine designs proposed herein have been optimized for minimum block fuel for a given aircraft mission (business case) and therefore for minimum $CO_2$ emissions. The market competitiveness of these fuel optimal designs however is highly dependent on the development of jet fuel prices in the years to come until 2020. The volatility of jet fuel price over the last 10 years is illustrated in Fig. 3.13. A further economic consideration for European markets may also be the development of the Euro/US$ exchange rate, as well as interest and inflation rates.

For the economic calculations conducted in this study certain assumptions were made. In order to retain consistency in the economic results, since the presented concept studies were carried out at substantially different moments in time, a common jet fuel price of 172c$/US gallon was assumed. It is worth noting that

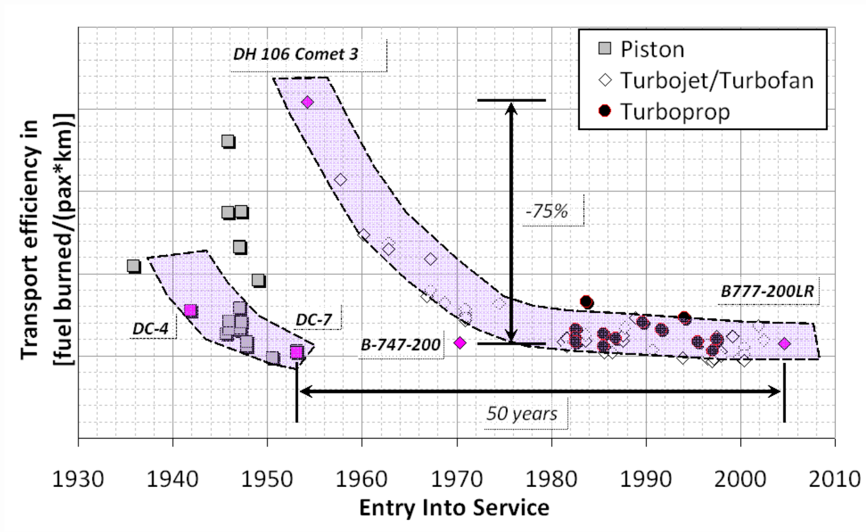


Figure 3.12: Evolution of aircraft transport efficiency (based on data from Avellán [95]).

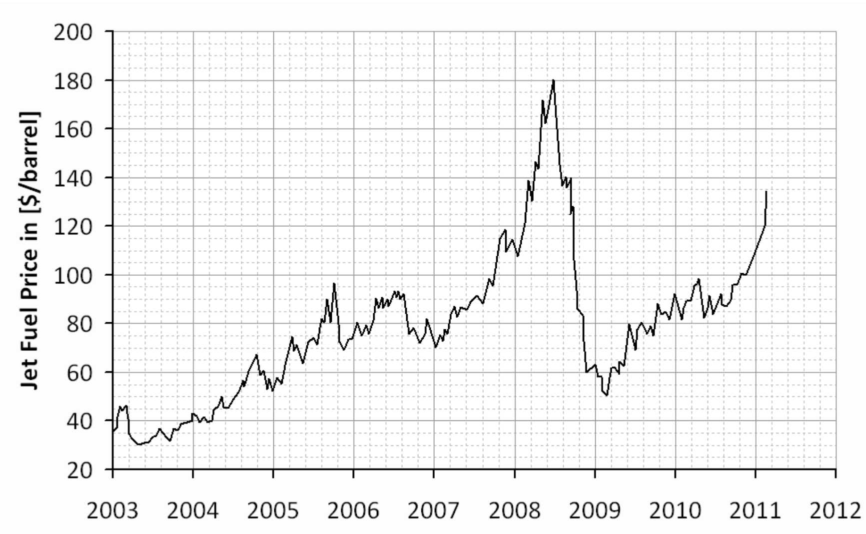


Figure 3.13: Long term perspective of jet fuel price movements (based on data from the International Air Transport Association [96] and Platts [97]).

at the time of writing the average jet fuel price was 320 [c$/US gallon] [96, 97]. Interest and inflation rates were assumed to be 6% and 2%, respectively, while the US$ to Euro exchange rate was assumed to be 0.8222.

It is worth noting that an increase in inflation rates from 2% to 3% can increase the net present cost by as much as 17%, over a period of 30 years. An increase in interest rates from 6% to 7% can increase Direct Operating Costs (DOC) by 2.5% and 4.5% for short and long range applications, respectively.

The cost of fuel as a fraction of the total DOC was predicted to be 13% and 19% for short and long range applications, respectively. An increase in block fuel by 1% translates in an increase of 0.13% and 0.19% in DOC, respectively, and as can be observed it is directly dependent on the ratio of fuel cost over DOC. A doubling of the fuel price would change this ratio to roughly 23% and 32%, respectively, and would also result in 13% and 19% higher DOC levels, respectively.

Higher levels of DOC, as a result of a significant increase in fuel price, would most probably be absorbed by airlines through an increase in fares. This could make fuel efficient designs increasingly market competitive, as the DOC optimal designs would further approach the fuel optimal designs. It would therefore be worthwhile to redirect further research investments towards developing fuel efficient aero engine designs, as has also been the case in the late 70's and through large part of the 80's. The introduction of carbon taxes could also have a similar effect.

### 3.2.4 Uncertainty analysis and technical risk

It is a common approach in system simulations to model component and system performance in a deterministic manner. In reality however, component performance is subject to various sources of uncertainty such as production scatter and performance deterioration. Therefore, real system performance will also be subject to uncertainty.

It is of paramount importance to quantify the technical risk emanating from such uncertainty during all stages of an aero-engine's life cycle, as illustrated in Fig. 3.14. During the transition from the conceptual design phase to the preliminary design phase for example, the cruise SFC figure must be locked and potentially offered to the customer in a contractual bid. If the SFC penalty due to in-service deterioration and production scatter is over-estimated, then product competitiveness will be lower than it could be. If the SFC penalty on the other hand is under-estimated, then the engine manufacturer risks having to pay expensive contractual penalties for those eventual under-performing production engines; or alternatively embark on an expensive product improvement programme. An accurate probabilistic performance modelling approach must

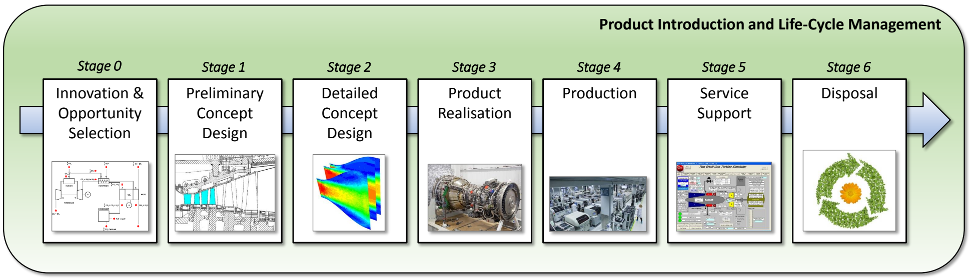


Figure 3.14: Product introduction and life-cycle management stages.

therefore be employed during the conceptual design stage. A key requirement is that it must be able to effectively capture the performance changes that will inevitably occur during the later stage of the product's life-cycle.

To model such aspects, performance deltas and factors need to be applied to some of the component performance parameters $P_1, P_2, ..., P_m$. For compressors and turbines, the parameters to modify are in principle efficiency and swallowing capacity. For inlets, bypass ducts, transition ducts, combustors, jet pipes and nozzles the parameters to modify are relative pressure losses as well as discharge and thrust coefficients.

The generic form for applying such deltas and factors on the nominal (deterministic) component performance parameter vector $\boldsymbol{P_{determ}}$ can be described through Eq. (3.16).

$$\boldsymbol{P_{prob}} = (\boldsymbol{P_{determ}} * \boldsymbol{c_{risk}}) + \boldsymbol{\Delta P_{risk}} \tag{3.16}$$

A fairly robust but computationally expensive method to estimate the effect of component performance deviations on overall system performance is the Monte Carlo method. Probability distribution functions for the delta $\boldsymbol{\Delta P_{risk}}$ and factor $\boldsymbol{c_{risk}}$ vectors are used for modelling the technical uncertainty in component performance. For example, the nominal efficiency of a turbomachinery component will be calculated in accordance with Eq. (3.17). The $\Delta\eta_{risk}$ parameter will follow some type of statistical distribution, for example a normal distribution, as described by Eq. (3.18). Other types of distributions may also be employed in a similar manner, such as uniform, triangular etc.

$$\eta_{prob} = \eta_{determ} + \Delta\eta_{risk} \tag{3.17}$$

$$\Delta\eta_{risk} \sim \mathcal{N}(\mu_{\eta,risk},\, \sigma^2_{\eta,risk}) \tag{3.18}$$

During a Monte Carlo analysis, a large number of simulations will be executed

- typically in the order of a few thousand. Sets of random deltas and factors are firstly derived and consequently applied on top of the assumed nominal component performance parameter vector $\boldsymbol{P_{determ}}$ and the performance model is executed. The probabilistic performance of the whole system is then derived through statistical analysis of the resulting performance simulations, as shown in Fig. 3.15. All the dependent whole system performance parameters $g_1, g_2, ..., g_k$ can be represented in their probabilistic form by a mean value and a standard deviation, as described through Eq. (3.19).

$$\boldsymbol{g_{prob}} \sim \boldsymbol{\mathcal{N}(\mu_g,\, \sigma_g^2)} \tag{3.19}$$

The individual whole system probabilistic performance parameters in the vector $\boldsymbol{g_{prob}}$ are expected to follow normal distributions, independently of the distributions used for deriving the probabilistic component performance parameter vector $\boldsymbol{P_{prob}}$, as conceptually illustrated in Fig. 3.16. The application of the Monte Carlo method for gas turbine applications is discussed in good detail by Kurzke [74]. The equivalent expressions for engine net thrust and specific fuel consumption are described by Eq. (3.20) and Eq. (3.21), respectively.

$$FN_{prob} \sim \mathcal{N}(\mu_{FN},\, \sigma_{FN}^2) \tag{3.20}$$

$$SFC_{prob} \sim \mathcal{N}(\mu_{SFC},\, \sigma_{SFC}^2) \tag{3.21}$$

The convergence of the Monte Carlo simulation itself can be confirmed easily through plots of the evolution of the mean and standard deviation of the deltas or factors being applied, as illustrated in Fig. 3.17, and Fig. 3.18, for a triangular, uniform and normal distribution. In principle, the Monte Carlo will converge after about three thousand simulations, albeit for academic studies one may consider using up to ten thousand simulations. For a quick study even about one thousand simulations may prove sufficient for yielding a reasonable result.

It must be noted that a probabilistic modelling approach based on Monte Carlo simulations (or even advanced uncertainty propagation techniques), allows the engine designer to develop a robust optimal conceptual design. This design will deliver optimal performance under all scenarios considered and will possess a well understood technical risk. Such risk can be quantified in terms of in-service SFC penalties as well as margins from future certification limits. In the conceptual design process these limits can be seen as technological targets to be confirmed (and certified) through type-tests during the later stages of the product development process.

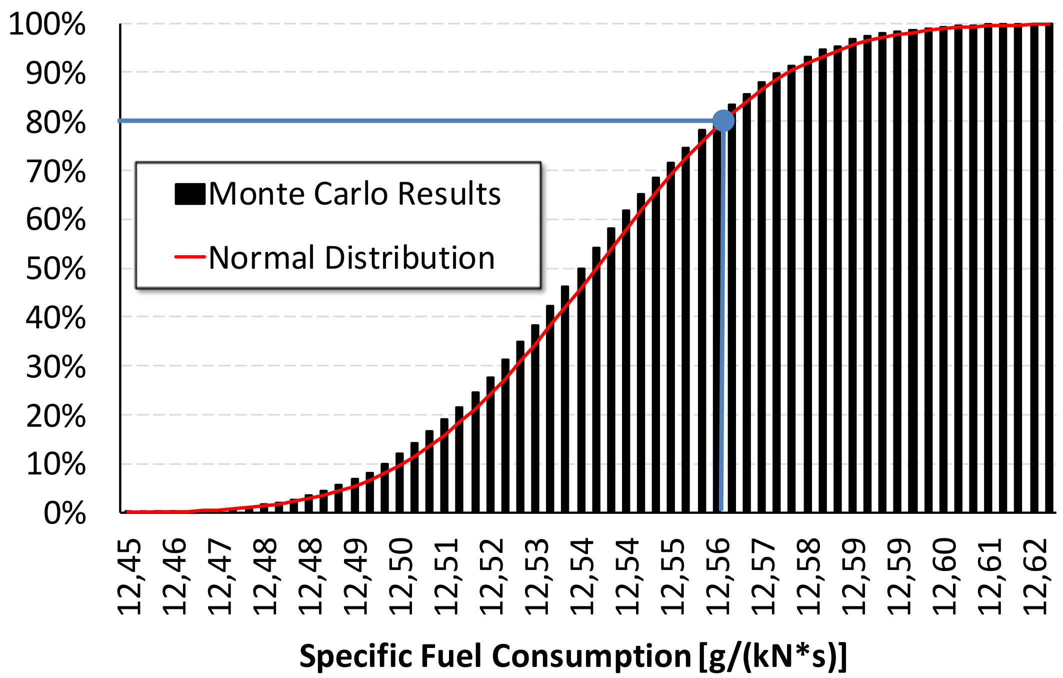


Figure 3.15: Example of cumulative distribution function of specific fuel consumption.

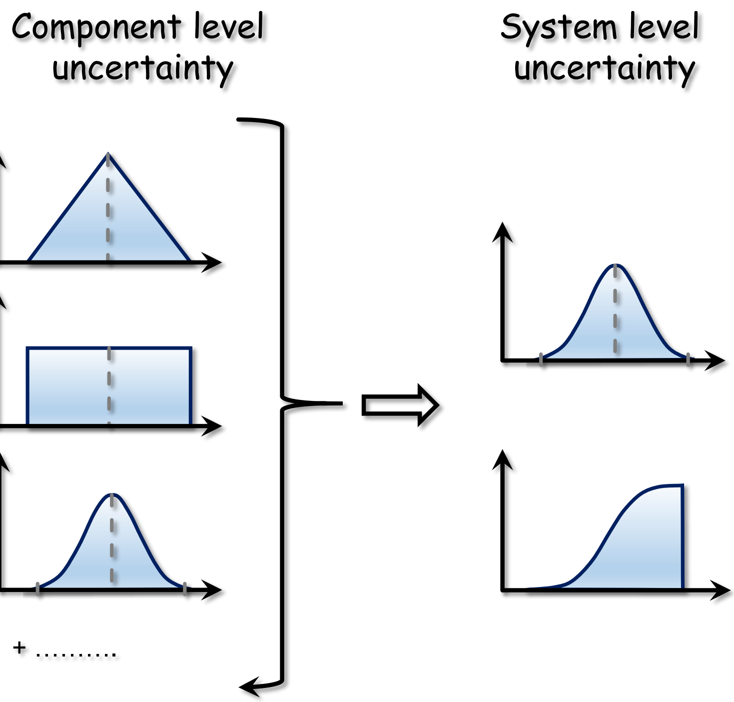


Figure 3.16: Combining component level uncertainty to derive system level uncertainty.

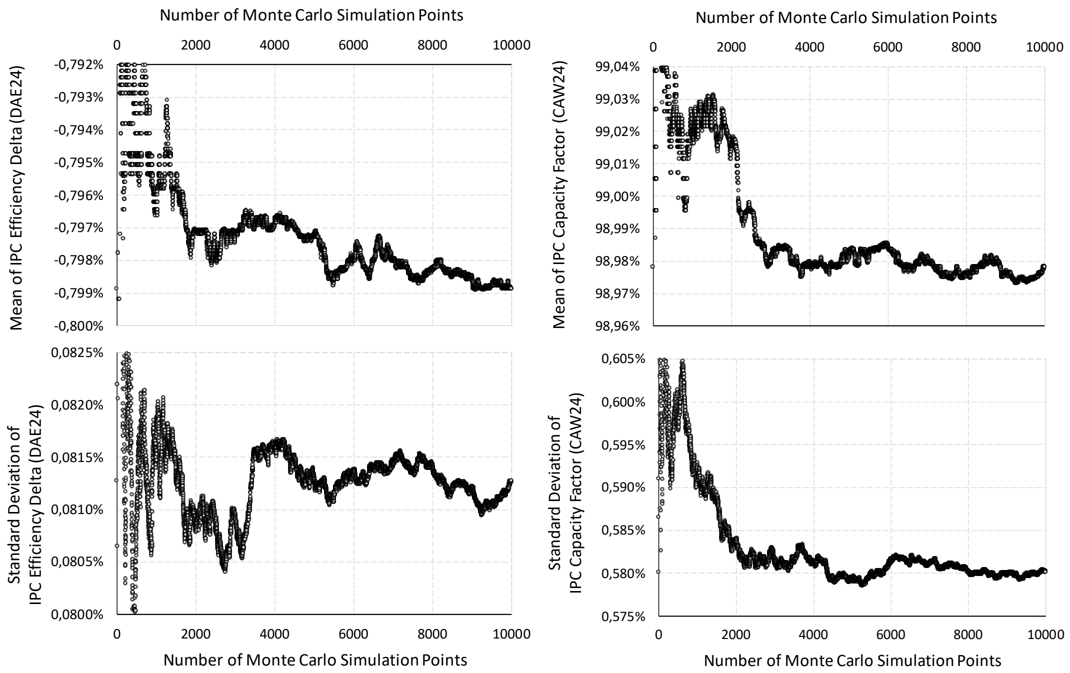


Figure 3.17: Evolution of the mean value (upper) and standard deviation (lower) of the delta or factor applied on IPC efficiency (left) or capacity (right), assuming a triangular or uniform distribution, respectively.

Engine manufacturers will typically maintain a database of probability distributions quantifying the performance uncertainty of key engine components and associated instrumentation – as integrated in different engine configurations within their product portfolio. Whilst such information can provide an excellent estimate on uncertainty in existing designs, some form of extrapolation and engineering judgment will need to be used to develop best estimates every time a new future engine conceptual design study is carried out.

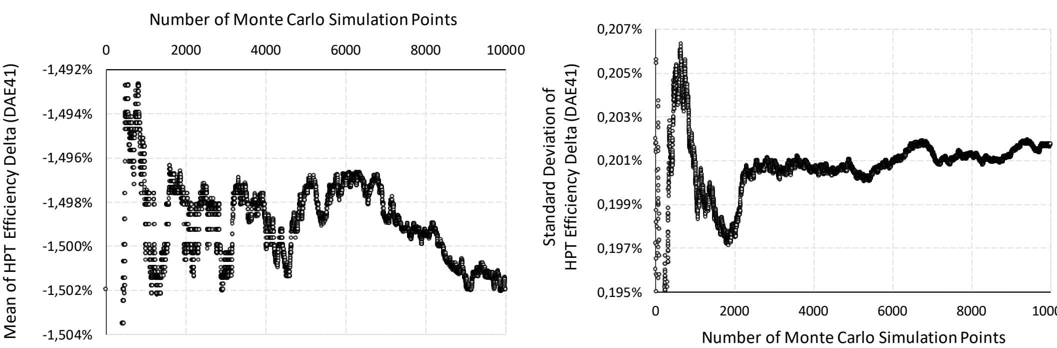


Figure 3.18: Evolution of the mean value (left) and standard deviation (right) of the delta applied on HPT efficiency assuming a normal distribution.

In the present work, a number of uncertainty distributions were used to estimate the effects of production scatter, deterioration as well as measurement uncertainty, as presented in Table 3.2 and Table 3.3. Whilst these distributions are not representative of any specific engine design, they can be considered reasonable for the purpose of analysing the technical risk of a future engine conceptual design, and are well within the expected order of magnitude of component uncertainty.

One of the disadvantages of performing a Monte Carlo simulation is the computational cost involved. For every set of values produced through the Monte Carlo and applied on the probabilistic component performance parameter vector $\boldsymbol{P_{prob}}$, the performance model needs to be executed to estimate the whole system probabilistic performance parameter vector $\boldsymbol{g_{prob}}$. The associated risk vector $\boldsymbol{\delta g_{risk}}$ is then estimated using Eq. (3.22).

$$\boldsymbol{\delta g_{risk}} = \boldsymbol{g_{prob}}\left(\boldsymbol{P_{prob}}\right) - \boldsymbol{g_{determ}}\left(\boldsymbol{P_{determ}}\right) \tag{3.22}$$

A fast alternative approach utilised in the present work employs the first-order Taylor expansion series to estimate the uncertainty effect of the probabilistic input parameter vector $\boldsymbol{P_{prob}}$ on the whole system probabilistic performance parameter vector $\boldsymbol{g_{prob}}$. In this approach, the Monte Carlo is used only to derive the $\boldsymbol{P_{prob}}$ vector which does not require an execution of the performance model. Then Eq. (3.23) is used for every instance of the $\boldsymbol{P_{prob}}$ vector to estimate the associated risk vector $\boldsymbol{\delta g_{risk}}$, rather than executing the performance model. The whole system probabilistic performance parameter vector $\boldsymbol{g_{prob}}$ can in turn be estimated using Eq. (3.22).

$$\begin{aligned}
\delta g_{1,risk} &\approx \sum_{i=1}^{m}\left(\frac{\partial g_{1,determ}}{\partial P_{i,determ}} * \left(P_{i,prob} - P_{i,determ}\right)\right)\\
\delta g_{2,risk} &\approx \sum_{i=1}^{m}\left(\frac{\partial g_{2,determ}}{\partial P_{i,determ}} * \left(P_{i,prob} - P_{i,determ}\right)\right)\\
&\vdots\\
\delta g_{k,risk} &\approx \sum_{i=1}^{m}\left(\frac{\partial g_{k,determ}}{\partial P_{i,determ}} * \left(P_{i,prob} - P_{i,determ}\right)\right)
\end{aligned} \tag{3.23}$$

The computational cost is reduced dramatically since the performance model only needs to be executed once for deriving the deterministic whole system performance parameter vector $\boldsymbol{g_{determ}}$, and a handful of additional times for estimating the partial derivatives (exchange rates) used in Eq. (3.23). The latter require only $m$ additional model executions - i.e., one per probabilistic input parameter $P_{1,prob}, P_{2,prob}, ..., P_{m,prob}$, if forward differences are used - or twice as many if central differences are used. The downside of the fast analytical approach has to do with its lower accuracy, which depends on the non-linear behaviour the whole system in the vicinity of the deterministic performance point. For small delta and factor values, the validity of using a first order approximation of the Taylor polynomial works well, but for increasingly larger values the accuracy will deteriorate.

Table 3.2: Component production scatter distributions.

| | Parameter | Distribution Type | Not Less Than | Most Likely | Not Higher Than |
|---|---|---|---|---|---|
| **Component** | | | | | |
| Fan (bypass side) | Efficiency Delta | Triangular | -0.3% | 0% | 0.1% |
| | Capacity Factor | Triangular | 99% | 100% | 101% |
| Intermediate Pressure Compressor | Efficiency Delta | Triangular | -1% | 0% | 0.5% |
| | Capacity Factor | Triangular | 99% | 100% | 101% |
| High Pressure Compressor | Efficiency Delta | Triangular | -0.6% | 0% | 0.6% |
| | Capacity Factor | Triangular | 99% | 100% | 101% |
| High Pressure Turbine | Efficiency Delta | Triangular | -0.5% | 0% | 0.5% |
| | Capacity Factor | Triangular | 99.2% | 100% | 100.8% |
| Intermediate Pressure Turbine | Efficiency Delta | Triangular | -0.35% | 0% | 0.15% |
| | Capacity Factor | Triangular | 98.5% | 100% | 101.5% |
| Low Pressure Turbine | Efficiency Delta | Triangular | -0.5% | 0% | 0.5% |
| | Capacity Factor | Triangular | 99.5% | 100% | 100.5% |
| **Measurements** | | | | | |
| Low Pressure Turbine Inlet | Temperature Delta | Uniform | -10K | – | +10K |

Table 3.3: Component deterioration distributions.

| | Parameter | Distribution Type | Not Less Than | Most Likely | Not Higher Than |
|---|---|---|---|---|---|
| **Component** | | | | | |
| Fan (bypass side) | Efficiency Delta | Triangular | -1% | -0.8% | -0.6% |
| | Capacity Factor | Uniform | 98% | – | 100% |
| Intermediate Pressure Compressor | Efficiency Delta | Triangular | -1% | -0.8% | -0.6% |
| | Capacity Factor | Uniform | 98% | – | 100% |
| High Pressure Compressor | Efficiency Delta | Triangular | -2% | -1.5% | -1% |
| | Capacity Factor | Uniform | 98% | – | 100% |
| High Pressure Turbine | Efficiency Delta | Triangular | -2% | -1.5% | -1% |
| | Capacity Factor | Uniform | 100% | – | 100.5% |
| Intermediate Pressure Turbine | Efficiency Delta | Triangular | -2% | -1.5% | -1% |
| | Capacity Factor | Uniform | 100% | – | 100.5% |
| Low Pressure Turbine | Efficiency Delta | Triangular | -2% | -1.5% | -1% |
| | Capacity Factor | Uniform | 100% | – | 100.5% |
| **Measurements** | | | | | |
| Low Pressure Turbine Inlet | Temperature Delta | Uniform | -10K | – | +10K |

## 3.3 Model validation

In order to yield useful information from sensitivity studies as well as reasonably accurate design optimisation results, when using the proposed approach, it is paramount that:

- A validation process is carried out for the engine/aircraft model.
- The uncertainty levels in the methodologies used are aligned and well understood.

In the validation process involving the presented approach the first step is to set up the engine performance model. For every new technology and engine configuration initial estimates of the potential performance will need to be made using expert knowledge from component specialists. As the research activities raise the Technology Readiness Level (TRL) of each technology, so improved component efficiency estimates become available. If such a computational framework is being used in a situation where a limited amount of information is being made available such as in integrated collaborative projects or in competitor product modelling - which implies for example the use of generic component characteristics - then further model calibration is required, typically against a specification provided by an Original Equipment Manufacturer (OEM).

The model validation exercise for the present work has been largely carried out as part of the work presented in [1], and the interested reader is refered to that for more detailed information. Examples of the accuracy of the calibrated performance models used in the present thesis - as developed for the intercooled core and intercooled recuperated core turbofan engines for long range applications, assuming a year 2020 entry into service technology - against information provided by OEMs, are illustrated in Fig. 3.19 and Fig. 3.20. Deviations between model predictions and OEM specification are restricted for all performance parameters to roughly 2% for the three major operating points. There is little merit in attempting to achieve better model alignment using generic component characteristics. An OEM engine performance model accuracy for a pre-production engine during the conceptual design phase may typically be no better than to within 1% SFC; at part-load the model uncertainty is expected to be significantly higher.

Where engine mechanical and aerodynamic design is concerned it is important that engine components are sized at the appropriate operating conditions. Component sizing methods need to be checked for physical behavior as the thermodynamic cycle is varied during the optimisation process. Similarly to engine performance models, there is again little merit in attempting to calibrate component weight models against an OEM specification to achieve deviations of less than 5%. Where aircraft weight and performance modelling is concerned the uncertainty levels may be roughly similar; 2% in block fuel and 5% in each aircraft weight group (wing, fuselage, landing gear etc.) pose as reasonable deviation targets.

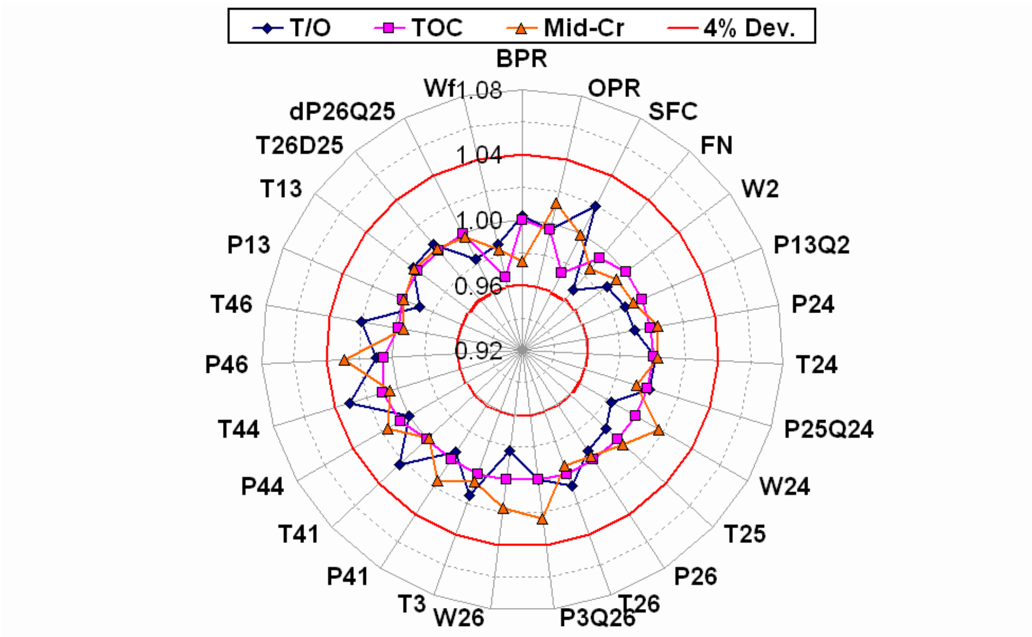


Figure 3.19: Deviations of engine performance model predictions from OEM specifications for the long range intercooled core turbofan engine.

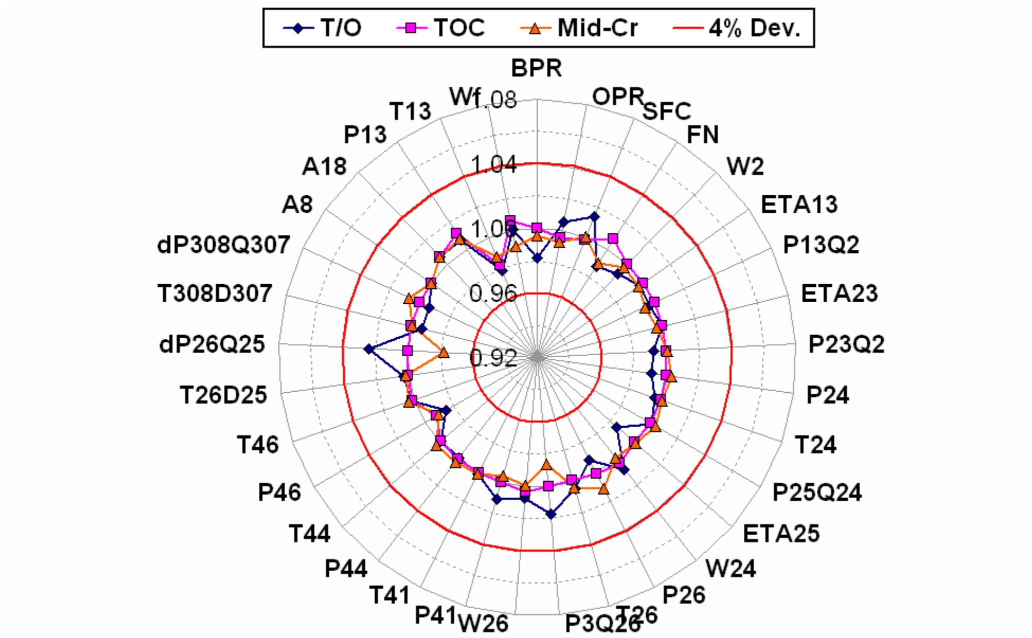


Figure 3.20: Deviations of engine performance model predictions from OEM specifications for the long range intercooled recuperated core turbofan engine.

| | Exchange rate | |
|---|---|---|
| Perturbation | Long range | Short range |
| 1000kg weight penalty per powerplant | 1.40% | 2.52% |
| +1% SFC shortfall | 1.22% | 1.09% |

Table 3.4: Block fuel exchange rates using the baseline long range and short range rubberised wing aircraft models.

Validating absolute block fuel predictions with public domain airline data is not a trivial task as different airlines will follow different operational practices. For example for the long range aircraft model, the business case prediction is 10% lower than the published annually-averaged value, given in [lt/(km*pax)], by SwissAir for 2009 for the Airbus A330-200 [98]. This does not necessarily mean that the model's business case is not a realistic one; nor that it wouldn't fit well with operational practices followed by other airlines. Furthermore, regional Air Traffic Management (ATM) practices can skew available block fuel data, while global ATM regulations may very well change significantly by 2020. It should be noted that fuel planning within the model respects the requirements defined for international flights by the Federal Aviation Administration [99] and the Joint Aviation Authorities [100].

Where conceptual design is concerned, exchange rates are perhaps a better type of parameter for evaluating the accuracy of a rubberized-wing model, rather than just simply comparing absolute values. Block fuel exchange rates produced with the rubberized-wing baseline aircraft models are presented in Table 3.4 for the business case of the long and short range models and are considered reasonable numbers. They have been produced by applying single perturbations i.e., 1% SFC shortfall and 1000 [kg] of weight penalty per powerplant.

It is important to note here that the proposed approach is primarily intended for system-level design optimization, as well as for comparing and helping to rank future technologies and design concepts. It is therefore trends that need to be captured properly (i.e., the effect on block fuel from introducing or improving a particular engine technology) rather than absolute values. Such trends can be predicted sufficiently accurately, if the engine/aircraft models have been calibrated at the above proposed accuracy levels, as long as the modelling has been performed on a formal and consistent basis. This of course implies that the systems expert carrying out the study has sufficient knowledge of the capabilities of the technologies under assessment.

Calibrating $NO_x$ prediction models to an accuracy to within about 10% is also reasonable. Actual uncertainty levels during the preliminary design of novel combustor concepts may be much higher; emission predictions at part-load will also be affected by uncertainties in the engine performance predictions.

Where cost estimates are concerned these are highly dependent on the assumptions being made. The presented framework is capable of performing risk analysis to consider fuel price volatility, engine lifing etc. The consideration of other key technical risk aspects such as production scatter and performance deterioration, as well as measurement uncertainty, is discussed in detail in the previous section.

# Chapter 4

# Results and Discussion

## 4.1 Concept comparison

The present chapter starts with a concept comparison based on the tools and algorithm described in Chapter 3. The focus is on the potential block fuel benefits resulting from the introduction of:

- An intercooled core in a direct drive UHBR turbofan configuration.
- An intercooled recuperated core in a geared UHBR turbofan configuration.
- An open rotor propulsor in a geared pusher configuration.

The aim is to set the stage for the detailed analysis that will be presented in the sections that follow. It should be noted that the results for the first two concepts are a summary of the work already presented in Kyprianidis et al. [1] while for the third concept details are given in Larsson et al. [2] – for the purposes of this thesis these results shall be considered as past work. The thrust requirements for the first two concepts are for an engine designed to power the long range aircraft model while the latter concept is centered around powering the short range aircraft model..

### 4.1.1 Intercooled core

For the intercooled core assessment, a year 2020 Entry Into Service (EIS) turbofan engine with a conventional core was set up as the baseline. The intercooled core engine is an ultra high OPR design with also year 2020 EIS level of technology, and features a tubular heat-exchanger, while the fan for both engines has

| | Conventional core DDTF LR EIS 2020 | Intercooled core DDIC LR EIS 2020 |
|---|---|---|
| Engine dry weight | Ref. | -5.9% |
| LPT weight | Ref. | -27.1% |
| Core weight | Ref. | -32.5% |
| Added components weight (as % of engine dry weight) | - | 7.7% |
| Block fuel weight | Ref. | -3.2% |
| Mid-cruise SFC | Ref. | -1.5% |
| Thermal efficiency | Ref. | +0.007 |
| Propulsive efficiency | Ref. | +0.000 |

Table 4.1: Comparison of an intercooled engine with a conventional core turbofan engine at aircraft system level (from Kyprianidis et al. [1]).

the same diameter and flow per unit of area. Business case block fuel benefits of approximately 3.2% are predicted for the intercooled engine, mainly due to the reduced engine weight and the core's higher thermal efficiency which results in a better SFC. **These intercooling benefits are highly dependent on achieving technology targets such as low intercooler weight and pressure losses**; the predicted lower dry weight, compared to the conventional core engine, can be attributed to various reasons. The intercooler weight penalty is largely compensated by the higher core specific output allowing a smaller core size and hence a higher BPR at a fixed thrust and fan diameter. The high OPR provides an additional sizing benefit, for components downstream of the HPC, by reducing further the corrected mass flow and hence flow areas. The intercooled core Low Pressure Turbine (LPT) was designed in this study with one less stage which reduced both engine weight and length, despite the high cycle OPR requiring a greater number of HPC stages. These observations are summarised in Table 4.1 with the added components weight group considering the intercooler and its installation standard; this group is not considered in the core weight group which also does not consider the core nozzle or the LPT and its casing.

### 4.1.2 Intercooled recuperated core

For the intercooled recuperated core assessment, a year 2000 EIS turbofan engine with a conventional core was set up as the baseline. The intercooled recuperated core configuration is an UHBR design with a year 2020 level of technology. Significant business case block fuel benefits of nearly 22% are predicted for the geared intercooled recuperated core engine due to its higher thermal and propulsive efficiency. The use of HPT cooling air bled from the recuperator exit [40, 50]

| | Conventional core BASE LR EIS 2000 | Intercooled recuperated core IRA LR EIS 2020 |
|---|---|---|
| Thrust/weight | Ref. | -12% |
| Engine dry weight | Ref. | +16.5% |
| Nacelle weight | Ref. | +29.7% |
| Fan weight | Ref. | +36.6% |
| LPT weight | Ref. | -17.1% |
| Added components weight (as % of engine dry weight) | - | 25.4% |
| Block fuel weight | Ref. | -21.6% |
| Mid-cruise SFC | Ref. | -18.3% |
| Thermal efficiency | Ref. | +0.024 |
| Propulsive efficiency | Ref. | +0.120 |

Table 4.2: Comparison of an intercooled recuperated engine with a conventional core turbofan engine at aircraft system level (from Kyprianidis et al. [1]).

results in a 1.3% SFC improvement due to more energy being recuperated from the exhausts, at a fixed effectiveness level - and despite the considerable increase in cooling air requirements (+3.5% of core mass flow). The predicted dry weight for the intercooled recuperated configuration is higher compared to the conventional core engine. There is a weight benefit from the use of EIS 2020 light-weight materials in most major engine components, as well as from the high speed LPT - due to the reduced stage count. Also, the relatively low engine OPR and the use of an intercooler increases core specific output, resulting in a smaller core. The introduction however of the gearbox, intercooler and recuperator components inevitably results in a significant weight penalty. It should be noted that a lower level of specific thrust, and hence a larger fan diameter, has been assumed for the intercooled recuperated core engine; this results in both a heavier fan and a heavier nacelle. These observations are summarised in Table 4.2 with the added components weight group considering the intercooler and recuperator and their installation standard, as well as the gearbox.

### 4.1.3 Geared open rotor

For the geared open rotor assessment, a year 2020 EIS geared turbofan engine with a conventional core was set up as the baseline. The geared open rotor concept design also assumes year 2020 EIS level of technology, and features two counter-rotating propellers in a pusher configuration powered by a geared low pressure turbine. Significant business case block fuel benefits of nearly 15% are predicted for the geared open rotor engine primarily due to its higher propulsive efficiency. Although, the geared turbofan engine benefits from a better thrust to

| | Geared turbofan<br>GTF SR<br>EIS 2020 | Geared open rotor<br>GOR SR<br>EIS 2020 |
|---|---|---|
| Engine installed weight | Ref. | +11% |
| Nacelle weight | Ref. | -88% |
| Fan/propeller weight | Ref. | +73% |
| LPT weight | Ref. | +20% |
| Core weight | Ref. | -31% |
| Block fuel weight | Ref. | -15% |
| Mid-cruise SFC | Ref. | -14% |
| Thermal efficiency | Ref. | -0.013 |
| Propulsive efficiency | Ref. | +0.16 |

Table 4.3: Comparison of a geared open rotor engine with a geared turbofan engine at aircraft system level (from Larsson et al. [2]).

weight ratio it suffers from significantly higher nacelle drag losses, compared to the open rotor design. These observations are summarised in Table 4.3.

## 4.2 Design space exploration

A study previously presented by the author compared conventional core and intercooled core turbofan engines for a long range application [82]. Both configurations had the same fan diameter and were designed to meet the same thrust requirements (70,000lbf). They were ultra-high bypass ratio three-shaft designs with direct drive front fans. The intercooled core configuration (illustrated in Fig. 4.1 and Fig. 4.2) featured an intercooler mounted inboard of the bypass duct and an auxiliary variable geometry nozzle to regulate the cooling flow. For designs to enter service between 2020 and 2025 the two concepts were evaluated for their potential to reduce mission fuel burn and $CO_2$ emissions through both thermal and propulsive efficiency improvements. The work demonstrated that an intercooled core could be designed for a significantly higher overall pressure ratio and with reduced turbine cooling air requirements, to give higher thermal efficiency than could otherwise be achieved with a conventional core.

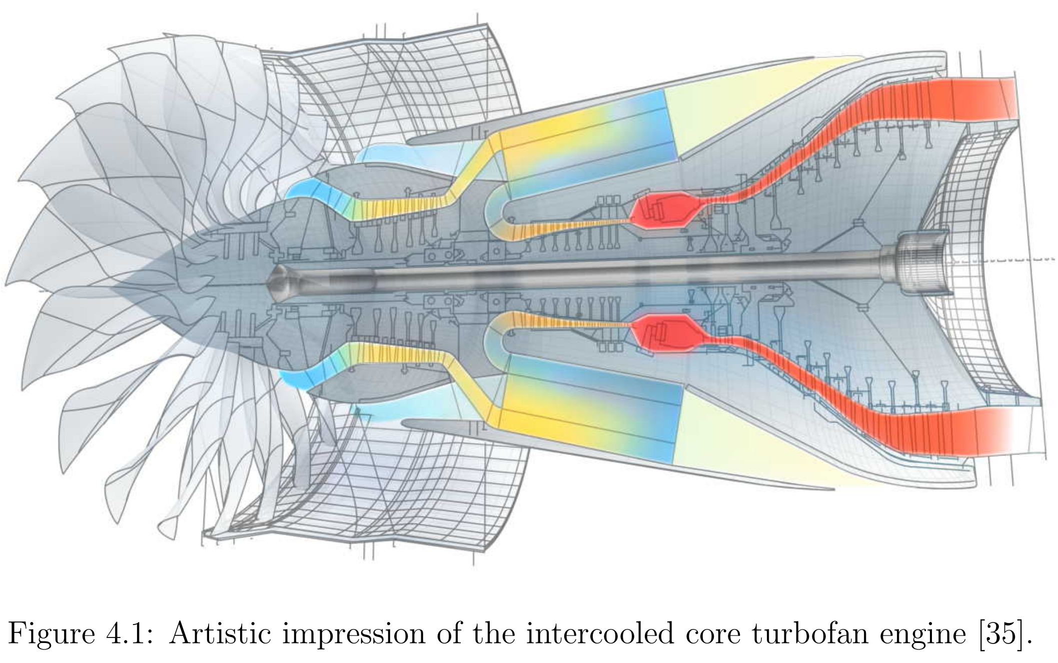

Figure 4.1: Artistic impression of the intercooled core turbofan engine [35].

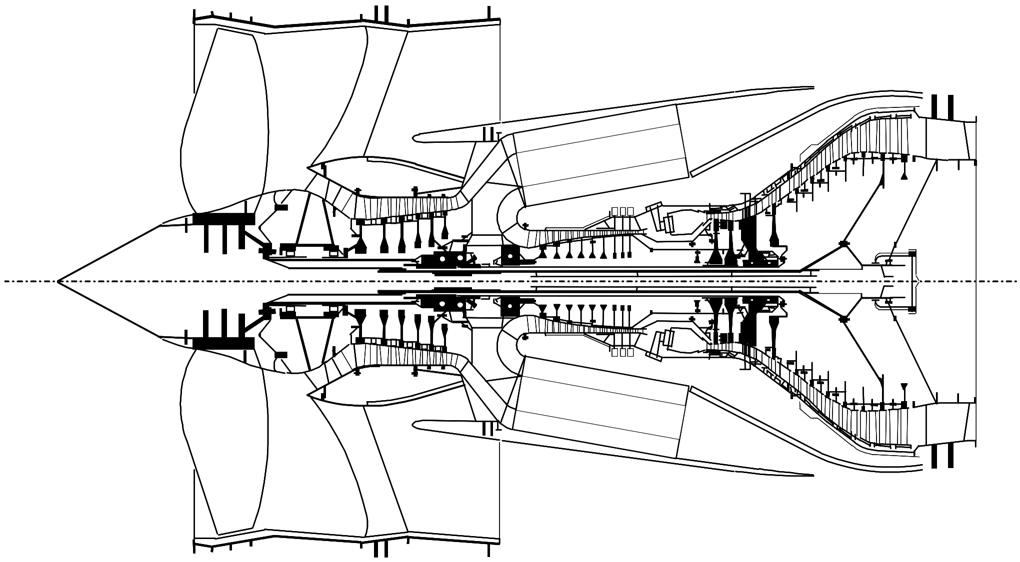

Figure 4.2: General arrangement of the direct-drive fan intercooled core configuration.

A further study presented by the author focused on the re-optimization of those same powerplants by allowing the specific thrust (and hence the propulsive efficiency) to vary [101]. Rather than setting fixed thrust requirements, a rubberised-wing aircraft model was fully utilised instead. The engine/aircraft combination was optimized to meet a particular set of customer requirements i.e. payload-range, take-off distance, time to height and time between overhaul. The work demonstrated that the optimal specific thrust for the intercooled core was somewhat higher than that of the conventional core turbofan engine. While the optimised high OPR intercooled core benefited from higher thermal efficiency, the optimised conventional core benefited more from higher propulsive efficiency. This result was mainly attributed to the minimum blade height limit applied at the back of the High Pressure Compressor (HPC), which tended to limit the intercooled engine OPR, particularly as specific thrust reduced, so negating part of the benefit of increased fan diameter.

This conclusion may appear specific to the thrust scale of the study engine (70,000lbf) and might not apply to more powerful engines, but it was considered likely to be generally applicable because all intercooled engines will have relatively small core components and so be more sensitive to the loss of efficiency from making them smaller still. As a partial remedy to this, the author proposes to remove the Low Pressure (LP) shaft diameter constraint to enable the intercooled engine to have a faster rotating lower hub to tip ratio core which should be more efficient because of its increased blade heights. This may be achieved by having:

- A geared fan and a high-speed Low Pressure Turbine (LPT) with a reduced shaft torque, or
- An aft fan arrangement with a geared or counter-rotating turbine, or
- A reverse-flow core.

Any of these arrangements might reduce the optimal specific thrust level significantly and hence merit further investigation although they would make 2020 a very ambitious target for entry into service. In the present work, the same multidisciplinary conceptual design tool as developed in [1] and discussed in Chapter 3 has been utilised to analyse the first option from the list above i.e., the option of an intercooled core geared fan aero engine for long haul applications.

The first part of the design space exploration study presented herein builds an understanding of the design space for this particular engine configuration. The focus is placed on identifying the isolated effects of several major design parameters on SFC, engine weight and mission fuel. In addition, a sensitivity analysis is carried out to assess the potential impact of technology shortcomings on the overall engine design.

The second part of the study, attempts to identify "globally" fuel burn optimal values for a set of engine design parameters by varying them all simultaneously. This permits the non-linear interactions between the parameters to be accounted. Special attention has been given to the fuel burn impact of the reduced HPC efficiency levels associated with low last stage blade heights. Three fuel optimal designs are considered, based on different assumptions. The first is for fixed HPC efficiency (not penalised by changes in blade height) and the second adjusts the HPC efficiency according to a correlation with HPC last stage blade height. Both are for fixed thrust requirements. In the third optimisation both the HPC efficiency and the design thrust levels are varied in order to maintain original customer requirements such as take-off field length.

For consistency with the previous studies the 2020 entry into service technology level assumption has been retained. With the direct drive fan intercooled core design from [101] used as reference, the original mechanical configuration has been converted to a 2-shaft geared fan variant. Relative to the direct drive concept, the geared variant futures a geared fan driven by a high-speed LPT while the high-speed Intermediate Pressure Compressor (IPC) is directly coupled with the LPT. Where appropriate the original performance assumptions (efficiencies, pressure losses) have been reworked to reflect changes in the modified mechanical and aerodynamic model. The engine size and take-off rating (70,000lbf) have been trimmed in order to achieve the same performance in terms of time to height and take-off distance as considered in [101]. A detailed schematic representing the engine configuration under investigation is illustrated in Fig. 4.3. A schematic of the engine performance model is illustrated in Fig. 4.4.

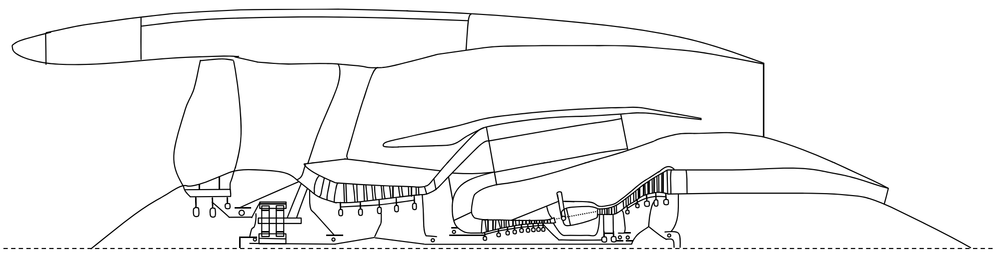

Figure 4.3: General arrangement of the geared fan intercooled core configuration.

### 4.2.1 Parametric design analysis

#### 4.2.1.1 Modelling assumptions

Engine design parameters including: specific thrust, jet velocity ratio, intercooler mass flow ratio, pressure ratio split exponent and overall pressure ratio have been varied - only one at a time - at the hot-day top of climb condition. The effect of intercooler effectiveness level at mid-cruise conditions has also been analysed. The parametric study has been carried out at fixed thrust levels at hot-day top of climb, end of runway hot-day take-off, and International Standard Atmosphere (ISA) mid-cruise conditions. The sensitivity analysis comprising a set of exchanged rates has been carried out also at fixed thrust levels. A full description of all the modelling assumptions for the parametric design analysis, as well as for the sensitivity analysis is presented in Fig. 4.5 and is discussed in further detail below.

Mass flow has been varied to achieve a thrust at hot-day top of climb conditions while combustor outlet temperature has been varied to achieve a thrust at end of runway hot-day take-off and ISA mid-cruise conditions. Fan pressure ratio and bypass ratio have been varied at hot-day top of climb conditions to achieve the required variation in specific thrust and jet velocity ratio, respectively. The core compressor pressure ratios (IPC and HPC) have been varied at hot-day top of climb conditions to achieve the required variation in pressure ratio split exponent and overall pressure ratio, respectively.

The following design parameters have been kept constant at hot-day top of climb conditions: combustor outlet temperature, turbine thermal barrier coating external surface blade metal temperature (by varying the HPT cooling flow), intercooler effectiveness, component polytropic efficiencies, duct, combustor and intercooler pressure losses, gearbox and shaft mechanical efficiencies, and LPT cooling flow mixing pressure ratio.

Although variable geometry has been assumed for the intercooler and bypass exhaust nozzles the total area has been kept constant at off-design. This was necessary in order to isolate the effects of the design parameters studied within

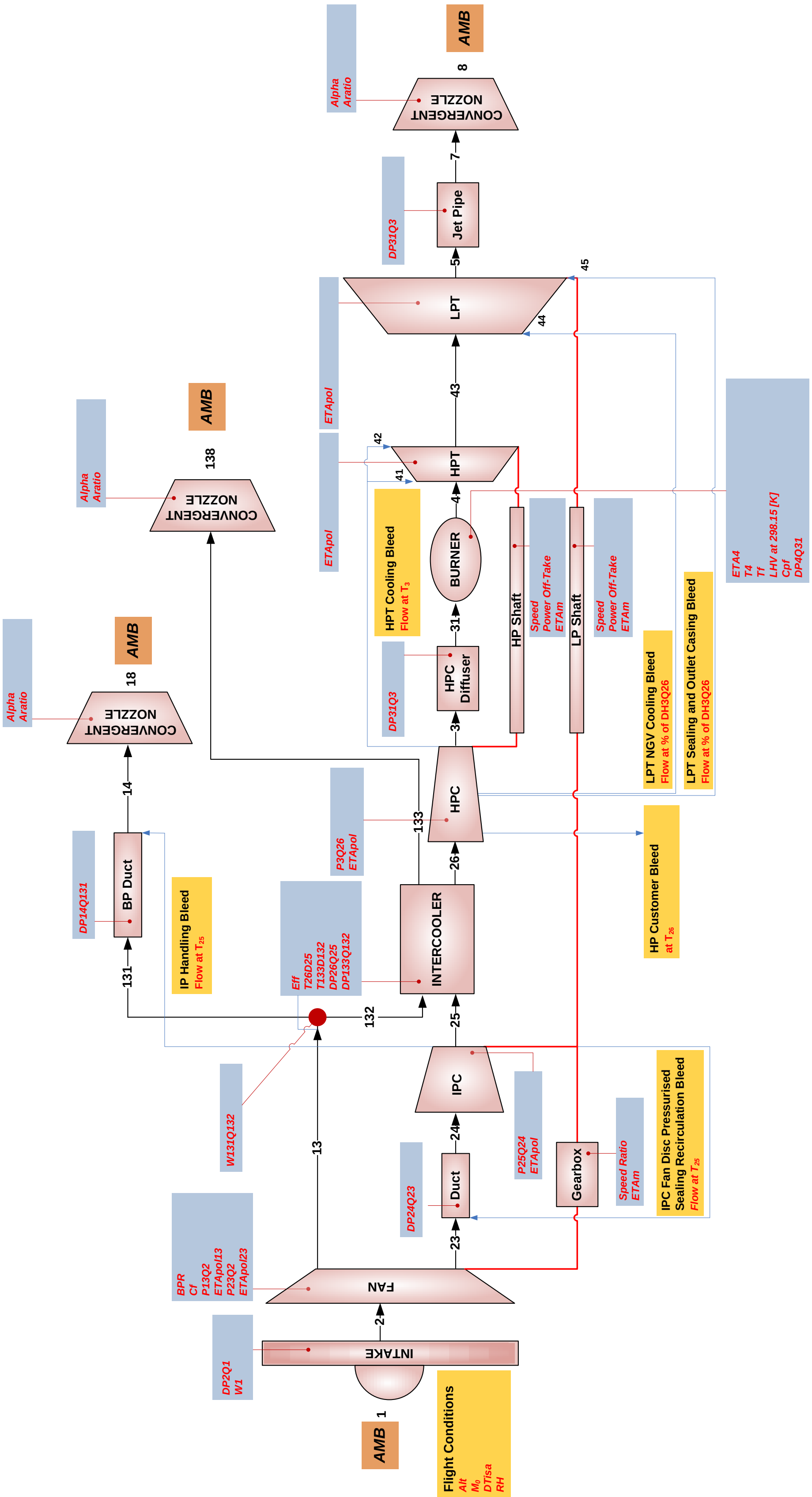


Figure 4.4: Performance model of the geared fan intercooled core configuration.

| Key engine parameters | Units | Hot-day top-of-climb conditions (ISA+10, FL350, Mach 0.82) | Hot-day end-of-runway take-off conditions (ISA+15, FL0, Mach 0.25) | Mid-cruise conditions (ISA, FL350, Mach 0.82) |
|---|---|---|---|---|
| Specific thrust | m/s | **Target*** | Out of the wash | Out of the wash |
| Jet velocity ratio | - | **Target*** | Out of the wash | Out of the wash |
| Intercooler mass flow ratio | - | **Target*** | Out of the wash | Out of the wash |
| Pressure ratio split exponent | - | **Target*** | Out of the wash | Out of the wash |
| Fan tip over hub pressure rise ratio | - | **Target** | Out of the wash | Out of the wash |
| Overall pressure ratio | kN | **Target*** | Out of the wash | Out of the wash |
| HPT TBC metal temperature | K | **Target** | Out of the wash | Out of the wash |
| LPT cooling flow mixing pressure ratio | - | **Target** | Out of the wash | Out of the wash |
| Thrust | - | **Target** | **Target** | **Target** |
| Engine inlet mass flow | kg/s | **Variable** | Out of the wash | Out of the wash |
| Fan tip pressure ratio | - | **Variable** | Out of the wash | Out of the wash |
| Bypass ratio | - | **Variable** | Out of the wash | Out of the wash |
| Intercooler LP inlet mass flow | kg/s | **Variable** | Out of the wash | Out of the wash |
| Fan root pressure ratio | - | **Variable** | Out of the wash | Out of the wash |
| IPC pressure ratio | - | **Variable** | Out of the wash | Out of the wash |
| HPC pressure ratio | - | **Variable** | Out of the wash | Out of the wash |
| HPT cooling flow (% HPC flow) | % | **Variable** | same as @ToC | same as @ToC |
| LPT cooling flow extraction point (% HPC enthalpy rise) | % | **Variable** | same as @ToC | same as @ToC |
| LPT cooling flow (% HPC flow) | % | Fixed | same as @ToC | same as @ToC |
| Combustor outlet temperature | K | Fixed | **Variable** | **Variable** |
| Intercooler nozzle area | m2 | Out of the wash | **Variable** | **Variable** |
| Bypass nozzle area | m2 | Out of the wash | **Variable** | **Variable** |
| Total cold nozzle area | m2 | Out of the wash | **Target** | **Target** |
| Core inlet mass flow | kg/s | Out of the wash | Out of the wash | Out of the wash |
| High pressure turbine rotor inlet temperature | K | Out of the wash | Out of the wash | Out of the wash |
| Fan tip polytropic efficiency | % | Fixed † | Out of the wash | Out of the wash |
| Fan root polytropic efficiency | % | Fixed | Out of the wash | Out of the wash |
| IPC polytropic efficiency | % | Fixed † | Out of the wash | Out of the wash |
| HPC polytropic efficiency | % | Fixed † | Out of the wash | Out of the wash |
| HPT polytropic efficiency | % | Fixed † | Out of the wash | Out of the wash |
| LPT polytropic efficiency | % | Fixed † | Out of the wash | Out of the wash |
| Intercooler temperature effectiveness | % | Fixed | **Target** | **Target*** |
| Intercooler bypass side pressure loss dP/P | % | Fixed † | Out of the wash | Out of the wash |
| Intercooler core side pressure loss dP/P | % | Fixed † | Out of the wash | Out of the wash |
| Combustor pressure loss dP/P | % | Fixed † | Out of the wash | Out of the wash |
| Jet pipe pressure loss dP/P | % | Fixed † | Out of the wash | Out of the wash |
| Bypass duct pressure loss dP/P | % | Fixed † | Out of the wash | Out of the wash |
| IPC inlet duct pressure loss dP/P | % | Fixed | Out of the wash | Out of the wash |
| HPC outlet diffuser pressure loss dP/P | % | Fixed | Out of the wash | Out of the wash |
| Engine intake pressure loss dP/P | % | Fixed | Out of the wash | Out of the wash |
| Intercooler nozzle thrust coefficient | % | Fixed | Out of the wash | Out of the wash |
| Bypass nozzle thrust coefficient | % | Fixed | Out of the wash | Out of the wash |
| Core nozzle thrust coeffficient | % | Fixed | Out of the wash | Out of the wash |
| HP shaft mechanical efficiency | % | Fixed | Out of the wash | Out of the wash |
| LP shaft mechanical efficiency | % | Fixed | Out of the wash | Out of the wash |
| Gearbox mechanical efficiency | % | Fixed | Out of the wash | Out of the wash |

**** A parametric analysis design variable*** ***† A sensitivity analysis parameter***

Figure 4.5: Geared fan intercooled core configuration modelling assumptions for parametric design and sensitivity analysis.

this paper from the potential benefits of using nozzle variable geometry to further optimise fan performance and propulsive efficiency. The use of variable geometry nozzles for such purposes could very well form the topic of a separate article and in the author's view the respective conclusions from such a study are likely to be - to a first order - independent of fan/LPT arrangement (geared or un-geared) and/or core arrangement (conventional or intercooled).

The study focuses primarily on the intercooled core with the geared fan/LPT arrangement acting as an enabler for high OPR and hence high core efficiency. Nevertheless, there is also focus on the propulsor through the evaluation of optimal specific thrust and jet velocity ratio values. Since the study considers engine weight the results on optimal specific thrust and jet velocity ratio are specific to the geared arrangement. Although, existing geared fan engines have not yet reached 70,000lbf thrust the author would expect them to continue to show a weight benefit relative to direct drive fan engines up to considerably higher thrust levels; this expectation is also supported by recent research on large geared turbofans [29, 102, 103]. Paul Adams, senior vice president of engineering at Pratt & Whitney was quoted in 2010 [104] as saying that "the overall concept of the geared turbofan is scalable up to pretty much any size". Eventually the geared solution may stop saving weight, but perhaps only in a much bigger engine. The gearbox ratio was not selected as a design variable in this study but was instead fixed to a value of 3 which is a reasonable choice for low pressure ratio and low tip speed fans. The interested reader is referred to the very valuable study presented in [105] for more details on gearbox ratio optimisation and the general advantages and disadvantages associated with geared fan configurations.

Fan pressure and/or bypass ratio often appear in the literature as design variables for turbofan engine optimisation studies. In the author's view, specific thrust (which directly relates to propulsive efficiency) and jet velocity ratio are instructive design variables for such studies. They are closely linked to fan pressure ratio and engine noise. Jet velocity ratios relate directly to the transfer of power from the core to the fan and to the trade-off between transfer and propulsive efficiency in optimising SFC and fuel burn. Bypass ratio has a big influence on the mechanical design of the engine, but this parameter is less fundamental to engine performance, being as much dependent on the assumptions made regarding core technology as it is on the specific thrust.

#### 4.2.1.2 Further considerations

The tools and algorithm described in Chapter 3 have been used here not only for predicting the engine performance but also for establishing the gas path layout for every design variant. The rubberized-wing aircraft model has been utilised to account for snowball effects. Furthermore, a second block fuel value has been calculated using a surrogate model based on the SFC and penalty weight exchange rates presented earlier through Table 3.4.

It must be noted that the study has not considered explicitly the potential effect that different thermo-mechanical and aerodynamic design choices may have on overall system performance. The author has chosen to fix or limit component aerodynamic performance parameters such as flow factors, tip Mach numbers and/or stage loadings to values that ensure that the assumed efficiencies can be established. The limits set on maximum mean stage loading (for the LPT) and minimum deHaller number (for the IPC and HPC) will be responsible in the results presented in the next sections for the changes observed in component stage count and the associated discontinuities in engine weight and block fuel. This approach is largely based on previous experience and engineering judgement and is in contrast to carrying out a full system level study for the optimal values of these parameters. Future research work could be focused on assessing these aspects and may merit a revisit of this study and some of its conclusions.

In the results presented in the next sections, the yellow square indicates the optimal design parameter value for mid-cruise SFC. The green circle indicates the optimal design parameter value for minimum business case block fuel when the rubberised-wing aircraft model has been used. The ordinate in the plots is relative to the corresponding optimum cruise SFC value. It should be noted that these symbols indicate different optimal designs for each single parameter study, not the global optima.

#### 4.2.1.3 Specific thrust

Within this investigation the specific thrust at hot-day top of climb was varied (at a fixed jet velocity ratio and thrust level) within a range considered reasonable. The specific thrust at ISA mid-cruise was consequently determined by executing the performance model at the corresponding operating condition. The variation of the main fan design parameters is shown in Fig. 4.6.

It is well known that propulsive efficiency will improve with reducing specific thrust, as illustrated in Fig. 4.7. The reducing fan pressure ratio at constant bypass duct pressure loss, leads to a deteriorating transfer efficiency and hence in a reduction in thermal efficiency which nearly halves the SFC benefit from the reduced specific thrust level [2, 106]. As specific thrust is reduced further - substantially below the range covered in this study - it is expected that minimum SFC will be reached when the diminishing rate of improvement in propulsive efficiency just balances the rate of reduction in transfer efficiency. For bypass duct pressure losses in the order of 1%, one can expect to start seeing parity at cruise specific thrust levels in the region of 60m/s.

Reduced specific thrust designs are directly associated with substantial increases in engine weight and hence reductions in engine thrust to weight ratio. As the specific thrust is reduced the fan and nacelle diameters increase leading to a substantial component weight increase. Furthermore, the increasing bypass ratio associated with the reducing fan pressure ratio makes the design of the LPT more difficult eventually leading to an increase in stage count. These observations are illustrated in Fig. 4.8.

The optimal specific thrust level (or fan diameter at given fan flow capacity) for business case block fuel is determined as a trade-off between the decreasing SFC and the rising engine weight and nacelle drag (with rising diameter), as can be observed in Fig. 4.9.

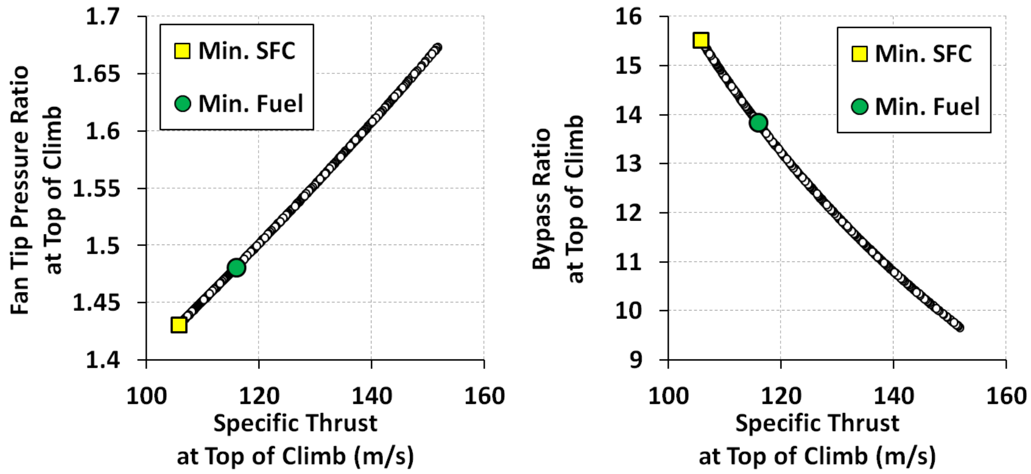


Figure 4.6: Fan design parameters at top of climb.

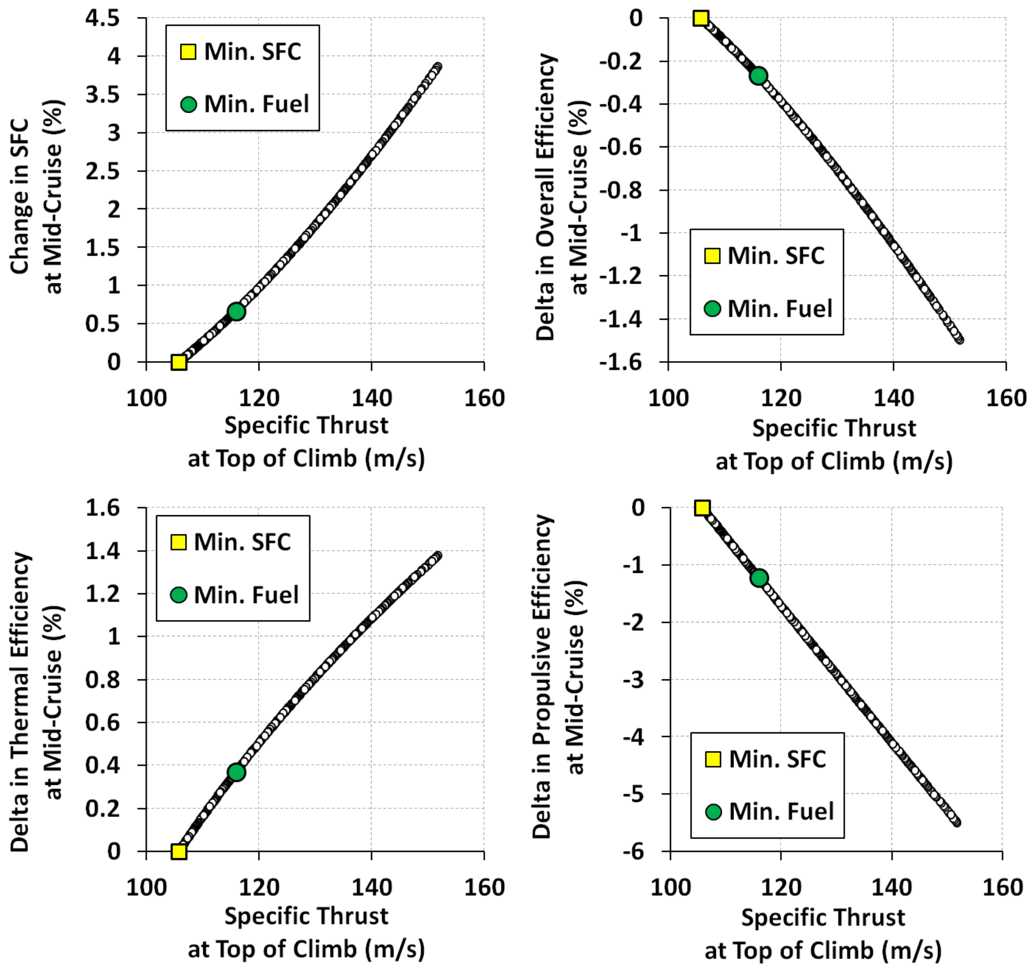


Figure 4.7: Specific thrust vs efficiency at mid-cruise.

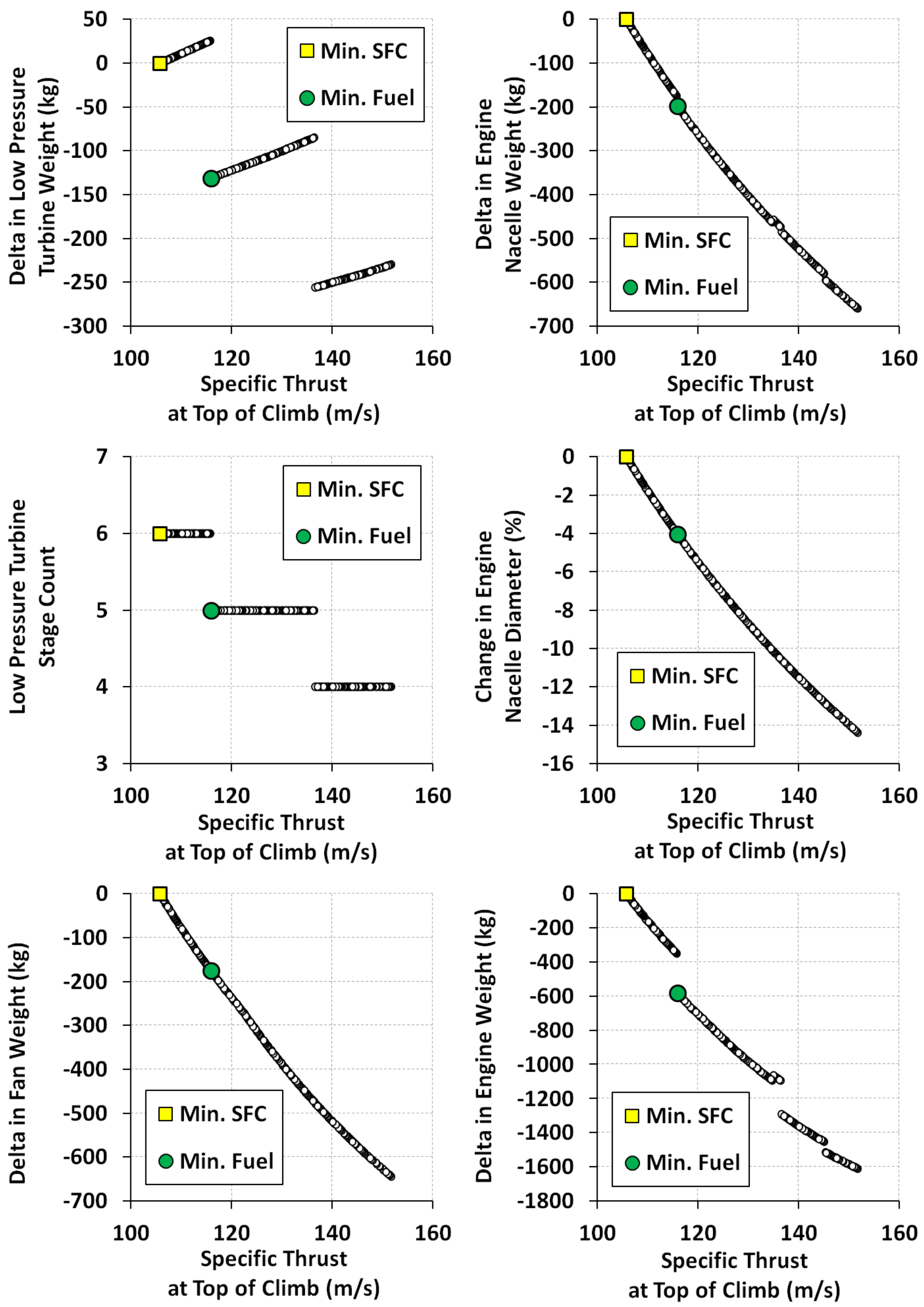


Figure 4.8: Specific thrust vs engine component weight, size and stage count.

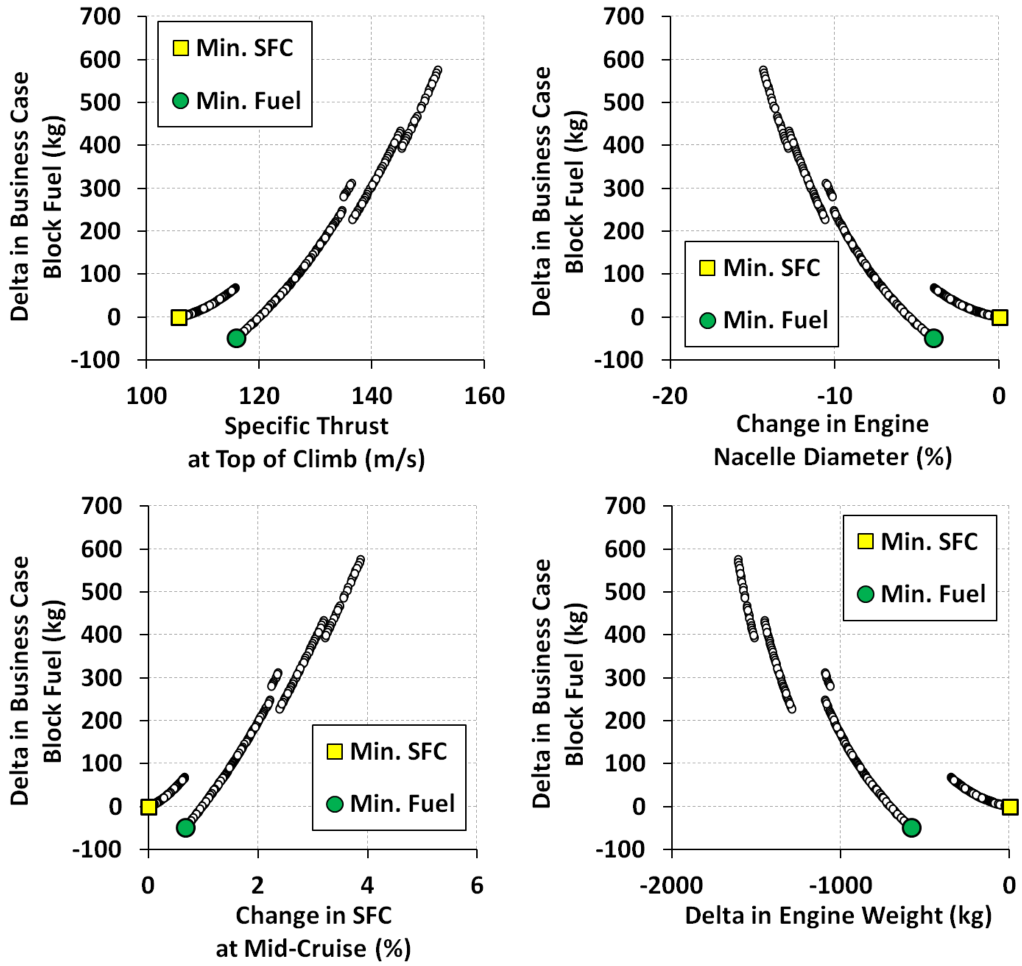


Figure 4.9: Specific thrust vs block fuel.

#### 4.2.1.4 Jet Velocity Ratio

As part of this investigation the jet velocity ratio at hot-day top of climb conditions was varied within a range considered reasonable (and hence the corresponding engine bypass ratio at a given specific thrust). The jet velocity ratio at ISA mid-cruise conditions has therefore been left to be the result of engine steady-state matching effects. Engine thrusts have been calculated using estimates of real nozzle performance, but the "jet velocity ratio" parameter is calculated assuming full expansion of each stream as in an ideal convergent-divergent nozzle.

Walsh and Fletcher [40] and Guha [107] both suggest an ideal value for the jet velocity ratio in the range of 0.8 to 0.85 for modern turbofans according to (4.1).

$$\left(\frac{V_{cold}}{V_{hot}}\right)_{optimal} = \eta_{Fan} \cdot \eta_{LPT} \cdot \eta_{LPshaft} \tag{4.1}$$

With jet velocity ratio increasing, propulsive efficiency improves while transfer efficiency deteriorates, as can be observed in Fig. 4.10. The optimal jet velocity ratio at mid-cruise for SFC is primarily determined by the fan, low pressure turbine, and shaft efficiencies, as well as by the bypass duct and core jet pipe pressure losses. Nevertheless, the optimal jet velocity ratio is actually higher than the value one would expect by using the formula presented in (4.1), particularly at mid-cruise. The main reason for this is that jet velocity ratio affects core efficiency at mid-cruise due to a combination of several different subtle changes to the core cycle and core component efficiencies at this condition. The presented formula does not consider changes in core efficiency and the beneficial effect of intercooling on transfer efficiency, nor account for losses in the bypass duct and jet pipe, whilst a relatively detailed engine performance model such as the one utilised in this study does. Although, the characteristics used in this study are scaled from existing characteristics of similar components the author considers that the observed behaviour in terms of engine performance is to some extent generic and also indicative of the inherent uncertainties in component and overall engine performance during the conceptual design phase. Using a relatively detailed engine performance model for optimising the jet velocity ratio will tend to yield more reliable results than the presented formula; it should be kept in mind however that the expected difference in terms of SFC is unlikely to be higher than 0.1%.

The optimal jet velocity ratio at top of climb for minimum mid-cruise SFC is significantly lower than the optimal value for top of climb SFC, as can be observed in Fig. 4.11. In fact, one has to trade SFC at top of climb even further when the figure of merit is business case block fuel. The reason for this is the detrimental effect that high jet velocity ratio values at top of climb have on engine weight and in particular on low pressure turbine weight. The jumps observed in component and overall engine weight are attributed to stage count changes in the respective components.

Block fuel results from the surrogate model are in good agreement with the results obtained from the rubberised-wing aircraft model, as can be observed in Fig. 4.12. These results indicate that it is possible to use SFC and weight penalty exchange rates for determining the optimal jet velocity ratio. It is interesting to note that the optimal jet velocity ratio at mid cruise conditions for business case block fuel is substantially closer to the value suggested by the formula presented in (4.1).

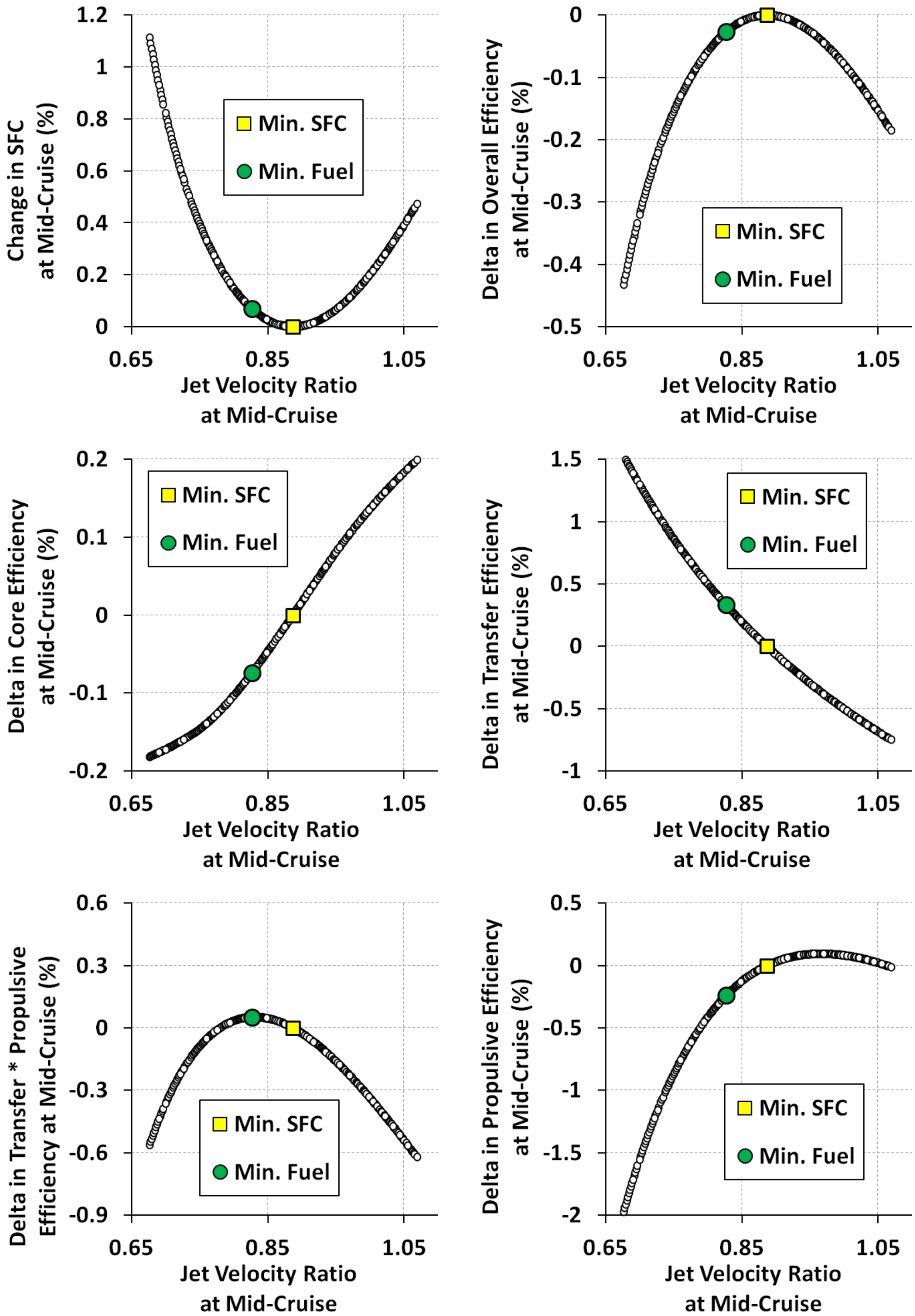


Figure 4.10: Jet velocity ratio vs mid-cruise SFC and efficiency.

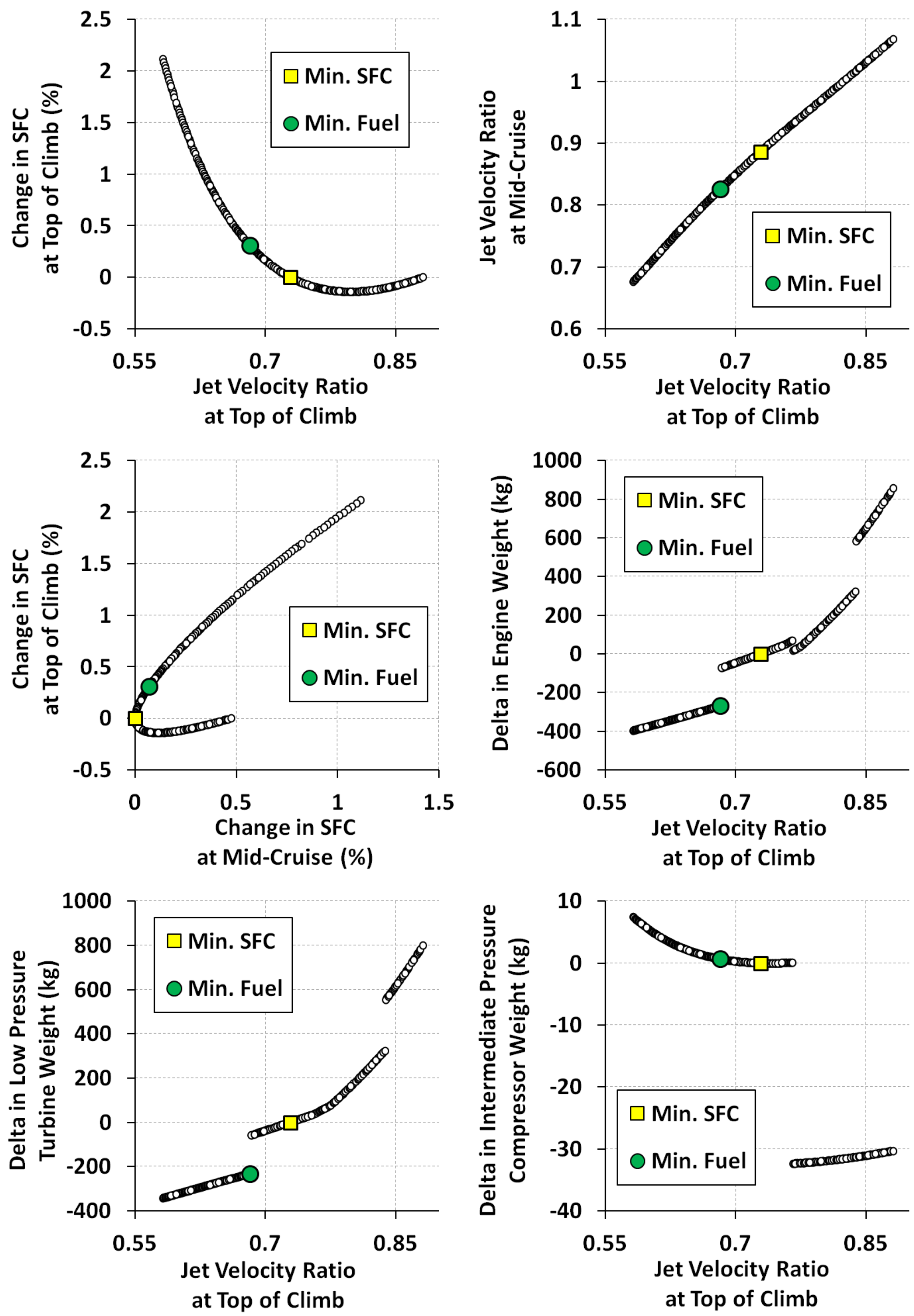


Figure 4.11: Jet velocity ratio vs top of climb behaviour and engine weight.

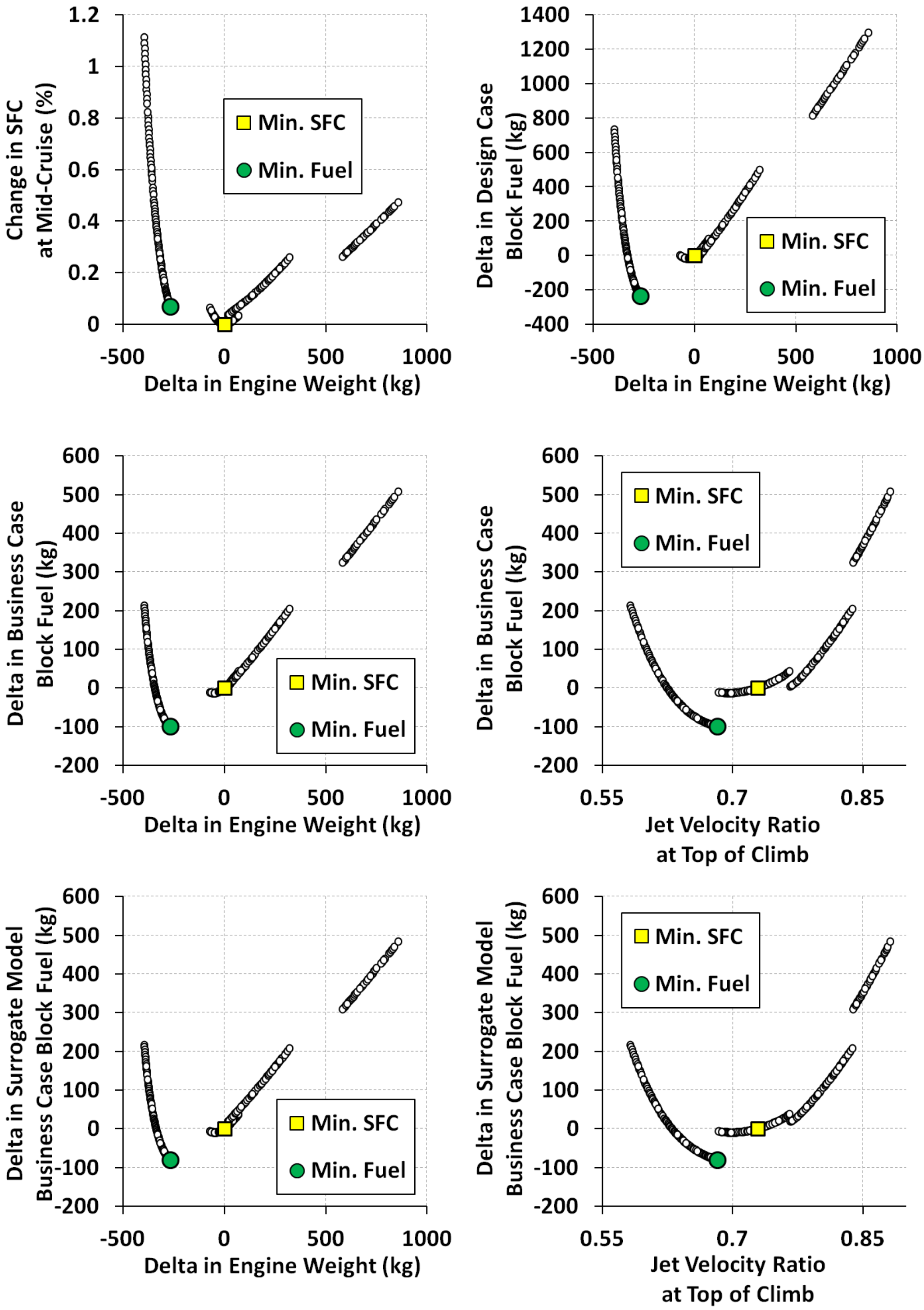


Figure 4.12: Jet velocity ratio vs block fuel.

#### 4.2.1.5 Intercooler mass flow ratio

As part of this investigation the intercooler mass flow ratio at hot-day top of climb has been varied within a range considered reasonable (and hence the corresponding intercooler splitter bypass ratio at a given total cold stream mass flow,) while the intercooler effectiveness at this condition has been held constant. The intercooler mass flow ratio at ISA mid-cruise conditions has been determined by the variable geometry setting required in the intercooler (auxiliary) cold nozzle in order to achieve the required effectiveness level.

As the intercooler mass flow ratio is increased transfer efficiency (and hence SFC) deteriorates since a larger part of the cold flow has to go through the high pressure loss route, as can be observed in Fig. 4.13. In the particular intercooler configuration, a high intercooler mass flow ratio is beneficial for intercooler weight (and hence engine weight) since it helps maintain higher temperature gradients across the length of the module and therefore higher heat transfer rates. In the design model utilised for this study, it is assumed that the intercooler size directly affects the engine nacelle diameter, since a larger intercooler will have the tendency to push the nacelle lines further outwards in order to maintain a satisfactory Mach number in the bypass duct. Increasing the intercooler mass flow ratio inevitably results in an increase in nacelle diameter which in turn can have an adverse effect on block fuel. As can be observed in Fig. 4.14, the optimal trade-off for block fuel is established at relatively low intercooler mass flow ratios. It can also be observed that the block fuel results from the surrogate model are not in good agreement with the results from the rubberised-wing aircraft model indicating that the use of SFC and penalty weight exchange rates alone is not sufficient for determining the optimal intercooler mass flow ratio. Drag count exchange rates must be utilised in order to properly consider intercooler sizing effects on nacelle diameter.

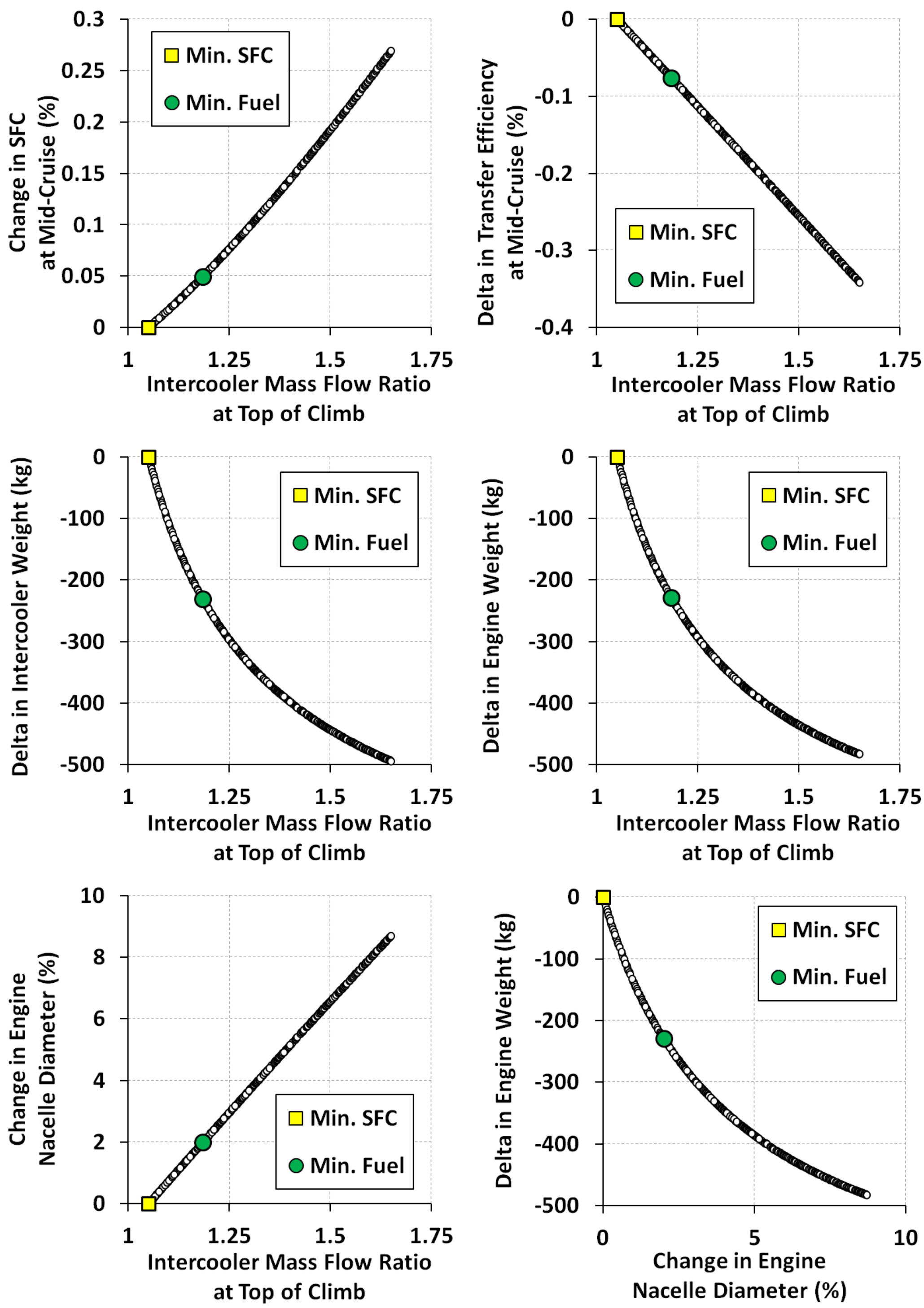


Figure 4.13: Intercooler mass flow ratio vs mid-cruise SFC, efficiency, weight and size.

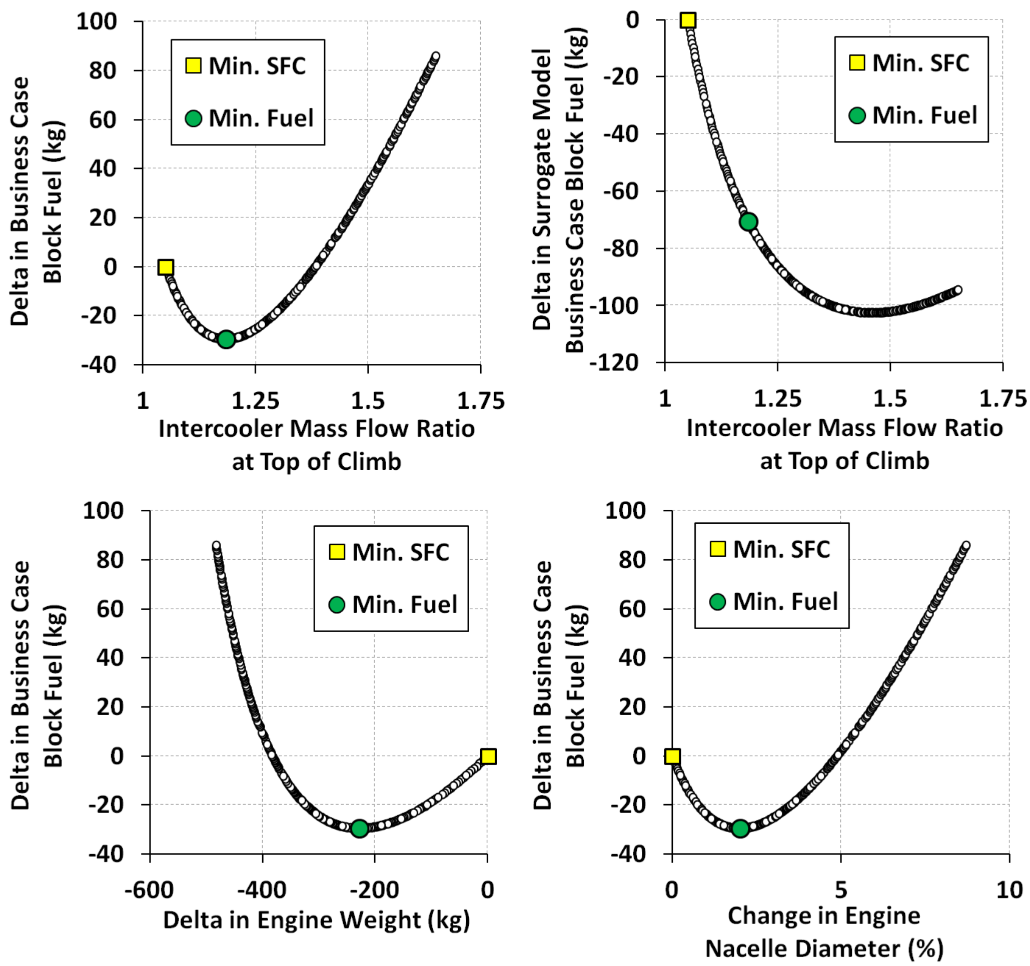


Figure 4.14: Intercooler mass flow ratio vs block fuel.

#### 4.2.1.6 Pressure ratio split exponent

As part of this investigation the pressure ratio split exponent at hot-day top of climb was varied within a range considered reasonable (and hence the intermediate and high pressure compressor pressure ratios at a given overall pressure ratio). The pressure ratio split exponent at ISA mid-cruise conditions was therefore left to be the result of engine steady-state matching effects.

To maximise core efficiency the intercooler should reject only relatively low grade heat to the cooling flow. Thus the split between the compressors should be biased towards the front end of the compression system with the IPC pressure ratio a relatively low proportion of the OPR. On the other hand, transfer efficiency deteriorates with reducing pressure ratio split exponent leading to a unique optimal design choice for thermal efficiency and SFC, as can be observed in Fig. 4.15. It is interesting to observe in Fig. 4.16 that the pressure ratio split exponent barely varies between top of climb and mid-cruise, and so does its optimal value for SFC. Shifting some of the pressure ratio to the IPC has a beneficial effect on engine weight and length, as shown in Fig. 4.17. As can be observed in Fig. 4.18, this is mainly attributed to the fact that a given pressure ratio can be achieved with less stages in the IPC, compared to the HPC, primarily due to the higher tip Mach number chosen for the former. The discontinuities in the engine weight trend are due to stage count changes in the IPC, HPC and LPT.

As can be observed in Fig. 4.19, the optimal design for business case block fuel is established at a substantially higher pressure ratio split exponent, compared to the optimal value for SFC. This is attributed to the beneficial effect on engine weight that is observed when shifting some of the pressure ratio to the IPC. It can also be observed that the block fuel results from the surrogate model are in good agreement with the results from the rubberised aircraft wing model indicating that the use of SFC and weight exchange rates alone is sufficient practice for determining the optimal pressure ratio split. It is interesting to note that Walsh and Fletcher [40] suggest a pressure ratio split exponent of 0.3 for thermal efficiency and 0.5 for specific power. Their work however looked at an intercooled cycle for power generation and hence did not consider engine weight and size effects nor the relatively small but beneficial effect of intercooling on transfer efficiency.

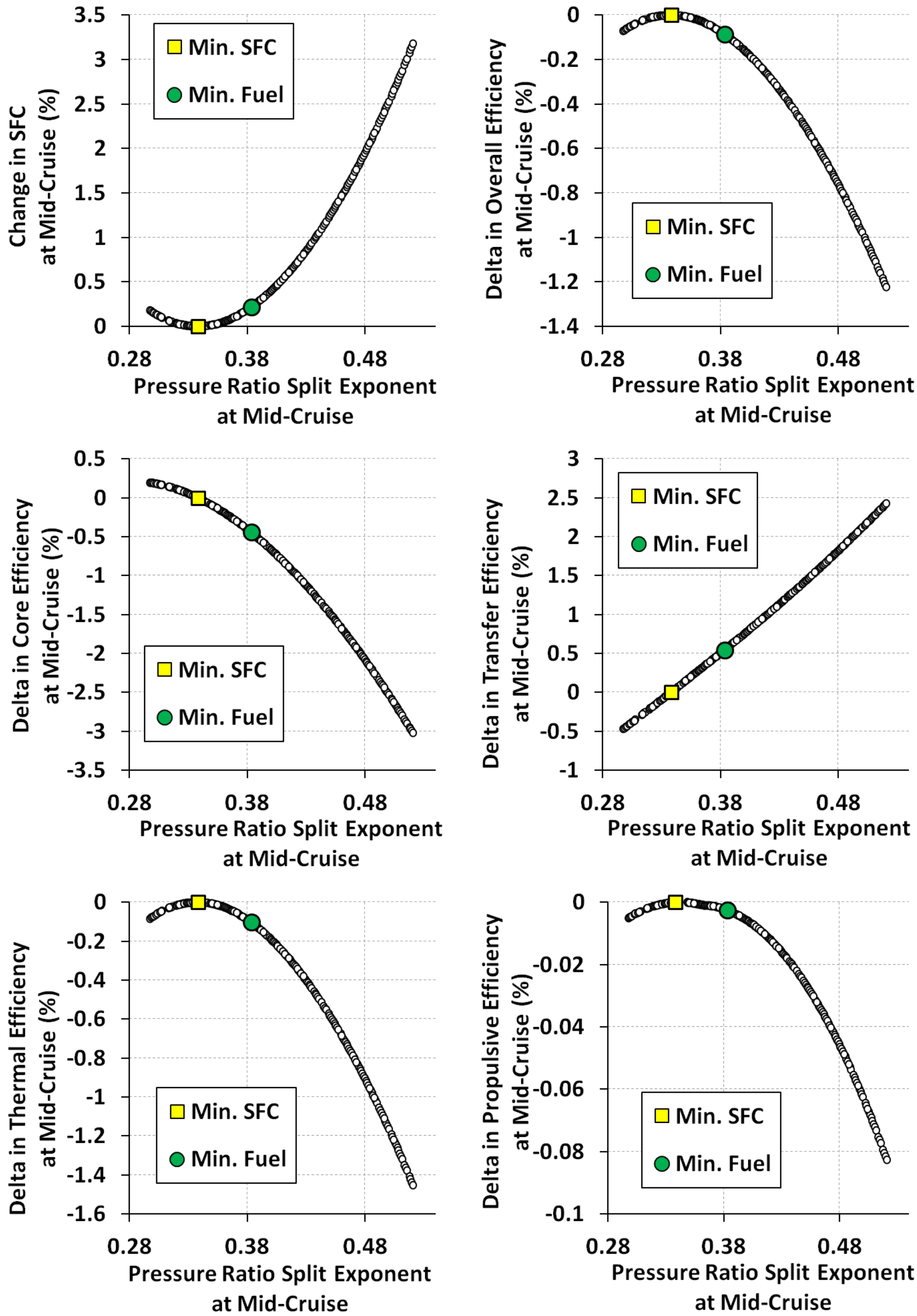


Figure 4.15: Pressure ratio split vs mid-cruise SFC and efficiency.

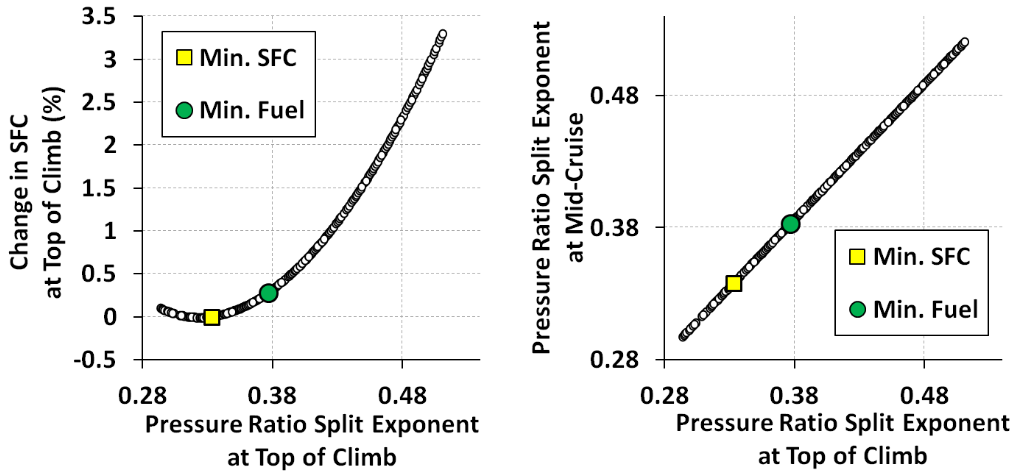


Figure 4.16: Pressure ratio split vs top of climb SFC.

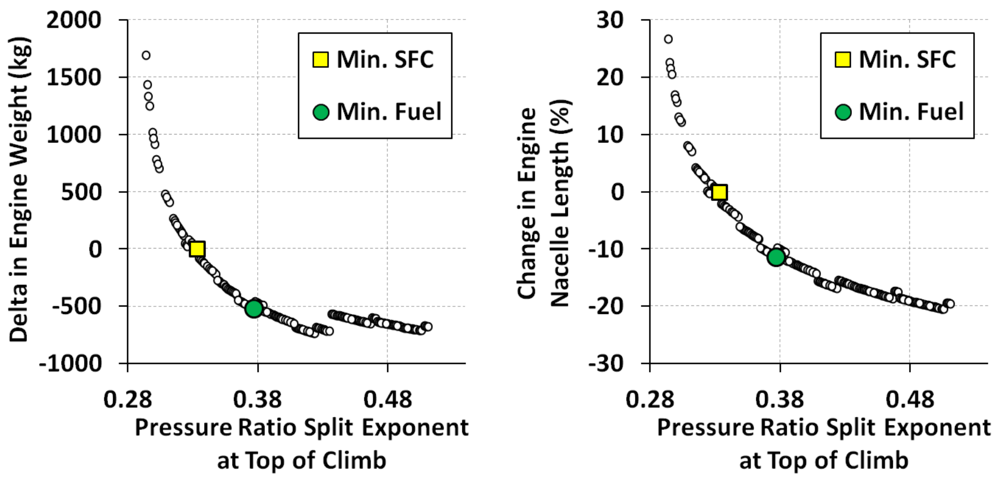


Figure 4.17: Pressure ratio split vs engine weight and size.

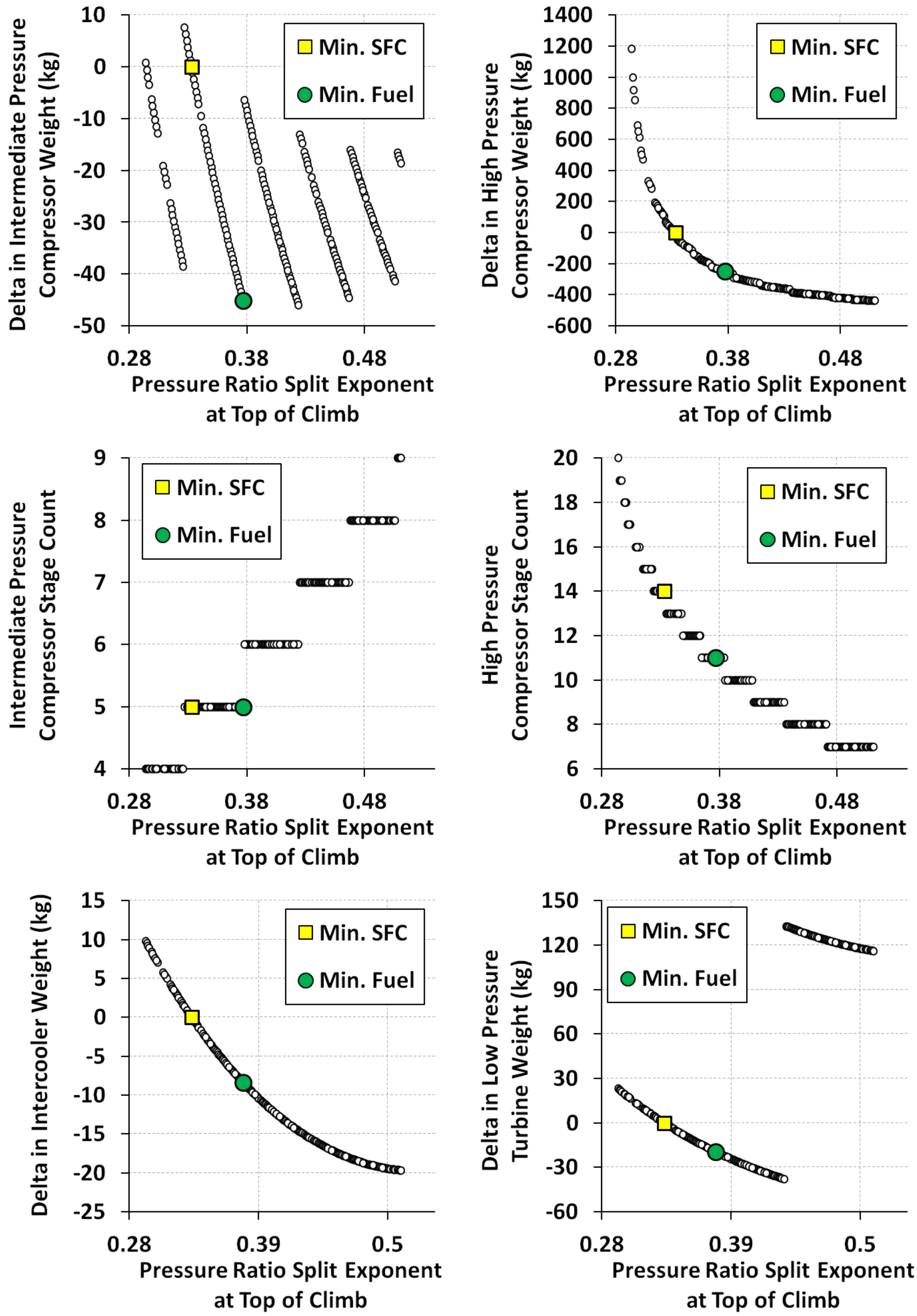


Figure 4.18: Pressure ratio split vs engine component weight and stage count.

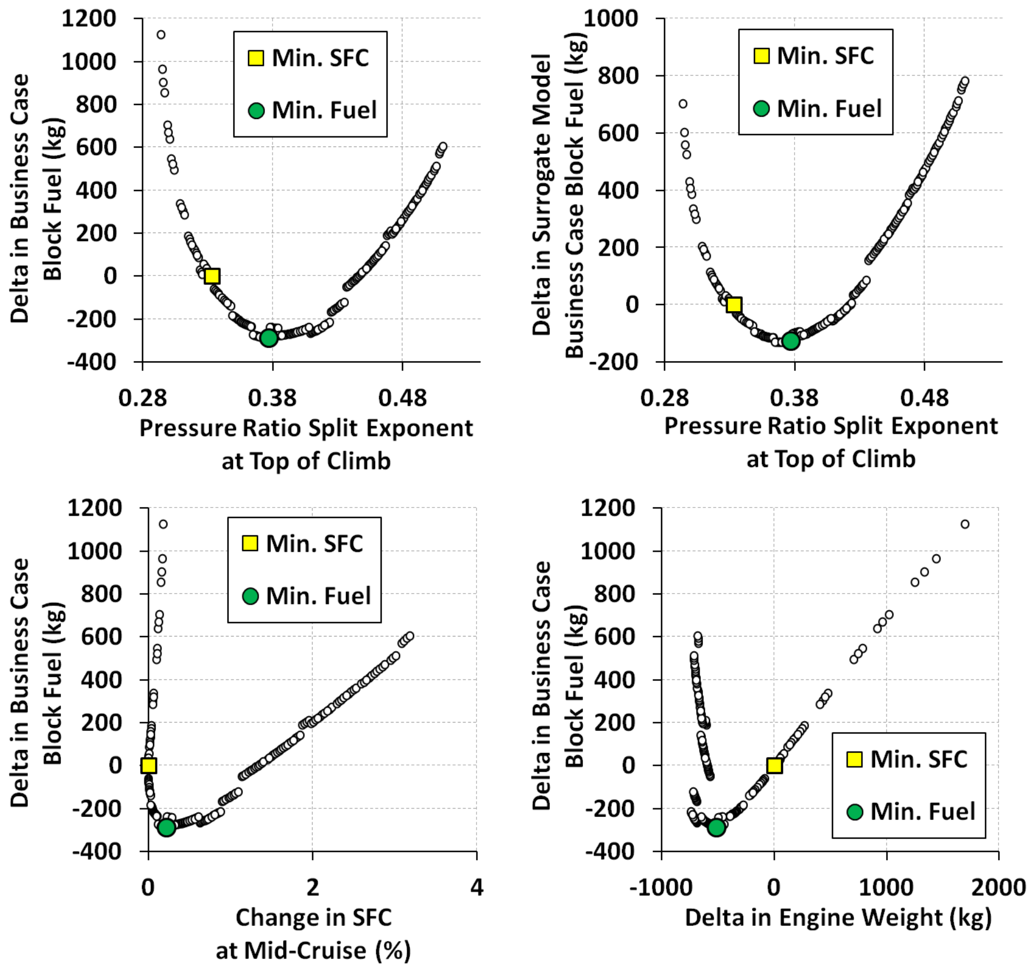


Figure 4.19: Pressure ratio split vs block fuel.

#### 4.2.1.7 Overall pressure ratio

As part of this investigation the OPR at hot-day top of climb was varied within a range considered reasonable (at a fixed pressure ratio split exponent). The OPR level at ISA mid-cruise conditions was therefore left to be the result of engine steady-state matching effects.

A first look at Fig. 4.20 indicates that a high OPR is required for optimal mid-cruise SFC. Furthermore, there is an engine weight benefit at high OPR values pushing the optimum for business case block fuel to even higher levels. As can be observed in Fig. 4.21, as OPR increases more heat is rejected to the intercooler cold stream which is beneficial to transfer efficiency but on the expense of a deteriorating core efficiency. The optimal OPR level for mid-cruise SFC is therefore a trade-off between the rising transfer efficiency and the decreasing core efficiency.

The beneficial effect of high OPR on engine weight is illustrated in Fig. 4.22. As OPR is increased the corrected mass flow at the HPT and LPT entry drops resulting in smaller flow areas and hence smaller and lighter blades. Increasing OPR at a constant jet velocity ratio at top of climb means that engine bypass ratio needs to be reduced (i.e. higher core mass flow) which eventually leads to a stage count drop in the LPT. A beneficial effect on engine component weight can also be observed for the HPC with rising OPR up to the level that an extra HPC stage is required. The weight saving can be attributed to the fact that at a constant pressure ratio split exponent and intercooler effectiveness level, rising OPR levels lead to a higher density at entry to the HPC and hence smaller and lighter blades. The IPC weight tends to increase with OPR primarily due to the increase in core mass flow.

The optimal OPR level for business case block fuel is determined as a trade-off between engine weight and SFC, as can be observed in Fig. 4.23. It should be noted however that SFC and engine weight are relatively insensitive to OPR when the latter ranges between 90 to 100. This indicates that the economic optimum is likely to be at a significantly lower OPR value than it may be for block fuel.

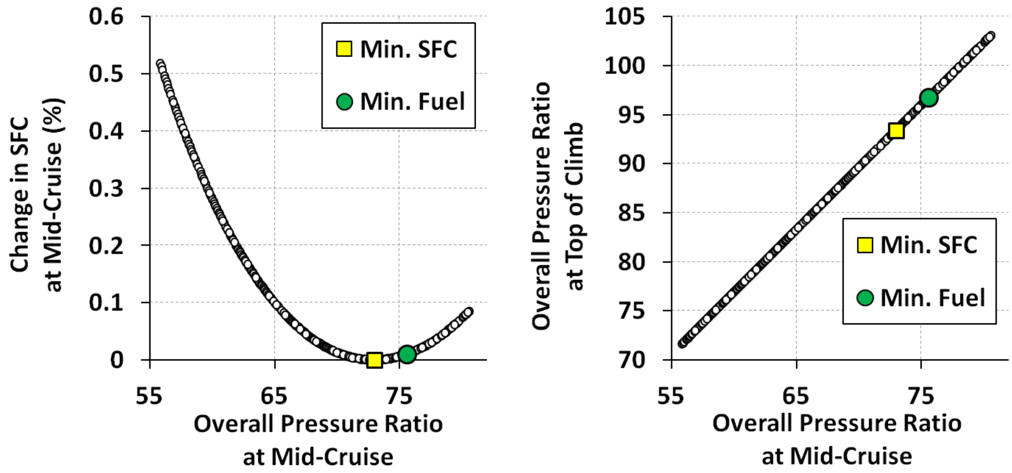


Figure 4.20: Overall pressure ratio vs SFC at mid-cruise.

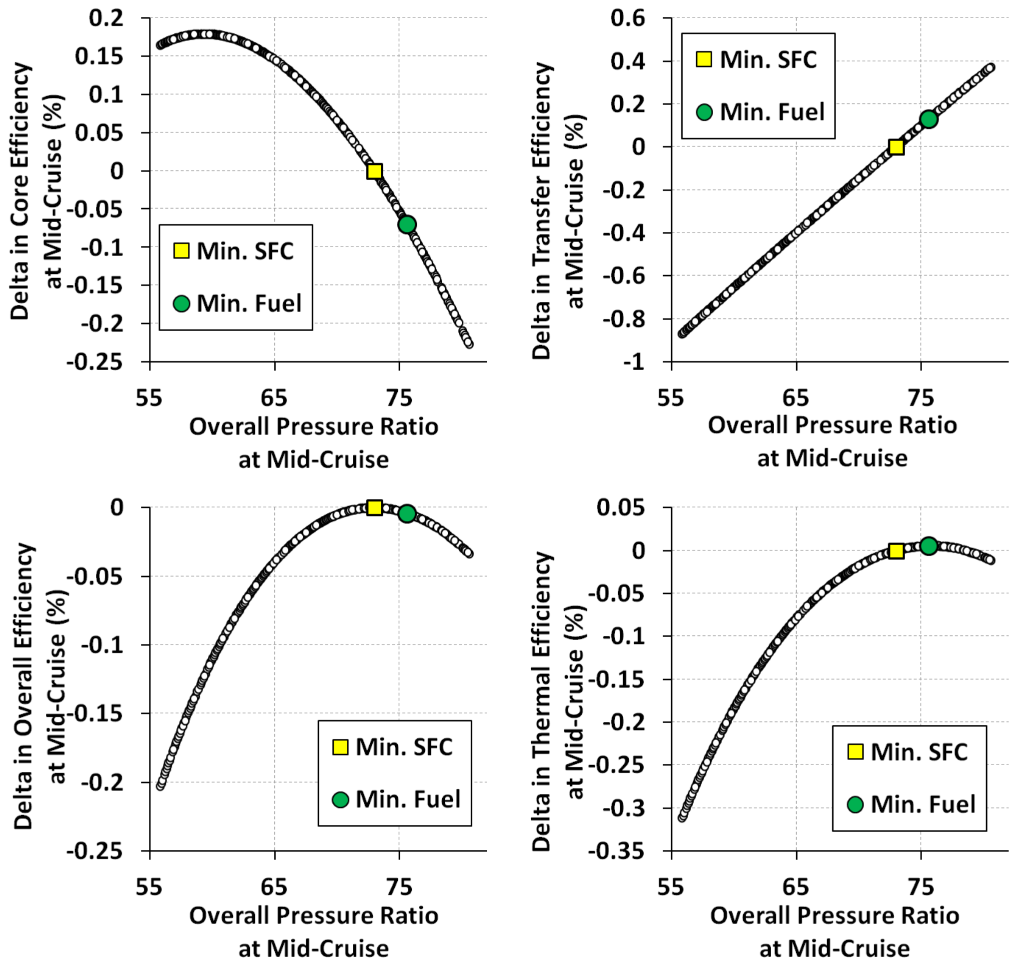


Figure 4.21: Overall pressure ratio vs efficiency at mid-cruise.

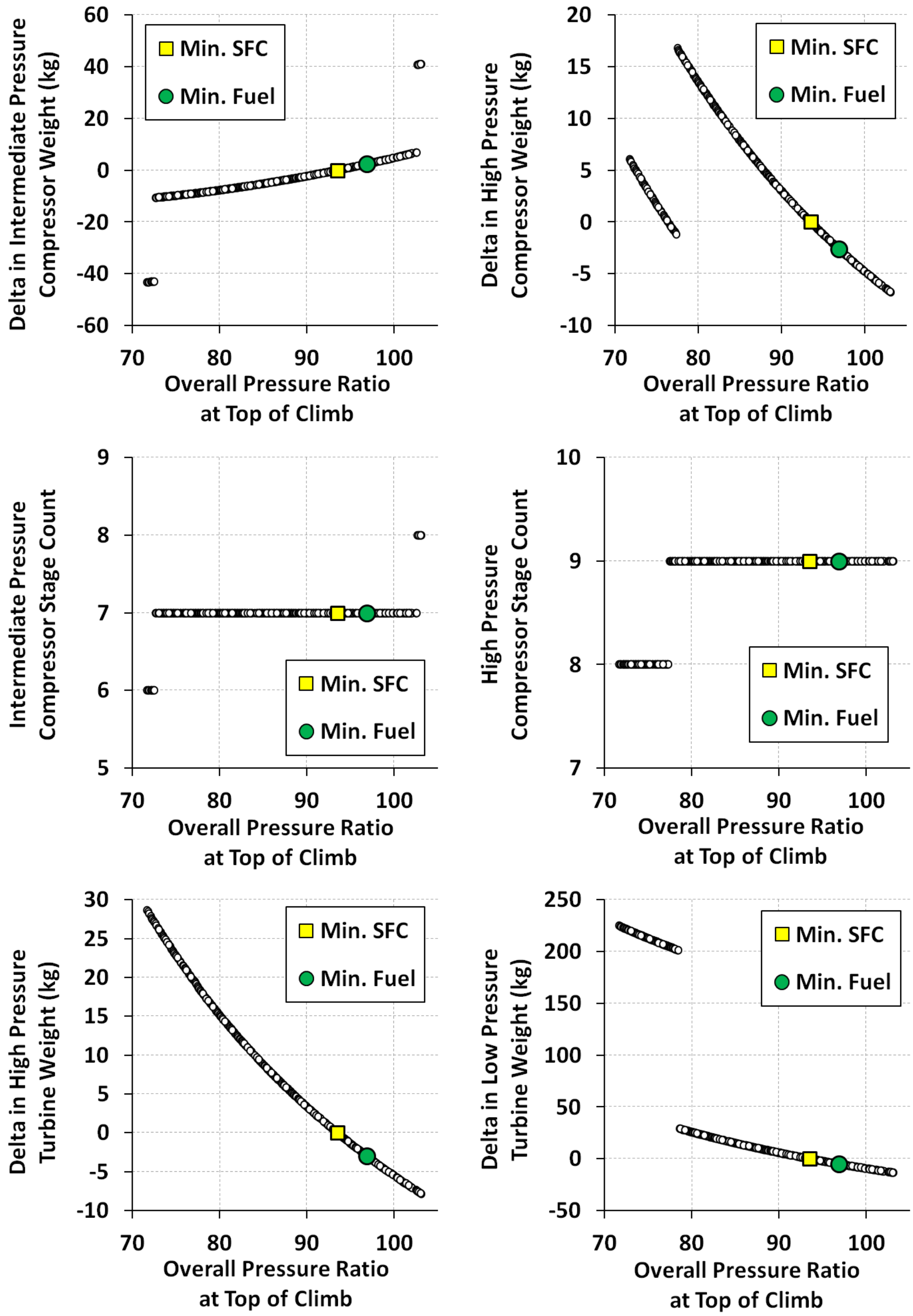


Figure 4.22: Overall pressure ratio vs engine component weight and stage count.

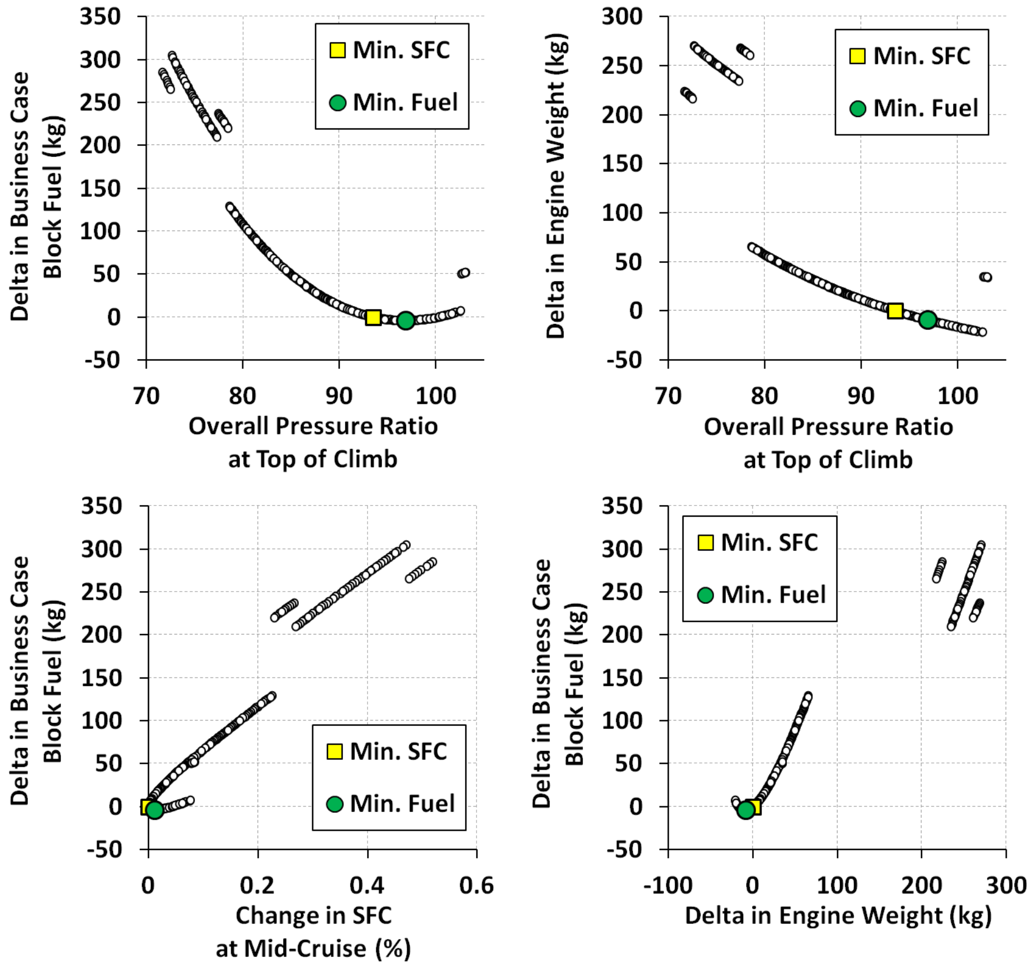


Figure 4.23: Overall pressure ratio vs block fuel.

#### 4.2.1.8 Intercooler effectiveness at mid-cruise

As part of this investigation the intercooler effectiveness at ISA mid-cruise was varied within a range considered reasonable (at a fixed hot-day top of climb thrust and jet velocity ratio) by utilising the variable geometry in the auxiliary intercooler nozzle. The intercooler effectiveness at top of climb conditions was kept constant throughout this study.

The variation of intercooler pressure losses, bypass ratio and combustor outlet temperature at mid-cruise is shown in Fig. 4.24. As can be observed, increasing intercooler effectiveness at a given thrust increases pressure losses in the intercooler hot and cold sides. Furthermore, it reduces both combustor outlet temperature and bypass ratio while fuel mass flow also drops up to a certain point where the increased core mass flow negates any benefit from the reduced combustor outlet temperature.

Through a close look at Fig. 4.25, it can also be observed that as intercooler effectiveness is increased, core efficiency drops and transfer efficiency improves since more heat is transferred from the core to the bypass stream. As intercooler effectiveness increases further, transfer efficiency eventually starts to drop as a result of the increasing pressure loss levels in the intercooler. As a second order effect, the jet velocity ratio at mid-cruise increases with increasing intercooling effectiveness - remembering that jet velocity ratio is fixed at top of climb - resulting in a marginally better propulsive efficiency.

The optimal levels of intercooler effectiveness for mid-cruise and business case block fuel are illustrated in Fig. 4.26. It can be observed that the optimal level of intercooling effectiveness will vary continuously during the cruise phase; the optimal value at every flight segment will be a function of altitude, flight Mach number and thrust requirement. At higher cruise altitudes a lower level of intercooling effectiveness will be optimal and this can help explain why the mid-cruise SFC and business case block fuel do not coincide i.e., the cruise phase for the business case takes place at a higher altitude than was assumed for the mid-cruise conditions.

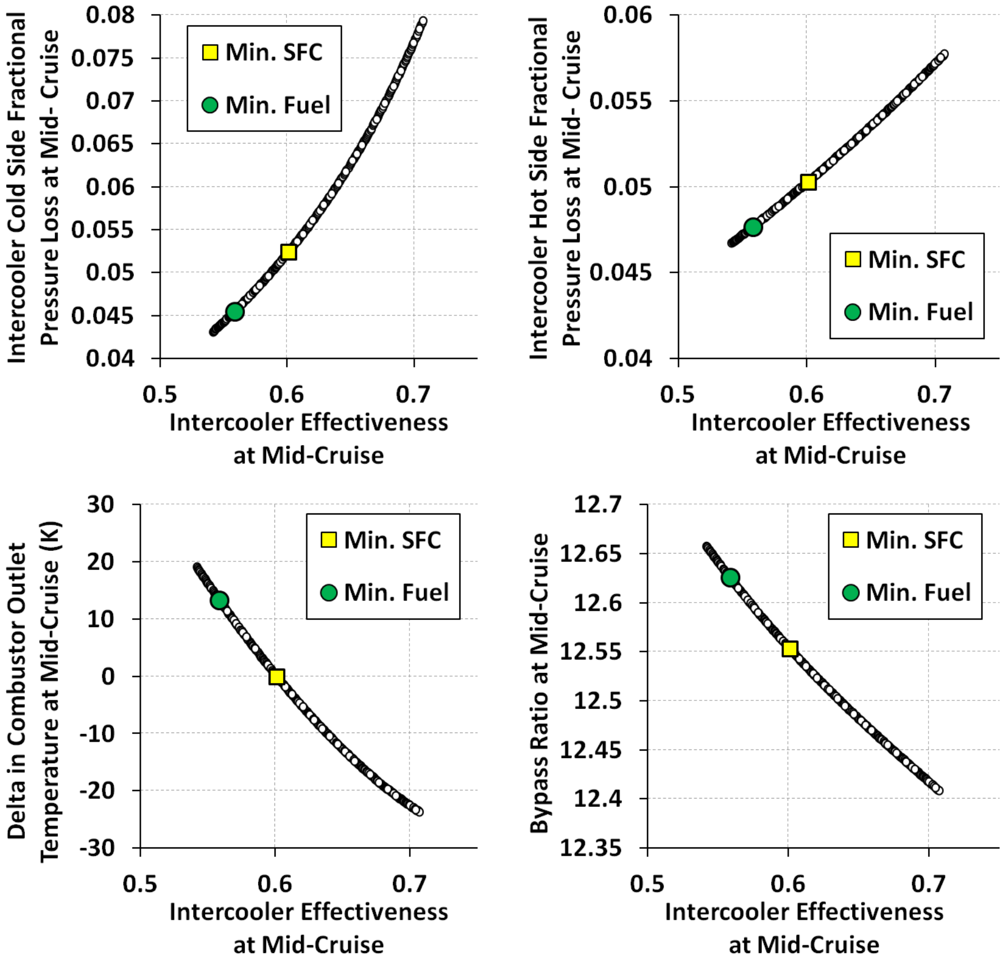


Figure 4.24: Intercooler effectiveness at mid-cruise vs combustor outlet temperature and bypass ratio.

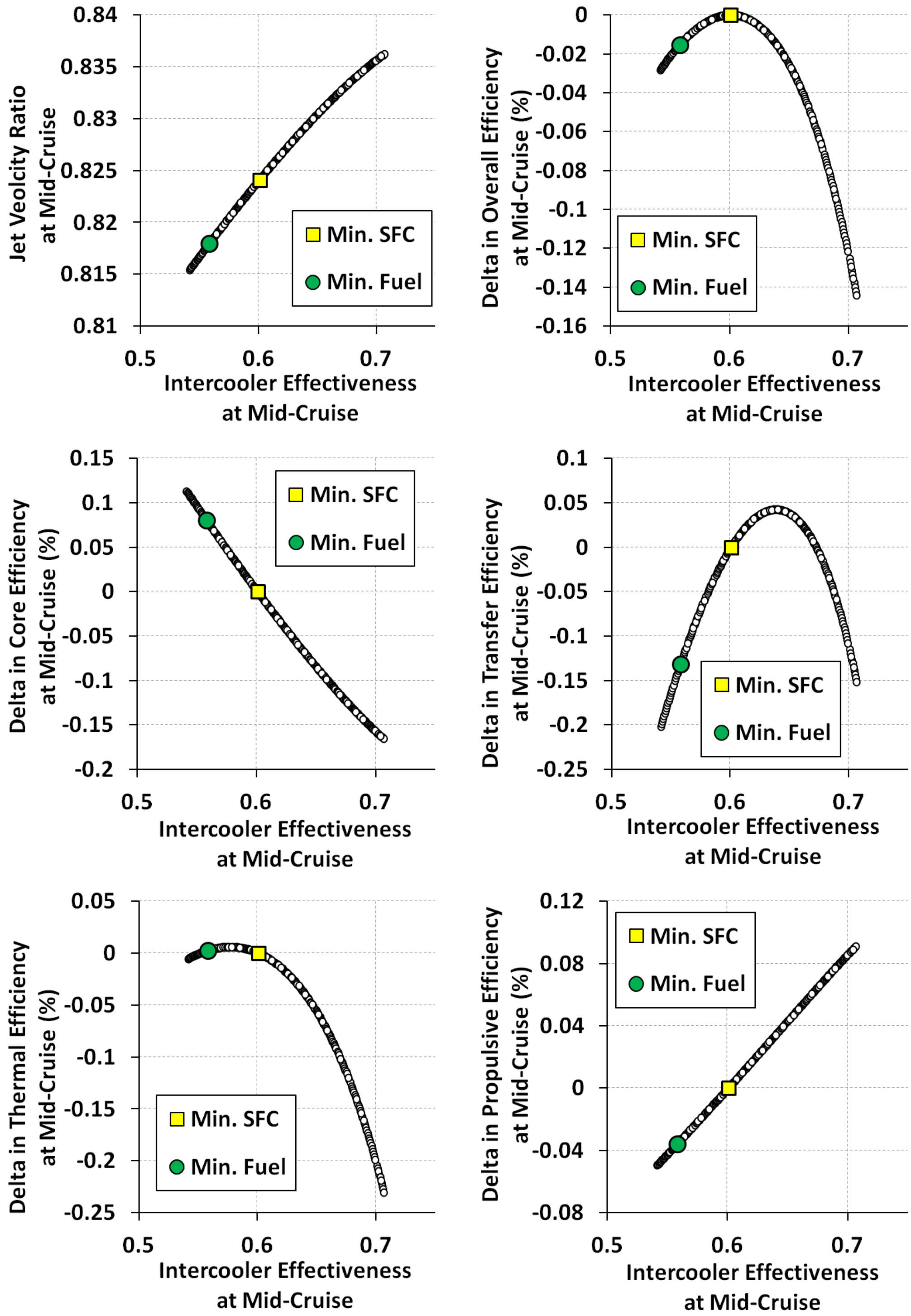


Figure 4.25: Intercooler effectiveness at mid-cruise vs efficiency.

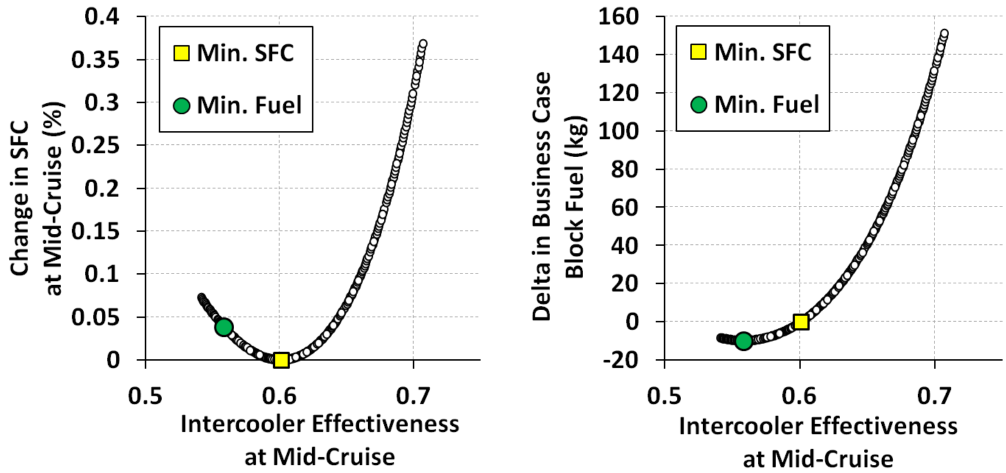


Figure 4.26: Intercooler effectiveness at mid-cruise vs block fuel.

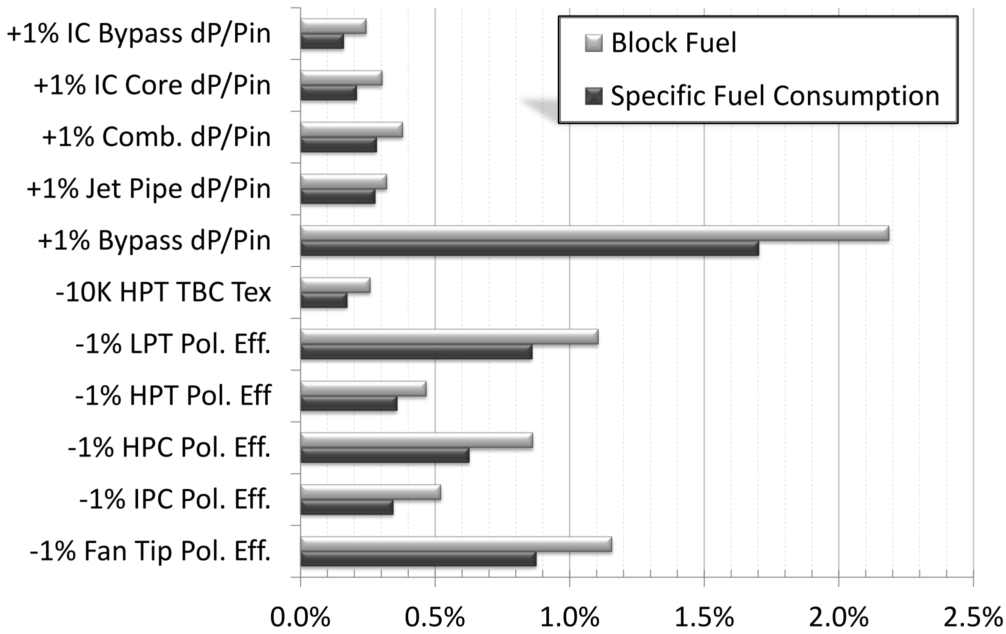


Figure 4.27: Sensitivity analysis for different technology target parameters.

#### 4.2.1.9 Exchange rates

The sensitivity analysis presented in this section aims to deliver averaged exchange rates which can be used to investigate the effect of technology parameter deviations on block fuel. These exchange rates were derived by keeping all design parameters including thrust at their datum values (as discussed in the modelling assumptions section) and introducing single perturbations, one for each technology target parameter, at hot-day top of climb conditions. The technology target parameters studied were: component polytropic efficiencies, duct, combustor and intercooler pressure losses, and HPT TBC average external surface metal temperature (by varying the HPT cooling flow).

The exchange rates are presented in Fig. 4.27 and should be perceived as variations from the technology target values that were assumed when deriving the nominal engine design. Each exchange rate figure represents the average of a set of 40 exchange rate values derived within a $\pm 1\%$ (or $\pm 10$ K) range through first order forward finite-differentiation. The derived values were visually inspected prior to being averaged and did not demonstrate considerable variation. It is the author's view that relatively small deviations from the datum cycle - as will be proposed in the following sections - will not invalidate the derived exchange rates and the specific conclusions presented in this section. The sensitivity parameters compiled allow for system level quantification of the importance of research on specific component technologies i.e. they can be used to assess the importance of progress in specific component technologies for this engine configuration.

Inversely, they also help quantify the impact of technology shortcomings.

The influence of the low pressure system component technology on performance is quite marked for the geared variant of the intercooled core configuration for long range applications. This is justified considering the fact that this a fairly low specific thrust design. In fact, the low pressure system component technology has the greatest influence on performance, as expected for an ultra high bypass ratio engine; significant fuel benefits are expected by improving fan and LPT efficiency. Inversely, shortcomings in meeting projected technology targets for the low pressure system will have a major impact on overall engine/aircraft performance.

With fan mass flow increasing and fan tip pressure ratio reducing, pressure losses in the bypass duct tend to have an increasingly dominant effect on transfer efficiency and, hence, on the impact of propulsive efficiency improvements on SFC. As can be observed in Fig. 4.27, a 1% increase in bypass duct pressure losses will reduce the projected block fuel benefits by roughly 2.2%. It should be noted here that previous work [101] has indicated that a 10 [in] increase in fan diameter and the consequent reduction in specific thrust is unlikely to give more than a 0.85% improvement in block fuel.

The efficiency of the IPC has a significantly smaller influence on block fuel, compared to the HPC, which reflects the significantly higher pressure ratio placed on the High Pressure (HP) shaft and despite the beneficial effects on compressor work due to intercooling. Similarly, the efficiency of the HPT has a substantially lower influence on block fuel, compared to the LPT for the same reasons. The influence of jet pipe and combustor pressure losses, as well as HPT external surface blade metal temperature on block fuel is far from negligible. Failure to deliver the expected efficiency levels for the compressor components will increase combustor inlet temperatures resulting in higher $NO_x$ levels and reduced component life; combustor designs are highly sensitive to inlet conditions and it is highly likely that a significant shortcoming in compressor efficiency would result in a re-design of the combustor.

It can be observed, that intercooler pressure losses have a non-negligible effect on block fuel. Losses in the intercooler hot stream are relatively more important compared to losses in the cold stream, although it should be expected that losses in the cold stream should become increasingly important as the intercooled mass flow ratio (W132Q25) is increased. Failure to achieve the intercooler pressure loss targets set can significantly reduce the projected block fuel benefits for the intercooled core configurations.

#### 4.2.1.10 Summary

The presented study has been focused on the isolated effect that six major design parameters have on specific fuel consumption, engine weight and mission fuel. A summary of these investigations is presented in Table 4.4 and is compared against the intercooled cycle from [82].

With minimum mission fuel in mind, the results indicate as optimal values a pressure ratio split exponent of 0.38 and an intercooler mass flow ratio of 1.18 at hot-day top of climb conditions. At ISA mid-cruise conditions a specific thrust of 86m/s, a jet velocity ratio of 0.83, an intercooler effectiveness of 56% and an overall pressure ratio value of 76 are likely to be a good choice.

| Parameter | Datum [82] | Parametric design analysis |
|---|---|---|
| Specific thrust* | 137m/s | 116m/s |
| Specific thrust** | 102m/s | 86m/s |
| Jet velocity ratio* | 0.68 | 0.68 |
| Jet velocity ratio** | 0.83 | 0.83 |
| Intercooler mass flow ratio* | 1.35 | 1.18 |
| Pressure ratio split exponent* | 0.43 | 0.38 |
| Overall pressure ratio* | 80 | 97 |
| Overall pressure ratio** | 62 | 76 |
| Intercooler effectiveness** | 61% | 56% |

***at hot-day top of climb***
*****at ISA mid-cruise***

Table 4.4: Summary of main design parameters.

The proposed optimal jet velocity ratio is actually higher than the value one would expect by using standard analytical expressions primarily because this design variable affects core efficiency at mid-cruise due to a combination of several different subtle changes to the core cycle and core component efficiencies at this condition. The presented formula does not consider changes in core efficiency and the beneficial effect of intercooling on transfer efficiency, nor account for losses in the bypass duct and jet pipe, whilst a relatively detailed engine performance model such as the one utilised in this study does.

The study has focussed on minimising fuel burn, but the overall economic optimum could be for a lower overall pressure ratio cycle. A simultaneous optimisation for all six design parameters will yield different optimal values particularly for those design parameters with strong interrelations, as will be shown in the next section. Nevertheless, only a relatively small improvement will be demonstrated in terms of overall system performance.

Mission fuel results from the surrogate model are in good agreement with the results obtained from the rubberised-wing aircraft model, at least for some of the design parameters. This indicates that it is possible - under some circumstances - to replace an aircraft model with specific fuel consumption and weight penalty exchange rates. Nevertheless, drag count exchange rates have to be utilised to properly assess changes in mission fuel for those design parameters that affect nacelle diameter.

Considering that the HPC last stage blade height (which is specific to engine thrust size) could have a substantial influence on the optimum OPR, it follows that different conclusions could be drawn for different engine sizes. High OPR intercooled engine cycles clearly become more attractive in larger engine sizes which can exploit higher overall pressure ratios without making the core components so small that they lose a significant amount of efficiency, but it is still possible that a smaller intercooled engine with an axi-centrifugal compressor could be considered. A 70,000lbf intercooled turbofan engine is large enough to make efficient use of an all-axial compression system, particularly within a geared fan configuration, but intercooling is perhaps more likely to be applied to even larger engines.

### 4.2.2 Design optimisation

#### 4.2.2.1 Optimisation problem

The parametric design analysis presented in the previous section focused on identifying the isolated effects of several major design parameters on SFC, engine weight and mission fuel. This was achieved by varying each design parameter - only one at a time.

An overall optimisation has also been carried out in order to establish the fuel optimal values of the following design parameters at hot-day top of climb conditions, by varying them all simultaneously: specific thrust, jet velocity ratio, intercooler mass flow ratio, pressure ratio split exponent, overall pressure ratio and HPT TBC average external surface metal temperature (by varying the HPT cooling flow). The intercooler effectiveness levels at end of runway hot-day take-off and at International Standard Atmosphere (ISA) mid-cruise conditions have also been varied. A full description of all the modelling assumptions for the design optimization is presented in Fig. 4.28 and is discussed in further detail below.

The initial optimisation work has been carried out at fixed thrust levels at hot-day top of climb, end of runway hot-day take-off and ISA day mid-cruise conditions. Similarly to the parametric design analysis, mass flow has been varied to achieve a thrust at hot-day top of climb conditions while combustor outlet temperature has been varied to achieve a thrust at end of runway hot-day take-off and ISA mid-cruise conditions. Fan pressure ratio and bypass ratio have been varied at hot-day top of climb conditions to achieve the required variation in specific thrust and jet velocity ratio, respectively. The core compressor pressure ratios (IPC and HPC) have been varied at hot-day top of climb conditions to achieve the required variation in pressure ratio split exponent and overall pressure ratio, respectively.

With regard to design parameters that have been kept constant, the same scheme has been used as in the parametric design analysis presented earlier, but with one exception. The turbine thermal barrier coating external surface blade metal temperature at hot-day top of climb conditions has not been kept constant, but has been chosen instead as a design parameter; the required variation in blade metal temperature has been achieved by varying the HPT cooling flow.

During the optimisation process, an intercooler auxiliary nozzle throat area variation from 50% to 100% has been considered as mechanically and aerodynamically feasible. This level of variation has therefore been set as the upper limit in order to ensure design feasibility. In addition, an HPT TBC average external surface metal temperature of 1233 K at end of runway hot-day take-off conditions has also been set as the upper limit. Any design that failed to meet these constraints has been discarded as infeasible.

| Key engine parameters | Units | Hot-day top-of-climb conditions (ISA+10, FL350, Mach 0.82) | Hot-day end-of-runway take-off conditions (ISA+15, FL0, Mach 0.25) | Mid-cruise conditions (ISA, FL350, Mach 0.82) |
|---|---|---|---|---|
| Specific thrust | m/s | **Target*, †** | Out of the wash | Out of the wash |
| Jet velocity ratio | - | **Target*, †** | Out of the wash | Out of the wash |
| Intercooler mass flow ratio | - | **Target*, †** | Out of the wash | Out of the wash |
| Pressure ratio split exponent | - | **Target*, †** | Out of the wash | Out of the wash |
| Fan tip over hub pressure rise ratio | - | **Target** | Out of the wash | Out of the wash |
| Overall pressure ratio | kN | **Target*, †** | Out of the wash | Out of the wash |
| HPT TBC metal temperature | K | **Target*** | **Out of the wash / Target** | Out of the wash |
| LPT cooling flow mixing pressure ratio | - | **Target** | Out of the wash | Out of the wash |
| Thrust | - | **Target †** | **Target / Out of the wash †** | **Target** |
| Engine inlet mass flow | kg/s | **Variable** | Out of the wash | Out of the wash |
| Fan tip pressure ratio | - | **Variable** | Out of the wash | Out of the wash |
| Bypass ratio | - | **Variable** | Out of the wash | Out of the wash |
| Intercooler LP inlet mass flow | kg/s | **Variable** | Out of the wash | Out of the wash |
| Fan root pressure ratio | - | **Variable** | Out of the wash | Out of the wash |
| IPC pressure ratio | - | **Variable** | Out of the wash | Out of the wash |
| HPC pressure ratio | - | **Variable** | Out of the wash | Out of the wash |
| HPT cooling flow (% HPC flow) | % | **Variable** | same as @ToC | same as @ToC |
| LPT cooling flow extraction point (% HPC enthalpy rise) | % | **Variable** | same as @ToC | same as @ToC |
| LPT cooling flow (% HPC flow) | % | Fixed | same as @ToC | same as @ToC |
| Combustor outlet temperature | K | Fixed | **Variable** | **Variable** |
| Intercooler nozzle area | m2 | Out of the wash | **Variable** | **Variable** |
| Bypass nozzle area | m2 | Out of the wash | **Variable** | **Variable** |
| Total cold nozzle area | m2 | Out of the wash | **Target** | **Target** |
| Core inlet mass flow | kg/s | Out of the wash | Out of the wash | Out of the wash |
| High pressure turbine rotor inlet temperature | K | Out of the wash | Out of the wash | Out of the wash |
| Fan tip polytropic efficiency | % | Fixed | Out of the wash | Out of the wash |
| Fan root polytropic efficiency | % | Fixed | Out of the wash | Out of the wash |
| IPC polytropic efficiency | % | Fixed | Out of the wash | Out of the wash |
| HPC polytropic efficiency | % | From correlation | Out of the wash | Out of the wash |
| HPT polytropic efficiency | % | Fixed | Out of the wash | Out of the wash |
| LPT polytropic efficiency | % | Fixed | Out of the wash | Out of the wash |
| Intercooler temperature effectiveness | % | Fixed | **Target*, †** | **Target*, †** |
| Intercooler bypass side pressure loss dP/P | % | Fixed | Out of the wash | Out of the wash |
| Intercooler core side pressure loss dP/P | % | Fixed | Out of the wash | Out of the wash |
| Combustor pressure loss dP/P | % | Fixed | Out of the wash | Out of the wash |
| Jet pipe pressure loss dP/P | % | Fixed | Out of the wash | Out of the wash |
| Bypass duct pressure loss dP/P | % | Fixed | Out of the wash | Out of the wash |
| IPC inlet duct pressure loss dP/P | % | Fixed | Out of the wash | Out of the wash |
| HPC outlet diffuser pressure loss dP/P | % | Fixed | Out of the wash | Out of the wash |
| Engine intake pressure loss dP/P | % | Fixed | Out of the wash | Out of the wash |
| Intercooler nozzle thrust coefficient | % | Fixed | Out of the wash | Out of the wash |
| Bypass nozzle thrust coefficient | % | Fixed | Out of the wash | Out of the wash |
| Core nozzle thrust coeffficient | % | Fixed | Out of the wash | Out of the wash |
| HP shaft mechanical efficiency | % | Fixed | Out of the wash | Out of the wash |
| LP shaft mechanical efficiency | % | Fixed | Out of the wash | Out of the wash |
| Gearbox mechanical efficiency | % | Fixed | Out of the wash | Out of the wash |

**** A fixed thrust optimization design variable*** ***† A fixed customer requirements optimization design variable***

Figure 4.28: Geared fan intercooled core configuration modelling assumptions for design optimization.

Table 4.5: Summary of optimisation problem.

| | Min | Max |
|---|---|---|
| **Optimisation design variables** | | |
| Specific thrust (at hot-day TOC), m/s | 105 | 155 |
| Jet velocity ratio (at hot-day TOC) | 0.55 | 0.90 |
| IC mass flow ratio (at hot-day TOC) | 1.05 | 1.65 |
| Pressure ratio split exponent (at hot-day TOC) | 0.25 | 0.60 |
| Overall pressure ratio (at hot-day TOC) | 70 | 105 |
| IC effectiveness (at hot-day EOR T-O), % | 60 | 80 |
| IC effectiveness (at ISA mid-cruise), % | 50 | 75 |
| HPT TBC Tex (at hot-day TOC)*, K | 1050 | 1250 |
| Net thrust (at hot-day TOC)**, 1,000 lbf | 11 | 18 |
| **Constraints** | | |
| IC auxiliary nozzle throat area variation, % | 50 | 100 |
| HPT TBC Tex (at hot-day EOR T-O)*, K | | 1233 |
| FAR T-O distance**, km | | 2.5 |
| Time to height (FL350)**, min | | 22.5 |
| **Optimisation function** | | |
| Minimum business case block fuel with and w/o the proposed HPC efficiency correction procedure | | |
| ***for fixed thrust optimisation only*** | | |
| *****for fixed customer requirements optimisation only*** | | |

A second optimisation study has also been carried out assuming fixed customer requirements rather than fixed thrust levels. Within this study, the same design procedure has been utilised but with some modifications. In more detail, thrust at hot-day top of climb conditions has been selected as an additional design variable; the required variation has been achieved by varying the engine mass flow at the same operating condition. Combustor outlet temperature at end of runway hot-day take-off conditions has also been varied to achieve an HPT TBC average external surface metal temperature of 1233 K at that condition, rather than a thrust. A maximum Federal Aviation Regulations (FAR) take-off distance of 2.5 km and a maximum time to height (Flight Level 35000 ft, FL350) of 22.5 min have been set as upper limits in order to ensure design feasibility. Any design that failed to meet these constraints - in addition to the constraints discussed earlier in this section - has been discarded as infeasible.

#### 4.2.2.2 Optimisation technique

A summary of the design variables, boundary conditions, constraints and objective function related to the described optimisation problem is presented in Table 4.5.

Best practice (industrial and academic) in the field of aero-engine conceptual design deterministic optimisation has been scarcely documented in the public domain, although the field is now receiving some interest [52, 108, 109]. In the author's view, the choice of optimisation strategy requires the consideration of several criteria such as gradient information, randomisation, globality and run-time. Smooth gradients are a crucial basis for successful optimisation, especially when a gradient-based technique is used. However, even with a zero-order optimisation strategy, a smooth sensitivity behaviour is desirable to prevent numerical pitfalls like noisy surroundings of the optima, local optima or discontinuities within the design domain.

The design space for a geared fan intercooled core engine is non-linear, while component stage count changes and physical infeasibility also create discontinuities. The Adaptive Simulated Annealing (ASA) [110] technique was chosen as it is well suited for this optimisation problem. The ASA technique can handle discontinuities, it employs randomisation to find a global optimum, it does not need gradient information, it works well for a low number of design variables (typically less than ten), and although it needs a large number of iterations to converge, it is at least as fast as genetic algorithms. The best solutions from the ASA technique were further investigated with a Sequential Quadratic Programming (SQP) technique. The SQP technique is gradient-based and therefore converges quickly and precisely to the local optimum. The combination of these two techniques can lead to precise and global optima even in discontinuous non-linear design spaces.

During the optimisation, the ASA technique was re-initialised several times from random corners of the design space. Although the technique took several thousands of iterations to converge after each re-initialisation, it always converged to the same optimal solution. The optimisation was complemented by running a large Design of Experiments consisting several thousands of points; the chosen method of sampling was the Latin Hypercube [111] modified so that the combination of factor levels for each design parameter is optimised, rather than randomly combined [112–114]. The DOE results verified the approximate location of the optimal design as suggested by the optimiser.

Approximate response surface models were not utilised in this study. This was because of the danger of distorting and/or missing local optimal solutions within a particularly discontinuous as well as non-linear design space. Such models are best suited for optimisation problems that rely on the use of computationally expensive models, whereas the models utilised in this study take typically less than a second per iteration.

#### 4.2.2.3 Aerodynamic considerations

Previous optimisation work on intercooled cycles and on conventional cycles for small turbofans, has indicated that a low HPC last stage blade height can have a substantial effect on optimal cycle selection. Within the optimisation studies presented in this work, an attempt to cater for this effect has been made by applying a correction delta on the HPC polytropic efficiency, as described in the methodology section of this thesis. The exchange rates presented in Fig. 4.27 have been used for this purpose.

It should be noted that the underlying engine and aircraft models are non-linear. Therefore, the linearised HPC correction method described above is most accurate within that region in the design space where the linear approximation holds well i.e., around the original nominal design. Nevertheless, the optimisation results presented in the next section do not reside in blade heights that cause significant efficiency reduction. The proposed cycle changes - particularly HPC pressure ratio - are also rather modest and as a result the exchange rates established in the sensitivity analysis section hold reasonably well. Therefore, it is the author's view that the HPC correction method is valid to a first-order and suitable for the purposes of this study.

#### 4.2.2.4 Optimisation at fixed thrust

In this section, results from a fixed thrust optimisation are presented based on the design procedure described earlier. The analysis has focused on identifying the "globally" fuel optimal values of several major design parameters.

Through the optimisation process, two fuel optimal designs have been determined (Fuel optimal 1 and 2) with details provided in Table 4.6. The corrected specific fuel consumption and block fuel values presented in this table have been derived using the HPC efficiency correction procedure as described already. The first design is therefore fuel optimal if no HPC efficiency correction is applied to account for low values of HPC last stage blade height. The second design delivers minimum business case block fuel when the HPC efficiency correction procedure is applied. The results are compared against the datum design presented in [82] and the single-parameter optimisation results presented in the parametric design analysis section.

In the results presented in Fig. 4.29 and Fig. 4.30, the yellow square indicates the fuel optimal design if no HPC efficiency correction is applied. The green circle indicates the fuel optimal design when the HPC efficiency correction procedure is applied. The approximate front of best designs (as determined by visual inspection of the results) is illustrated through a dashed red line, while results from the parametric design analysis are illustrated using black circles (line). It should be noted that Fig. 4.29 and Fig. 4.30 contain those points - from the fixed

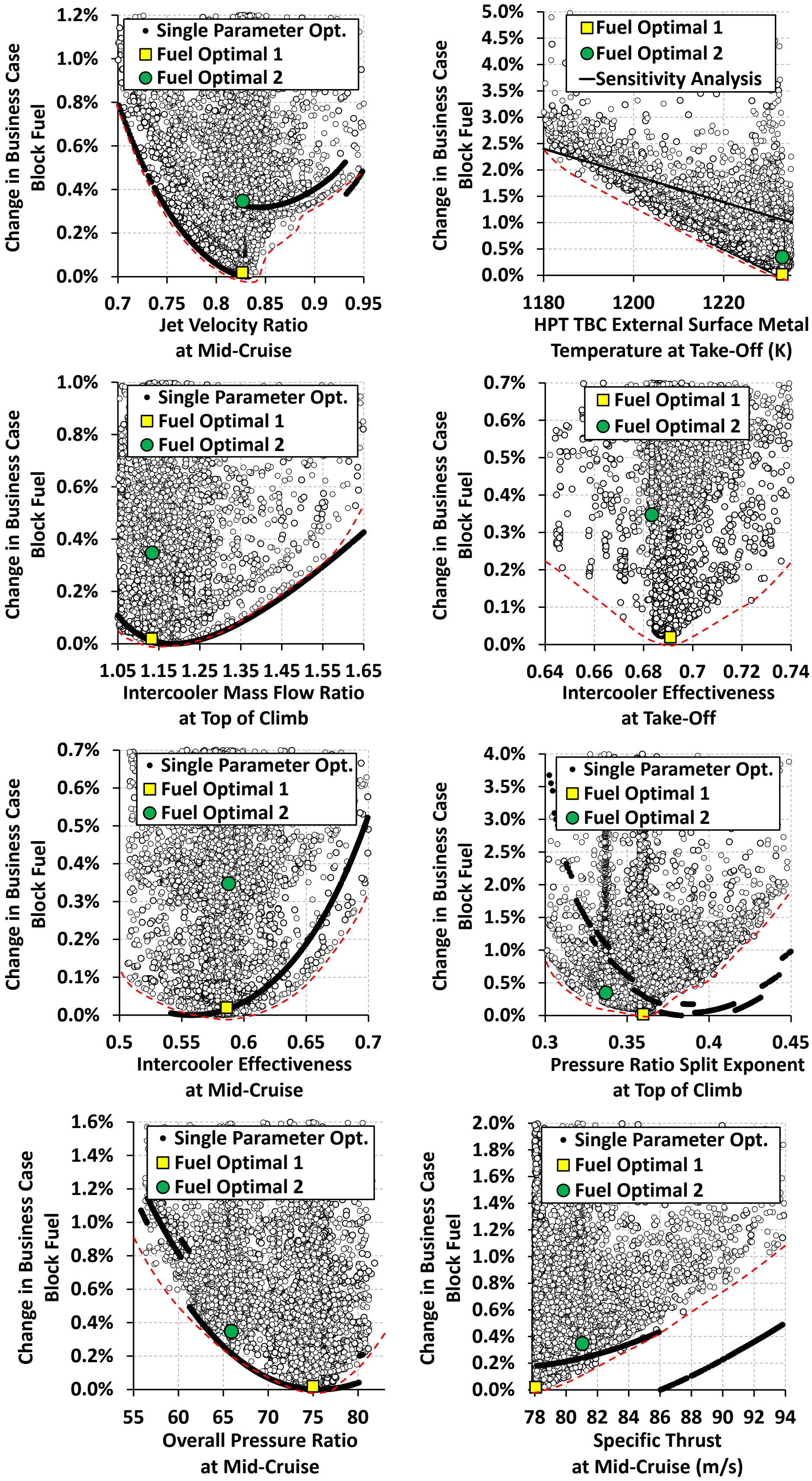


Figure 4.29: Optimal design parameter values for minimum business case block fuel.

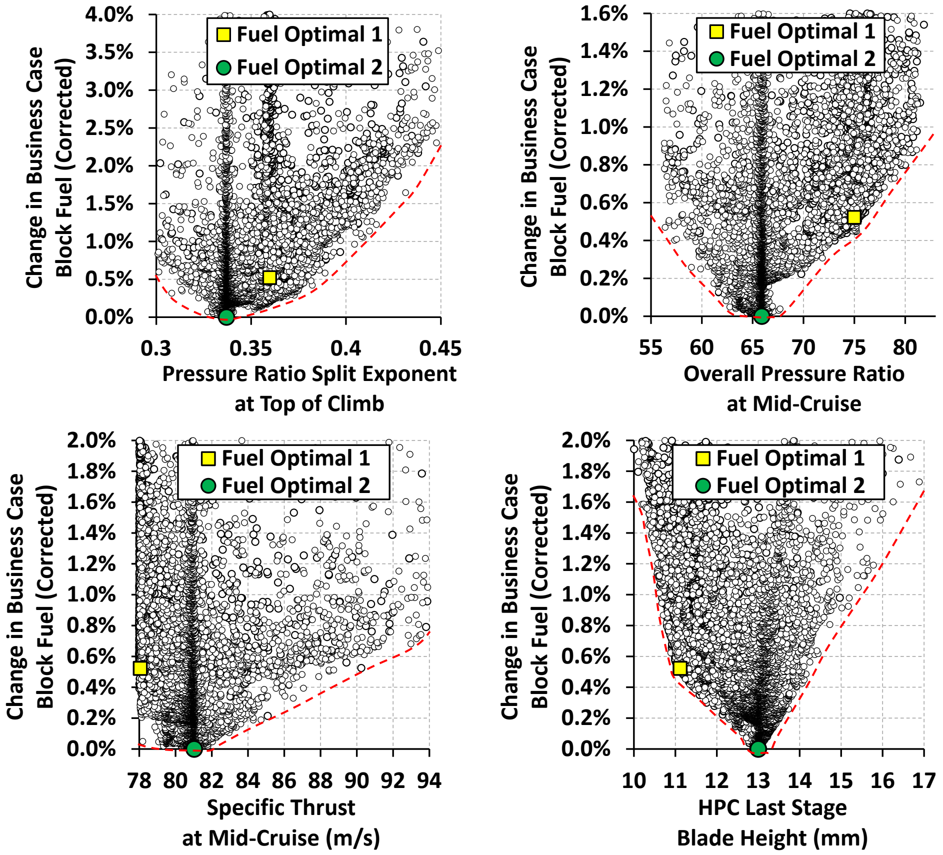


Figure 4.30: Optimal design parameter values for minimum business case block fuel with correction for HPC efficiency.

Table 4.6: Summary of optimisation results.

| | Datum [82] | Parametric design analysis | Fuel optimal 1 | Fuel optimal 2 | Fuel optimal 3 |
|---|---|---|---|---|---|
| **Input (optimisation design variables)** | | | | | |
| Specific thrust (at hot-day TOC), m/s | 137 | 116 | 106 | 109 | 111 |
| Overall pressure ratio (at hot-day TOC) | 80 | 97 | 95 | 84 | 90 |
| Pressure ratio split exponent (at hot-day TOC) | 0.43 | 0.38 | 0.36 | 0.34 | 0.36 |
| HPT TBC Tex (at hot-day TOC), K | 1165 | 1165 | 1165 | 1158 | 1170 |
| Jet velocity ratio (at hot-day TOC) | 0.68 | 0.68 | 0.68 | 0.68 | 0.68 |
| IC effectiveness (at ISA mid-cruise), % | 61 | 56 | 59 | 59 | 57 |
| IC effectiveness (at hot-day EOR T-O), % | 72 | 72 | 69 | 68 | 67 |
| IC mass flow ratio (at hot-day TOC) | 1.35 | 1.18 | 1.13 | 1.13 | 1.15 |
| **Output** | | | | | |
| Specific thrust (at ISA mid-cruise), m/s | 102 | 86 | 78 | 81 | 80 |
| Overall pressure ratio (at ISA mid-cruise) | 62 | 76 | 75 | 66 | 69 |
| Bypass ratio (at hot-day TOC) | 11.2 | 12.8 | 14.4 | 13.9 | 13.7 |
| Jet velocity ratio (at ISA mid-cruise) | 0.83 | 0.82 | 0.83 | 0.83 | 0.83 |
| HPT TBC Tex (at hot-day EOR T-O), K | 1233 | 1232 | 1233 | 1233 | 1233 |
| Business case block fuel, % | Datum | -2.2 | -2.8 | -2.5 | -2.9 |
| Business case block fuel (corrected), % | Datum | -1.5 | -2.0 | -2.5 | -2.5 |
| SFC (at ISA mid-cruise), g/(kN*s) | 14.39 | 13.98 | 13.85 | 13.87 | 13.95 |
| SFC (at ISA mid-cruise), % | Datum | -2.8 | -3.7 | -3.6 | -3.1 |
| SFC (at ISA mid-cruise, corrected), % | Datum | -2.4 | -3.0 | -3.6 | -2.7 |
| Time to height (FL350), min | 22.5 | 23.0 | 22.8 | 23.0 | 22.3 |
| FAR take-off distance, km | 2.5 | 2.45 | 2.42 | 2.43 | 2.48 |
| HPC last stage blade height, mm | 14.6 | 11.7 | 11.1 | 13.0 | 12.0 |
| Engine weight, % | Datum | +16.5 | +22.3 | +21.8 | +17.8 |
| Stage count (Fan-IPC-HPC-HPT-LPT) | 1-7-9-2-4 | 1-7-10-2-5 | 1-6-10-2-5 | 1-5-11-2-5 | 1-6-10-2-5 |
| Production cost, % | Datum | +12.2 | +13.1 | +13.9 | +10.1 |

thrust optimisation and corresponding DOE runs - that satisfy all the relevant constraints presented in Table 4.5.

It can be observed that the fuel optimal values for most of the chosen cycle design parameters depend rather weakly on whether the HPC efficiency correction procedure has been applied or not. This is not the case for overall pressure ratio, pressure ratio split exponent and specific thrust. The corrected block fuel difference between the two proposed designs is 0.5%.

Whereas the sensitivity analysis presented earlier suggests a reduction of about 0.25% in aircraft fuel burn per 10 K increase in HPT TBC average external surface metal temperature, the optimisation results suggest a reduction of about 0.5%. This higher exchange rate is the result of an optimal rematching of all other cycle design parameters as the blade metal temperature is increased. Reducing intercooling at take-off conditions will reduce pressure loss levels and engine weight, but will also result in increased HPT cooling flow levels; the present study suggests that the fuel optimal value is less than 70%.

In principle the trends from the parametric design analysis can also be observed when all parameters are varied simultaneously. The simultaneous matching of all design parameters however can help identify additional corners in the design space that are of interest. Such corners can be missed when varying jet velocity ratio or specific thrust in isolation due to LPT stage count changes. Furthermore, the fuel optimal value of the pressure ratio split exponent is weekly dependent on the value of intercooler effectiveness at mid-cruise conditions; introducing intercooling earlier in the compression process requires a higher intercooler effectiveness at mid-cruise conditions.

The fuel optimal values for overall pressure ratio, pressure ratio split exponent and specific thrust are different when the HPC efficiency correction is applied, as illustrated in Fig. 4.30. It can be observed that both the overall pressure ratio and the pressure ratio split exponent need to be reduced, in order to increase the HPC discharge corrected flow and therefore increase the HPC last stage blade height. Specific thrust is also affected but to a lesser degree and primarily due to the mechanical and aerodynamic design choices made within this study.

#### 4.2.2.5 Optimisation at fixed customer requirements

In this section, results from a fixed customer requirements optimisation are presented based on the design procedure described earlier. Once again, the analysis has focused on identifying the "globally" fuel optimal values of several major design parameters.

Through the optimisation process, an additional fuel optimal design has been determined (Fuel Burnt Optimal 3) with details provided in Table 4.6. This third design delivers minimum business case block fuel when the HPC efficiency

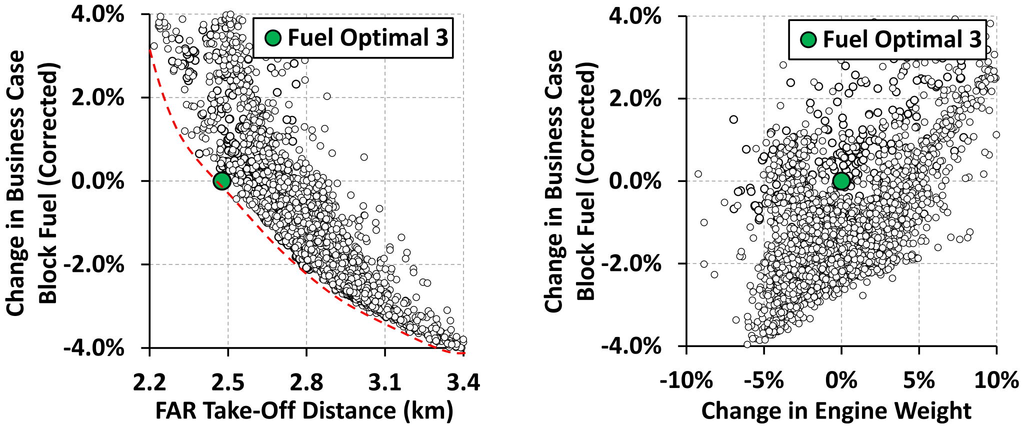


Figure 4.31: Effect of customer requirements on engine weight and business case block fuel.

correction procedure is applied. The fuel optimal values for the different cycle parameters are generally similar to the ones determined through the fixed thrust optimisation and the discussion presented is still applicable.

In the results presented in Fig. 4.31, the green circle indicates the fuel optimal design when the HPC efficiency correction procedure is applied. It can be observed that customer requirements such as FAR take-off distance play a very important role in determining a fuel optimal engine design. Tougher customer requirements result in bigger and heavier engines that burn more fuel. It should be noted that Fig. 4.31 contains those points - from the fixed customer requirements optimisation and corresponding DOE runs - that satisfy the maximum intercooler auxiliary nozzle throat area variation constraint presented in Table 4.5.

#### 4.2.2.6 Summary

The same multidisciplinary conceptual design tool has been utilised, as in the parametric design analysis, to analyse the option of an intercooled core geared fan aero engine for long haul applications. The presented study has been focused on identifying “globally” fuel burn optimal values for a set of engine design parameters by varying them all simultaneously. This permits the non-linear interactions between the parameters to be accounted. Special attention has been given to the fuel burn impact of the reduced HPC efficiency levels associated with low last stage blade heights. The proposed design methodology is capable, with the utilised tool, of exploring the interaction of design criteria and providing critical design insight at engine-aircraft system level.

Three fuel optimal designs are considered, based on different assumptions. The results indicate that it is preferable to trade overall pressure ratio and pressure ratio split exponent, rather than specific thrust, as means of increasing blade height and hence reducing the associated fuel consumption penalties. It is interesting to note that even when considering the effect of HPC last stage blade height on efficiency there is still an equivalently good design at a reduced overall pressure ratio. This provides evidence that the overall economic optimum could be for a lower overall pressure ratio cycle. Customer requirements such as take-off distance and time to height play a very important role in determining a fuel optimal engine design. Tougher customer requirements result in bigger and heavier engines that burn more fuel. Higher overall pressure ratio intercooled engine cycles clearly become more attractive in aircraft applications that require larger engine sizes.

## 4.3 Trade-off analysis

A trade-off analysis based on the tools and algorithm described in Chapter 3 is presented here. The work looks at the trade-off between the ever-increasing energy efficiency (propulsive and thermal) of modern aero-engines and their $NO_x$ performance. Two different combustor designs are considered:

- A Rich–burn Quick–quench Lean–burn (RQL) combustor.
- A Lean Direct Injection (LDI) combustor.

The primary novelty of the present study lies on the insight provided on the effects of reducing engine specific thrust (propulsive efficiency), and increasing overall pressure ratio and turbine operating temperature (thermal efficiency) on $NO_x$ emissions.

### 4.3.1 System performance modelling

In the parametric studies presented in this section three major engine operating points were considered: Hot–Day Top–of–Climb (HD TOC), End–Of–Runway Hot–Day Take–Off (EOR HD TO), and ISA Mid–Cruise (ISA MCR). The engine configuration chosen was a three–shaft turbofan engine for long–haul applications, i.e., 70,000lbf thrust. A schematic of the engine performance model is illustrated in Fig. 3.2.

At the hot–day top–of–climb condition (performance reference point) the following technology parameters have been kept constant: component polytropic efficiencies, duct and combustor pressure losses, shaft mechanical efficiencies, and Intermediate Pressure Turbine (IPT) cooling flow mixing pressure ratio. The selected component technology levels were in general consistent with an engine designed to enter service in 1995, consistent with the work presented in Kyprianidis et al. [1] and Samuelsson et al. [115]. The technology factors for RQL and LDI combustors were established under the NEWAC project, and all non-confidential elements have been presented in Kyprianidis et al. [1]. Whilst there are several challenges in the sizing of such types of combustors, the approach utilised is considered appropriate for considering the influence of combustor inlet pressure, temperature and operating fuel-to-air ratio on overall system design.

A complex multi-point synthesis matching scheme was used to cover key design constraints as typically considered in the conceptual design phase [115]. A full description of the scheme, including modelling assumptions, is presented in Fig. 4.32 and is discussed in further detail below.

| Key engine parameters | Units | Hot-day top-of-climb conditions (ISA+10, FL350, Mach 0.82) | Hot-day end-of-runway take-off conditions (ISA+15, FL0, Mach 0.25) | Mid-cruise conditions (ISA, FL350, Mach 0.82) |
|---|---|---|---|---|
| Specific thrust | m/s | Out of the wash | Out of the wash | **Synthesis Target 1** |
| Jet velocity ratio | - | Out of the wash | Out of the wash | **Synthesis Target 2** |
| Pressure ratio split exponent | - | Out of the wash | Out of the wash | **Synthesis Target 3** |
| Fan tip over hub pressure rise ratio | - | **Target** | Out of the wash | Out of the wash |
| Overall pressure ratio | - | Out of the wash | Out of the wash | **Out of the wash / Synthesis Target 4** |
| HPC outlet temperature | K | Out of the wash | **Synthesis Target 4 / Out of the wash** | Out of the wash |
| HPT NGV TBC metal temperature | K | Out of the wash | **Synthesis Target 5** | Out of the wash |
| HPT rotor TBC metal temperature | K | Out of the wash | **Synthesis Target 6** | Out of the wash |
| IPT NGV TBC metal temperature | K | Out of the wash | **Synthesis Target 7** | Out of the wash |
| IPT rotor TBC metal temperature | K | Out of the wash | **Synthesis Target 8** | Out of the wash |
| IPT cooling flow mixing pressure ratio | - | **Target** | Out of the wash | Out of the wash |
| LPT NGV TBC metal temperature | K | Out of the wash | **Synthesis Target 9** | Out of the wash |
| Combustor outlet temperature | K | Out of the wash | Out of the wash | Out of the wash |
| Thrust | kN | **Target** | **Target** | **Target** |
| Engine inlet mass flow | kg/s | **Variable** | Out of the wash | Out of the wash |
| Fan tip pressure ratio | - | **Synthesis Variable 1** | Out of the wash | **Out of the wash †** |
| Bypass ratio | - | **Synthesis Variable 2** | Out of the wash | **Out of the wash †** |
| Fan root pressure ratio | - | **Variable** | Out of the wash | Out of the wash |
| IPC pressure ratio | - | **Synthesis Variable 3** | Out of the wash | **Out of the wash †** |
| HPC pressure ratio | - | **Synthesis Variable 4** | **Out of the wash †** | **Out of the wash †** |
| HPT NGV cooling flow (% HPC flow) | % | **Synthesis Variable 5** | **same as @ToC †** | same as @ToC |
| HPT rotor cooling flow (% HPC flow) | % | **Synthesis Variable 6** | **same as @ToC †** | same as @ToC |
| IPT NGV cooling flow (% HPC flow) | % | **Synthesis Variable 7** | **same as @ToC †** | same as @ToC |
| IPT rotor cooling flow (% HPC flow) | % | **Synthesis Variable 8** | **same as @ToC †** | same as @ToC |
| IPT cooling flow extraction point (% HPC enthalpy rise) | % | **Variable** | same as @ToC | same as @ToC |
| LPT sealing flow (% HPC flow) | % | **User Input** | same as @ToC | same as @ToC |
| Fan disc pressurised sealing flow (% IPC flow) | % | **User Input** | same as @ToC | same as @ToC |
| Combustor fuel flow | kg/s | **Synthesis Variable 9** | **Variable** | **Variable** |
| Core nozzle area | m2 | Out of the wash | Out of the wash | Out of the wash |
| Bypass nozzle area | m2 | Out of the wash | Out of the wash | Out of the wash |
| Core inlet mass flow | kg/s | Out of the wash | Out of the wash | Out of the wash |
| High pressure turbine rotor inlet temperature | K | Out of the wash | Out of the wash | Out of the wash |
| Fan tip polytropic efficiency | % | **User Input** | Out of the wash | Out of the wash |
| Fan root polytropic efficiency | % | **User Input** | Out of the wash | Out of the wash |
| IPC polytropic efficiency | % | **User Input** | Out of the wash | Out of the wash |
| HPC polytropic efficiency | % | **User Input** | Out of the wash | Out of the wash |
| HPT polytropic efficiency | % | **User Input** | Out of the wash | Out of the wash |
| IPT polytropic efficiency | % | **User Input** | Out of the wash | Out of the wash |
| LPT polytropic efficiency | % | **User Input** | Out of the wash | Out of the wash |
| Combustor pressure loss dP/P | % | **User Input** | Out of the wash | Out of the wash |
| Jet pipe pressure loss dP/P | % | **User Input** | Out of the wash | Out of the wash |
| Bypass duct pressure loss dP/P | % | **User Input** | Out of the wash | Out of the wash |
| IPC inlet duct pressure loss dP/P | % | **User Input** | Out of the wash | Out of the wash |
| IPC/HPC intercompressor duct pressure loss dP/P | % | **User Input** | Out of the wash | Out of the wash |
| HPC outlet diffuser pressure loss dP/P | % | **User Input** | Out of the wash | Out of the wash |
| Engine intake pressure loss dP/P | % | **User Input** | Out of the wash | Out of the wash |
| Bypass nozzle thrust coefficient | % | **User Input** | Out of the wash | Out of the wash |
| Core nozzle thrust coeffficient | % | **User Input** | Out of the wash | Out of the wash |
| HP shaft mechanical efficiency | % | **User Input** | Out of the wash | Out of the wash |
| IP shaft mechanical efficiency | % | **User Input** | Out of the wash | Out of the wash |
| LP shaft mechanical efficiency | % | **User Input** | Out of the wash | Out of the wash |

***† Varied as needed for convergence of synthesis target using corresponding synthesis variable at top-of-climb condition***

Figure 4.32: Multi-point matching scheme for 3-shaft turbofan.

Engine mass flow $W_2$ at hot-day top-of-climb has been varied to achieve a net thrust $FN$ at the same condition. Combustor outlet temperature $T_4$ at end–of–runway hot–day take–off and ISA mid–cruise has been varied to achieve a net thrust $FN$ at the respective condition. Bypass Ratio ($BPR$) and Fan Pressure Ratio ($FPR$) at hot-day top-of-climb have been varied to achieve a jet velocity ratio $\frac{V_{cold}}{V_{hot}}$ and specific thrust $SFN$, respectively, at ISA mid–cruise conditions.

Combustor outlet temperature $T_4$ at hot-day top-of-climb has been varied to achieve a Low Pressure Turbine (LPT) entry temperature $T_{47}$ at end–of–runway hot–day take–off. The HPT and IPT blade and vane TBC average external surface metal temperatures where kept constant at the end–of–runway hot–day take–off by varying the respective cooling flows as set at the hot-day top-of-climb condition. The High Pressure Compressor (HPC) pressure ratio $\frac{P_3}{P_{26}}$ has been varied at hot-day top-of-climb to achieve a combustor entry temperature $T_{31}$ at the end-of-runway hot-day take-off condition.

The Intermediate Pressure Compressor (IPC) pressure ratio $\frac{P_{25}}{P_{24}}$ at hot-day top-of-climb conditions has been varied to achieve a pressure ratio split exponent $n$ at ISA mid–cruise conditions. All selected material technology levels were consistent with an engine designed to enter service in 1995, unless otherwise indicated in the plots that follow. For plots in which OPR was purposely varied (by varying $\frac{P_3}{P_{26}}$), the combustor entry temperature $T_{31}$ at the end–of–runway hot–day take–off condition was not matched.

### 4.3.2 NO$_x$ emissions

An assessment focused on the prediction of $NO_x$ emissions levels for the ICAO LTO cycle of advanced novel aero-engine designs is presented. The $NO_x$ predictions are compared through Fig. 4.33 against ICAO Annex 16 Volume II legislative limits [116], as well as the Medium Term (MT) and Long Term (LT) technology goals set by CAEP [117]. Balloons have been used to indicate the uncertainty in the $NO_x$ predictions. The author has considered a ±10% overall uncertainty in the predicted $NO_x$ emissions when using the proposed correlations. In addition, a relatively small experience-based uncertainty is considered in the estimated overall pressure ratio of the various future cycles. The uncertainty is meant to cover the lower Technology Readiness Level (TRL) associated with some of the proposed future aero-engine designs. In the case of those engines already in service, namely the CFM-56, Trent 800 and GE90, the bubbles have been sized to cover the spread in the information contained in the ICAO databank for the different variants of each engine model.

The results demonstrate that a sufficient margin against the ICAO CAEP/8 LTO cycle $NO_x$ certification limit may be achieved for all the configurations that have been assessed assuming technology levels consistent with a year of entry into service around 2020. Lean-burn combustion technology can offer improved $NO_x$

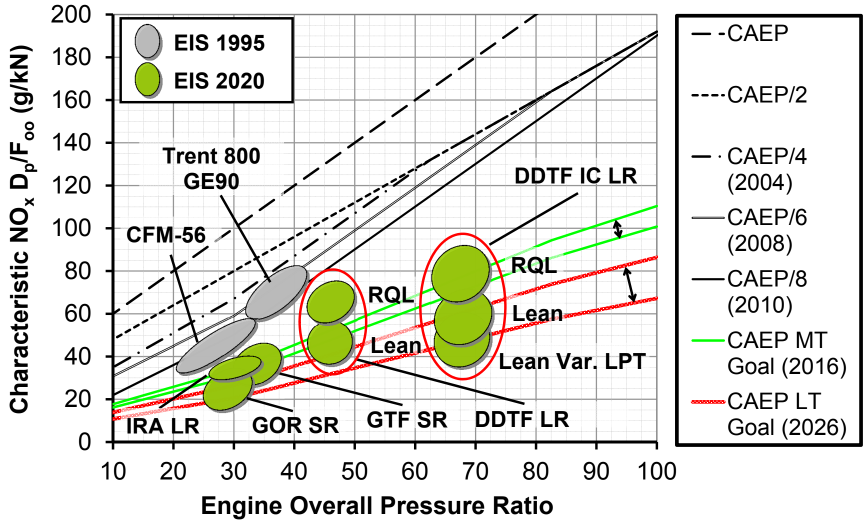


Figure 4.33: $NO_x$ emissions assessment for different future aero engine design concepts (DDTF LR: Direct–Drive TurboFan for Long Range applications; DDTF IC LR: Direct-Drive TurboFan with Intercooled Core for Long Range applications; IRA LR: Intercooled Recuperated turbofan for Long Range applications; GTF SR: Geared TurboFan for Short Range applications; GOR SR: Geared Open Rotor for Short Range applications).

performance when compared to RQL technology, particularly if coupled with variable geometry LPT nozzle guide vanes that can help modulate the combustor AFR at part-load conditions.

Nonetheless, it can been observed in Fig. 4.33 that despite the improved certification margin, absolute $NO_x$ emissions per passenger-kilometer are likely to increase at least for some of the proposed novel concepts. It is not fully clear which design parameters drive this increase and what their impact might be on high-altitude $NO_x$ emissions, which are currently not covered by any legislation. An earlier study presented in [118] did attempt to shed some light on this topic but had several shortcomings. The authors failed to separate the effect of specific thrust (propulsive efficiency) and OPR (thermal efficiency) on $NO_x$ emissions. A fully rigorous engine performance model was also not utilised, which meant that it was not possible to study the engine behaviour at different operating conditions i.e., sea-level versus high-altitude. These important interrelationships shall be investigated and discussed in detail in the subsections that follow.

### 4.3.3 Propulsive efficiency

Reducing specific thrust increases engine propulsive efficiency, which is beneficial for cruise SFC, as illustrated in Fig. 4.34. This has been the subject of several thermodynamic studies and has been well covered in the literature. What has

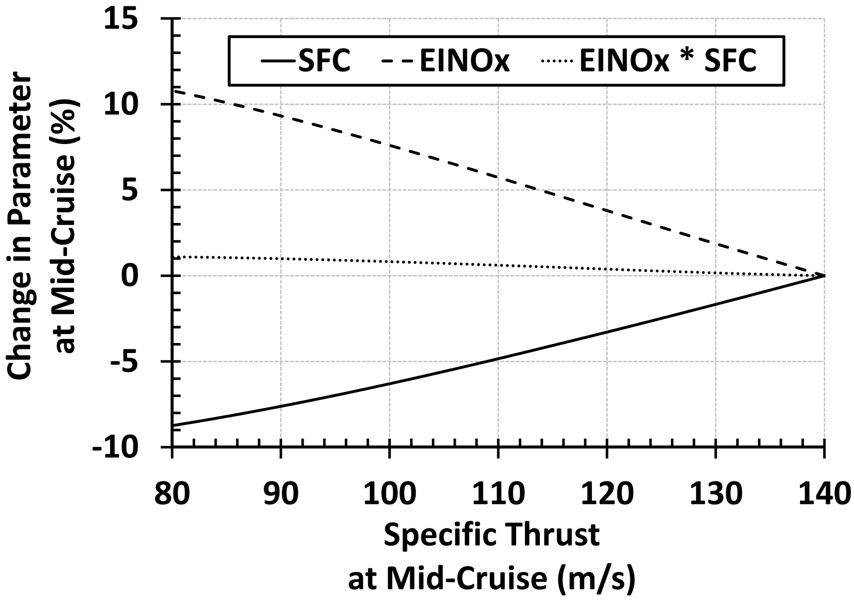


Figure 4.34: Variation in ISA mid-cruise SFC and $NO_x$ emissions with specific thrust for an RQL combustor.

not been adequately assessed is the effect of specific thrust on $NO_x$ emissions. As shown in Fig. 4.34, the $NO_x$ emissions index ($EINO_x$) for an RQL combustor increases with reducing specific thrust i.e., more $NO_x$ are emitted per unit of fuel burned. This is because cruise OPR tends to increase with reducing specific thrust at a set combustor entry temperature limitation at end-of-runway take-off conditions. Nonetheless, the total amount of $NO_x$ emitted per unit of thrust i.e., the product of $EINO_x$ and SFC, remains approximately constant with decreasing specific thrust.

At end-of-runway take-off conditions, $EINO_x$ for an RQL combustor remains approximately constant with reducing specific thrust, as illustrated in Fig. 4.35. This is because the engine OPR at this condition has to remain approximately constant at the set combustor entry temperature limitation. Due to the low forward Mach number, the reduction in specific thrust has a much more pronounced effect on SFC. Therefore, the total amount of $NO_x$ emitted per unit of thrust reduces with decreasing specific thrust.

The absolute amount of $NO_x$ emitted during a typical long–haul flight decreases with decreasing specific thrust, as illustrated in Fig. 4.36. This behaviour can be observed for both RQL and LDI combustor technology and is attributed primarily to aircraft-level snowball effects from the resulting reduction in SFC. Cruise $NO_x$ emissions are particularly low for LDI combustors – and are largely independent of specific thrust level – since around this point the primary zone tends to operate at its optimum performance.

The amount of $NO_x$ emitted during a typical LTO cycle also decreases with

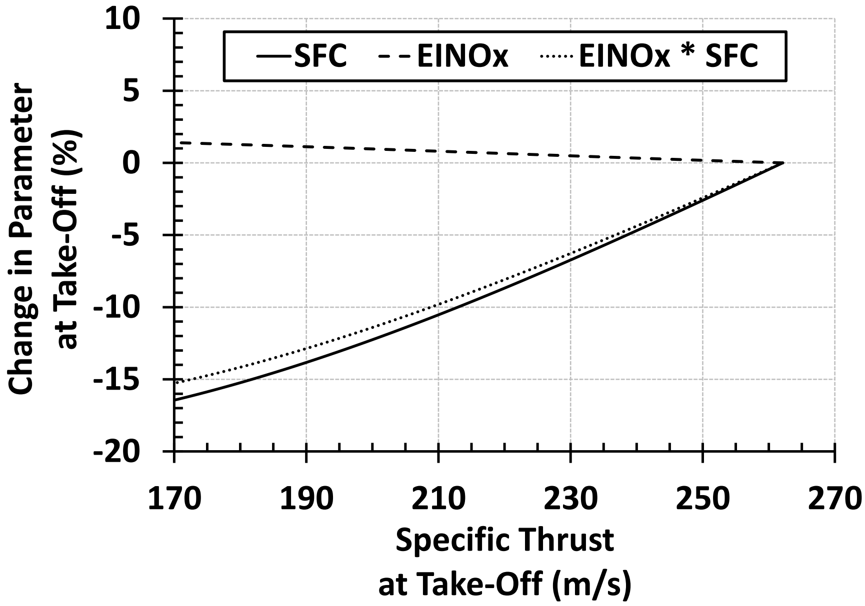


Figure 4.35: Variation in end-of-runway hot-day take-off SFC and $NO_x$ emissions with specific thrust for an RQL combustor.

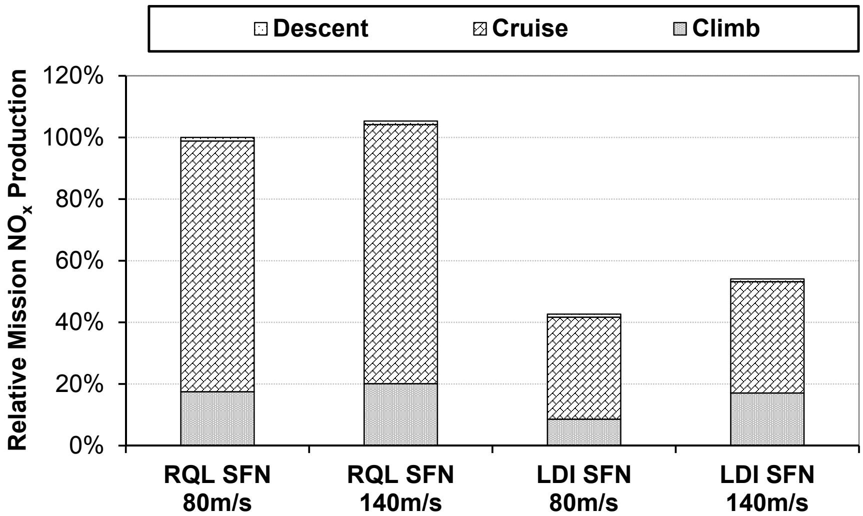


Figure 4.36: Variation in total mission $NO_x$ emissions with specific thrust and combustor technology.

decreasing specific thrust, as illustrated in Fig. 4.37. This behaviour can be observed for both RQL and LDI combustor technology and is attributed primarily to the expected reduction in $EINO_x$ at high-power. LDI combustors are particularly sensitive at high-power conditions; their performance is largely dependent on the primary zone flame temperature ratio between take-off and cruise. This ratio tends to reduce with reducing specific thrust and therefore LDI technology is found to be particularly suitable for low specific thrust turbofan designs.

Overall, reducing specific thrust has a more pronounced (and beneficial) effect on LTO $NO_x$, rather than mission $NO_x$, and this holds particularly true for LDI combustors. This suggests a gap in the current certification legislation which seems to favour reduced sea-level $NO_x$ over high altitude $NO_x$. The full potential and competitive advantage of lean burn technology lays in fact at cruise conditions but these are currently not covered by emissions regulations. The results presented demonstrate that a lean-burn combustor with similar (or better) $NO_x$ performance at sea-level relative to an RQL combustor would outperform the RQL design at altitude.

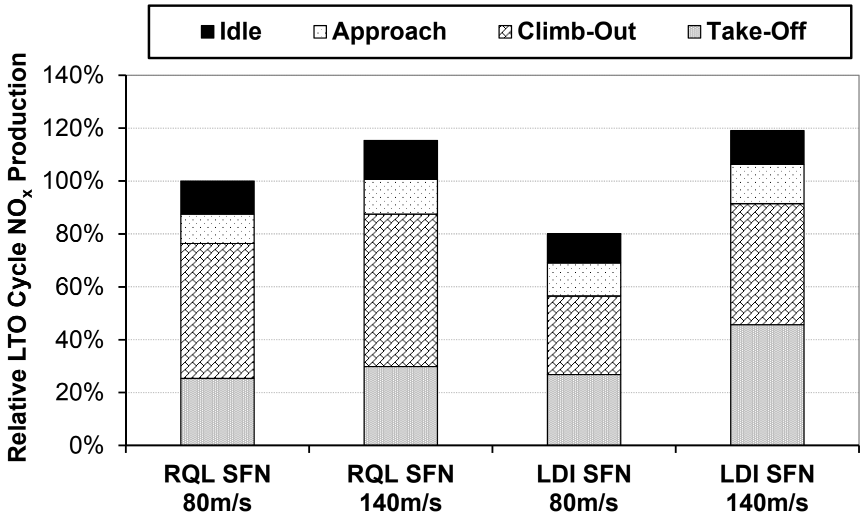


Figure 4.37: Variation in LTO cycle $NO_x$ emissions with specific thrust and combustor technology.

### 4.3.4 Thermal efficiency

Increasing OPR generally increases engine thermal efficiency, which is beneficial to cruise SFC, as illustrated in Fig. 4.38. The optimal level of OPR for minimum cruise SFC depends largely on material technology, and the associated cooling requirements to ensure safe operation within a given set of maximum operating temperature limitations. As can be observed, improvements in material technology tend to reduce cruise SFC and increase the optimal OPR level. However, increased OPR levels are associated with elevated combustor entry temperature and pressure levels. As expected from the basic theory of thermal $NO_x$ formation, and as shown in Fig. 4.39, increasing OPR results in an exponential increase in cruise $EINO_x$ for an RQL combustor. This increase is even more pronounced at end–of–runway hot–day take–off conditions due to the higher absolute combustor entry temperature and pressure levels encountered at this operating point, as shown in Fig. 4.40.

The absolute amount of $NO_x$ emitted during a typical long–haul flight increases significantly with increasing OPR for an RQL combustor, as illustrated in Fig. 4.41. This behaviour is not observed for LDI combustor technology since the AFR in the combustor primary zone can be increased to compensate for the negative effect of increased combustor entry temperature levels on $NO_x$ emissions. Furthermore, the reduced SFC fully compensates for the negative effect of the increased combustor entry pressure levels on $NO_x$ emissions.

The amount of $NO_x$ emitted during a typical LTO cycle also increases significantly with increasing OPR for an RQL combustor, as illustrated in Fig. 4.42. Again, this behaviour is not observed for LDI combustor technology for the same reasons as with mission $NO_x$. LDI combustors can therefore help decouple $NO_x$ emissions performance and engine thermal efficiency. Overall, increasing OPR has a more pronounced (and detrimental) effect on LTO $NO_x$, rather than mission $NO_x$, and this holds particularly true for RQL combustors.

Current certification legislation allows higher $NO_x$ emissions levels with increasing OPR. In other words, it permits trading $NO_x$ emissions to improve engine energy efficiency, and hence reduce $CO_2$ emissions through reduced fuel consumption. This also leads to lower direct operating costs for airliners, which can be seen as beneficial for aviation growth.

### 4.3.5 Summary

The same multidisciplinary conceptual design tool has been utilised, as in the previous sections, to assess the trade-off between the ever-increasing energy effi-

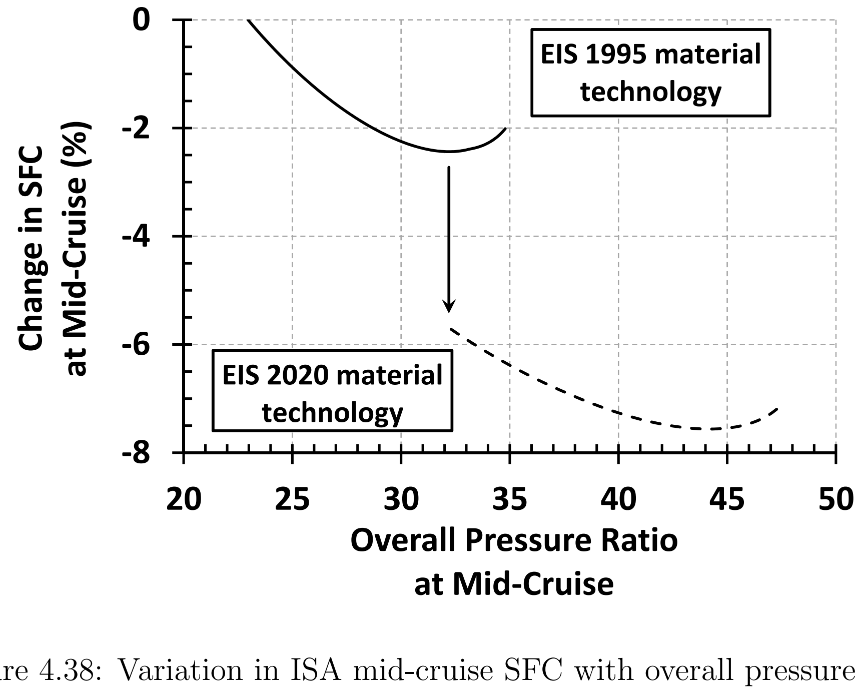


Figure 4.38: Variation in ISA mid-cruise SFC with overall pressure ratio.

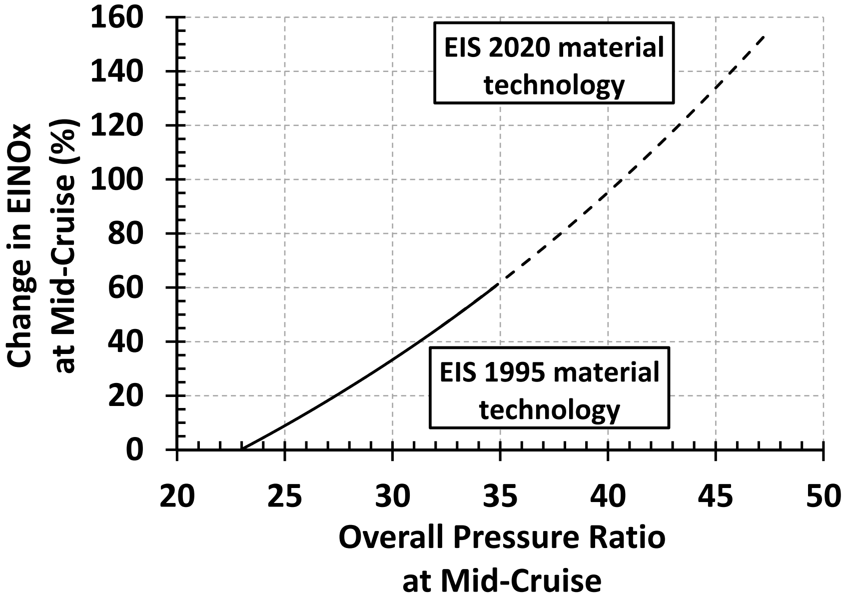


Figure 4.39: Variation in ISA mid-cruise $EINO_x$ with overall pressure ratio for an RQL combustor.

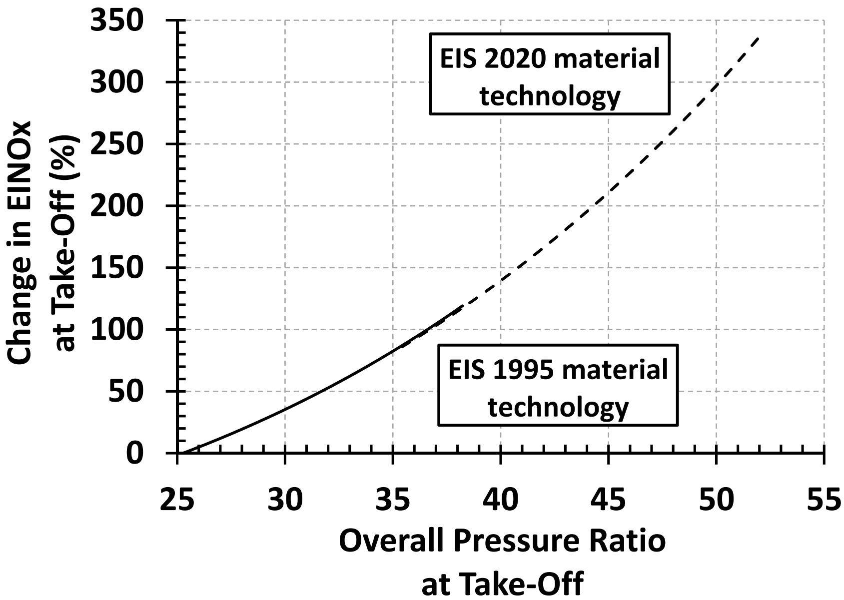


Figure 4.40: Variation in end-of-runway hot-day take-off $EINO_x$ with overall pressure ratio for an RQL combustor.

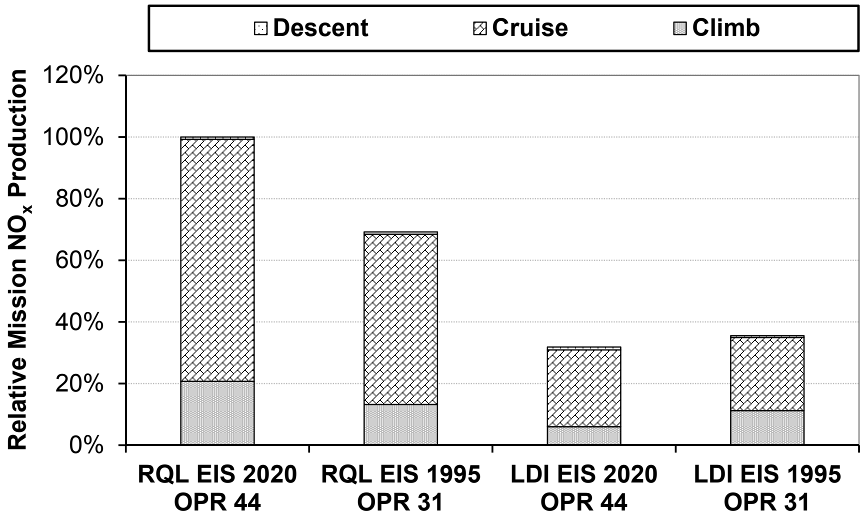


Figure 4.41: Variation in total mission $NO_x$ emissions with overall pressure ratio and combustor technology.

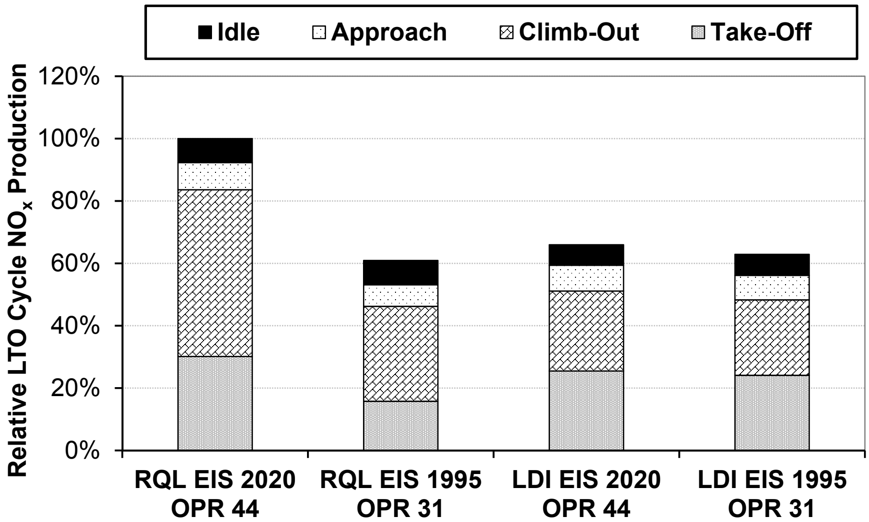


Figure 4.42: Variation in LTO cycle $NO_x$ emissions with overall pressure ratio and combustor technology.

ciency of modern aero-engines and their $NO_x$ performance. The simulation results show that improving engine propulsive efficiency is likely to have a benign effect on $NO_x$ emissions at high altitude; at sea-level conditions $NO_x$ emissions are particularly likely to reduce. Improving engine thermal efficiency however has a detrimental effect on $NO_x$ emissions from RQL combustors, both at high altitude and particularly at sea-level conditions. LDI combustor technology does not demonstrate such behaviour and can therefore help decouple $NO_x$ emissions performance from engine thermal efficiency.

The current legislation permits trading $NO_x$ emissions to improve engine efficiency and hence reduce $CO_2$ emissions through reduced fuel consumption. This also leads to lower direct operating costs for airliners, which can be seen as beneficial for aviation growth. If we are to reduce the contribution of aviation to global warming, however, future certification legislation may need to become more stringent and comprehensive, i.e., cover high altitude conditions. By doing so we can help unlock the competitive advantage of lean burn technology in relation to cruise $NO_x$ and mission performance.

## 4.4 Technical risk

A technical risk analysis based on the tools and algorithm described in Chapter 3 is presented here. The work looks at quantifying the performance impact of the uncertainties involved in production scatter, component deterioration and measurements used for engine control. The focus is on the turbofan configuration for which the trade-off analysis was carried out in the preceding section.

The primary novelty of the present study lies on the insight provided when quantifying such risks early in the engine development process, i.e., the conceptual design phase. A comparison between Monte Carlo sampling and a fast analytical approach is also given.

### 4.4.1 System performance modelling

In the studies presented in this section three major engine operating points were considered: Hot–Day Top–of–Climb (HD TOC), End–Of–Runway Hot–Day Take–Off (EOR HD TO), and ISA Mid–Cruise (ISA MCR). The engine configuration chosen was the 3–shaft turbofan engine for long–haul applications, i.e., 70,000lbf thrust, that was utilised also in the trade-off analysis section and is illustrated in Fig. 3.2. The selected component technology levels were in general consistent with an engine designed to enter service in 2020.

The simulations presented herein where based on the steady-state performance mathematical description shown in Table 3.1. A number of uncertainty distributions were used to estimate the effects of production scatter, deterioration as well as measurement uncertainty, as presented in Table 3.2 and Table 3.3. Based on these uncertainty distributions, a number of Monte Carlo studies were carried out and are presented in the next section. For each study, 10,000 random points were simulated and analysed statistically. In addition, key parameters such as $SFC$, $T_4$, $T_{46}$ and $N_{46}$ were estimated using the fast analytical approach presented earlier in this work. This was based on the use of traditional Taylor expansion series and the assumption of constant first derivatives around the datum engine operating point. All simulations where run either at a constant thrust or at a constant measured parameter.

### 4.4.2 Production scatter and component deterioration

A comparison of Monte Carlo simulations against the fast analytical approach, for an engine operated at constant thrust with full deterioration at the end–of–runway hot–day take–off condition, is illustrated in Fig. 4.43. It can be observed that the analytical approach consistently under-predicts the expected increase in $SFC$ and $T_4$ by up to 0.4% and 4K, respectively. Similar trends are observed when looking at the cumulative probability curves, with the best agreement found for $N_{46}$. Nonetheless, these differences are well within the accuracy of any engine deterioration estimates made during the conceptual design stage.

The fully deteriorated engine demonstrates a significant increase in key type test certificate parameters such as $T_{46}$ and $N_{46}$, in excess of 40K and 0.6%, respectively, for engine variations within one standard deviation. Although often not a type-test certificate parameter itself, $T_4$ plays a key role in establishing maximum $T_{46}$ levels. It can be observed that $T_4$ for a fully deteriorated engine can increase in excess of 45K for engine variations within one standard deviation. $SFC$ also deteriorates significantly which is particularly important when the manufacturer's contractual obligations include performance retention guarantees. The simulations suggest an increase in $SFC$ in excess of 3.5% for engine variations within one standard deviation.

The same trends are observed when repeating the analysis at ISA mid-cruise conditions, as illustrated in Fig. 4.44. It is therefore critical to consider deteriorated performance during the conceptual design phase, particularly for determining type-test rotational speeds and temperatures, as well as $SFC$ guarantees. Furthermore, the fast analytical approach is suitable accuracy-wise for use in conceptual design optimisation studies; this holds particularly true considering that it is several orders of magnitude faster than the rigorous Monte Carlo approach i.e., it only requires the simulation of a handful of operating points.

A comparison of Monte Carlo simulations against the analytical approach, for an engine operated at constant thrust with typical production scatter at the end–of–runway hot–day take–off condition, is illustrated in Fig. 4.45. Similar conclusions can be deduced as with the deteriorated engine case, albeit the under-prediction is not always present. The fast analytical approach is even more suitable in the production scatter case, since the assumption of constant model sensitivities holds better the closer to the datum operating point one remains i.e., under-predicting $SFC$ and $T_4$ by up to 0.1% and 1K, respectively.

The same trends are observed when repeating the analysis at ISA mid-cruise conditions, as illustrated in Fig. 4.46. It is important to note that when considering production scatter, the average engine (i.e., the engine that has a worse performance than 50% of the engines produced) will deviate mildly from the spec design, albeit within 0.1% and 2K for $SFC$ and $T_4$, respectively. The 80% engine (i.e., the engine that has a worse performance than 80% of the engines produced) will suffer from up to +0.3% $SFC$, +0.2% $N_{46}$, +5K for $T_4$ and +4K for $T_{46}$. This is particularly important for establishing correct $SFC$ guarantees as well as making preliminary estimates of engine production margins. These are elements to be considered in robust conceptual design.

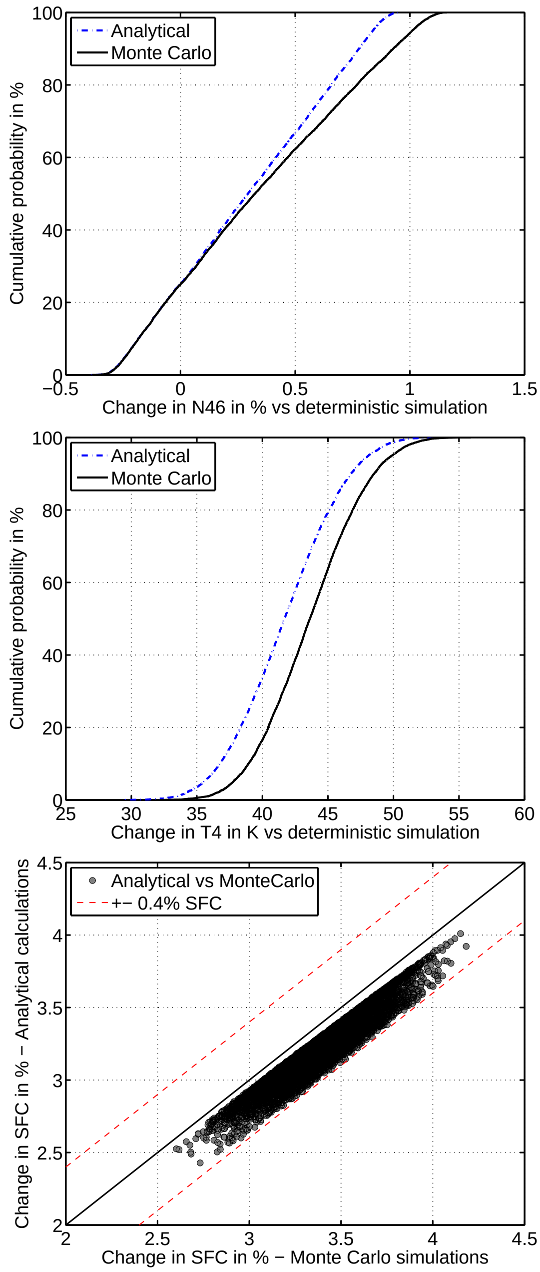


Figure 4.43: Analytical vs Monte Carlo - Full deterioration, constant take-off thrust.

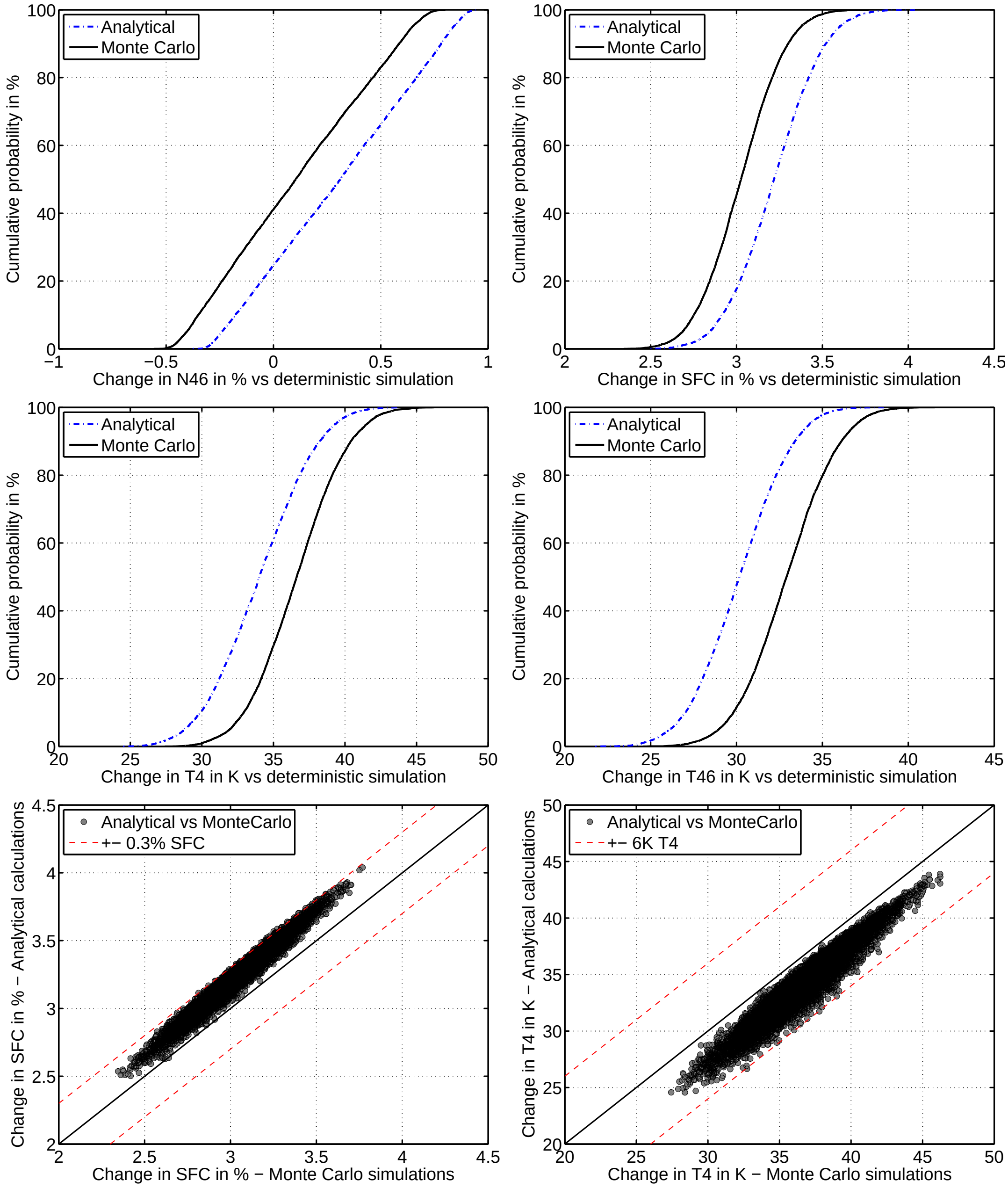


Figure 4.44: Analytical vs Monte Carlo - Full deterioration, constant cruise thrust.

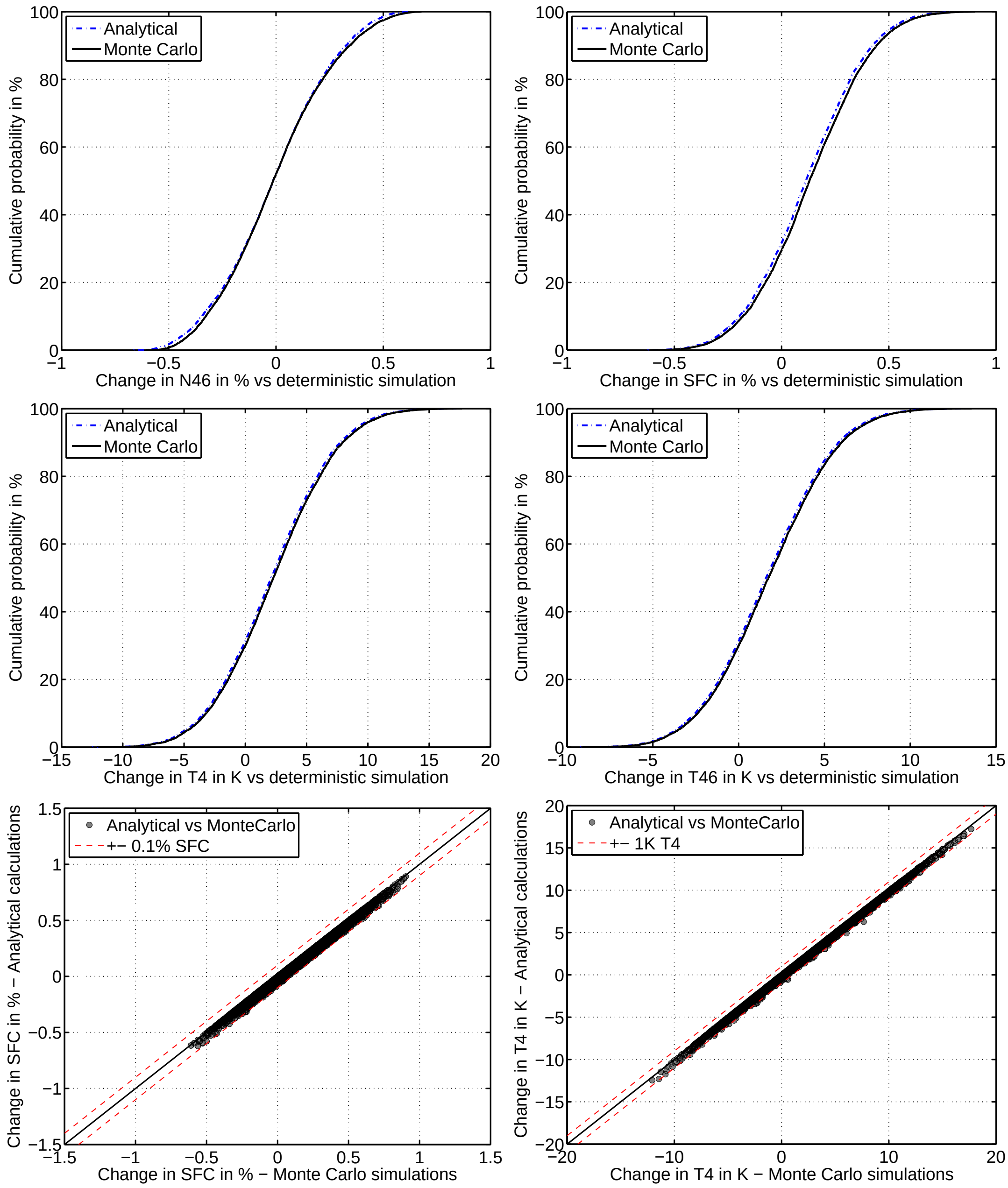


Figure 4.45: Analytical vs Monte Carlo - Production scatter, constant take-off thrust.

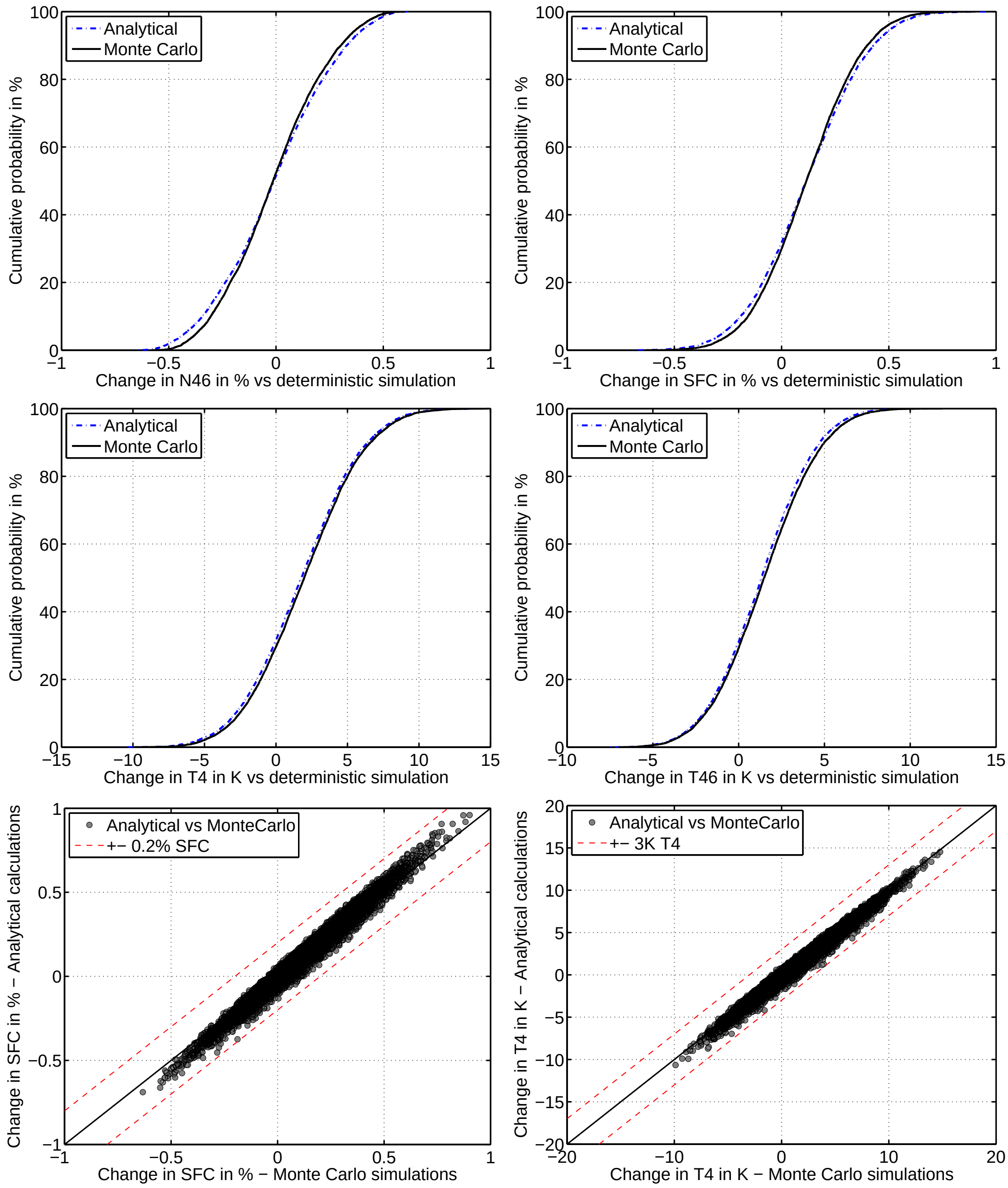


Figure 4.46: Analytical vs Monte Carlo - Production scatter, constant cruise thrust.

### 4.4.3 Measurement uncertainty and engine control

A comparison of Monte Carlo simulations against different control approaches, for an engine operated with full deterioration at the end–of–runway hot–day take–off condition, is illustrated in Fig. 4.47. The engine is simulated operating at three different constant parameters, $FN$, $N_{46}$ and $T_{46}$, respectively. It can be observed that the choice of measured parameter against which to rate the engine has a significant effect on performance. The ideal case is set as being able to run the engine at constant thrust i.e., make use of direct in-flight thrust measurements with zero error. In reality, however, thrust can only be directly measured directly on a test bed. Therefore, alternative measured parameters must be used for the purposes of engine control during actual flight.

Operating the engine at a constant $N_{46}$ will yield similar performance over time, with loss of thrust limited to about 2.5% $FN$. Lower levels of $SFC$, $T_4$, $T_{46}$ and $P_3$ are estimated in this scenario, as a result of operating the engine at a lower power level.

Operating the engine at a constant $T_{46}$ will yield significantly deteriorated performance over time, particularly if one accounts for the typical measurement uncertainties associated with thermocouples operating in harsh environments. The loss of thrust can be as high as 10% $FN$, while $P_3$ can drop by as much as 8%. Operating the engine at such reduced thrust levels results in significantly lower levels of $SFC$, $T_4$, and actual $T_{46}$.

It is therefore paramount to consider control system design - including measurement uncertainty - when assessing the performance of a deteriorated engine during the conceptual design stage. This is particularly important for determining type-test rotational speeds and temperatures, as well as for providing competitive SFC guarantees that can be achieved without excessive risk during the engine development programme.

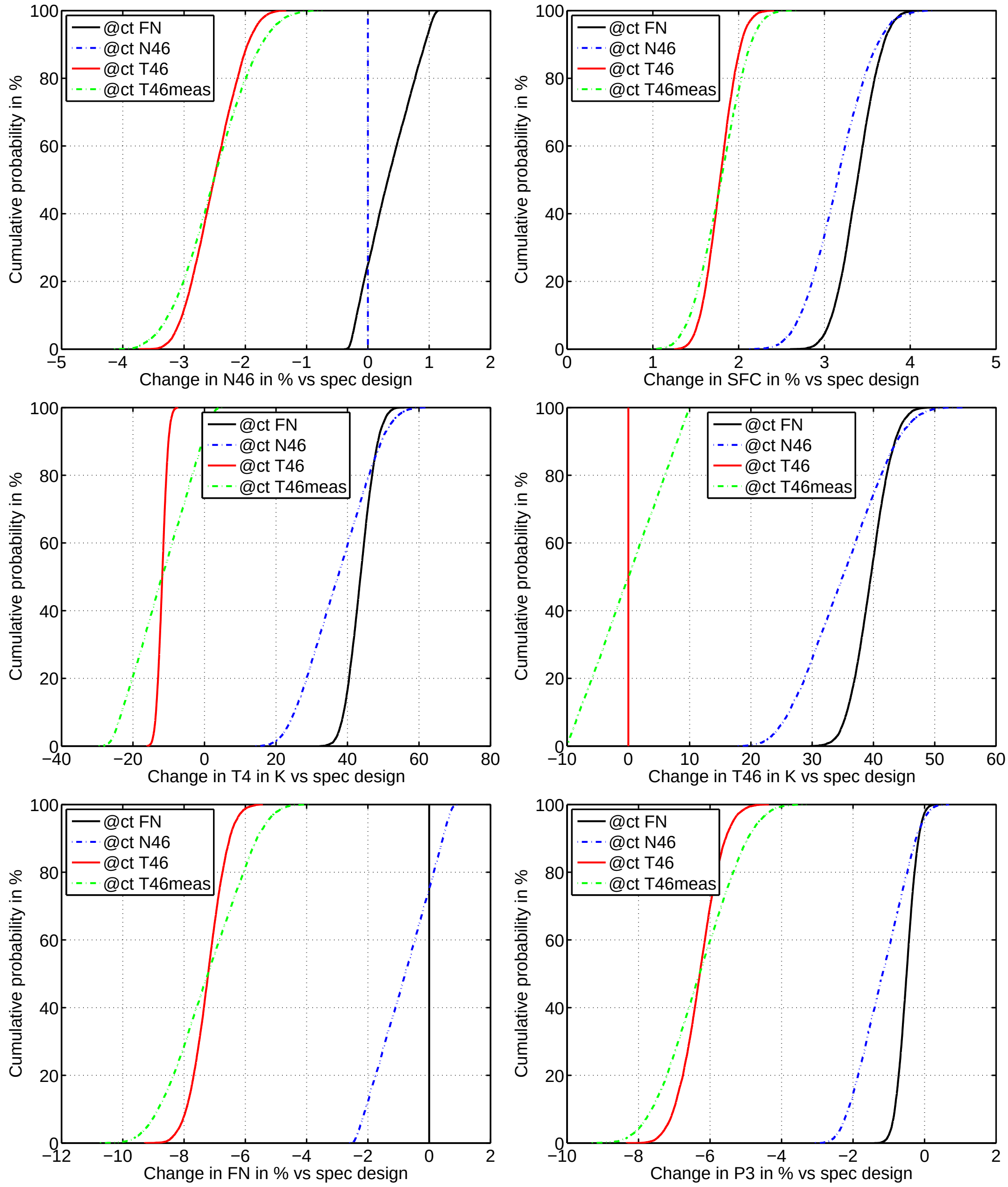


Figure 4.47: Measurement uncertainty and engine control - Full deterioration, various control parameters at take-off.

### 4.4.4 Summary

Insight has been provided on the potential benefits to be tapped from a transition from the traditional deterministic approach for system analysis to a stochastic (robust design) approach for economic decision-making under uncertainty. A basic methodology has been outlined and applied on a specific conceptual design case for a conventional turbofan engine. Use has been made of the same multidisciplinary conceptual design tool, as in the previous sections.

The sensitivity of an optimal engine design obtained deterministically to real-life uncertainties has been found to be far from negligible. The considerable impact of production scatter, measurement uncertainties as well as component performance deterioration, on engine performance must be catered for; this includes taking into consideration control system design aspects. A fast analytical approach has been shown to be sufficiently accurate for the the conceptual design process, particularly for estimating key performance parameters. These relate to type-test certification and performance retention guarantees including preliminary estimates of engine production margins.

# Chapter 5

# Pedagogical Perspectives

Despite the need for highly qualified experts, multi-disciplinary gas turbine conceptual design has not been a common study topic in traditional undergraduate and post-graduate curriculums. Although many courses on specialised topics in gas turbine technology take place, limited attention is given on connecting these individual topics to the overall engine design process. Teaching conceptual design as part of an engineering curriculum, or as an intensive short course, may help to address the industrial need for engineers with early qualifications on the topic i.e., prior to starting their careers in the gas turbine industry.

This chapter presents details and lessons learned from:

- The integration of different elements of conceptual design in an existing traditional MSc course on gas turbine technology through the introduction of group design tasks.

- The development and evaluation of an intensive (short) course on gas turbine multi-disciplinary conceptual design as a result of an international cooperation between academia and industry.

- The development of a new BSc course where gas turbine technology is an integral part.

Within the short course, the students were grouped in competing teams and were asked to produce their own gas turbine conceptual design proposals within a given set of functional requirements. The main concept behind the development of the new design tasks, and the new intensive course, has been to effectively mimic the dynamics of small conceptual design teams, as often encountered in industry. The results presented are very encouraging, in terms of enhancing student learning and developing engineering skills.

## 5.1 Approach to course development

Just like the research methodology employed in the main part of the present thesis, the approach to course development also needs to be an iterative one. There are 4 key stages to follow - in an iterative manner - during the development of a course, as discussed by Haggis [119], and illustrated in Fig. 5.1: (i) design, (ii) implement, (iii) evaluate, and (iv) improve. Each stage is inherently linked to answering a key question as follows:

- What are the desired learning outcomes the students need to achieve?
- How to ensure that students achieve the desired learning outcomes?
- How well did the learning process work?
- How to enhance the effectiveness of the learning process?

The approach therefore starts by setting up appropriate learning outcomes that capture the skills and knowledge the students must attain after successfully completing the course. This has been the default praxis in higher education for a number of years, although some studies critical to this approach have surfaced in recent years [120]. In the context of learning outcomes, the role of the teacher as a mind developer and a mentor emerges, as opposed to that of an expert [121]. Choice of learning outcomes that promote life-long skills development, including the capacity for independent learning, is therefore of particular importance.

In the next stage of the course development process, appropriate teaching and learning methods are implemented to fit the desired learning outcomes. Biggs [122] covers in great detail a large number of such modern methods. The choice among such methods is a non-trivial task and can be heavily influenced by the way both faculty, as well as students, view the learning process in higher education [123].

In a perfect scenario the teaching learning methods employed go hand-in-hand with the assessment methods used to evaluate student learning [124]. Possible examples of this can be extensive course assignments and group projects employing formative assessments with continuous feedback loops [125]. The term assessment in this context may refer to any form of appraisal of student performance [126]. Formative assessments empower the students to identify by themselves their own weaknesses and focus on ways to address them. At the same time it also allows for teachers to adjust their teaching approach to support more effectively struggling students [127]. Depending on the educational environment it may be possible to completely remove summative assessment practices; this however may be inhibited by learning outcomes focused on low-level cognitive skills, such as knowledge and as opposed to analysis and synthesis [128].

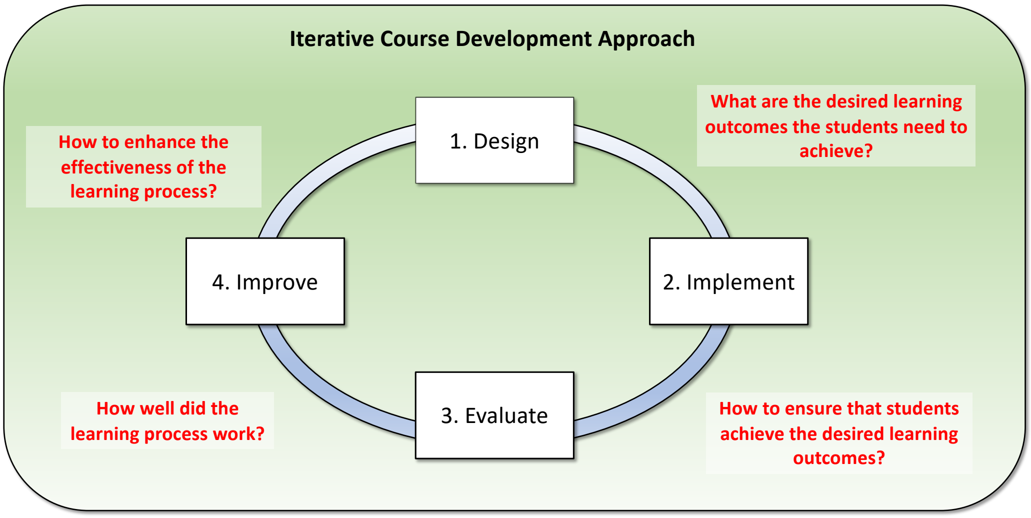


Figure 5.1: Iterative course development approach.

While the course is given it is then very important to evaluate how well the educational process is working. The focus here must be set both on identifying shortfalls in the methods employed, as well as those elements whose implementation was successful in terms of enhancing student learning. Through critical reflection the teaching team is then tasked with making changes in the teaching and learning methods used. If needed, the course learning outcomes may also need to be revised at this stage [129]. At this point one full circle of the course development process will have been completed, and the iterative process is then repeated anew.

## 5.2 Gas turbine education

Gas turbine designs have evolved dramatically over the past 50 years. The know-how has been hard won and is a result of strong and continuous research and development efforts from industry, in collaboration with academia. The achievement of high technology levels however, is inevitably linked with increased development costs, and for the industry to remain viable, cost-effective research and development is needed. This need has led to the development of complex in-house methods and tools for multi-disciplinary gas turbine conceptual design. Practitioners of these methods and users of such tools are, and can of course only be, experts in gas turbine conceptual design.

Despite the need for such highly qualified experts, gas turbine conceptual design has not been a common study topic in traditional post-graduate curriculums. In fact, the provision of formal education on multi-disciplinary gas turbine conceptual design to future engineers has been rather rare. Conceptual design specialists are often people simply rising to the challenge after having been formally educated in gas turbine performance, and less often in some of the general fundamentals of system analysis. Within the premises of a gas turbine manufacturer, multi-disciplinary gas turbine conceptual design is often taught almost by word of mouth over a period of several years of employment. Conceptual design specialists are expected to develop their knowledge through consecutive secondments within different departments in the company and through a continuous mentoring process performed by senior specialists; this is often referred to as industrial experience.

Within this learning process, it is rather uncommon for any form of structured academic teaching to take place. In some cases, company employees may be offered the possibility of taking a one-week short course on a particular gas turbine technology subject. This typically occurs when moving to a new department within the same company i.e., as an introduction to the new line of work to be carried out. Such courses are typically either university products, or internal company products, and are focused on the particular subject at hand. Especially within the academic environment, limited attention is given to connecting the individual topic to overall engine design.

Teaching conceptual design as part of a post-graduate curriculum, or as an intensive short course, may therefore help to address the industrial need for engineers with early qualifications on the topic i.e., prior to starting their careers in the company. Despite the fact that many details in gas turbine conceptual design and advanced technologies tend to be well kept company secrets, there is a good amount of information available in the public domain. This information can be used within the university environment for educational purposes, by developing courses that fulfill specific industrial needs and are hence of high value to the gas turbine industry.

### 5.2.1 Problem-based learning

In the author's view, courses on gas turbine conceptual design can benefit if problem-based learning is made an integral part of the course. This may be achieved by means of extended hands-on design tasks that focus on real-life multidisciplinary design problems. Within the higher education community there has been an increasing emphasis placed on student learning through inquiry and the use of problem-based learning [130]. Benefits from the introduction of hands-on design projects include improvement of important cognitive and personal skills and a higher probability that students may pursue a post-graduate degree [131]. Furthermore, introducing design problems with industrial relevance in the curriculum can help students develop engineering skills that are typically picked up after graduation but "can make the difference between success and failure in one's engineering career" [132].

Some positive experiences from the use of problem-based learning in teaching gas turbine technology have previously been presented in Hourmouziadis et al. [133], Mund et al. [134], and Svensdotter et al. [135], but these efforts have essentially focused on developing new project courses, in cooperation with industrial sponsors. These courses comprised very limited lecture time (primarily invited lectures by industrial experts) and were engineered to help students relate lecture material - taught in parallel (or in previous years) as part of more traditional courses - to particular real-life multi-disciplinary design problems, as typically encountered in the gas turbine industry.

No experiences have been reported in the literature with respect to introducing problem-based learning as an integral part of an existing stand-alone traditional course on gas turbine technology. Furthermore, with the exception of the collaboration presented in [136], little attention has been given in introducing problem-based learning in (the rather niche market of) intensive courses on gas turbine multi-disciplinary conceptual design. In the next sections, details and lessons learned will be presented from: (i) the integration of different elements of conceptual design by means of extended design tasks in an existing traditional MSc course on gas turbine technology, and (ii) the development of an intensive course on gas turbine multi-disciplinary conceptual design that was designed for the specific needs of an industrial sponsor.

### 5.2.2 The Swedish university environment

At Chalmers University of Technology the academic year is divided into four study quarters, each seven weeks long, followed by a dedicated exam week during which a 4-hour written exam is taken. The study year is thus comprised four times eight weeks equalling in total 32 weeks of study. During each study quarter, the students normally follow two to three courses in parallel. At Mälardalen University a similar form is used with the difference that each study year comprises four times 10 weeks equalling in total 40 weeks of study.

This imposes some constraints on how conceptual design can be integrated into the learning process. Preferably, it should be made possible for the students to complete their conceptual design tasks within five to six weeks, to allow them to fully concentrate on preparing for the final examination. Furthermore, the workload should be evenly distributed over the course weeks so as not to conflict with the student effort requirements by other courses that run in parallel.

Several MSc programs in Sweden allow longer project-oriented courses to run over extended periods, covering several study quarters. The examination may then be replaced with a series of hand-in tasks, reports and the examiner's assessment of the students' performance as they cooperate to tackle a joint project. Still, the traditional and predominant course structure in Sweden is the 7-week or 9-week study period (followed by a written examination given during the dedicated exam week) and over the past years, teaching of gas turbine technology has followed this approach.

### 5.2.3 The Brazilian university environment

At Instituto Technológico de Aeronáutica (ITA) the teaching of gas turbine technology takes place primarily at the graduate level in a much similar approach as the one described for Chalmers University of Technology; this holds particularly true for the ITA Professional MSc programme. The programme has a duration of two years and each year is divided into three 4-month periods. During the first year all of the lecturing take place, with each course comprising two periods of eight weeks; this sums up to a total of 48 weeks of lecturing for the entire year. The students are expected to achieve 24 credits during this year. Two credits are awarded for written exam scores of at least 8 out of 10, whilst one credit is awarded for scores between 6.5 and 8; no credit is awarded for scores under 6.5. The students must also produce and submit a paper to an international congress or journal. For accepted articles the students can be awarded up to 2 credits per paper, totalling a maximum of 3 credits. During their second year the students must focus solely on their research and are expected to produce a dissertation. To be awarded the title of Professional MSc they must, additionally, defend and have their dissertation approved during a *viva voce* session.

## 5.3 Improvement of an existing MSc course

### 5.3.1 Integration of conceptual design elements

Various elements of conceptual design have been integrated in an existing gas turbine technology course, through group design tasks, with the purpose of supporting the understanding of the course material and ensuring that students commit to the course early in the study quarter. Students are given bonus credits for their efforts on the group design tasks, and despite the fact that the latter are not mandatory, a large majority of the students choose to work on them to improve their learning. The integration of different elements of conceptual design within a MSc course on gas turbines can help:

- Provide cohesion between different disciplines and aspects studied.
- Resolve particular learning obstacles.

- Subject students to tasks that allow them to exercise engineering skills and judgement.

Cohesion in this context should be understood as the process of synthesis by which the students begin to appreciate subject interrelationships, by viewing thermodynamics, turbomachinery, systems analysis, etc., not as separate topics, but as a whole.

The next two sections are intended to provide some experiences from integrating different elements of gas turbine multidisciplinary conceptual design into an existing curriculum, based on what is viewed as more traditional academic learning. In more detail, lessons learned are presented from the development of two different design tasks, used within an existing 7-week MSc course on "Gas Turbine Technology" at Chalmers University of Technology. It should be pointed out that due to the student effort required, these two design tasks were never run in parallel, but were instead handed out during different academic years.

### 5.3.2 Design task 1 - The Whittle W1 engine

This group design task comprised three parts and was developed with the purpose of introducing some cohesion between the various subjects studied as part of the gas turbine technology course. The assignment concentrated on repeating some of the design work carried out by Sir Frank Whittle [137]. This allowed groups consisting of three to four students to work on developing a thermodynamic design point model, a mean line design of the one stage axial turbine and an altitude performance assessment of the engine. The task was normally completed within a total effort of about 40 hours.

The design task was specifically engineered so that the students would have to re-use their design point performance data of the W1 engine for establishing boundary conditions for the mean-line turbine model, as well as for setting a starting point for the final performance work. Setting the focus of the design task over a basic turbojet cycle made it possible for the students to program their own performance models with a limited effort. The modelling of more complex aero engine cycles requires either a more substantial student effort, or forces the tutor to introduce an existing performance code. From a learning perspective, it is always a considerable advantage if the modelling is totally transparent and preferably performed, line by line, by the students. On the other hand, since only few students have an intuitive and strong understanding of numerical analysis, the solution of more than a few non-linear coupled equations tends to shift the focus from the understanding of engine performance to the struggle of using existing (or developing new) numerical routines.

Basic turbojet performance theory, as it is developed in Saravanamuttoo et al. [138] makes the solution process quite transparent, but the exercises accompanying the text suffer from the obvious challenge of effectively illustrating the complete performance solution process. The consequence of this is that students who learn primarily by working through examples tend to have difficulties in grasping the overall process associated with performance calculations and also have difficulties in applying the approach on more complex cycles. Thus, the gas turbine conceptual design task, as described above, can assist in resolving this learning obstacle.

When it comes to subjecting students to design tasks that allow (or demand) exercising engineering judgement, an initial reflection on the predominant examination form at Chalmers should be made. Since the students are graded primarily by their performance in the written exams, students will tend to concentrate their study efforts on handling problems that could be asked in an exam paper. Problems that the students have not seen in a course, or problems that require quite innovative use of the knowledge acquired, are often not suitable for exams. Still, the ability to find a solution to a rather challenging task within a few days is typical for everyday engineering work. There can be several difficult steps involved in solving an exam problem, or providing a proof, but the complexity will ultimately be limited by the examination time available. A typical engineering problem, however, such as developing a computer code, may contain hundreds of more or less complex calculations. To be successful in handling such a task, different skills are required, and therefore need to be developed within an engineering educational framework. Another class of problems that is infrequent in engineering education, but is quite frequent in engineering work, are problems that do not have a solution. Such a problem may, for instance, require that a constraint is relaxed, or that the physics used to describe the problem are made more complex, or in some cases reduction of complexity may provide a solution.

For all these reasons, there is good merit in giving opportunities (and incentives) to students for spending their study time on solving problems that for practical reasons cannot be part of a traditional 4-hour examination. In the context of a course on gas turbine technology, the introduction of different elements of conceptual design through group design tasks helped assist in the training of important engineering abilities. The design of the Whittle engine provided a framework where a number of data ranging from several disciplines had to be handled simultaneously. The solution process initially looks straightforward, but proves to be quite open-ended and results in the need for substantial reverse engineering. In more detail, a careful read through [137] eventually makes it clear that the radial compressor efficiency provided in the paper should be seen as a design target set by Sir Frank Whittle, rather than a number that was actually achieved. What the students then need to do, is to estimate the work input based on the rotational speed and impeller geometry together with a guessed efficiency. A number of educated estimates, together with a somewhat uncertain value for the turbine inlet temperature, eventually leads the students to establish a value for the static thrust, which can be considered as relatively accurate measured information.

Apart from the observations presented associated with learning basic gas turbine theory, this design task also serves as a good example of how the introduction of radical innovations many times is associated with personal sacrifice and years of struggle. It is the belief of the author that students who have been exposed to the discussion of what is needed to radically change a business are more likely to have the courage and persistence to pursue such a direction in their future carriers.

### 5.3.3 Design task 2 - Conceptual design of a future turbofan engine

This group design task also comprises three parts concentrating on the analysis of the installed performance of a future turbofan engine. The positive experiences drawn from the Whittle task have been retained, in terms of attempting to introduce more cohesion between the different subjects studied. More focus however is given on the use of rigorous performance estimation procedures, mean line design of all the turbomachinery components, and finally an assessment of the impact of nacelle size and engine weight on installed performance. The design task aids the student in establishing a connection between thermodynamics, component design and overall system analysis.

This design task relies on the students having a better understanding of turbomachinery prior to taking this course. Thus, this implementation may provide some new ideas to teachers who wish to present gas turbine theory to students with a prior experience in turbomachinery. As mentioned above, it is a more demanding assignment in the sense that it brings in a wider range of concepts and more advanced theory than what is presented in the introductory text by Saravanamuttoo et al. [138]. It is expected that the students commit about 60 hours to complete all three parts of the assignment with the work being carried out by teams of three to four people.

In the first part of the assignment, the students are again requested to developed an engine design point performance model. Rather than using simplified relations in their models, such as the ones presented in Saravanamuttoo et al. [138] and other similar introductory texts, thermodynamics are dealt in a rigorous way [40, 139] based on the argumentation given by Kurzke [140]. For instance, the use of constant specific heat ratios (i.e. perfect gas) is replaced with the use of enthalpy and entropy tables and the Gibbs equation (i.e., half-ideal gas). The performance data derived are subsequently used in the next part of the assignment comprising the mean-line design of the turbomachinery components.

Students that have taken a course in turbomachinery are aware of most of the basic concepts that are introduced in [138], related to axial and radial compressor theory as well as axial turbines. An approach that may then be suitable is to bring in material that addresses technology levels on current state-of-the-art or future turbofan engines. To accomplish this, data on the conceptual design of different gas turbine components have been collected and correlated based primarily on the work by [141]. Axial Mach numbers, tip Mach numbers, aspect ratios, stage loadings and hub to tip ratios can be used to work out stage numbers and define a gas path. Checks on turbine stress levels can be made in a systematic manner. Students are then asked to implement these correlations as part of the code they developed for predicting the design point performance of the engine.

In the last part of the design task, emphasis is placed upon deriving the steady-state performance of the engine at 3 major operating points (hot-day end-of-runway take-off, hot-day top-of-climb, mid-cruise), as well as establishing nacelle size and engine weight. This information is subsequently used by the students for assessing the installed performance of their designs. The learning obstacle associated with coming to grips with the complexity of turbofan engine steady state performance and weight prediction cannot be tackled directly by letting the students develop their own codes, and in-house tools are therefore provided to the students.

Feedback and discussion during the course of this design task brings the student into a fairly realistic framework for understanding how the design constraints of turbofan engines limit their performance. It is rather difficult to ensure that the students get this overview of how the various disciplines interrelate based solely on traditional teaching and a written exam. The task retains the environment of relatively open-ended problems that may have to be iterated on, or may even lack a solution, and confronts the student with a number of design dilemmas. It should be pointed out however, that the value of approaching the complexity of a turbofan engine is to some extent compromised by the fact that the students are not able to fully work through all the information needed, and their efforts in the last parts of the design task have to be assisted by the use of pre-developed codes.

## 5.4 Development of a new intensive course

### 5.4.1 Course partners and delegates

Although many courses on specialised topics in gas turbine technology take place within ITA and the MSc programme, limited attention is given on connecting these individual topics to the overall engine design process. Teaching of gas turbine conceptual design as part of a post-graduate curriculum, or as an intensive short course, may help to address the industrial need for engineers with early qualifications on the topic i.e., prior to starting their careers in the gas turbine industry.

With that need in mind, the author developed and delivered an intensive course on gas turbine conceptual design that was specifically targeted for the needs of 20 students of the ITA Professional MSc programme in Gas Turbine Technology, and 9 employees of VALE Soluções em Energia. All ITA students had a minimum of 5 years of engineering education prior to the course (i.e., Bachelors + MSc) and were pursuing their second MSc degree; some also possessed limited working experience. The large majority of VALE students were holders of a PhD degree and had between 5 and 20 years of working experience in different disciplines of mechanical engineering.

The short course was held in São José dos Campos, São Paulo, Brazil as a joint effort between Chalmers University of Technology, and Instituto Technológico de Aeronáutica, and VALE Soluções em Energia. The course material was prepared by Chalmers University and was delivered at ITA facilities in Brazil as part of the ITA MSc programme. ITA acted as the overall coordinator of the project whilst VALE acted as the main sponsor.

### 5.4.2 Course description

#### Technical contents

The developed intensive course capitalises on the experience gained from previous teaching efforts, and also from the practical knowledge gained through participation in several integrated projects [27,32,35] in collaboration with some of the major stakeholders in the European aero engine industry. Substantial know-how has been gained whilst attempting to capture and emulate within an advanced multidisciplinary conceptual design tool [82] the essential details and high level performance of the actual conceptual design process, as typically applied in the gas turbine industry.

As illustrated in Fig. 5.2, the technical focus of this course was limited to only two out of several major topics in gas turbine conceptual design: engine performance and sizing. Complementary lectures on other topics were also provided, but due to time constraints this could not be pursued at the same level of detail. The main aim of the course was to introduce the students to the interdependence of different disciplines (and engineering groups) in the overall engine design process.

The course covered material on several disciplines utilising public domain sources for each topic. The lectures on engine performance were based on the work of Walsh and Fletcher [40], Kurzke [83], Kyprianidis [139], and Gronstedt [142]. The lectures on component preliminary design were based on the work of Saravanamuttoo [138], Dixon and Hall [143], Grieb [141], Lefebvre [8], Doerr [144], and Gronstedt [145].

Table 5.1: Lecture structure for Week 1, 2 and 3.

| | Hrs | Topic |
|---|---|---|
| Day 1 | 1 | Welcome and Course Overview |
| | 2 | Introduction to Gas Turbines |
| | 1 | Introduction to Conceptual Design |
| Day 2 | 2 | Non-dimensional Theory for Gas Turbines |
| | 2 | Fan Sizing |
| Day 3 | 2 | Component Modelling for Real Cycles |
| | 2 | Axial Compressor Sizing |
| Day 4 | 2 | Axial Turbine Sizing |
| | 2 | Design Task Hand-Out |
| Day 5 | 2 | Cascades and Loss Modelling |
| | 2 | Steady State and Transient Performance |
| Day 6/7 | | No lectures |
| Day 8 | 4 | Introduction to Automated Gas Turbine Performance and Design Calculations |
| Day 9 | 4 | Conceptual Design of a Modern Turbofan |
| Day 10 | 4 | Conceptual Design of a Modern Turbofan |
| Day 11 | 2 | Combustor Design for Low Emissions |
| | 2 | Gas Turbine Materials and Lifing |
| Day 12 | 2 | Design Space Exploration |
| | 2 | Future Component Technology |
| Day 13 | 2 | Noise abatement |
| | 1 | Alternative Fuels (Group Hand-In) |
| | 1 | Future Applications of Gas Turbines |
| Day 14 | 2 | Advanced Concepts and Technologies |
| | 2 | Industrial vs. Aero Gas Turbines |
| Day 15 | 4 | Evaluation of Final Engine Designs |

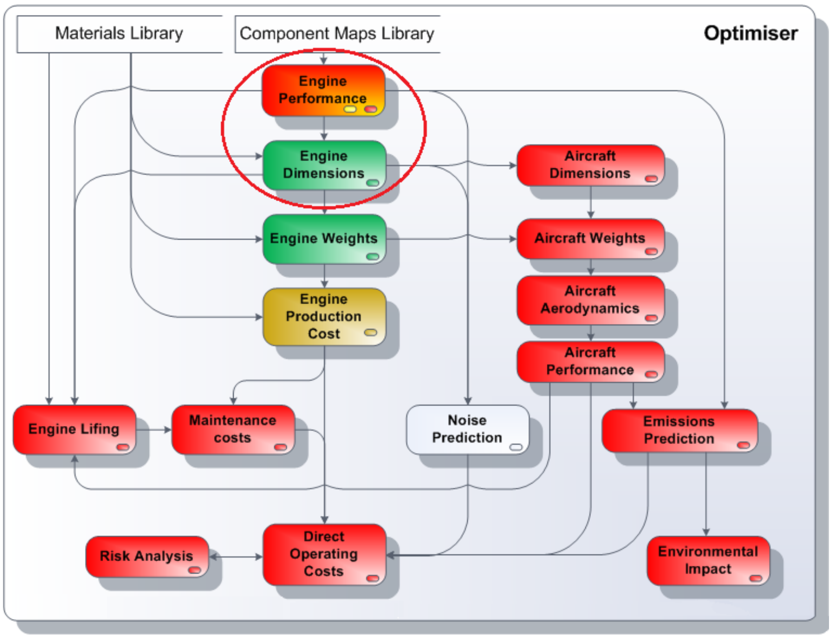


Figure 5.2: Conceptual design algorithm [82].

### Lecture structure and participant efforts

The structure of the lectures for all three weeks of the short course is given in Table 5.1. The learning focus for each week was substantially different. During Week 1, the lectures focused primarily on presenting basic gas turbine theory, as well as on explaining design methods that would later on be utilised within a group design task. During Week 2, the focus was shifted to the presentation of more advanced topics in gas turbine multi-disciplinary design. During the last week, lectures were given on 'exotic' topics, aiming to provide students with a broader perspective on the conceptual design process. The total lecture effort was 52 hours with a maximum of 4 lecture hours per day.

During Week 1, the students were given short daily assignments and were asked to work on them in groups. The hand-out of the group engine design task was set for the end of Week 1 with the teams being requested to deliver their final designs near the end of Week 3. The evaluation of the final engine designs took place during the last day of the course during which time the students were provided with feedback on the flaws and merits of their work.

Regular tutoring took place during the entire short course for about 2 hours per day i.e., 30 hours in total. Tutoring during Week 1 focused on the daily assignments. Expert advice was provided to the students, primarily in the form of technical design reviews that took place during Week 2 and Week 3 i.e., from the hand-out up until the conclusion of the design task. No lectures were scheduled for the beginning of Week 2, which gave time to the students to assimilate lecture material from Week 1 and initiate work on the design task.

The expected overall effort from the student side (including participation in the lectures, group work, and personal study) was about 150 hours over a period of 3 weeks. Nevertheless, some of the more motivated students actually exceeded this target and invested up to 200 hours, primarily by utilising the time available during the two interim weekends.

### Group Formation

An effort was made to group the students in such a way as to ensure that a good spread of different (and ultimately necessary) technical skills was present in each team. The students were therefore grouped into 8 preliminary design teams with the selection being based primarily on their previous educational and professional background. No significant effort was made towards considering Belbin roles [146] as an additional criteria for forming the groups. Consideration was given only in avoiding the formation of Apollo teams (pure teams for example were allowed).

In retrospect, team formation based on technical skills alone proved to be a rather poor choice. Some teams demonstrated lack of effective leadership, whilst others lacked motivation, innovation or the capacity to bring closure to their tasks at hand. Some of these shortfalls could very well have been avoided if the students were asked to undertake a formal Belbin Self Perception Inventory [146]. Such an assessment could have helped the tutors during the early stages of the course to asses each student's best team roles, and the resulting knowledge could have been used in the team formation process.

### Group Design Task

As part of the learning process the student groups were given a design task and were asked to complete it by the end of the short course. Their task at hand was to carry out a competitive conceptual design of a 3-shaft turbofan configuration including: general arrangement, engine installed weight, nacelle drag, and installed performance.

As a first step in the design task, the students were asked to carry out a full thermodynamic calculation of the performance of the engine at 3 major operating points: (i) hot-day top-of-climb, (ii) mid-cruise, and (iii) hot-day end-of-runway take-off. The calculations were carried out using an in-house gas turbine performance synthesis code [78]. As part of this process the students were asked to determine expert input (i.e., turbomachinery component efficiencies) from technology charts.

Table 5.2: Design task input parameter datasets as used by each group.

| Group | Entry Into Service | Specific Thrust |
|---|---|---|
| 1 | 1995 | Reference |
| 2 | 2010 | Reference |
| 3 | 2020 | Reference |
| 4 | 2030 | Reference |
| 5 | 1995 | -10% |
| 6 | 2010 | -10% |
| 7 | 2020 | -10% |
| 8 | 2030 | -10% |

Although the customer requirements were the same for all teams (net thrust, power off-takes, customer bleeds), 4 different company technology levels were assumed through an engine Entry Into Service (EIS) term. Furthermore, some groups were asked to design their engines at a lower specific thrust level. The different input parameter datasets provided to each group are given in Table 5.2. All groups designed their cores at the same overall pressure ratio and the same pressure ratio distribution between the high pressure compressor and the fan and intermediate pressure compressor together.

The different technology levels that each team was asked to assume focused primarily on turbomachinery aerodynamic design aspects. This was achieved by providing the students with technology correlations where several major component design choices, such as fan hub to tip ratio, were parameterised against EIS. Furthermore, the students were asked to correct all of their turbomachinery efficiency values (calculated from the methods presented in Grieb [141] and Samuelsson et al. [115]) with correction factors based again on EIS. Weight savings resulting from the use of more advanced materials and manufacturing techniques were not to be considered. The effect of high pressure turbine blade material capability on engine efficiency, however, was explicitly taken into account by setting restrictions on maximum blade metal temperature (and hence minimum cooling flow), based again on EIS.

For the limits or corrections set on different parameters, to account for the use of advanced materials and methods, it was assumed that a Technology Readiness Level (TRL) of 9 would have been achieved at the chosen EIS. Whilst the realism of the values used for the said limits or corrections is of some educational importance, what is of the highest importance is different: the approach followed is aimed towards helping students to understand that conceptual design of future systems must always consider estimates of what is likely to be achieved by the time the product will enter service.

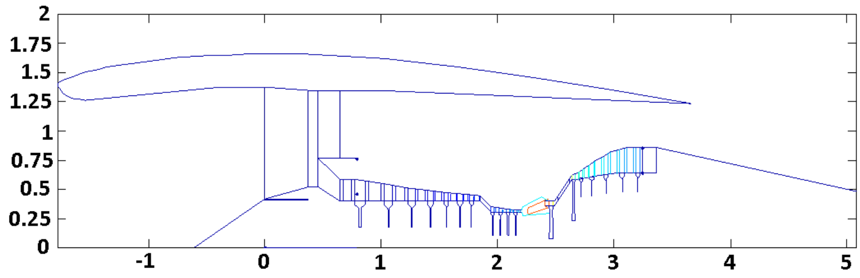


Figure 5.3: Example of group engine sizing results - Engine general arrangement.

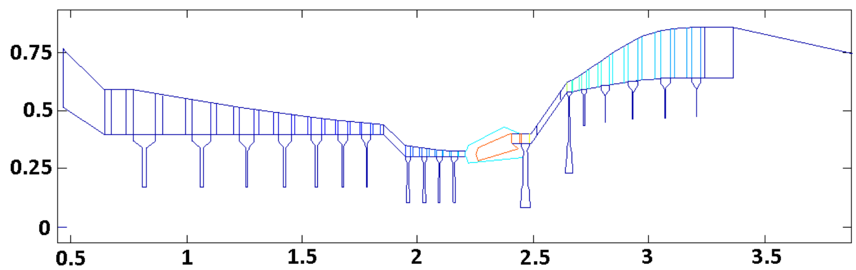


Figure 5.4: Example of group engine sizing results - Core general arrangement.

As a second step in the design task, the students were asked to perform a preliminary aerodynamic and mechanical design of all major engine components. The aerodynamic design was focused on deriving the engine flow path (annulus) and drawing the nacelle lines. The mechanical design was primarily focused on component material choices, disc and casing sizing, and designing the fan for bird strike. The calculations were carried out using an in-house gas turbine weights and dimensions estimation code [79]. As part of this process the students were asked to determine expert input (i.e., fan hub to tip ratio, compressor blade tip speed and axial inlet Mach number, swan neck duct parameter, combustor tilt angle, etc) either from technology charts, or by exercising engineering judgement. The students were permitted to vary the stage count for the two core compressors and the low pressure turbine, whilst the stage count for the fan and the two core turbines was fixed.

An example of a general arrangement as produced by one of the groups is illustrated in Fig. 5.3 and Fig. 5.4. These drawings effectively demonstrate the level of design detail at which the students were expected to work. Basic design choices had to be made for several components including: inlet, fan, intermediate and high pressure compressor, combustor, high pressure and intermediate turbine, low pressure turbine, intercompressor and interturbine duct, bypass duct, jet pipe, core and bypass nozzle, disks, shafts, and nacelle.

As a final step in the design task, the students were asked to summarise their

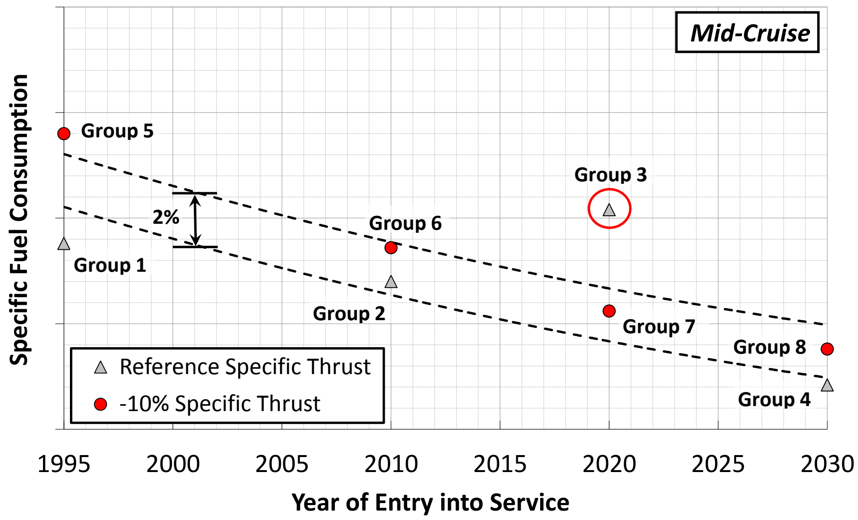


Figure 5.5: Summation and quality assessment of group engine performance results.

efforts in a technical report. This document had the character of a turbofan engine preliminary assessment report. The students had to include not only a short description of the major methods used and their numerical results, but also attempt to quantify uncertainties in the engine design by means of sensitivity analysis.

A high-level summation of the engine performance results as produced by the different student groups is given in Fig. 5.5. These results can be correlated both against EIS and specific thrust and the resulting trends are illustrated in the chart with dashed lines. It is relatively easy to qualitatively assess the group performance estimates through such correlations. For example, it is straightforward to see that the results from Group 3 are not following the expected trends, and a thorough check of the team's performance calculations, and design choices, should be made. For all other groups, the maximum observed deviation from the correlation trend in terms of specific fuel consumption is within 1%.

Such deviations are rather reasonable considering the amount of design freedom the groups were given when producing their general arrangement, and the fact that component efficiencies are derived from the latter and fed back to the performance tool in an iterative manner. A high-level summation of the engine sizing results as produced by the different student groups is given in Table 5.3. It should be noted that the stage count column refers to the following order: fan, intermediate pressure compressor, high pressure compressor, high pressure turbine, intermediate pressure turbine, and low pressure turbine. These results are rather hard to correlate, and the only easily identifiable trend is the change in engine weight and nacelle diameter with specific thrust. In this case, the nacelle

Table 5.3: Summation of group engine sizing results.

| Group | Engine Weight [kg] | Nacelle Length [m] | Nacelle Diameter [m] | Stage Count |
|---|---|---|---|---|
| 1 | 7030 | 5.85 | 3.50 | 1-6-5-1-1-6 |
| 2 | 7060 | 6.05 | 3.61 | 1-6-4-1-1-6 |
| 3 | 7125 | 5.82 | 3.46 | 1-5-4-1-1-7 |
| 4 | 7190 | 5.82 | 3.43 | 1-5-4-1-1-7 |
| 5 | 6680 | 5.52 | 3.32 | 1-7-4-1-1-5 |
| 6 | 6200 | 5.50 | 3.29 | 1-6-4-1-1-6 |
| 7 | 6150 | 5.53 | 3.27 | 1-5-5-1-1-5 |
| 8 | 6210 | 5.49 | 3.27 | 1-5-3-1-1-7 |

diameter choice of Group 2 is in question. The design freedom - together with the fact that all students were asked to work with the same level of materials and manufacturing technology (with the exception of the high pressure turbine blade material) - makes it hard to distinguish in the group results any trend in engine weight with EIS.

### 5.4.3 Course evaluation

At the end of the course a questionnaire was provided to the students to fill out. The results from the questionnaire have been very encouraging and are presented below:

**Q1.**

What is your view on the daily group assignments during Week 1?

1. Not very helpful - difficult to learn from (0%).
2. I knew it already (5%).
3. I learned a bit (20%).
4. It helped my learning a great deal (75%).

**Q2.**

What is your view on the in-house code tutorials?

1. Not very helpful - difficult to learn from (10%).
2. Quite useful for the later work (90%).

**Q3.**

What is your view on the lecture series?

1. Not very helpful - difficult to learn from (0%).
2. I knew it already (0%).
3. I learned a bit (10%).
4. It helped my learning a great deal (90%).

**Q4.**

What is your view on the group design task activity during Week 2 and Week 3?

1. Not very helpful - difficult to learn from (0%).
2. I knew it already (0%).
3. I learned a bit (5%).
4. It helped my learning a great deal (95%).

**Q5.**

What is your overall view on the course?

1. Not very helpful - difficult to learn from (0%).
2. I knew it already (0%).
3. I learned a bit (5%).
4. I learned a great deal. The course was very valuable (95%).

**Student comments.**

The overall rating of the course from the students perspective has been very positive. Nevertheless, the students did raise a few critical points through their feedback.

The technical contents of the course were considered rather hard by about 15% of the delegates; interestingly enough, this came primarily from individuals with higher qualifications (PhD degree holders) in different fields. About 50% of the VALE employees considered the course to be too time demanding, requiring from them time investments that were incompatible with their personal and work obligations (most of them had to resume their company work during the afternoons of Week 1). These two points brought forward an interesting realisation. Teaching complex design interrelations to senior engineers (compared to less-experienced younger delegates) is not always easier. Slightly different teaching approaches may need to be employed for mature students, while care also has to be given during the selection process to ensure that prospective delegates are well aware of the time investment that will be required from them during the course.

The use of automated in-house codes for the group design task in some circumstances inhibited a portion of the students from understanding the influence of different cycle and component design parameters on the overall engine design. Although this was the case for only a portion of the delegates, it did bring forward another interesting realisation. Not all students will come to terms with the fact that *"it is about the design problem, not the software"*, even after several years of formal higher education. Therefore, more care needs to be given in helping all students develop a better understanding of the fact that the engineering importance in the conceptual design process lays primarily on critically analysing numbers and trends, and less on deriving them using a particular piece of software. It should not be underestimated that some course delegates (including mature/senior students) may have yet to come to terms with the latter fact - and this holds true even for a specialised post-graduate course. On the other hand, students should be able to derive the equations that describe the physics behind a particular engineering problem. Since the available course time did not permit for teaching at this level of detail, supplemental material was provided to the students with complete derivations and descriptions of the physics involved in gas turbine conceptual design.

From the teachers' perspective, it was felt that communicational problems did rise between team members, for some of the groups, which generally led to an overall team inefficiency. This mismatch of team roles led to a lack of motivation for some team members and to work overloading for others who had to pick up the slack in order to bring the design task to closure on time.

The most positive student comments that could be highlighted were:

- *"I could never have imagined that in a 3-week course I could end up with such a comprehensive preliminary design project..."*
- *"I now understand how to deal with concepts that I only understood theoretically before..."*
- *"I now understand several important points that require close attention within a whole-engine design..."*

Overall the course was considered successful from the students' perspective, and both the lectures and the group design task requirements were well appreciated. The course did reach its main goal i.e., to introduce the students to the interdependence of different disciplines (and engineering groups) in the overall engine design process. In the future, all delegates would be happy to recommend this course to their colleagues, but only if they possess the necessary determination and time resources for tackling the intensive nature of the lectures and all course requirements i.e., the daily group assignments of Week 1, and the group design task of Week 2 and 3.

## 5.5 Development of a new BSc course

### 5.5.1 About the course

This section presents the structure of a new BSc course, "Heat and Power Technology II", where gas turbine technology is an integral part. The course is given at Mälardalen University in Sweden and is part of two 3-year undergraduate degree programs (Swedish Högskoleingenjör) on Heat and Power technology and Electrical technology, and a 5-year degree program (Swedish Civilingenjör) on Energy Systems. Student intake will vary from year to year and will range from 25 to 50 students. As a prerequisite, the students must have completed courses in Heat Transfer, Applied Thermodynamics, Fluid Mechanics, and Mathematics prior to enrolling to this course.

This undergraduate course acts as a stepping stone for students following the 5-year program helping them to develop the skills needed to follow MSc-level courses. For those students following instead the 3-year programs a key aim is to be able to independently acquire new knowledge and apply existing knowledge on real life problems, as they embark on their professional careers. For these reasons, the course employs a number of different teaching and learning approaches including traditional theory lectures and tutorials, lectures on current research, invited lectures from industry as well as high-profile academics, study visits to industrial facilities, MATLAB labs, as well as a comprehensive assignment that includes preparing a lengthy technical report.

### 5.5.2 Intended learning outcomes and assessment

During the initial stage of the course development a set of intended learning outcomes (ILOs) was set. Although the course is meant to also cover specific technical topics focus was given on the skills the students need to develop. A set of constructive teaching and learning activities was consequently selected, as well as appropriate assessments of student performance, largely based on best practices proposed by Biggs [122]. In total 6 learning outcomes were set:

1. *Describe* the basic design and operation principles of different gas turbine concepts and their components, as well as combined cycles and fuel cells.
2. *Describe* the current state-of-the-art (research and development) in the field of gas turbine and turbomachinery technology.
3. *Apply* existing knowledge from Thermodynamics and Fluid Mechanics to *compute and analyse* different gas turbine concepts in terms of economy, technology and environment.
4. *Communicate* effectively in writing own technical analysis results and conclusions related to gas turbine concepts and turbomachinery.
5. *Optimize* the operational plan of a powerplant from an economic point of view.
6. *Compare and contrast* the environmental and economic impact of different thermal processes.

The students are examined in their achievement of the ILOs through an assignment as well as a written exam. The written exam, which consists of both theory questions and calculation problems, is linked to learning outcomes 1-3, 5, and 6 and provides just over half the credits for the course. The assignment consists of gas turbine performance calculations, turbomachinery conceptual design, and a technical report. The assignment is linked to learning outcomes 3, 4, and 5. A successful completion of the assignment provides 3.5 higher education credits and passing the written exam provides an additional 4 credits. The students have the opportunity to improve their grade in the assignment by submitting a corrected version. The final grade is calculated by combining the grades of the two examination modules, provided the student has passed the written exam (achieved at least 41% of the marks) as shown in Table 5.4.

### 5.5.3 Lecture structure

Lectures on gas turbine performance and component design take place during the first six weeks, with the last three weeks of the course discussing the topics

Table 5.4: Final grade calculation (3 is pass, 5 is maximum)

| **Assignment** | **Exam marks (at least)** | | | | |
|---|---|---|---|---|---|
| **marks** | **41%** | **50%** | **60%** | **65%** | **80%** |
| **-** | 3 | 3 | 4 | 4 | 5 |
| **3** | 3 | 3 | 4 | 4 | 5 |
| **4** | 3 | 4 | 4 | 4 | 5 |
| **5** | 3 | 4 | 4 | 5 | 5 |

of combined cycles, fuel cells, and energy economics. The focus of the lectures each week is shown in Table 5.5. The teaching team comprises a large number of lecturers, each focusing on one thematic topic or unit, including the MATLAB labs. Learning outcomes for each lecture are also provided to the students along with the lecture slides and all associate teaching material.

The assignment follows the lessons learned from the MSc-level course as well as the short-course presented earlier. It comprises two parts: gas turbine performance calculation and turbomachinery conceptual design. In the first part, the students are asked to perform a design point calculation for a two-shaft turbofan. The second part requires the use of non-dimensional parameters to estimate the component dimensions and the velocity triangles based on the performance data from the first part of the assignment. A number of assumptions for the operating conditions, cycle parameters, and component efficiencies are given, along with guidelines for the completion of the task. The values for selected parameters (specific thrust, HPC pressure ratio, combustor outlet temperature) are different for each student to prevent them from cheating. It is also recommended that they use MATLAB to carry out the calculations because an iterative approach is required to achieve the above mentioned individual parameters. The students can develop their code in partnership with one other student but should have full individual ownership of their code and report. For evaluation, they have to submit their code, a filled out template with their calculation results for approximately 200 parameters, and a technical report. The report should include a description of the key methods, the assumptions made, and sketches of the engine configuration, the velocity triangles for the high pressure components (HPC and HPT), a sketch of the HPC flow path, and a good discussion. The assignment itself is presented in Appendix A A. An example data set is also provided to the students as a reference, so that they can check their calculations.

In order to assist with the students' understanding of gas turbine operation,

Table 5.5: Course lecture structure.

| **Week** | **Subject matter** |
|---|---|
| 1a | Introduction to the course, Applications of gas turbines and basic theory & Presentation of course assignment |
| 1b | Ideal cycles, Compressible flow & Inlet and nozzles: design principles and performance |
| 2a | Introduction to MATLAB (laboratory activity) |
| 2b | Real cycles and component modelling |
| 3a | Building subroutines and outputting data in MATLAB (laboratory activity) |
| 3b | Aero gas turbines & Advanced topics in gas turbine performance |
| 4a | Dimensional analysis & Axial flow compressors: design principles and velocity triangles |
| 4b | Invited lecture & Combustors: design principles and emissions |
| 5a/b | Study visit and advanced calculations with MATLAB (laboratory activity) |
| 6a | Axial flow turbines: design principles and velocity triangles |
| 6b | Principles of gas turbine conceptual design |
| 7a | Combined cycles: basic theory and applications |
| 7b | Invited lecture & Fuel cells: basic theory and applications |
| 8a | Introduction to energy economics: basic theory |
| 8b | Fuel cells: basic theory and applications Intercoolers and recuperators |
| 9a | Case studies in energy economics |
| 9b | Repetition exercises and course wrap-up |

a model of a two shaft turbofan engine was manufactured using 3D printing, with the aim to provide the students with a better understanding of how the individual components are combined in an engine. The possibility to look at a rotating model of the engine rather than a sketch or picture during the lecture provides a significant improvement to their understanding of the subject before the study visits. The 3D-printed model is seen in Figure 5.6. In addition to the 3-D printed model a large number of different types of turbomachinery components (blades, discs etc.) are made available to the students during class.

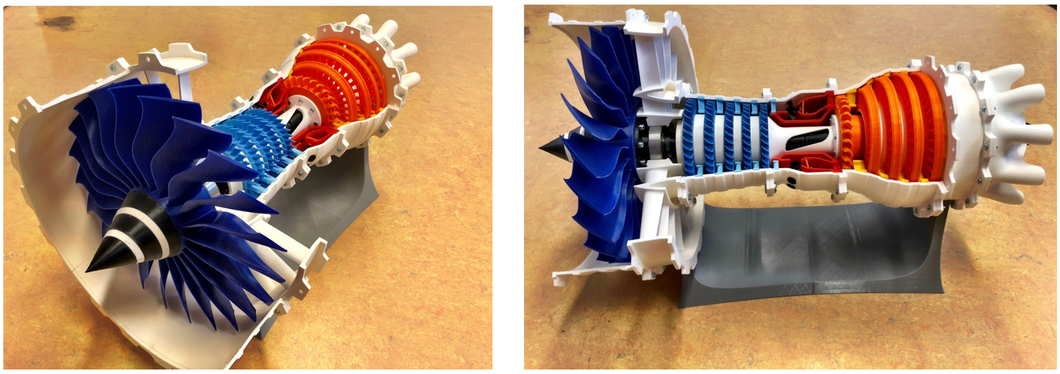

Figure 5.6: 3D-printed model of a gas turbine engine.

### 5.5.4 Course evaluation

The course has been run successfully over a number of years, with improvements carried out after every "Design-Implement-Evaluate-Improve" cycle. A comprehensive assessment of all teaching, learning and assessment activities is presented by Aslanidou et al. [147]. As the evaluation part was primarily driven by another researcher with support from the author, it will not be covered within the present thesis; the interested reader is instead referred to [147].

## 5.6 Summary

Details have been presented from the development of courses on gas turbine multi-disciplinary conceptual design. The lessons learned can be summarised as follows:

- Problem-based learning can enhance student learning, provide cohesion and foster appreciation for the importance and interdependence of different disciplines in the overall engine design challenge. It can also assist in the early development of engineering skills that are typically picked up only after graduation.

- The use of problem-based learning and automated in-house codes are simply a means to an end. Strong effort should be given throughout the course by the tutors in helping the students develop a better understanding of the fact that the engineering importance in the conceptual design process lays primarily on critically analysing numbers and trends, and less on deriving them.
- The intensive nature of the developed course may not be suitable for all prospective candidates. Strong determination and time investment is required from the students in order to tackle the high demands of the curriculum.
- Group formation should be based not only on technical skills but also on a critical assessment of each student's best team roles. This can lead to more efficient teams with fewer communicational problems.
- Teaching complex design interrelations to senior engineers (compared to less-experienced younger delegates) is not always easier and perhaps slightly different teaching approaches may need to be employed for mature students.

# Chapter 6

# Conclusion

The research work presented started with a review of the evolution of the industry's vision for the aero engine design of the future. Appropriate research questions were set that can influence how this vision may further involve in the years to come. Design constraints, material technology, customer requirements, noise and emissions legislation, technology risk and economic considerations and their effect on optimal concept selection were discussed in detail. Different aspects of the pedagogy of gas turbine conceptual design as well as information on the Swedish and Brazilian educational systems were also presented.

The multi-disciplinary aero engine conceptual design tool utilised here is - at this level of integration and to such evidence that were encountered during this research - of higher fidelity than previous efforts reported in the literature. It is based on an explicit algorithm and considers the following disciplines: engine performance, engine aerodynamic and mechanical design, aircraft design and aerodynamic performance, emissions prediction and environmental impact, engine and airframe noise, and production, maintenance and direct operating costs.

It should be noted that this design tool is targeted towards identifying an appropriate design space where more complex and time-consuming tools could be utilised. In many cases the modelling carried out is based on correlations that are available in the public domain or have been supplied by original equipment manufacturers within the European collaborative projects VITAL, NEWAC, and DREAM. It is recognized that such correlations have a limited range of validity and are dependent on supporting engineering science base. As an appropriate design space is defined, a more rigorous iterative design procedure would typically be set involving a large number of company specialists.

With respect to addressing the research questions set, several novel engine cycles and technologies - currently under research - were identified. It was shown that there is a great potential to reduce fuel consumption for the different concepts identified, and consequently decrease the $CO_2$ emissions. Furthermore, this can be achieved with a sufficient margin from the $NO_x$ certification limits set by International Civil Aviation Organisation, and in line with the medium term and long term goals set through it's Committee on Aviation Environmental Protection.

The option of an intercooled core geared fan aero engine for long haul applications was assessed by means of a detailed design space exploration. An attempt was made to identify the fuel burn optimal values for a set of engine design parameters by varying them all simultaneously, as well as in isolation. Different fuel optimal designs were developed based on different sets of assumptions. The trade-off between the ever-increasing energy efficiency of modern aero-engines and their $NO_x$ performance was also assessed for an advanced three-shaft turbofan engine using a novel engine multi-point synthesis design approach. Furthermore, a practical methodology for accounting for uncertainty has been outlined and applied on a specific conceptual design case for a conventional turbofan engine.

Finally, lessons learned were also presented from: (i) the integration of different elements of conceptual design in an existing traditional MSc course on gas turbine technology, (ii) the development of an intensive course on gas turbine multi-disciplinary conceptual design.

### *R.Q.1: How low can we really go on specific thrust?*

There are still benefits to be tapped from further reducing specific thrust, but these are limited due to installations losses i.e., engine weight and nacelle drag, as well as operability issues i.e., fan surge margin. It is unlikely that direct-drive or geared fan designs can yield any significant propulsive efficiency benefits at cruise specific thrust levels below 70-80 [m/s]. As with the first high bypass ratio turbofans, it is probable that their design will be driven primarily by engine noise considerations and may once again prove sub-optimal in terms of engine installed efficiency. Higher propulsive efficiency could be achieved using an open-rotor configuration at the expense of significantly increased noise levels. Due to the large propeller/rotor diameters involved such designs would be in principle only appropriate for short-haul aircraft. Whilst distributed propulsion and boundary layer ingestion could offer some further limited improvements, these would require a radical aircraft configuration that is decades away from being developed.

### *R.Q.2: How high can we really go on OPR and $T_{41}$?*

Some core efficiency improvements can be achieved by further increasing engine firing temperature and overall pressure ratio. This is largely driven by improvements in material and cooling technology that could push optimal cruise OPR levels in the region of 60-65 for engines designed for long-haul aircraft. Small compressor blade heights in the last stages of the high pressure compressor, and the associated losses, place an upper limit on OPR. High OPR intercooled engine cycles become more attractive in aircraft applications that require larger engine sizes. Such a concept may allow efficiency-optimal cruise OPR values in the region of 80-90.

> ***R.Q.3: What is the trade-off between low $CO_2$ and $NO_x$ considering the influence of current and future emissions legislation?***

Improving engine thermal efficiency has a detrimental effect on $NO_x$ emissions for traditional combustors, both at high altitude and particularly at sea-level conditions. Lean-combustion technology does not demonstrate such behaviour and can therefore help decouple to some extend $NO_x$ emissions performance from engine core efficiency. If we are to reduce the contribution of aviation to global warming, however, future certification legislation may need to become more stringent and comprehensive, i.e., cover high altitude conditions. By doing so we can help unlock the competitive advantage of lean burn technology in relation to cruise $NO_x$ and mission performance.

> ***R.Q.4: How sensitive is an optimal design obtained deterministically to production scatter, component deterioration as well as measurement uncertainty?***

There are potential benefits to be tapped from a transition from the traditional deterministic approach for system analysis to a stochastic (robust design) approach for economic decision-making under uncertainty. The sensitivity of an optimal engine design obtained deterministically to real-life uncertainties is far from negligible. The considerable impact of production scatter, measurement uncertainties as well as component performance deterioration, on engine performance must be catered; this includes taking into consideration control system design aspects. A fast analytical approach can be sufficiently accurate for the conceptual design process, particularly for estimating key engine performance parameters. The latter relate to type-test certification and performance retention guarantees including preliminary estimates of engine production margins.

> ***R.Q.5: How can gas turbine conceptual design be introduced effectively in traditional post-graduate curriculums?***

The results from the use of problem-based learning are encouraging, in terms of enhancing student learning and developing engineering skills. Traditional turbomachinery courses can be improved by introducing in the curriculum design tasks based on automated in-house tools. Such an approach can fit fairly different university environments with relatively small adjustments by the responsible teacher and on a case-by-case basis. The use of a design task and group project work, based on real-life industrial challenges and functional requirements, is likely the most effective way to teach elements of gas turbine conceptual design. A key element to leverage this is to set aside time for group and individual student tutoring, at key stages of competition of the design task. Furthermore, student group formation based not only on technical skills but also on a critical assessment of each student's best team roles may also help the learning process.

On a final reflection, it must be noted that aero-engine design is primarily driven by economic considerations. As fuel prices increase, the impact of fuel consumption on direct operating costs also increases. Furthermore, novel engine concepts and associated technologies tend to carry with them a large development cost and associated risk. The question therefore rises:

> **Can the potential reduction in fuel consumption and direct operating costs outweigh the technological risks involved in introducing novel concepts into an uncertain market?**

The answer is left to be given by the choices policy-makers and the aero-engine industry make in the years to come.

## 6.1 Contribution to knowledge

The author's contribution to knowledge from this work can be summarised as follows:

**I.** Derivation of new design methods and further development of an existing multi-disciplinary aero engine conceptual design tool aimed towards identifying an appropriate design space where more complex and time-consuming tools could be utilised. The author's efforts have been focused primarily on: (i) the consideration of innovative engine technologies and associated system design effects, (ii) the consideration of emissions certification legislation, and (iii) the consideration of production scatter, deteriorated engine performance and measurement uncertainty.

**II.** Assessment of future environmentally friendly power and propulsion systems, using the developed tool, including:

- Quantification of potential benefits from the introduction of innovative engine technologies and identification of fuel optimal designs for year 2020+ entry into service.

- Assessment of the sensitivity of the optimality of different designs when considering emissions legislation.
- Assessment of the sensitivity of the optimality of different designs when considering production scatter, performance deterioration over an engine's life cycle as well as measurement uncertainty.

**III.** Pedagogical lessons learned from the development of courses on gas turbine conceptual design.

Considering item [I.] above, a specific contribution is the simultaneous engine multi-point synthesis design method, as well as the aircraft-level optimization process that have been pursued. The parametric design analysis, looking at the effect of key non-dimensional and quasi-dimensional parameters on system performance, while keeping all other at consistent values using the said synthesis approach is also novel. As this work has spanned many years, it is particularly encouraging to see in the open literature that other researchers have already begun using similar approaches, following first publication of the presented system design method by the author.

It is likely that detailed studies and such tools exist internally in companies. Nevertheless, it is worth having such a tool and future aero engine design and policy assessments available for the broader research community. Whilst the detailed effort carried out by the author will be presented in the main body of the final thesis, it is important to note that this work is expected to be supported by an appropriate number of conference and journal papers.

## 6.2 Recommendations for future work

Future work on the developed methods and concept assessments should focus on:

- **Consideration of design and analysis method uncertainty.** The transition from the traditional deterministic approach for energy system analysis to a stochastic approach for decision making under uncertainty can lead to the selection of more robust engine designs.
- **Consideration of more disruptive technologies.** Concepts such as pulse detonation and constant volume combustion, as well as the double bypass and selective bleed cycles could be considered. The tool could also be further developed to perform a more rigorous assessment - compared to previous efforts - of distributed propulsion and supersonic flight for commercial transport.

- **Introduction of policy scenarios as well as ATM and airline fleet operational aspects.** Interesting and more realistic assessments could come out of this development, including looking into ways of reducing an airline's environmental footprint.

# References


[1] Konstantinos G. Kyprianidis. *Multi-disciplinary Conceptual Design of Future Jet Engine Systems.* PhD thesis, Cranfield University, Cranfield, Bedfordshire, United Kingdom, April 2010.

[2] L. Larsson, T. Grönstedt, and K.G. Kyprianidis. Conceptual Design and Mission Analysis for a Geared Turbofan and an Open Rotor Configuration. In *ASME TURBO EXPO 2011 Proceedings, GT2011-46451*, Vancouver, Canada, June 2011. DOI: 10.1115/GT2011-46451.

[3] J.E. Penner, D.H. Lister, D.J. Griggs, D.J. Dokken, and M. McFarland, editors. *Aviation and the Global Atmosphere: A Special Report of IPCC Working Groups I and III in Collaboration with the Scientific Assessment Panel to the Montreal Protocol on Substances that Deplete the Ozone Layer.* Cambridge University Press, ISBN 978-0521663007, Cambridge, United Kingdom, 1999. 373 pp.

[4] The Core Writing Team, R.K. Pachauri, and L.A. Meyer, editors. *Climate Change 2014: Synthesis Report. Contribution of Working Groups I, II and III to the Fifth Assessment Report of the Intergovernmental Panel on Climate Change.* IPCC, ISBN 978-92-9169-143-2, Geneva, Switzerland, 2015. 151 pp.

[5] Advisory Council for Aeronautical Research in Europe. European Aeronautics: A Vision for 2020 – Meeting Society's Needs and Winning Global Leadership. See also URL `http://www.acare4europe.org`, January 2001.

[6] J.H. Horlock, D.T. Watson, and T.V. Jones. Limitations on Gas Turbine Performance Imposed by Large Turbine Cooling Flows. *ASME Journal of Engineering for Gas Turbines and Power*, 123(3):487–494, July 2001.

[7] R.C. Wilcock, J.B. Young, and J.H. Horlock. The Effect of Turbine Blade Cooling on the Cycle Efficiency of Gas Turbine Power Cycles. *ASME Journal of Engineering for Gas Turbines and Power*, 127(1):109–120, January 2005.

[8] A.H. Lefebvre. *Gas Turbine Combustion.* Taylor & Francis, PA, USA, 2nd edition, 1999.

[9] D.E. Gray and J.W. Witherspoon. Fuel conservative propulsion concepts for future air transports. Technical Report SAE-760535, Society of Automotive Engineers, 1976.

[10] R. Hirschkron and R.E. Neitzel. Alternative concepts for advanced energy conservative transport engines. Technical Report SAE-760536, Society of Automotive Engineers, 1976.

[11] A.J.B. Jackson. Some Future Trends in Aero Engine Design for Subsonic Transport Aircraft. *ASME Journal of Engineering for Power*, 98:281–289, April 1976.

[12] A.J.B. Jackson. *Optimisation of Aero and Industrial Gas Turbine Design for the Environment*. PhD thesis, Cranfield University, Cranfield, Bedfordshire, United Kingdom, 2009.

[13] G.L. Wilde. Future large civil turbofans and powerplants. *RAeS Aeronautical Journal*, 82:281–299, July 1978.

[14] P.H. Young. The future shape of medium and long-range civil engines. *RAeS Aeronautical Journal*, pages 53–61, February 1979.

[15] G.G. Pope. Prospects for reducing the fuel consumption of civil aircraft. *RAeS Aeronautical Journal*, pages 287–295, August 1979.

[16] J.M. Swihart. The Promise of the Supersonics. In *AIAA 7th Annual Meeting and Technical Display Proceedings, AIAA 70-1217*, Houston, Texas, USA, October 1970.

[17] R.E. Bates and J. Morris. A McDonnell Douglas Perspective – Commercial Aircraft for the Next Generation. In *AIAA Aircraft Design, Systems and Technology Meeting Proceedings, AIAA-83-2502*, Fort Worth, Texas, USA, October 1983.

[18] R. Watts. European air transport up to the year 2000. *RAeS Aeronautical Journal*, pages 300–312, July 1978.

[19] J.A. Borradaile. Towards the optimum ducted UHBR engine. In *Proceedings of AIAA/SAE/ASME/ASEE 24th Joint Propulsion Conference, AIAA-89-2954*, Boston, Massachusetts, USA, July 1988.

[20] R.A. Zimbrick and J.L. Colehour. An investigation of very high bypass ratio engines for subsonic transports. In *Proceedings of AIAA/SAE/ASME/ASEE 24th Joint Propulsion Conference, AIAA-88-2953*, Boston, Massachusetts, USA, July 1988.

[21] N.J. Peacock and J.H.R. Sadler. Advanced Propulsion Systems for Large Subsonic Transports. *ASME Journal of Propulsion and Power*, 8(3):703–708, May-June 1992.

[22] N.T. Birch. 2020 vision: the prospects for large civil aircraft propulsion. *RAeS Aeronautical Journal*, pages 347–352, August 2000.

[23] P.C. Ruffles. The future of aircraft propulsion. *Proceedings of the IMechE, Part C: Journal of Mechanical Engineering Science*, 214(1):289–305, 2000.

[24] J Sieber. Aerodynamic Design and Experimental Verification of an Advanced Counter-Rotating Fan for UHB Engines. In *Third European Propulsion Forum*, Paris, France, 1991.

[25] P. Schimming. Counter Rotating Fans – An Aircraft Propulsion for the Future. *Journal of Thermal Science*, 12(2):97–103, 2003.

[26] H.I.H. Saravanamuttoo. The Daniel and Florence Guggenheim Memorial Lecture - Civil Propulsion; The Last 50 Years. In *ICAS 2002 Congress Proceedings*, Toronto, Canada, September 2002.

[27] enVIronmenTALly friendly aero engines. `http://www.project-vital.org`, 2009.

[28] J.-J. Korsia and S. Guy. VITAL – European R&D Programme for Greener Aero-Engines. In *ISABE 2007 Proceedings, ISABE-2007-1118*, Beijing, China, September 2007.

[29] J.-J. Korsia. VITAL – European R&D Programme for Greener Aero-Engines. In *ISABE 2009 Proceedings, ISABE-2009-1114*, Montreal, Canada, September 2009.

[30] Devaiah Nalianda, Konstantinos G. Kyprianidis, Vishal Sethi, and Riti Singh. Techno-economic Viability Assessments of Greener Propulsion Technology under Potential Environmental Regulatory Policy Scenarios. *Applied Energy*, 157(1):35–50, November 2015. DOI:10.1016/j.apenergy.2015.07.017.

[31] GE36 Design and Systems Engineering. Full-scale technology demonstration of a modern counterrotating unducted fan engine concept - engine test. NASA-CR-180869, GE Aircraft Engines, Cincinnati,, OH, USA, December 1987.

[32] valiDation of Radical Engine Architecture systeMs. `http://www.dream-project.eu`, 2011.

[33] Clean Sky Joint Technology Initiative. `http://www.cleansky.eu`, 2011.

[34] J. Kurzke. Achieving maximum thermal efficiency with the simple gas turbine cycle. In *Proceedings of 9th CEAS European Propulsion Forum: "Virtual Engine – A Challenge for Integrated Computer Modelling"*, Rome, Italy, October 2003.

[35] NEW Aero engine Core concepts. `http://www.newac.eu`, 2011.

[36] G. Wilfert, J. Sieber, A. Rolt, N. Baker, A. Touyeras, and S. Colantuoni. New Environmental Friendly Aero Engine Core Concepts. In *ISABE 2007 Proceedings, ISABE-2007-1120*, Beijing, China, September 2007.

[37] Andrew Martin Rolt and Konstantinos G. Kyprianidis. Assessment of New Aero Engine Core Concepts and Technologies in the EU Framework 6 NEWAC Programme. In *ICAS 2010 Congress Proceedings, Paper No. 408*, Nice, France, September 2010.

[38] J.P. Downs and K.L. Kenneth. Turbine Cooling Systems Design – Past, Present and Future. In *ASME TURBO EXPO 2009 Proceedings, GT2009-59991*, Orlando, Florida, June 2009.

[39] H.I.H. Saravanamuttoo, G.F.C. Rogers, and H. Cohen. *Gas Turbine Theory*. Pearson Education Limited, United Kingdom, 5th edition, 2001.

[40] P.P. Walsh and P. Fletcher. *Gas Turbine Performance*. Blackwell Science, United Kingdom, 1st edition, 1998.

[41] H. Canière, A. Willcokx, E. Dick, and M. De Paepe. Raising cycle efficiency by intercooling in air-cooled gas turbines. *Applied Thermal Engineering*, 26(16):1780–1787, November 2006.

[42] M.A. da Cunha Alves, H.F. de Franca Mendes Carneiro, J.R. Barbosa, L.E. Travieso, P. Pilidis, and K.W. Ramsden. An insight on intercooling and reheat gas turbine cycles. *Proceedings of the Institution of Mechanical Engineers, Part A: Journal of Power and Energy*, 215(2):163–171, 2001.

[43] T. Papadopoulos and P. Pilidis. Introduction of Intercooling in a High Bypass Jet Engine. In *ASME TURBO EXPO 2000 Proceedings, 2000-GT-150*, Munich, Germany, May 2000.

[44] L. Xu, B. Gustafsson, and T. Grönstedt. Mission Optimization of an Intercooled Turbofan Engine. In *ISABE 2007 Proceedings, ISABE-2007-1157*, Beijing, China, September 2007.

[45] L. Xu and T. Grönstedt. Design and Analysis of an Intercooled Turbofan Engine. *ASME Journal of Engineering for Gas Turbines and Power*, 132(11), November 2010. doi:10.1115/1.4000857.

[46] A.M. Rolt. UK Patent GB 2 413 366 B, September 2006.

[47] Andrew Martin Rolt and Nick J. Baker. Intercooled Turbofan Engine Design and Technology Research in the EU Framework 6 NEWAC Programme. In *ISABE 2009 Proceedings, ISABE-2009-1278*, Montreal, Canada, September 2009.

[48] A.D. Walker, J.F. Carrotte, and A.M. Rolt. Duct Aerodynamics for Intercooled Aero Gas Turbines: Constraints, Concepts and Design Methododology. In *ASME TURBO EXPO 2009 Proceedings, GT2009-59612*, Orlando, Florida, June 2009.

[49] A. Lundbladh and A. Sjunnesson. Heat Exchanger Weight and Efficiency Impact on Jet Engine Transport Applications. In *ISABE 2003 Proceedings, ISABE-2003-1122*, Cleveland, USA, September 2003.

[50] S. Boggia and K. Rud. Intercooled Recuperated Gas Turbine Engine Concept. In *Proceedings of 41st AIAA/ASME/SAE/ASEE Joint Propulsion Conference and Exhibit, AIAA 2005-4192*, Arizona, USA, July 2005.

[51] L. Xu, K.G. Kyprianidis, and T. Grönstedt. Analysis of an Intercooled Recuperated Aero-engine. In *ISABE 2011 Proceedings, ISABE-2011-1318*, Göteborg, Sweden, September 2011.

[52] L. Xu, K.G. Kyprianidis, and T. Grönstedt. Optimization Study of an Intercooled Recuperated Aero-Engine. *AIAA Journal of Propulsion and Power*, 29(2), March-April 2013. DOI: 10.2514/1.B34594.

[53] G. Pellischek and B. Kumpf. Compact Heat Exchanger Technology for Aero Engines. In *ISABE 1991 Proceedings, ISABE-91-7019*, Nottingham, United Kingdom, September 1991.

[54] H. Schoenenborn, E. Ebert, B. Simon, and P. Storm. Thermomechanical Design of a Heat Exchanger for a Recuperated Aeroengine. *ASME Journal of Engineering for Gas Turbines and Power*, 128(4):736–744, October 2006.

[55] C.F. McDonald, A. Massardo, C. Rodgers, and A. Stone. Recuperated gas turbine aeroengines, part I: early development activities. *Aircraft Engineering and Aerospace Technology: An International Journal*, 80(2):139–157, 2008.

[56] C.F. McDonald, A. Massardo, C. Rodgers, and A. Stone. Recuperated gas turbine aeroengines, part II: engine design studies following early development testing. *Aircraft Engineering and Aerospace Technology: An International Journal*, 80(3):280–294, 2008.

[57] C.F. McDonald, A. Massardo, C. Rodgers, and A. Stone. Recuperated gas turbine aeroengines, part III: engine concepts for reduced emissions, lower fuel consumption, and noise abatement. *Aircraft Engineering and Aerospace Technology: An International Journal*, 80(4):408–426, 2008.

[58] A. Wulff and J. Hourmouziadis. Technology Review of Aeroengine Pollutant Emissions. *Aerospace Science and Technology*, 1(8):557–572, December 1997.

[59] Hukam C. Mongia. Commercial Propulsion Engines Emissions. In Richard Blockley and Wei Shyy, editors, *Encyclopedia of Aerospace Engineering, Volume 2: Propulsion and Power*. John Willey & Sons, Ltd, ISBN: 978-0-470-75440-5, October 2010. DOI: 10.1002/9780470686652.eae589.

[60] Sigrun Matthes, Ulrich Schumann, Volker Grewe, Christine Frömming, Alexander Dahlmann, Katrin Koch, and Hermann Mannstein. Climate Optimized Air Transport. In Ulrich Schumann, editor, *Atmospheric Physics*, chapter 44, pages 727–746. Springer-Verlag Berlin Heidelberg, ISBN 978-3-642-30182-7, Germany, July 2012. Part of the series Research Topics in Aerospace, DOI: 10.1007/978-3-642-30183-4.

[61] Timothy C. Lieuwen and Vigor Yang, editors. *Gas Turbine Emissions*. Cambridge University Press, ISBN 978–0–521-76405–6, New York, NY, USA, 1st edition, 2013.

[62] Mauro Masiol and Roy M. Harrison. Aircraft engine exhaust emissions and other airport-related contributions to ambient air pollution: A review. *Elsevier, Atmospheric Environment*, 95:409–455, October 2014. DOI: 10.1016/j.atmosenv.2014.05.070.

[63] R.W. Claus, A.L. Evans, J.K. Lylte, and L.D. Nichols. Numerical Propulsion System Simulation. *Computing Systems in Engineering (ISSN 0956-0521)*, 2(4):357–364, 1991.

[64] J.K. Lytle. The Numerical Propulsion System Simulation: An Overview. NASA/TM-2000-209915, NASA Glenn Research Center, June 2000.

[65] E. Onat and G. W. Klees. A method to estimate weight and dimensions of large and small gas turbine engines. NASA-CR-159481, NASA, January 1979.

[66] M.T. Tong, I. Halliwell, and L.J. Ghosn. A computer code for gas turbine engine weight and disk life estimation. *ASME Journal of Engineering for Gas Turbines and Power*, 126(2):265–270, April 2004.

[67] M.T. Tong and B.A. Naylor. An Object-Oriented Computer Code for Aircraft Engine Weight Estimation. In *ASME TURBO EXPO 2008 Proceedings, GT2008-50062*, Berlin, Germany, June 2008.

[68] L.A. McCullers. Aircraft configuration optimization including optimized flight profiles. In *NASA Symposium on Recent Experiences in Multidisciplinary Analysis and Optimization, NASA-CP-2327, Part 1, pp. 395-412*, Hampton, Virginia , USA, April 1984.

[69] K. Kontos, B. Janardan, and P. Gliebe. Improved NASA-ANOPP Noise Prediction Computer Code for Advanced Subsonic Propulsion Systems. NASA-CR-195480, NASA Lewis Research Center, August 1996.

[70] N. Antoine, I. Kroo, K. Willcox, and G. Barter. A Framework for Aircraft Conceptual Design and Environmental Performance Studies. In *10th AIAA/ISSMO Multidisciplinary Analysis and Optimization Conference Proceedings, AIAA 2004-4314*, Albany, New York, September 2004.

[71] C.R. Mercer, W.J. Haller, and M.T. Tong. Adaptive Engine Technologies for Aviation CO2 Emissions Reduction. In *42nd AIAA/ASME/SAE/ASEE Joint Propulsion Conference and Exhibit, AIAA-2006-5105*, Sacramento, California, USA, July 2006.

[72] R.B. Abernethy and J.C. Sammons. Three Applications of Monte Carlo Simulation to the Development of the F100 Turbofan Engine. In *12th Propulsion Conference, Joint Propulsion Conferences, AIAA Paper No. 76-731*, Palo Alto, CA, USA, July 1976. 10.2514/6.1976-731.

[73] Dimitri N. Mavris and Bryce Alexander Roth. Assessment of Uncertainty in Aerospace Propulsion System Design and Simulation. In *2003 JANNAF Joint Meeting*, Colorado, USA, December 2003.

[74] Joachim Kurzke. Some Applications of the Monte Carlo Method to Gas Turbine Performance Simulations. In *ASME TURBO EXPO 1997 Proceedings, 97-GT-048*, Florida, USA, June 1997. DOI:10.1115/97-GT-048.

[75] Bryce Alexander Roth and Dimitri N. Mavris. Commercial Engine Architecture Selection in the Presence of Uncertainty and Evolving Requirements. In *ISABE 2001 Proceedings, ISABE-2001-1169*, Atlanta, USA, September 2001.

[76] Bryce Alexander Roth, M.D. Graham, Dimitri N. Mavris, and N.I. Mascotai. Adaptive Selection of Aircraft Engine Technologies in the Presence of Risk. *ASME Journal of Engineering for Gas Turbines and Power*, 126(1):40–44, January 2004. DOI:10.1115/1.1639006.

[77] Mattia Padulo, M.S. Campobasso, and M.D. Guenov. Novel Uncertainty Propagation Method for Robust Aerodynamic Design. *AIAA Journal*, 49(3):530–543, 2011.

[78] Konstantinos G. Kyprianidis, R.F. Colmenares Quintero, D.S. Pascovici, S.O.T. Ogaji, P. Pilidis, and A.I. Kalfas. EVA - A Tool for EnVironmental Assessment of Novel Propulsion Cycles. In *ASME TURBO EXPO 2008 Proceedings, GT2008-50602*, Berlin, Germany, June 2008. DOI:10.1115/GT2008-50602.

[79] Konstantinos G. Kyprianidis, A. Dax, S.O.T. Ogaji, and T. Grönstedt. Low Pressure System Component Advancements and its Impact on Future Turbofan Engine Emissions. In *ISABE 2009 Proceedings, ISABE-2009-1276*, Montreal, Canada, September 2009.

[80] Isight & the SIMULIA Execution Engine. http://www.3ds.com/ products-services/simulia/portfolio/isight-simulia-execution-engine/ overview/, 2014.

[81] S. Bretschneider, O. Arago, and S. Staudacher. Architecture of a Techno and Environmental Risk Assessment Tool Using a Multi-Modular Build Approach. In *ISABE 2007 Proceedings*, Beijing, China, September 2007. ISABE-2007-1103.

[82] Konstantinos G. Kyprianidis, T. Grönstedt, S.O.T. Ogaji, P. Pilidis, and R. Singh. Assessment of Future Aero-engine Designs with Intercooled and Intercooled Recuperated Cores. *ASME Journal of Engineering for Gas Turbines and Power*, 133(1), January 2011. doi:10.1115/1.4001982.

[83] J. Kurzke. Preliminary Design. Lecture Notes, von Karman Institute for Fluid Dynamics, Sint-Genesius-Rode, Belgium, April 2003. In Lecture Series 2002-2003, Aero-Engine Design: A State of the Art.

[84] Konstantinos G. Kyprianidis, Devaiah Nalianda, and Erik Dahlquist. A $NO_x$ Emissions Correlation for Modern RQL Combustors. *Energy Procedia*, 75:2323–2330, March 2015. *Presented at the 7th International Conference on Applied Energy ICAE2015, Paper ID 238, Abu Dhabi, United Arab Emirates,* **Recommended for publication in Applied Energy,** DOI:10.1016/j.egypro.2015.07.433.

[85] W.M. Kays and A.L London. *Compact Heat Exchangers*. Krieger Publishing Company, Malabar, Florida, USA, 3rd edition, 1998.

[86] B. Lakshminarayana. Methods of Predicting the Tip Clearance Effects in Axial Flow Turbomachinery. *ASME J. Basic Eng.*, 92(3):467–480, September 1970. DOI: 10.1115/1.3425036.

[87] A.J. Fawke and H.I.H. Saravanamuttoo. Digital Computer Methods for Prediction of Gas Turbine Dynamic Response. SAE-710550, pp. 1805-1813, Society of Automotive Engineers, February 1971.

[88] W.L. MacMillan. *Development of a Modular Type Computer Program for the Calculation of Gas Turbine Off-Design Performance*. PhD thesis, Cranfield University, Cranfield, Bedfordshire, United Kingdom, 1974.

[89] A. Alexiou, I. Roumeliotis, N. Aretakis, A. Tsalavoutas, and K. Mathioudakis. Modeling Contra-Rotating Turbomachinery Components for Engine Performance Simulations: The Geared Turbofan With Contra-Rotating Core Case. *ASME J Gas Turb Pwr*, 134(11), November 2012. DOI: 10.1115/1.4007197.

[90] L.R. Jenkinson, P. Simpkin, and D. Rhodes. *Civil Jet Aircraft Design*. Arnold, London, United Kingdom, 1st edition, 1999.

[91] J. Roskam. *Airplane Design - Part V: Component Weight Estimation*. Design, Analysis and Research Corporation, Lawrence, Kansas, USA, 1st edition, 2003.

[92] E. Torenbeek. *Synthesis of Subsonic Airplane Design: An Introduction to the Preliminary Design of Subsonic General Aviation and Transport Aircraft, with Emphasis on Layout, Aerodynamic Design, Propulsion and Performance*. Delft University Press and Kluwer Academic Publishers, The Netherlands, student edition, 1982.

[93] ESDU. Estimation of Airframe Drag by Summation of Components – Principles and Examples. ESDU-97016, London, United Kingdom, September 1997.

[94] P. Laskaridis. *Performance Investigations and Systems Architectures for the More Electric Aircraft*. PhD thesis, Cranfield University, Cranfield, Bedfordshire, United Kingdom, 2004.

[95] R. Avellán. Towards Environmentally Friendly Aero Engines. Master's thesis, Chalmers University, Göteborg, Sweden, 2008.

[96] International Air Transport Association. `http://www.iata.org`, 2011.

[97] Platts. `http://www.platts.com`, 2011.

[98] Swiss International Air Lines. Flying Smart. *Swiss Magazine, Issue 12.2009 / 1.2010*, pages 100–105, December 2009.

[99] Federal Aviation Administration. Federal Aviation Regulation Part 121 - Operating Requirement: domestic, flag and supplemental operations. FAR 121, Washington, DC, USA.

[100] Joint Aviation Authorities. Joint Airworthiness Requirements OPS Part 1 – Commercial Air Transportation (Aeroplanes). Ammendment 14, Hoofddorp, The Netherlands, 2008.

[101] Konstantinos G. Kyprianidis, Andrew Martin Rolt, and Vishal Sethi. On Intercooled Turbofan Engines. In Benini, E., editor, *Progress in Gas Turbine Performance*, chapter 1, pages 3–24. InTech, ISBN 979–953–51–1166–5, Rijeka, Croatia, June 2013. DOI: 10.5772/54402.

[102] C. Hughes, W. Lord, and S. Masoudi. NASA/Pratt and Whitney Collaborative Partnership Research in Ultra High Bypass Cycle Propulsion Concepts. In *Fundamental Aeronautics Program 2nd Annual Meeting*, Atlanta , USA, October 2008.

[103] B.K. Kestner, J.S. Schutte, J.C. Gladin, and D.N. Mavris. Ultra High Bypass Ratio Engine Sizing and Cycle Selection Study for a Subsonic Commercial Aircraft in the N+2 Timeframe. In *ASME TURBO EXPO 2011 Proceedings, GT2011-45370*, Vancouver, Canada, June 2011.

[104] Kjelgaard, C. Gearing Up for the GTF. *Aircraft Technology, Issue 105*, pages 86–95, May 2010.

[105] J. Kurzke. Fundamental Differences Between Conventional and Geared Turbofans. In *ASME TURBO EXPO 2009 Proceedings, GT2009-59745*, Orlando, Florida, June 2009.

[106] Konstantinos G. Kyprianidis. Future Aero Engine Designs: An Evolving Vision. In E. Benini, editor, *Advances in Gas Turbine Technology*, chapter 1. InTech, November 2011. doi:10.1115/1.4001982.

[107] Abhijit Guha. Optimum Fan Pressure Ratio for Bypass Engines with Separate or Mixed Exhaust Streams. *AIAA Journal of Propulsion and Power*, 17(5):1117–1122, September-October 2001.

[108] I. Goulos, F. Hempert, V. Sethi, V. Pachidis, R. d'Ippolito, and M. d'Auria. Rotorcraft Engine Cycle Optimization at Mission Level. *ASME J Gas Turb Pwr*, 135(9), September 2013. DOI: 10.1115/1.4024870.

[109] Esmail Najafi Saatlou, Konstantinos G. Kyprianidis, Vishal Sethi, A.O. Abu, and Pericles Pilidis. On the Trade-Off Between Minimum Fuel Burn and Maximum Time Between Overhaul for an Intercooled Aeroengine. *Proceedings of the IMechE, Part G: Journal of Aerospace Engineering*, 228(13):2424–2438, October 2014. DOI: 10.1177/0954410013518509.

[110] L. Ingber. Simulated Annealing: Practice versus Theory. *Mathematical Computer Modeling*, 18(11):29–57, 1993.

[111] M.D. McKay, R.J. Beckman, and W.J. Conover. A Comparison of Three Methods for Selecting Values of Input Variables in the Analysis of Output from a Computer Code. *Technometrics published by the American Statistical Association*, 21(2):239–245, May 1979.

[112] R. Jin, W. Chen, and A. Sudjianto. An Efficient Algorithm for Constructing Optimal Design of Computer Experiments. *Journal of Statistical Planning and Inference*, 134(1):268287, 2005.

[113] M. Johnson, L. Moore, and D. Ylvisaker. Minimax and Maximin Distance Designs. *Journal of Statistical Planning and Inference*, 26:131148, 1990.

[114] M.D. Morris and T.J. Mitchell. Exploratory Designs for Computational Experiments. *Journal of Statistical Planning and Inference*, 43:381402, 1995.

[115] Sebastian Samuelsson, Konstantinos G. Kyprianidis, and Tomas Grönstedt. Consistent Conceptual Design and Performance Modeling of Aero Engines. In *ASME TURBO EXPO 2015 Proceedings, GT2015-43331*, Montreal, Canada, June 2015. DOI:10.1115/GT2015-43331.

[116] ICAO. International Standards and Recommended Practices – Environmental Protection, Annex 16 to the Convention on International Civil Aviation, Volume II - Aircraft Engine Emissions. 3rd edition plus ammendments, Montreal, Canada, 2008.

[117] P. Newton, C. Holsclaw, M. Ko, and M. Ralph. Long Term Technology Goals for CAEP/7. presented to the Seventh Meeting of CAEP, February 2007.

[118] A. Döpelheuer and M. Lecht. Influence of Engine Performance on Emission Characteristics. In *RTO AVT Symposium on "Gas Turbine Engine Combustion, Emissions and Alternative Fuels" Proceedings, RTO-MP-14*, Lisbon, Portugal, October 1998.

[119] Tamsin Haggis. What have we been thinking of? A critical overview of 40 years of student learning research in higher education. *Studies in Higher Education*, 34(4):377–390, 2009.

[120] Nicholas Addison. Doubting Learning Outcomes in Higher Education Contexts: from Performativity towards Emergence and Negotiation. *The International Journal of Art & Design Education*, 33(3):313–325, 2014.

[121] David Scott Yeager and Carol S. Dweck. Mindsets That Promote Resilience: When Students Believe That Personal Characteristics Can Be Developed. *Educational Psychologist*, 47(4):302–314, 2012.

[122] J. Biggs and C. Tang. *Teaching for Quality Learning at University.* McGraw-Hill/Society for Research into Higher Education, Oxford, United Kingdom, 4th edition, 2011.

[123] K.L. Dandy and K. Bendersky. Student and Faculty Beliefs About Learning in Higher Education: Implications for Teaching. *International Journal of Teaching and Learning in Higher Education*, 26(3):358–380, 2014. ISSN 1812-9129.

[124] G.S. Hanna and P.A. Dettmer. *Assessment for effective teaching: Using context-adaptive planning.* Pearson A&B, Boston, MA, USA, 1st edition, 2004.

[125] B.S. Bloom, J.T. Hastings, and G.F. Madaus. Handbook on the formative and summative evaluation of student learning. *Studies in Art Education*, 14(1):487–494, 1971. doi:10.2307/1319918.

[126] D. Royce Sadler. Formative assessment and the design of instructional systems. *Instructional Science*, 18(2):119144, June 1989.

[127] Carol Ann Tomlinson. The Bridge Between Today's Lesson and Tomorrow's. *Educational Leadership: Using Assessments Thoughtfully*, 71(6):10–14, March 2014. doi:10.2307/1319918.

[128] B.S. Bloom, M.D. Engelhart, E.J. Furst, W.H. Hill, and D.R. Krathwohl. *Taxonomy of educational objectives: The classification of educational goals. Handbook I: Cognitive domain.* David McKay Company, New York, USA, 1st edition, 1956.

[129] Edith Braun and Bernhard Leidner. Academic Course Evaluation: Theoretical and Empirical Distinctions Between Self-Rated Gain in Competences and Satisfaction with Teaching Behavior. *European Psychologist*, 14(4):297306, 2009. doi:10.1027/1016-9040.14.4.297.

[130] J. Kinkead. Learning Through Inquiry: An Overview of Undergraduate Research. *New Directions for Teaching and Learning*, 2003(93):5–18, 2003. doi:10.1002/tl.85.

[131] A.L. Zydney, J.S. Bennett, A. Shahid, and K.W. Bauer. Impact of Undergraduate Research Experience in Engineering. *Journal of Engineering Education*, pages 151–157, April 2002.

[132] D.C. Wisler. Engineering - What You Don't Necessarily Learn in School. In *ASME TURBO EXPO 2003 Proceedings, GT2003-38761*, Atlanta, USA, June 2003.

[133] J. Hourmouziadis, N. Schroeder, K. Biegi, K.-J. Schmidt, S. Servaty, and W. Gärtner. A Multimedia Aeroengine Design Course with Industry Support. In *ASME TURBO EXPO 2000 Proceedings, 2000-GT-585*, Munich, Germany, May 2000.

[134] F.C. Mund, A.I. Kalfas, R.S. Abhari, Y. Turcan, J. Hourmouziadis, I. Trébinjac, and A. Vouillarmet. A Multi-Component and Multi-Disciplinary Student Design Project Within an International Academic and Industrial Collaboration. In *ASME TURBO EXPO 2003 Proceedings, GT2003-38163*, Atlanta, USA, June 2003.

[135] S. Svensdotter, P. Almqvist, and T.H. Fransson. Introduction of Project Based Learning for Designing a Heat and Power Plant Into the Last Year Curriculum. In *ASME TURBO EXPO 2000 Proceedings, 2000-GT-583*, Munich, Germany, May 2000.

[136] J.R. Barbosa and P. Pilidis. GEOPHILES – GEneration Of Power with HIgh Levels of Environmental Friendliness: A Technology Transfer Project Between Europe and South America. In *ASME TURBO EXPO 2000 Proceedings, 2000-GT-586*, Munich, Germany, May 2000.

[137] C.B. Meher-Homji. The Development of the Whittle Turbojet. *ASME Journal of Engineering for Gas Turbines and Power*, 120:249–256, April 1998.

[138] H.I.H. Saravanamuttoo, G.F.C. Rogers, H. Cohen, and P.V. Straznicky. *Gas Turbine Theory.* Pearson Education Limited, United Kingdom, 6th edition, 2009.

[139] Konstantinos G. Kyprianidis. Gas Turbine Performance. Lecture Notes, Chalmers University of Technology, Gothenburg, Sweden, 2011.

[140] J. Kurzke. About Simplifications in Gas Turbine Performance Calculations. In *ASME TURBO EXPO 2007 Proceedings, GT2007-27620*, Montreal, Canada, May 2007.

[141] H. Grieb. *Projektierung von Turboflugtriebwerken.* Birkhäuser Verlag, Basel, Switzerland, 1st edition, 2004.

[142] T. Grönstedt. Conceptual Aero Engine Design Modelling: Efficiency Modelling. Lecture Notes, Chalmers University of Technology, Gothenburg, Sweden, 2011.

[143] S.L. Dixon and C.A. Hall. *Fluid Mechanics and Thermodynamics of Turbomachinery.* Elsevier Butterworth-Heinemann, MA, USA, 6th edition, 2010.

[144] T. Doerr. Introduction to Aero-Engine Gas Turbine Combustion. Lecture Notes, von Karman Institute for Fluid Dynamics, Sint-Genesius-Rode, Belgium, February 2010. In Lecture Series 2009-2010, Combustion in Aero-Engines.

[145] T. Grönstedt. Conceptual Aero Engine Design Modelling: Engine Sizing. Lecture Notes, Chalmers University of Technology, Gothenburg, Sweden, 2011.

[146] M. Belbin. *Management Teams: Why They Succeed or Fail.* Elsevier Butterworth-Heinemann, Oxford, United Kingdom, 3rd edition, 2010.

[147] Ioanna Aslanidou, Valentina Zaccaria, Evangelia Pontika, Nathan Zimmerman, Anestis I. Kalfas, and Konstantinos G. Kyprianidis. Teaching Gas Turbine Technology to Undergraduate Students in Sweden. In *ASME TURBO EXPO 2018 Proceedings, GT2015-77074*, Oslo, Norway, June 2018. 10.1115/GT2018-77074.

# Appendices

# Appendix A

# Course Assignment

### 1. Introduction

#### Part A - Gas Turbine Performance

The first part of this design task comprises a design point calculation for a two-shaft separate jets turbofan according to the set of assumptions provided in the section below. The engine low pressure spool shall comprise a single-stage fan and a low-speed booster coupled mechanically to a Low Pressure Turbine (LPT). The high pressure spool shall comprise a High Pressure Compressor (HPC) coupled mechanically to a High Pressure Turbine (HPT). The air shall be introduced to the fan through a subsonic intake and shall travel from one turbomachinery component to the next through appropriate ducts. Both the bypass air as well as the core exhaust air shall expand in separate convergent nozzles.

The values for a few selected parameters shall be different for each student and will be provided separately on Blackboard. It is recommended that all calculations be carried out in MATLAB since they will be iterative in nature. An alternative but less good option is MS Excel.

#### Part B - Turbomachinery Conceptual Design

The second part of this design task focuses on the use of key non-dimensional turbomachinery parameters for establishing estimates on component dimensions and velocity triangles. The performance data established in the first part of the design task are used for analysing the following engine components: the HPC and the HPT. The working style should be to extend the MATLAB code or spreadsheet that you have established from the first part to analyse the HPC flow path, as well as study the velocity triangles of the HPT.

## 2. Assumptions

### Operating conditions

Altitude = 10668m

dTISA = 10K

Flight Mach number = 0.82

### Cycle

Engine net thrust = 70kN

Fan pressure ratio = 1.4-1.9 (first guess range suggestion, iterate)

Bypass ratio = 4-13 (first guess range suggestion, iterate)

Booster pressure ratio = 1.5

### Individual input data

Specific thrust = ? (see spreadsheet)

High pressure compressor pressure ratio = ? (see spreadsheet)

Combustor outlet temperature = ? (see spreadsheet)

### Component efficiencies

Intake pressure loss = 0.3%

Bypass duct pressure loss = 1.5%

Intercompressor duct pressure loss = 1%

Combustor pressure loss = 4%

Interturbine duct pressure loss = 1%

Jet pipe pressure loss = 1%

Fan polytropic efficiency = 90%

Booster polytropic efficiency = 90%

High pressure compressor (HPC) polytropic efficiency = 90%

Combustor efficiency = 0.9999

High pressure turbine (HPT) polytropic efficiency = 90%

Low pressure turbine (LPT) polytropic efficiency = 90%

High pressure shaft mechanical efficiency = 99.5%

Low pressure shaft mechanical efficiency = 99.5%

**High Pressure Compressor conceptual design**

- Multi-stage constant-mid radius design.
- 1st stage relative tip Mach number of 1.35
- Purely axial flow at each stage entry and exit i.e., $C_{stg1,1} = C_{ax,stg1,1}$ and $C_{stg1,3} = C_{ax,stg1,3}$ etc.
- Constant axial velocity between first stage rotor entry and exit.
- You may linearly interpolate axial Mach numbers and aspect ratios at each stage entry based on the conceptual design values used for HPC entry and exit.
- You may assume that every compressor stage has the same polytropic efficiency of 90%.
- You may assume that in a given stage the rotor and stator have the same aspect ratios. Use the blade and vane entry height for determining the length of each blade and vane.

**High Pressure Turbine conceptual design**

- Two-stage constant-mid radius design.
- Purely axial flow at each stage entry and exit i.e., $C_{stg1,1} = C_{ax,stg1,1}$ and $C_{stg2,3} = C_{ax,stg2,3}$
- Constant axial velocity between first stage rotor entry and exit.
- The HPT NGV entry mid radius is 125% of the HPC exit mid radius i.e., $r_{mid,hpt,entry} = r_{mid,hpc,exit}/0.8$
- You may linearly interpolate axial Mach numbers between stages.
- Equal enthalpy drop across the two turbine stages.

- You may assume a constant mass flow across the HPT $1^{st}$ stage rotor in your conceptual design calculations.

**Further assumptions**

- Assume that 20% of the HPC inlet mass flow (taken from the HPC outlet) is used for cooling purposes in the HPT.
- Assume that 60% of the total cooling flow is used for HPT $1^{st}$ stage NGV cooling and does work in the HPT i.e., it is mixed before the HPT $1^{st}$ stage rotor inlet.
- Assume that the rest (40%) of the total cooling flow is used for HPT $1^{st}$ stage rotor cooling and does not do any work in either rotor of the HPT due to very low momentum, i.e., it is therefore mixed downstream of the HPT $2^{nd}$ stage rotor.
- Assume ideal convergent nozzles.
- Assume that the incoming working fluid is dry air and that it behaves as an ideal gas i.e., variable properties with temperature and fuel-to-air ratio.
- Assume an expected year of Entry Into Service EIS = 2020
- Assume that flow properties at mid radius represent the average flow across the blade/vane height.

All further assumptions made must be stated explicitly in your report and justified. You may use the information provided in your lecture slides and compendiums, or information available in the public domain.

## 3. Key Calculations

As part of this design task you must:

- Calculate the total pressure and temperature at all engine stations (including HPT $1^{st}$ stage NGV entry and exit, and HPT $2^{nd}$ stage rotor outlet before and after mixing the cooling air).
- Calculate the fuel mass flow, momentum draft, gross thrust from each nozzle, net thrust, specific fuel consumption, intake mass flow, core mass flow, fan pressure ratio, bypass ratio, ideal jet velocity ratio, HPT $1^{st}$ stage NGV and rotor blade metal temperature and cooling effectiveness, propulsive efficiency, thermal efficiency and overall efficiency.

- Use the bypass ratio value provided only as a first guess. You shall iterate on the bypass ratio value to achieve the approximate optimal ideal jet velocity ratio suggested by the formula $V_{jet,bypass}/V_{jet,core} = \eta_{fan}\eta_{LPT}\eta_{LP,mech}$ (see lecture slides). You must demonstrate the optimality of this bypass ratio. HINT: Prepare a "Specific Fuel Consumption vs Ideal Nozzle Jet Velocity Ratio" plot to illustrate your point.

- Use the fan pressure ratio value provided only as a first guess. You shall iterate on it to achieve the required net thrust level.

- Determine the number of stages for your high pressure compressor. Calculate the stage loading and (rotor) flow coefficient of every stage at mid radius.

- Sketch the flow path of the high pressure compressor based on your blade/vane length and height estimates.

- Calculate and sketch the inlet velocity triangle at the high pressure compressor $1^{st}$ stage rotor tip. What is the relative tip speed?

- Calculate and sketch the inlet and outlet velocity triangles at the high pressure compressor $1^{st}$ stage rotor mid. What is the total flow deflection?

- Calculate and sketch the mid velocity triangles for the $1^{st}$ stage of the high pressure turbine. What is the total flow deflection?

- Determine the high pressure turbine $1^{st}$ and $2^{nd}$ stage loading and (rotor) flow coefficients. Is the stage loading sufficiently high to merit two stages, or would it be better to go for a single-stage design instead? Justify your view.

- Re-calculate the high pressure turbine $1^{st}$ stage rotor metal temperature by determining the rotor inlet relative total temperature. In doing so you must use the velocity information available from you velocity triangle calculations. Do you think that cooling is necessary for the second stage? Why so?

- Calculate the high pressure turbine $1^{st}$ stage AN2 value and cross-check if it is within acceptable limits.

In addition to the above calculations, you will also need to carry out all necessary calculations in order to fill out the stand-alone results spreadsheets provided separately and in conjunction with this assignment on Blackboard.

You may develop your code or spreadsheet alone, or in partnership with one (1) other student. Nonetheless, you must have full individual ownership of the code or spreadsheet developed, and be ready to explain and justify the work in detail in an individual oral examination, if requested.

Brainstorming sessions between larger groups of students are encouraged, but separate codes must in all cases be developed and submitted on Blackboard to complete this assignment.

### 4. Reporting and Submission

You shall prepare and submit electronically an individually prepared technical report, prepared in English, according to the deadline schedule provided on Blackboard.

You may NOT co-author your report with another student.

Your report must be structured according to the official report template and include (as minimum) the following information:

- Your name and student ID
- The name and student ID if you developed your code/spreadsheet in partnership.
- A summative description of the key methods implemented and all assumptions made.
- A detailed sketch of the gas turbine configuration.
- A sketch of the required velocity triangles for the high pressure compressor $1^{st}$ stage (rotor inlet and outlet) and the high pressure turbine $1^{st}$ stage (NGV inlet, rotor inlet and outlet) including appropriate blade and vane shapes.
- A detailed sketch of the high pressure compressor flow path showing the variation in cross flow area and rotor/stator length across all stages of the HPC. You should clearly identify each stage rotor and stator. The sketch should be on scale i.e., you must use your calculated geometric values for each stage rotor and stator.
- A 2-page discussion of your key results and overall conclusions focusing on the bullet point questions raised in Section 3 of this assignment description. The detailed Excel results templates that you will fill out should not be included in this report (apart from the sketches) and should be uploaded as separated files.

In preparing your report please keep in mind that it will be sent to URKUND for plagiarism checking. All cases of plagiarism will be report to the MDH disciplinary committee.

In addition to the technical report, you must also:

- Submit the complete MATLAB code or Excel spreadsheet that you have developed in order to carry out your calculations. If you have partnered with another student in developing the code, you must clear identify this in your submission, by including the name and student ID of your partner.
- Fill out completely and submit electronically the stand-alone separate Excel results templates that contain the parameters that must be calculated. These templates are provided in conjunction with this task through Blackboard. DO NOT MODIFY THE SPREADSHEET TEMPLATES PROVIDED!

All illustrations used in your report should be produced by yourself and must not be taken from literature.